12-2021

An Assessment of the Neurovascular Structures of the Trigeminal Nerve and Their Relationship to Diet in Primates

Caitlin Yoakum
University of Arkansas, Fayetteville

An Assessment of the Neurovascular Structures of the Trigeminal Nerve and Their Relationship to Diet in Primates:

A dissertation submitted in partial fulfillment
of the requirements for the degree of
Doctor of Philosophy in Anthropology

by

Caitlin Yoakum
Texas Tech University
Bachelor of Arts in Anthropology, 2014
Texas Tech University
Master of Arts in Anthropology, 2016

December 2021
University of Arkansas

This dissertation is approved for recommendation to the Graduate Council.

_____
Claire Terhune, Ph.D.
Dissertation Director

_____
J. Michael Plavcan, Ph.D.
Committee Member

_____
Peter Ungar, Ph.D.
Committee Member

ABSTRACT

The inferior alveolar nerve (IAN) enters the mandible via the mental foramen, supplies nervous sensation to the mandibular teeth as it travels through the mandibular canal, and exits the mandibular foramen to send information to the brain to maintain chewing cycles and protect the teeth from damage. Although bony canals and foramina have been shown to form around soft-tissue structures, there are some examples (e.g., the hypoglossal nerve/canal) where the nervous structures do not comprise most of the canal/foramina space. It is important to know the size of nerves because it has been established that larger nerves convey more information at faster rates. However, no previous work has established the size of the IAN in primates or if the mandibular canal and associated foramina can be used as proxies for the nervous tissues. The purpose of this dissertation is to assess the variation seen in the IAN in using both a hard-tissue dataset comprised of tooth and mandibular canal measurements and a soft-tissue dataset comprised of the cross-sectional area (CSA) and volumetric measurements of the IAN. These two datasets explore the relationship between the IAN and the roots and enamel surfaces of I_1, C_1, P_4, and M_1, the CSA and volume of the mandibular canal, and the dietary categories of primates.

Overall, the IAN is related to the bony structures of the mandible by size across primates. There were significant relationships between the tooth surface areas and the IAN throughout the mandible, with most showing either isometric or negatively allometric relationships. Additionally, the nerve CSA measurements at the mental foramen, mandibular foramen, beneath P_4, beneath M_1, and overall canal volumes showed significant relationships with the corresponding IAN measurements. However, while these relationships may be significant there is no evidence to support the hypothesis that the IAN fills most of the mandibular canal.

Teeth are under strong selective pressure to change shape in response to a change in environment or diet in primate species. Therefore, it was hypothesized that the nervous tissues

– because of their direct relationship to the teeth by supplying somatic sensation – would be under these same selective pressures. However, there was only one significant relationship found between the shape of the premolar tooth and the nervous tissue variables, with no other teeth showing significant relationships with the shape of the tooth's surface. These relationships were further supported when there were no significant relationships between the IAN and dietary categories – reinforcing the conclusion that there are little to no differences in IAN size across primates based on diet.

All cranial nerves in mammals are highly conserved in their shape, pathways, and functions, indicating strong selective pressures to maintain these nerves for their vital functions. These data showed that the IAN – a termination of cranial nerve V – is highly constrained across primates (and some mammal species) and is more likely related to the overall size of the mandible rather than selective pressures such as diet.

ACKNOWLEDGEMENTS

As far as writing dissertation sections goes, this was the most fun and the greatest privilege to write. Obtaining a Ph.D. is not a miraculous feat of a single person but rather an enormous marathon that lasts for four (and sometimes five or six) years of an individual's life. Not only do I have academic advisors to thank but also the people that kept me sane, with a foot in the real world outside of academia. There have been tears, there has been stress, there have been moments where quitting seemed like the most tantalizing option, but the support network that I have built around me has never allowed me to truly fail. Thus, the next few pages will be the thanks that I owe those individuals, and can likely never repay in full, but will attempt a few kind words.

My advisor, Claire Terhune, Ph.D., has borne the brunt of my stumbling along through graduate school and has always been available to offer advice for both academic and personal questions. She has not only helped me develop a dissertation that I care greatly about but has also helped me develop all of skills I will need as I embark on a career in academia. She has created whole classes, made sure we were included on publications, encouraged funding opportunities for travel, introduced us to anyone we asked at conferences and in academic spaces, and read my NSF DDRIG proposal for this very project at least fifty times. Claire is the advisor I needed to complete this project, even if she drove me crazy for a large percentage of the time.

Along with Claire, my committee members have been invaluable in making this project the best that it could be. Dr. Mike Plavcan and Dr. Peter Ungar have rigorously evaluated my methods and ideas during the formation of this project and throughout. When I needed help with teeth, jaw mechanics, statistics, or anatomy, both were always willing to lend an ear and give advice. They have sat in meetings, written my qualifying exams, sat through proposals, and answered every email ever sent. They have been a model committee and it has been a privilege to be mentored by them all.

Ashly was my roommate for most of the time during this project and best friend for the entirety of it. I owe 90% of the knowledge I have in statistics to her and will likely continue to ask for help long after this project gets put on to a shelf and (hopefully) never read again. She has been a personal therapist since the day we moved in together and is the only other person here in Arkansas that has the exact same shared experience I have gained in this program. Most of the good times and all the bad times have been shared with her and she is irreplaceable in helping me complete this project. There is no one else I go to for advice here and no one else I would get a matching tattoo with.

Simon Tye might not have been around for the formation of this project, but he did manage to catch the tail end. While he has always been willing to offer me advice on coding and the science of evolution, the love that he has offered me personally is second to none. He is my support system and the home I get to come home to every day. He has been weekend projects and hunting for treasures. He is a constant adventure buddy and my very best friend in the entire world. We have built a life together, along with Magnolia, that I never dreamed I would have. There are not enough words in the English language (or any language in my opinion) that can describe how happy I am with him and how much he means to me in this lifetime. Every laugh, every tear, every bike ride, every insomnia order, and every other moment has been the privilege of my life to spend with you.

Apart from the singular most important people in my life, there are groups of individuals that have helped in ways I couldn't have imagined when I set out on this journey. Particularly Ben Wadsworth and the Evans lab as well as the Alverson lab and its many graduate students that have unlocked doors for me and my cart of rattling bottles. Being housed in a historic building means that no distilled water taps exist in our caves and thus I have traveled to Ferritor Hall more times that I can count to fill up my plethora of mismatched jugs. Without this water, none of the iodine solutions could be made and thus the simple act of having access to a distilled water tap has made this entire project even possible.

Similarly, all those who donated specimens to this project (free of charge, I might add) have made the project possible. When we began, Claire and I agreed that 50 specimens would be adequate to complete the research. In a year, we had managed to find 181 specimens that people from a variety of universities were willing to part with for a few years, which I think shows just how kind and miraculous the academic world can be when we work together. Manon Wilson, Paul Gignac, Haley O'Brien and the rest of the MICRO team were always willing to provide advice on scanning, staining, and barium-latex injection techniques whenever asked, allowing me to refine my protocols and make this study better overall. Zach Throckmorton has also always been available when anatomy (or job market) advice was needed. It is these small moments and contributions of senior academics that can make or break the future of a graduate student and I am proud to say that all these people who have believed in me to get this project done have constantly inspired me to always help others.

This project would not have been completed without the help of several key undergraduate researchers: Amber Cooper, Alice Stubbs, and Autumn Sanders. They have spent hours helping me with data collection, specimen preparation, and have listened to me talk about any and everything. They have become friends as well as colleagues and I hope that I have prepared them for future research endeavors that they might pursue and for all of life's problems within academia. Undergraduates are often undervalued in the work that they produce in labs, but these researchers kept this project going and gave me the momentum and courage that I needed.

Outside of academia, I have been anchored to the real world by my family and my friends. My parents, Donna and Dennis Yoakum, have always allowed me to chase whatever wild dream that I have. My mother has always told people that I "march to the beat of my own drum" which I have recently decided to take as a compliment. They have, for many years, attempted to explain my work with decapitated monkey and ape heads to a variety of horrified friends. This horror has not, however, ever caused them to waver in their support of my career

goals. Their outdoor freezer may bear the stench of death (from a variety of animal corpses), but their unwavering support has meant the world to me. My sister and brother-in-law, Catherine and Larry Pineda, have similarly helped me in all of my endeavors. From helping me label and tag (decomposing and very smelly) lemurs to always offering free pharmacy consults (to a poor graduate student with school insurance) their support has also been constant. Their children, Jack and Hazel, have inspired me in more ways than I can count. They make me want to constantly participate in outreach and scientific education as each new thing I can teach them inspires wonder and constant questioning of the natural world. They are my main motivators to stay within academia so that I can keep chasing that feeling of knowing I have taught someone something that may change their life entirely.

My very best friends in life have constantly reminded me that the real world continues to move after everyone else has already graduated from college. Katie Waller forced me to take two vacations for the celebration of her bachelorette party and wedding, causing me to realize that rest and fun with friends is vital during graduate school. Taylor West has inspired to chase my dreams from starting out her career as a labor and delivery nurse (with all the staggering stories you'd expect), to teaching in Thailand, to now starting and owning her own business – reminding me that you do not have to continue a career path that is no longer bringing you joy. Audrya Houde has helped me see that even if I had a career outside of academia, the same problems would exist in life. I have learned so much about the admin of speech therapy, moving to new cities, making new friends, overcoming medical hardships, and chasing dreams from her than she will ever know. She has encouraged my shopping habits, my workout habits, my whole30 attempts, and has constantly reminded me that if something doesn't bring you joy in life you should immediately find a proper receptacle for it (whether that is recycling or the trash). Luckily, and because of these people, I have been able to hold on to mostly joyous things for the last 10 years and will continue to do so through life for many more. We always say we

should make the time to get together more often (doesn't everyone after graduation?), but we really should find some time to get together more often.

Finally, I'd like to thank all the people around me that made graduate school bearable and most of the time fun. My bosses for many years as I taught, Lucas Delezene and Amelia Villasenor. All the faculty members whose classes I got to take as I made my way through coursework earning my degree. The other graduate students in the Anthropology department who were amazing supporters and sounding boards for projects both academic and personal. Sideways bar and Smoke and Barrel, for always being a meeting place with a few familiar faces and plenty of taps behind the bar. Dickson street in general, for always being a place we could gather when we needed out of our work and our classrooms. The biology crew – James, Eric, Zach, Connor - for making me say "I don't even understand why I'm friends with you guys" at least three times every weekend. And the many, many other people that have impacted my life in one way or another and have helped me grow into the person that I am today.

Throughout this journey I have fumbled and bumbled my way to making sense of this project and my life. I have spent all my formative years on a college campus giving my all to my research and my future career. I have learned that science is less sitting in an ivory tower and more failing in a dark lab about a hundred times before you find the answer you've been searching for. I used to think that when I stumbled up the back steps of academia that I'd be able to walk gracefully out of the front door at the end, diploma in hand and ready for the world. In reality, I've discovered that we are all just beluga whales in a dolphin show, slowly jumping and splashing along to fast paced music that someone else has set but doing the absolute best we could. In the end, the audience still claps.

TABLE OF CONTENTS

CHAPTER 1: INTRODUCTION

For most mammals, particularly primates, the orofacial region is the first part of the body that interacts with potential food objects. Primates use numerous senses to choose their food and optimize nutrition intake. For example, frugivorous primates frequently interact with food via their hands, eyes, face, and olfactory system to determine if a given fruit has reached the appropriate ripeness. In contrast, primates that eat leaves or seeds use fewer external sensations to determine the toughness of these food objects and often chew on these objects briefly to decide if it is worthwhile to process further. If a leaf is too tough—which tends to indicate high fiber content, low levels of nitrogen, and/or low levels of protein—the primate will not ingest the leaf to avoid filling their stomach with bulky, non-nutritious materials (Davies et al., 1988; Lucas, 1994; Ganzhorn et al., 2017). This suggests that these animals are using tactile sensory feedback from orally testing tough/stiff plant parts to determine which leaves or shoots to eat. Presumably the tactile sensory structures of the mouth are under considerable selective pressure, particularly among taxa that eat a more resistant diet. The purpose of this dissertation is to establish that, in addition to the well-studied visual and manual sensory adaptations, primate food processing and acquisition is also heavily dependent on the sensory nerves of the oral cavity and teeth. This underlying assumption arises partly out of observation that the nervous tissues of the oral cavity are all uniquely positioned to inform primates and other mammals about the material properties of the food they ingest, as well as to provide sensory feedback during complex masticatory behaviors such as incision or other oral processing.

All oral structures are innervated through branches of the trigeminal nerve (CN V), of which the three main branches pass through the infratemporal fossa (V_1), maxillary body (V_2), and mandibular canal (V_3). The mandibular canal is often thought of as a single bony tube terminating at both the mental and mandibular foramen, although the tubular nature of this structure has been contested based on small studies in humans (Anderson et al., 1991; Chávez-Lomeli et al., 1996; Olivier, 1928). This canal runs through the body of the mandible,

thereby providing passage for the inferior alveolar nerve (IAN) and the inferior alveolar artery (Anderson et al., 1991). Variation in the anatomy of the mandibular canal has only been noted in humans, with no study addressing the variation seen in non-human primates.

Previous research indicates that the size of some nerves is directly correlated to their total axon count, with higher amounts of axons relaying more information at a faster speed (Cull et al., 2003; Jamniczky & Russell, 2004; Jonas et al., 1992; Muchlinski & Deane, 2014). Therefore, knowing the size of nerves and their amount of myelination could give some insight into the sensitivity of these tissues and the types of sensation they are able to process. While some studies have estimated the number of axons within the human mandible (Edin & Trulsson, 1992; Rood, 1978) and cats (Holland, 1978) no study has assessed the variation seen in the IAN across primates. This dissertation aims to discuss the relative size of the IAN across primates and the variation seen in this nerve to fill this gap in the literature.

While it has been established that primate diets are related to tooth form and masticatory patterns (Kay, 1973, 1975; Lucas, 2006), it remains largely unknown whether the accompanying nerves are under the same selection pressures. Because teeth are the direct interface with the outside environment and have been shown to be under selective pressure for different shapes based on diet, it is assumed that the nervous structures that supply these teeth would be under similar evolutionary pressures. However, because there is little knowledge on the variation of the IAN in primates, no study has assessed if this is the case.

ORGANIZATION OF THIS DISSERTATION

Chapter 2 of this dissertation provides a literature review of the known research on the trigeminal nerve (with particular emphasis on V_3), the mandibular canal and its bony correlates, the specific innervation of the overall masticatory system, food material properties, foraging efficiency in primates, and the implications this research may have on human evolutionary studies. While not exhaustive, this background research discusses what is known on the topics necessary to examine the data collected for this research.

Chapter 3 of this dissertation discusses the materials and methods used for this research. This dissertation uses two sets of separate but related data: a hard-tissue dataset that focuses on the bony structures of the mandible and teeth in primates, and a soft-tissue dataset that is comprised of digital three-dimensional (3D) models of the IAN. Using these two datasets I investigate three research questions that inform on the relationships between the hard- and soft-tissue structures of the mandible. This research employs diceCT staining methods to visualize soft-tissue structures in microCT scans, programs such as Avizo and Geomagic to create 3D models and take measurements, and a series of statistical analyses performed in RStudio or Microsoft Excel.

The first research question (Chapter 4) examines the relationship between tooth morphology and the IAN. Because the tooth is the direct interface with the external environment, it should have a relationship to the nervous tissues that supply information from the teeth to the brain. Thus, these nervous tissues should be under similar selective pressure as the teeth which are heavily influenced by diet. To discuss this question, I test a series of three hypotheses to establish if there is a relationship between the surface of the tooth and both the root structures and the nervous tissues that directly innervate it.

The second research question (Chapter 5) examines the relationship between the mandibular canal and the IAN that runs through it. It is assumed that bony canals and foramina form around nervous and vascular tissues as they are the first to form during development. However, no previous research has established if the size and shape of the mandibular canal is equal to that of the IAN and corresponding vascular structures. This chapter discusses the relationship between the cross-sectional areas (CSA) of the IAN and the corresponding CSA of the bony canal as well as the IAN volume and the mandibular canal volume.

The third research question (Chapter 6) examines the relationship between the nervous tissues and diet in primates. This chapter uses traditional dietary categories (i.e., frugivore, folivore, etc.), resistant vs. non-resistant categories, and dietary percentages of foods

consumed. These dietary categories were culled from the literature based on field observations of primates in their natural habitats. Additionally, this chapter focuses on how nervous tissue size might change in relation to its location in the mandible. Specifically, I test two separate hypotheses: 1) primates with more resistant diets – and thus more oral processing – will have larger nerves in the posterior aspect of the oral cavity and, 2) primates that have primarily frugivorous diets will have more nervous tissues in the anterior aspect of the mandible – where the nerve exits the mandible and provides somatic sensation to the lower face – to aid in the external processing and manipulation of foodstuff prior to ingestion.

The final chapter of this dissertation (Chapter 7) gives a general discussion and conclusion of all research questions together as well a discussion on future avenues of research. First, I discuss the relationships of the IAN to the hard-tissue components (i.e., the teeth, the mandibular canal, and the mental/mandibular foramina). Second, I discuss the IAN and its relationship to primate diet.

This dissertation is the first to collect data of this kind using the novel technique of iodine staining and 3D segmentation of nervous tissues. Knowing the variation in these structures is vital for understanding the cranial nerves and how they look across primates (and some mammals). This work is the first to compare the size of nervous structures within the mandible to the shape and size of the teeth, the size of the mandibular canal, and diet across a wide range of primates giving integral information of how nervous structures change in relation to environmental selective pressures.

CHAPTER 2: BACKGROUND

Cranial nerves, although crucial for most of the sensory information and injury treatment to the brain, are grossly understudied in their function, development, evolution, and morphology (Trejo, 2019). Although cranial nerves are highly conserved across vertebrates, their functions, evolution, and intraspecific variation are highly complex (Trejo, 2019). However, the evolutionary trajectory of these nerves has been superficially established: paired sensory structures allowed organisms to transition from filtering animals without brains to animals that exhibit predatory behaviors, while coevolving in a coordinated way with the neck, heart, and gastrointestinal tract (Trejo, 2019). This coevolution of the neural crest, neural placodes, and the cardiopharyngeal fold has allowed for increased cephalization in vertebrates and particularly primates and humans (Martínez-Marcos & Sañudo, 2019; Trejo, 2019). Due to the current advances in technology and our increased ability to study cranial nerves, we are at a critical point in the field of anthropology in understanding how much of an effect these nerves, and in particular the trigeminal nerve, have had on the evolution of the primate masticatory system.

The trigeminal nerve (cranial nerve V, CNV) is the largest of all 12 recognized cranial nerves and is named from the Latin word “trigeminus,” meaning Three Twins (Singh, 2019). There are three main branches to CNV: the ophthalmic branch (V_1), the maxillary branch (V_2), and the mandibular branch (V_3) (Figure 2.1). This dissertation focuses on the size and path of a single terminal nerve of the mandibular branch (V_3), the inferior alveolar nerve (IAN). The IAN runs through the mandibular canal, supplying nervous sensation from the teeth to the brain and muscular function to the muscles of mastication.

This background section will be a review of the current literature known on the trigeminal nerve and its bony correlates, specifics on the innervation of the masticatory system, food material properties, foraging efficiency, and a brief discussion on human evolutionary implications. While not exhaustive, this chapter aims to address what questions have already been asked about the IAN and indicate the areas that need further study.

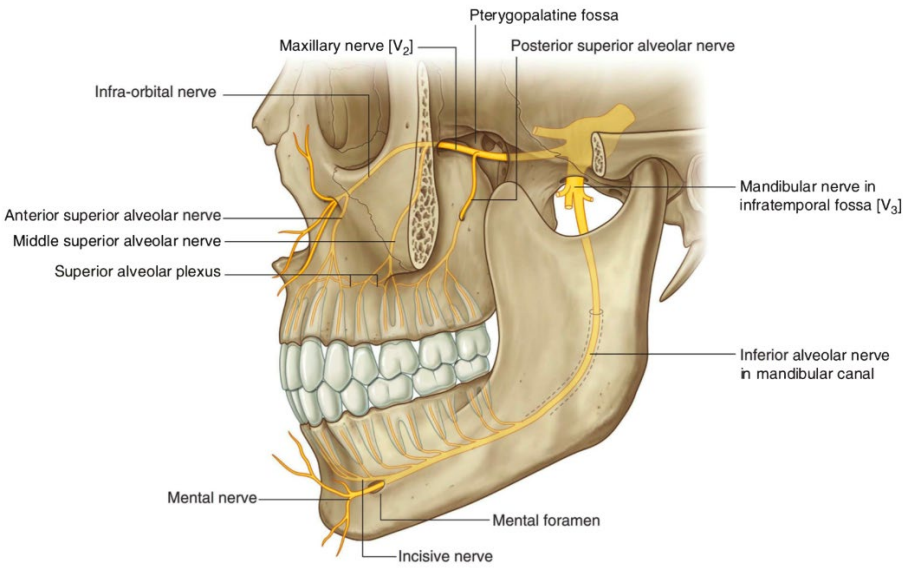

Figure 2.1. Demonstration of the typical course of the trigeminal nerve with the maxillary (V_2) and mandibular (V_3) branches labeled. Image from Gray's Anatomy (2015).

THE TRIGEMINAL NERVE AND ITS BONY CORRELATES

This section will aim to discuss the main branches of the trigeminal nerve with somatic sensory information pathways described towards the brain (afferent) and motor pathways described from the brain (efferent). The trigeminal nerve becomes a single structure as its two roots, a sensory and motor root, converge in Meckel's cave at the trigeminal ganglion (Booth et al., 2013; Edwards & Gaughran, 1971). The nerve is divided into three subsequent branches, the ophthalmic branch (V_1), the maxillary branch (V_2), and the mandibular branch (V_3) (Figure 2.1). The ophthalmic branch (V_1) enters the brain case via the superior orbital fissure and carries somatic sensory information along its three main branches: the lacrimal, frontal, and nasociliary. The frontal nerve enters the cranium at the supraorbital foramen and carries cutaneous somatic sensation from the upper portion of the face to the brain. The maxillary branch (V_2) enters the brain case via the foramen rotundum and carries somatic sensory information along three main branches: the maxillary nerve (which includes the alveolar branches), zygomatic, and posterior dental. The infraorbital nerve enters the infraorbital foramen (becoming the superior alveolar nerve) and carries cutaneous innervation from tissues below

the eyes and beneath the nose to the brain. The mandibular branch (V_3) enters (and exits for motor pathways) the brain case via the foramen ovale and is divided into both sensory and motor branches. The motor branches (the muscular, masseteric, deep temporal, lateral pterygoid, and inferior alveolar) all provide innervation to the various muscles of mastication.

The somatic sensory branches (meningeal, buccal, auriculotemporal, and lingual) all carry sensory innervation from the mucosal tissues of the oral cavity to the brain. One branch of V_3, the mental nerve, transmits somatic sensory information from the skin of the chin, lower lip, and labial gum as it passes through the mental foramen. The mental nerve is continuous with the inferior alveolar nerve (IAN) which passes through the mandibular canal and through the mandibular foramen towards the brain (Blackmore & Jennett, 2001; Edwards & Gaughran, 1971; Morris & Jackson, 1933; Sandring, 2015). The IAN also serves as the sole sensory innervation for the lower tooth row.

For the purposes of this review, the terminology used in this work will reflect the current thinking in that regardless of branching patterns, all nervous tissue that enters the mental foramen (proceeding posteriorly) and innervates the teeth is called the inferior alveolar nerve (IAN). The IAN runs through the body of the mandible until it exits in a bundle at the mandibular foramen, joining the main trunk of the mandibular branch. When the mental nerve passes through the mental foramen, an additional branch, the incisal nerve, also provides somatic sensory information from the canines and incisors (Jacobs et al., 2007). Some argue that the mandibular incisal nerve is not a true neurovascular bundle (i.e., nerve, artery, and vein) but is much better described as an incisal plexus (Jacobs et al., 2007). This nerve contains no motor fibers and only serves a sensory function as objects are placed on the chin, lips, or anterior teeth (Jacobs et al., 2007).

Mastication and Oral Structures

The primary function of the mandible is mastication, or a rhythmic activity of food processing in the oral cavity that is automatic and dependent upon the physical properties of food materials (Luschei & Goldberg, 2011). At the most basic level, mastication must involve movement of the temporomandibular joint (TMJ) to allow the maxillary teeth to come into occlusion with the mandibular teeth for food processing (Ahlgren, 1976). Often classified as a hinge joint with a movable socket, the TMJ is composed of the mandibular condyle, the glenoid fossa, the articular eminence, the articular disc, and the articular capsule and ligaments (Crompton, 1989; Hylander, 2006; Lucas, 2006; Luschei & Goldberg, 2011; Rees, 1954). The intermediate zone of the articular eminence bears the highest load during mastication, causing this portion of the articulating disc to have a lack of neurovascular structures (Hylander, 2006; Luschei & Goldberg, 2011). However, the posterior portions of the articular disc, articular capsule, and articular ligament are highly vascularized and innervated by the trigeminal nerve (Hylander, 2006). Muscles involved in the movement of the TMJ are numerous: the masseter, temporalis, medial pterygoid, lateral pterygoid, digastric, mylohyoid, geniohyoid, stylohyoid, and various infrahyoid muscles (Crompton, 1989; Lucas, 2006; Luschei & Goldberg, 2011). Those most important for mastication in terms of neurological impulses from occlusal movements are the masseter, temporalis, and hyoid muscles (Hylander, 2006).

The masticatory muscles are typically divided into two groups: 1) jaw-closing muscles (temporalis, masseter, and medial pterygoid) and 2) jaw-opening muscles (digastric, lateral pterygoid, and the suprahyoid group) (Lucas, 2006; Luschei & Goldberg, 2011; McNamara, 1974). The jaw-closing muscles can be thought of as extensors whereas the jaw-opening muscles are thought of as flexors, although the jaw-opening muscles are aided significantly by gravity (Luschei & Goldberg, 2011). The TMJ is capable of two basic movements: 1) rotary or hinge movements and 2) translation or sliding movements (Hylander, 2006). While the mandible is considered a class III lever in primates, there is a working side and a balancing side, with the

latter bearing most total condylar reaction forces (Daegling & Grine, 2006; Hylander, 1975b, 2006; Luschei & Goldberg, 2011; Smith, 1978; Werner et al., 1991). These movements are influenced heavily by the shape and size of the muscles that control them. The jaw-closing muscles have many nervous proprioceptors (i.e., receptors that transmit information on how the muscles are moving and working to the brain), indicating they are capable of more sensory input whereas the jaw-opening muscles have been shown to have very few, if any proprioceptors (Luschei & Goldberg, 2011).

The ability of any mammal to adjust the chewing cycle and sense the material properties of food is directly related to the innervating structures within and around the teeth. Chewing is composed of a three-part cycle: 1) the opening stroke where the mandible moves downward to a specific amount of jaw opening (gape), 2) a closing stroke where the mandible moves rapidly upward and laterally to engage the food between the molars, and 3) a power stroke where the mandible moves upward and medially at a slower rate back to the point of the maximum intercuspation of the teeth (Luschei & Goldberg, 2011). Many authors separate the opening stroke portion (gape) of mastication into four stages: fast close, slow close, slow open, and fast open (Crompton, 1989; Hiiemae, 1974; Thexton et al., 1980). This cycle has been well-defined and holds true for most mammals, as they tend to use only one side of the mandible at a time for chewing. However, significant variation exists in mammals in terms of specific chewing cycles that are entirely dependent on food properties. The fast close to slow close transition is consistently related to tooth-food-tooth contact and the slow open to fast open transition is correlated with any changes in the direction of the hyoid caused by hyoid muscle contraction (Crompton, 1989). It is very difficult, however, to recognize these two divisions in primates because there are no large hyoid movements typically involved in their mastication (Crompton, 1989).

In humans, chewing cycles have been shown to be unique to specific individuals regardless of food properties, indicating that the way we chew is in some way pre-programmed

based on previous experiences (Luschei & Goldberg, 2011). Many authors assume that if this pre-programming is true for human subjects, the same can be inferred across primates due to their overall similarities with humans in food choice and mastication. Chewing and gape cycles are predominantly controlled by motor fibers in the mandible that transmit impulses to activate the temporalis, masseter, and hyoid muscles to control chewing with complex movements (Booth et al., 2013; Crompton, 1989; Rees, 1954). Sensory fibers from the scalp, skin of the face, gums, teeth, and lips relay information on tooth processing to alert the masticatory apparatus to the necessary gape required for certain food types (Booth et al., 2013; Cartmill et al., 1987; Crompton, 1989). Length of the chewing cycle can be affected by the stiffness and toughness of the food, particularly when the food is on the cheek teeth (Lund & Kolta, 2006; Luschei & Goodwin, 1974; Thexton et al., 1980).

The Periodontal Membrane

Mastication is often studied as a single process with a variety of moving parts. The purpose of this section is to break down the individual portions of the oral cavity and its innervating structures (i.e., teeth, gums, mandible, etc.) in detail. While the teeth are arguably one of the most important components of mastication, they are held in place by the periodontal membrane (or PM), that is composed of the periodontal ligament, the gingiva, and the periosteum (Figure 2.2) (Hannam, 1976, 1982). The periodontal ligament is a series of small fibers that attach the root surface of the tooth to the alveolar bone that surrounds it, allowing the tooth some movement in its socket. The gingiva, often called the “gums”, are soft-tissue structures that are found at the neck of the tooth, the dividing point between the crown surface and the root surface. The periosteum is a thin, fibrous tissue layer surrounding the alveolar bone that is richly innervated and vascularized.

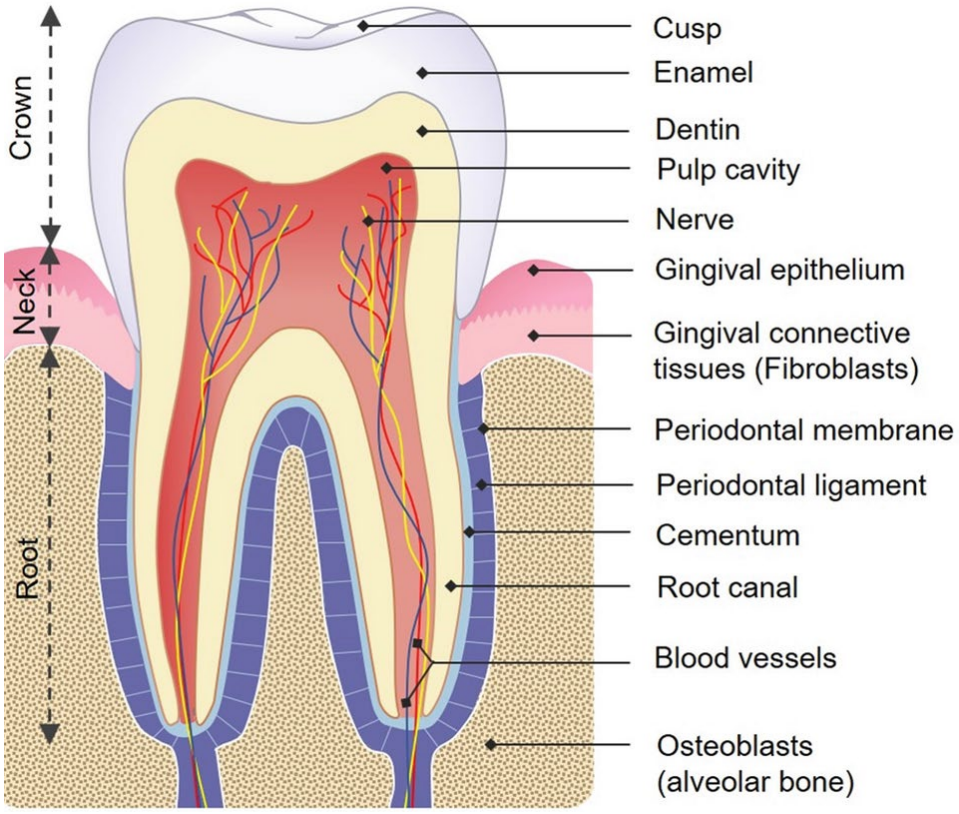

Figure 2.2. Example of a molar tooth that shows the periodontal membrane (periodontal ligament, gingiva, and alveolar bone). Image from Iranparvar et al. (2020).

The PM serves two main functions: hold the teeth in their correct place within the alveolar bone and provide a large portion of the sensory information generated in the mouth during oral movements. Because of these integral roles in tooth function, the PM of the maxillary and mandibular process is well established before tooth development begins, giving nerve axons a path to follow as they grow in the direction of the future tooth crown (Beertsen et al., 2000; Fearnhead, 1967). There is some evidence that neural richness in the PM increases from anterior to posterior along the mandibular arch, although the opposite is true for the maxillary arch (Desjardins et al., 1971). Transmedian innervation (i.e., some nerve axons appear to cross the midline) has been shown in both incisors and canines, although it is rare that it extends as far as the canines (Chiego et al., 1980; Starkie & Stewart 1931). All these innervating structures within the PM are relaying information regarding touch or pressure within the oral cavity during

all mouth movements (Anderson et al., 1970; Avery & Cox, 1977; Brashear, 1936; Plaffman, 1939).

There are many different systems with the overall nervous system that relay an enormous amount of information that cannot be exhaustively discussed here. However, there are three main categories of sensation that help regulate mastication: proprioception, mechanoreception, and pressoreceptors. Proprioception is a vital process that the nervous system performs as it allows the body to perceive its own position in space. There are three main types of proprioceptors: Golgi-tendon organs, muscle spindles, and joint receptors. Within the PM, most of the proprioception is sensed via Golgi tendon organs (sometimes referred to as Golgi-Mazzoni type or GTO) and muscle spindles (Hannam, 1976; Luschei & Goldberg, 2011). Golgi tendon organs and muscle spindles are part of the system that protects the muscles of mastication, by sending information to the central nervous system (CNS) as to the amount of tension or stress a muscle is exerting to prevent excess use and potential damage.

A large portion of the research on the masticatory apparatus focuses on a group of somatosensory receptors called mechanoreceptors. Mechanoreceptors relay external stimuli to internal cellular structures via mechanically gated ion channels. Feedback mechanisms in the mandible are most likely controlled by mechanoreceptors in the periodontal ligament and are crucial components to understanding the mammalian masticatory cycle (Byers & Dong, 1989; Crompton, 1995; Falin, 1958; Inoue et al., 1989; Linden, 1991; Ross et al., 2010). This feedback mechanism reduces the risk of tooth breakage, wear, and loss during mastication. Additionally, it has been noted that the mechanoreceptors related to the oral cavity are able to transmit information on incredibly high forces much faster (compared to sensory neurons of the skin) and for long periods of time (Hannam & Farnsworth, 1977; Van Steenberghe, 1979). Individual periodontal mechanoreceptors are not able to inform on either force direction or the tooth to which a force was applied, and instead work as a population of receptors in groups of at least 25 (Edin & Trulsson, 1992; Hannah, 1982; Johnsen & Trulsson, 2003; Linden, 1991; Matthews,

1977; Trulsson et al., 1992). While the molar teeth have higher pressure thresholds, the degree of mobility that is needed to evoke excitation does not differ greatly between all tooth types (Yamada & Kumano, 1969).

There are two types of nerve fibers found in the nervous system: myelinated fibers that are surrounded by a myelin (or fatty) sheath that help to transmit information faster, and unmyelinated fibers that are not surrounded with myelin and thus transmit information at a slower rate. The amount of myelinated vs. nonmyelinated nerve fibers and the size of these fibers varies significantly by species (Brashear, 1936; Byers, 1985; De Lange et al., 1969). The sizing of nerve fibers is typically divided into three categories: 1) small (smaller than 6μ), medium (between 6μ and 10μ), and large (larger than 10μ). Knowing the size of a nerve fiber and if it is myelinated can often inform as to its sensory function. For example, larger and myelinated fibers are often associated with touch, all medium fibers (both myelinated and unmyelinated) are associated with temperature, and small fibers (both myelinated and unmyelinated) are associated with pain (Brashear, 1936; Byers, 1985; Hannam, 1982; Van Steenberghe, 1979; Young, 1977).

The PM is supplied with both unmyelinated and myelinated fibers up to 14μ in diameter and are derived from some apical nerves and many nerves branching from the alveolar bone. The terminal branches are divided into both arborized (spider-like) and close (spiral-like) coils, which are suggested to be pressoreceptors (i.e., pressure receptors) (Bernick, 1952; Brashear, 1936; Byers et al., 1986; Capra & Wax, 1989; Kubota & Osanai, 1977; Kuzentsova & Smirnov, 1969; Linden, 1991; Loewenstein & Rathkamp, 1955; Plaffman, 1939; Trulsson et al., 1992; Yamada & Kumano, 1969). These apical nerve fibers pass vertically towards the gingival margin and are reinforced at intervals by nerve bundles entering the PM through small foramina in the alveolar bone (Bernick, 1952). The nerve fibers on the peripheral portion of the PM have specialized knob-like end organs and the finer nerve fibers that pass to the deeper part of the

PM break up into fine arborizations (spider-like) without terminal organs (Bernick, 1952; Byers, 1977; Griffin & Spain, 1972; Lewinsky & Steward, 1937; Stewart, 1927).

Because primates minimize overall variation in the gape cycle while switching stages (e.g., fast close to slow close, etc.) and maintain a relatively constant cycle duration, they can achieve optimal chewing frequencies based on the size and shape of the masticatory feeding system (Inoue et al., 1989; Ross et al., 2010). Some studies (Capra & Wax, 1989; Harputluoglu, 1990; Inoue et al., 1989; Luschei & Goldberg, 2011; Zeigler et al., 1984) have used numbing, the removal of portions of the PM, and putting pressure on individual teeth to show that if the PM is blocked in some way from sharing information with the CNS, individuals would have trouble keeping the bolus in position in the mouth, would have insufficient occlusion during all stages of the masticatory cycle, they could not chew forcefully or at a steady rate, jaw movements became irregular, teeth failed to erupt and alveolar bone growth was inhibited, or there was an increase in chewing cycles. This research has led to conclusions that the PM is integral to maintaining regular chewing and helps aid in the protection of tooth surfaces.

There has been a noted connection between salivary volume and stress response in that as the pressure on teeth increases, more saliva fills the oral cavity (Anderson et al., 1985; Hector, 1985; Watanabe & Dawes, 1988). Saliva increase can be an indicator as to the pressure capture in the posterior teeth because the output of saliva increases as much as three times with a more resistant diet and the force of biting (Anderson & Hector, 1987; Anderson et al., 1985; Linden, 1991; Lucas, 1979, 2006; Hofmann et al., 2008; Hector, 1985; Watanabe & Dawes, 1988). This masticatory salivary reflex depends entirely on afferent information from intra-oral mechanoreceptors, with particular emphasis on receptors in the PM (Anderson & Hector, 1987; Herring, 1985; Watanabe & Dawes, 1988). Saliva is an important process in food processing as it begins the chemical breakdown of food materials by helping form the bolus. An increase in saliva while consuming tougher or stiffer foods may aid in softening the foodstuff and easing the process of mechanical food breakdown.

The arborized endings in the PM help regulate mastication more than knob-like endings and are what constitutes classifying the PM as a reflexogenic field (Falin, 1958; Seto, 1972). Reflexogenic fields (or zones) are areas of the body where specific stimulations will cause an involuntary reflex. The PM is sensitive to both the beginning and end of pressure applied during a chewing cycle as well as the rate of application of that tension. Reflex inhibition (provided by receptor input from the periodontal ligament) of the masseter and temporalis muscles occurs after tooth contact in normal occlusion, allowing an animal to maintain its teeth from being damaged and help maintain the rhythmic chewing cycle (Anderson et al., 1970; Hannam, 1982; Hannam & Lund, 1981; Van Steenberghe, 1979). Teeth with and without pulp have unchanged sensibilities in response to pressure, giving further evidence to the hypothesis that the PM is responsible for the tactile perception of pressure and may have an important significance in protecting the teeth during normal occlusion (Adler, 1949; Gordon, 1979; Kennett & Linden, 1987; Kubota & Osanai, 1977; Loewenstein & Rathkamp, 1955; Plaffman, 1939). Edentulous patients also show very similar reflex responses to mechanical stimulation (Heasman, 1984; Linden, 1991; Maeda, 1987).

The mandible of humans is suggested to have at least 5,000 PM nervous receptors, with at least 15,513 myelinated nerves in the IAN overall (Edin & Trulsson, 1992; Rood, 1978). By comparison, cats have been shown to have only 6,856 myelinated nerves (Holland, 1978). Baron et al. (1990) investigated the overall volume of the trigeminal complex in Insectivora, Scandentia, and Primates and notes that Insectivora had the highest volume of nervous tissues, Scandentia the second, and Primates had the lowest volumetric measurements. Little else has been published on direct volumetric measurements, but overall conclusions have been drawn that explain differences in volume based on the role of orofacial involvement in exploratory behaviors (Baron et al., 1990).

Tooth Types and Innervation

The basic mammalian tooth consists of a variety of structures that vary across tooth types in size/shape. The four basic tooth types are the incisors, canines, premolars, and molars. The tooth row is typically divided into anterior teeth (the incisors and canines) and the posterior or post-canine teeth (the premolars and molars). Figure 2.2 shows the basic set up of each tooth type with the structures (from superior to inferior) of the enamel surface, dentin layer, pulp cavity, cementum layer, root surface, and the surrounding periodontal membrane.

Although all mammals share the same four basic tooth types, they vary substantially in size and shape in response to diet and environment. One variation that is often studied is whether teeth are of finite growth or continuously growing. Studies have shown that continuously growing anterior teeth do have innervating structures for sensory information in both the tooth crown and periodontal membrane (Kubota & Osanai, 1977; Lewinsky & Steward, 1937; Ness, 1954; Stewart, 1927). Similarly, continuously growing posterior dentition has also been shown to have innervating structures, although there appears to be overall fewer nerve endings than what is seen in finite posterior dentition (Bernick, 1966; Kubota & Osanai, 1977; Lund et al., 1971; Van Steenberghe, 1979; Weijs & De Jong, 1977). In teeth with finite growth, many studies have shown that the anterior dentition have more nerve endings than the posterior dentition, while the periodontal membrane has more innervating structures surrounding the posterior dentition and the apical portion of the tooth root (Byers & Dong, 1989; Cash & Linden, 1980; Kubota & Osanai, 1977; Lewinsky & Steward, 1937; Hassanali, 1997; Maeda, 1987).

It is generally agreed upon (Anderson et al., 1970; Avery & Cox, 1977; Brashear, 1936; Dubner et al., 1978; Luschei & Goldberg, 2011; Plaffman, 1939) that pain is related to the nervous fibers found within the pulp of the teeth. Tooth pulp is supplied with small, myelinated fibers between 2μ and 10μ in size, that vary in their terminations that arise from the IAN and enter the pulp through the root canal (Figure 2.2) (Brashear, 1936; Byers & Dong, 1983; Griffin & Harris, 1968; Linden, 1991; Plaffman, 1939; Seto, 1972). The arborized (bush-like, spider-like)

nerve endings, the most dominant form of endings in the pulp, innervate the dentin and odontoblast layer (a layer of cells between the pulp and dentin that help regenerate dentinal cells over a tooths lifetime) (Figure 2.3) (Avery, 1959; Byers, 1977; Falin, 1958; Frank, 1968; Seto, 1972). These nerve endings are always associated with specific and nonspecific cholinesterase in the odontoblast processes within the odontoblast layer. Cholinesterase is a group of enzymes that break down certain acids in nerve endings that afferent pain information, indicating there is a direct path of pain transmission through the dentin (Anderson et al., 1970; Avery, 1959; Byers & Dong, 1983). Both reparative dentin and radicular dentin are rarely innervated, but both cervical and coronal dentin are extensively innervated and are responsible for most pain sensation (Byers & Dong, 1983).

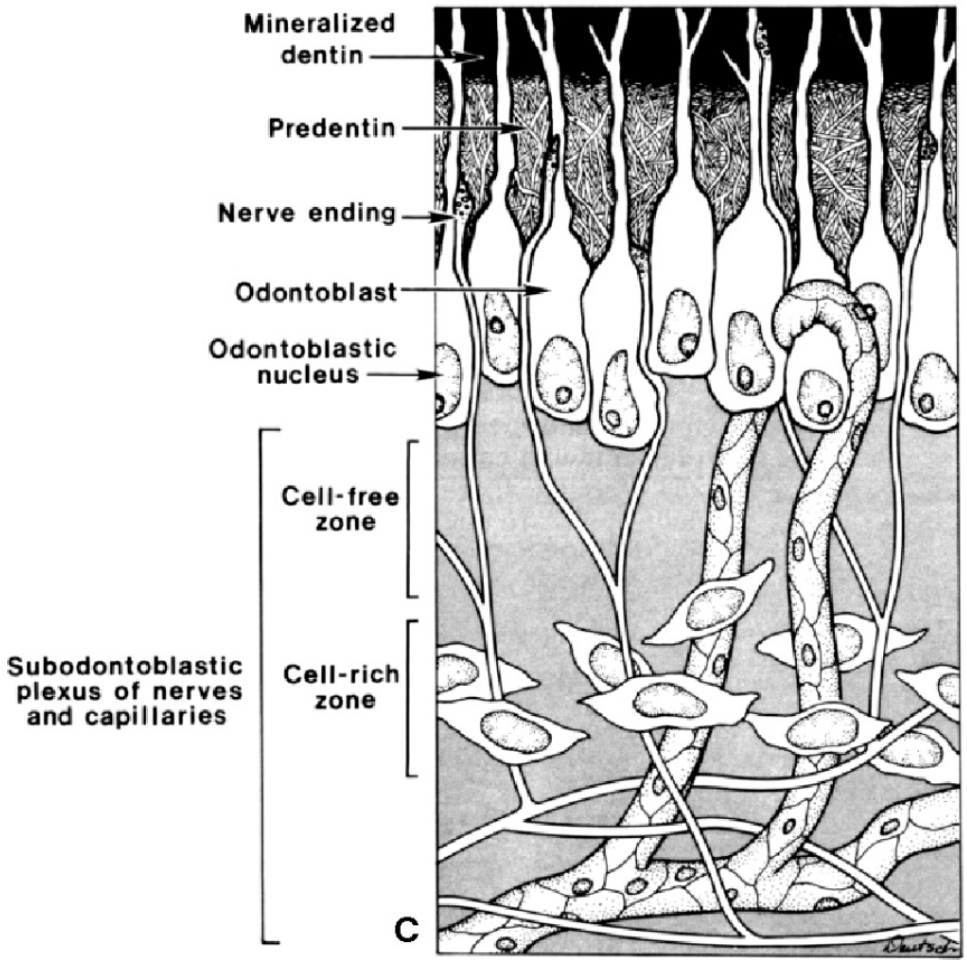

Figure 2.3. Example of the odontoblast layer between the predentin layer and the subodontoblast layer filled with nerve endings and blood vessels. Image from Pashley et al. (2002).

While the information above tells us the specifics of innervation and sensory reception in all oral structures, the most studied trait related to primate diet and mastication is tooth form (Hiiemäe & Kay, 1973; Kay, 1975; Leighton, 1993; Strait, 1997, 2001; Taylor, 2002). Teeth are the direct interface between the food that an animal is consuming and the mechanical breakdown process. In tooth studies, there is a critical assumption made in fracture scaling in that bite force will match tooth size/shape in mammals that have similar dietary patterns (Lucas, 2006; Teaford et al., 2006). In other words, the amount of force necessary to break down food is directly related to the size/shape of the tooth that breaks it down. There is an overall agreement that tooth shape, and more specifically the amount of contact area on the cusps of the teeth,

has undergone strong selection tied to improving mechanical efficiency for chewing different kinds of foods (Kay, 1975; Lund et al., 1998). Contact areas on teeth are typically related to the diet a specific species is adapted to, with two general tooth shapes: blades vs. mortar and pestle (Lucas & Luke, 1980; Lucas, 2006; Strait, 1997). Blade-like teeth have high peaks and deep crevices (i.e., have higher shearing quotients) to retain the food within the crevices so that when the upper and lower teeth meet, the food is trapped in place for multiple fractures (Lucas, 1979, 2006; Lucas & Luke, 1980; Lumsden & Osborn, 1977; Strait, 1997). Mortar and pestle-like teeth have less relief to the tooth crown and large contact areas on the cusps during occlusion, which are more useful with food that is not tough (Kay, 1973, 1975; Rosenberger & Kinzey, 1976).

The anterior teeth are most involved in the acquisition and manipulation of food (incision) as it enters the mouth, while the posterior teeth are most involved in the processing (mastication) of food and the formation of a bolus. Anterior tooth size, and particularly the incisors, have been shown to reflect the degree of incision during ingestion (Highlander, 1975a, 2006; Lucas, 2006; Murphy, 1968; Ungar, 1998, 2002). Anterior teeth, like all teeth in the mouth, are supplied with nervous structures via the IAN to the pulp of the tooth and the surrounding PM. Because food encounters the anterior teeth before any other portions of the mouth, it has been assumed that they are important in the process of acquiring foods and understanding the initial characteristics of food (Trulsson, 2006; Trulsson & Johansson, 1996). Some research has shown that the anterior teeth are particularly relevant for adjusting contact force and for providing information on the direction of stimulation when food is processed at the front of the mouth (Trulsson, 2006; Trulsson & Johansson, 1996).

The post-canine teeth are of particular interest in anthropological studies because they are used for mastication rather than incision. These teeth are often larger and are responsible for eliciting the feedback mechanism via nervous stimulation required for tooth protection. Larger teeth, such as the molars, also provide more attachment sites for the periodontal

ligament via the tooth root. Lucas (2012) explains that more attachment sites allow these teeth to resist masticatory stress more efficiently compared to teeth with less root surface area, indicating they will be more informative than other tooth types for mastication. For most mammals, molar surface areas scale at 0.75 power of body mass, a direct correlation between metabolism and body mass (Kleiber, 1961). Studies show that molar size varies isometrically within dietary categories, but is positively allometric across them (Kay, 1975; Ungar, 1998, 2002). This is likely because larger primates eat less nutrient and energy dense foods, while smaller animals eat foods with higher energy and protein content (Ungar, 2002). Larger primates that need to eat more food (due to their diets consisting of low energy foods) will have larger molar surface areas to process larger quantities. Thus, the molars are particularly useful when estimating the diet of species, particularly across primates.

While much research has focused on tooth size and shape, enamel surface area and complexity, and other soft tissues of the mouth, very few studies have examined the relationship between tooth root size and the enamel surface. Spencer and others (Deines et al., 1993; Lucas, 2012; Spencer, 2003) have shown that tooth root surface area is larger in teeth that are more heavily loaded during mastication, whether by more chewing cycles or tougher diets. This hypothesis would also explain the tendency of the first mandibular molar to be the largest, as the maximum bite force decreases from the first to third molar (Spencer, 2003). By calculating tooth root size and scaling it against crown area for the posterior teeth, Spencer et al. (2003) was able to show significant differences in maxillary tooth root area in *Cebus albifrons* (untufted) and *Cebus apella* (tufted) who have been documented to eat a variety of foods with different mechanical properties in similar environments. This work hypothesized that the reason for this may be related to the need to distribute occlusal forces across the tooth row when high loads are applied to the teeth. However, no studies to date have examined the link between the size of the tooth crown and roots and the nervous structures that innervate them.

Canals and Foramina

Bony canals and foramina have been shown to develop around neurovascular pathways and thus are often studied to determine how structures are innervated rather than the actual nervous structures themselves (Albrecht, 1967; Aldridge et al., 2005; Benoit et al., 2018; Chávez-Lomeli et al., 1996; Greer et al., 2017; Jamniczky & Russell, 2004). However, little research has been done to establish if a bony structure like a canal can be used to accurately represent the size and shape of the soft tissues that run through it. Often, this research is done only on human cadavers, an arguably poor species representation of primates as a whole. Some canals in humans, like the hypoglossal, do not accurately represent the size and shape of the nerve that runs through them (Mackinnon & Dellon, 1995). Others have shown that nerves such as the optic and infraorbital nerve do accurately represent the size and shape of the corresponding canals (Jamniczky & Russell, 2004; Jonas et al., 1992). It is essential to establish if the mandibular canal can be used as a proxy for the mandibular nerve because the mandibular canal is highly variable in size and shape but is often cited as a single bony canal that contains the IAN and the inferior alveolar artery (IAA) (Anderson et al., 1991; Angelopoulos, 1966; Barclay, 1971; Blackmore & Jennett, 2001; Booth et al., 2013, Wyman & Stoia, 2013; Edwards & Gaughran, 1971; Gershenson et al., 1986; Mardinger et al., 2000; Morris & Jackson, 1933; Murphy & Grundy, 1969; Olivier, 1927, 1928; Starkie & Stewart, 1931; Sutton, 1974; Wadu et al., 1997). Without confirmation that the IAN and canal are not significantly different in size and pathway, studying the bony structures to assess the soft tissues is impossible. Due to the close relationship the IAN has for protection of the teeth during mastication, being able to study the hard-tissue component when the nerve is not present is vital for understanding the evolution of the masticatory system.

Research on the mandibular canal, the mental foramen, and the mandibular foramen and its variation was introduced by Olivier (1927) and Cryer (1901) who argued that the canal is not necessarily a continuous, bony tunnel but could be better described as a cribriform tube.

Using 50 human mandibles, Olivier (1928) established that the mandibular foramen is a slit rather than an oval, and contrary to published literature, is not placed at an equal distance from the base of the sigmoid notch and the lower border of the mandible (Anderson et al., 1991). Often the posterior portion of the canal is clearly defined, forming a tunnel with thick walls, with the nerve forming a round cord that conforms to the canal (Gowgiel, 1992; Olivier, 1928; Starkie & Stewart, 1931). Others argue that the tubular nature of the canal is lost at the molars, suggesting a widening of the IAN (Wadu et al., 1997). However, in all cases, moving from posterior to anterior in the canal the walls become progressively thinner with few instances of clear divisions of the mental and incisive nerve at the anterior portion of the mandibular body (Cryer, 1901; Gowgiel, 1992; Mardinger et al., 2000; Olivier, 1928; Starkie & Stewart, 1931; Wadu et al., 1997).

In humans, small lateral tubes join each tooth root to the main canal, which pass upward and forward in a curved direction depending on the position of the teeth (Figure 2.1) (Anderson et al., 1991; Polland et al., 2001; Sutton, 1974; Wadu et al., 1997). While, the third molar tube is nearly vertical, the second pre-molar has the longest curve and tube of all, and often the tube passing to the second pre-molar is found as an offshoot of that going to the anterior root of the first molar (Anderson et al., 1991; Cryer, 1901; Littner et al., 1986; Polland et al., 2001; Wadu et al., 1997). The largest (in diameter) of these tubes connect the nerve to the lower second premolar and the lower first molar, suggesting more nervous sensory tissues located in and around these teeth (Erisen et al., 1989; Kress et al., 2004). Often, the roots of the third molar extend around and into the mandibular canal, causing damage if the tooth is removed without care (Kress et al., 2004; Miles & West, 1954; Stockdale, 1959). Where the two nerves of the corresponding sides of the mandible meet at the mandibular symphysis, they turn sharply superiorly, so that the two nerves run parallel to each other to innervate the central incisors (Starkie & Stewart, 1931). Studies show very low degrees of asymmetry in mandibular canals except in cases of pathological processes (Littner et al., 1986; Matsuda, 1929; Nortje et al.,

1977). Other work suggests that sexual dimorphism does not play a significant role in mandibular canal configuration or asymmetry (Anderson et al., 1991; Nortje et al., 1977).

The mandibular canal is comprised of two openings: the anterior mental foramen and posterior mandibular foramen. While little research has been done to assess variation in the mandibular foramen, an extensive body of research exists on the size, shape, and number of the mental foramen. Many studies have attempted to show uniformity in the mental foramen placement, but this varies extensively across humans (Barclay, 1971; Gershenson et al., 1986; Matsuda, 1929; Olivier, 1928). Many studies have shown that a large variety of factors can change the size, placement, and presence of the mental foramen: growth and development in children (Anderson et al., 1991, Salah El-Beheri, 1985; Williams & Krovitz, 2004), the presence of accessory mental foramina (AMF) (Agthong et al., 2005; Apinhasmit et al., 2006; Budhiraja et al., 2013; Gershenson et al., 1986; Gupta & Soni, 2012; Göregen et al., 2013; Hanihara & Ishida, 2001; Imada et al., 2012; Iwanaga et al., 2015; Kalender et al., 2012; Katakami et al., 2008; Kieser et al., 2002; Liang et al., 2009a; Matsuda, 1929; Montagu, 1954; Mwaniki & Hassanali, 1992; Naitoh et al., 2009a; Naitoh et al., 2009b; Naitoh et al., 2010; Naitoh et al., 2011; Oliveira-Santos et al., 2011; Orhan et al., 2013; Paraskevas et al., 2015; Prabodha & Nanayakkara, 2006; Riesenfeld, 1956; Robinson & Yoakum, 2019; Sawyer et al., 1998; Senyurek, 1946; Simonton, 1923; Udhaya et al., 2013), differences in feeding behaviors and side preferences during mastication (Agarwal & Gupta, 2011; Amorim et al., 2008; Voljevica et al., 2015; Yesilyurt et al., 2008), diet (Moore et al., 1968), and the resorption of bone during tooth loss (Charalampakis et al., 2017; Gabriel, 1958; Gershenson et al., 1986; Heasmen, 1984; Iwanaga et al., 2019; Wadu et al., 1997; Xie et al., 1997).

At present, one study addresses if the size of the mental foramen can be used as a proxy for touch sensitivity and would thus be correlated to diet (Muchlinski & Deane, 2016). Muchlinski and Deane (2016) base their assessment on the assumption that the size of the mental nerve is equal to the size of the mental foramen, without providing gross dissection

evidence for this assumption other than its apparent similarities to the infraorbital foramen (IOF) and nerve (ION). Muchlinski and Deane (2016) conclude that there is no correlation between diet and size of the mental foramen in groups of strepsirrhine primate frugivores and folivores. Further, Muchlinski and Deane (2016) argue that these results are likely because primates in all dietary categories use the upper lip and nose (as opposed to the lower lip and chin) far more often in food handling and acquisition. However, no study has adequately shown that the size of the IAN/mental nerve are accurately represented in the bony architecture that surrounds them. This is in opposition to studies showing that the infraorbital nerve (ION, the maxillary correlate to the mental nerve) positively correlates with the size of the infraorbital foramen (IOF) and can accurately predict the dietary patterns in major groups across primates (Muchlinski, 2008; Spriggs et al., 2016).

Blood Supply to the Inferior Alveolar Nerve and Connected Tooth Structures

Because the cardiovascular and neuronal systems are the first to develop, blood vessels and nerve bundles are often arranged in parallel patterns, allowing them to be both functionally and physically interdependent (Shadad et al., 2019). The sympathetic peripheral sensory nerves that supply teeth are crucial for mediating sensory function, blood vessel growth, oxygen and nutrient supply, and the disposal of waste products (Shadad et al., 2019). These dental sensory nerves follow a strict, developmentally regulated pattern of growth, navigation, and patterning that is directly linked to crown morphogenesis and cell differentiation in the tooth structures (Shadad et al., 2019). The tooth vascular supply formation precedes tooth innervation, and there is evidence that the navigation and patterning of the dental sensory neuronal process (a projection from the cell body, Figure 2.4) is at least partly influenced by the path of blood vessels (Shadad et al., 2019). However, later in development there is some evidence that neural processes can appear where there are no blood vessels present, although most neuronal processes appear where vascularization has been previously established. Therefore, it has

been suggested that while the initial neuronal supply to the teeth is dependent on blood supply, the development of neurons can also be viewed as a separate and independent process.

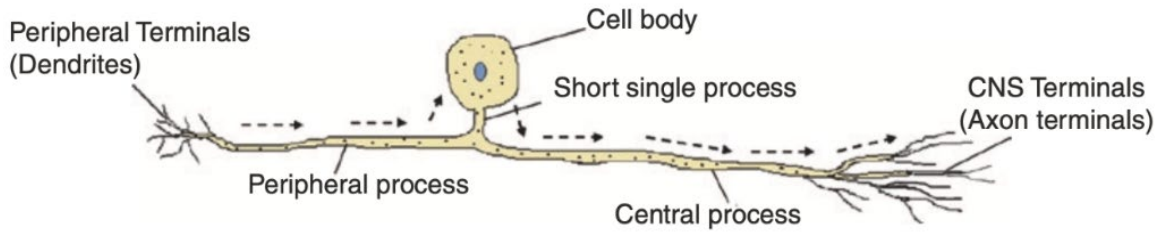

Figure 2.4. Example of a pseudo-unipolar neuron. Image from Singh (2019).

While the development of blood supply and neurons in the alveolar region is well established, the adult blood supply to the IAN is contested in the medical literature. Most often, the contents of the mandibular canal are described as only the IAN and inferior alveolar artery (IAA) (Blackmore & Jennett, 2001; Booth et al., 2013; Edwards & Gaughran, 1971; Morris & Jackson, 1933). However, the dental literature often teaches students that the canal contains a true neurovascular bundle of a nerve, artery, and vein (Anderson et al., 1991; Frank, 1966; Gowgiel, 1992; Lindh et al., 1995; Littner et al., 1986; Rosenquist, 1996). It is often cited that this neurovascular bundle is positioned 4 to 6 mm lingual to the external buccal surface of the mandible to help dentists establish where to insert certain medications, however this is highly contested because of the known variation observed in the mandibular canal (Anderson et al., 1991; Frank, 1966, 1968; Gowgiel, 1992; Lindh et al., 1995; Littner et al., 1986; Rosenquist, 1996). Some texts (Murphy & Grundy, 1969; Wadu et al., 1997) assert that the vein provides protection to both the blood supply and the nervous tissue along the inferior aspect of the canal (Murphy & Grundy, 1969; Wadu et al., 1997). Further, many publications argue that if the IAA is even present, it quickly anastomoses throughout the trabecular bone of the mandible and does not follow the full course of the canal to the mental foramen (Anderson et al., 1991; Lindh et al., 1995; Wadu et al. 1997; Booth et al., 2013).

In short, the blood supply to the IAN is incredibly variable with few publications agreeing on its exact course, location, or existence. The external carotid artery ultimately supplies the IAN with blood through various channels including the facial artery (via the submental branch) to the superficial masseter and mylohyoid muscles, which then supply the sub-lingual branch, the inferior labial artery, and finally the mental branch of the inferior alveolar artery (Edwards & Gaughran, 1971). This has been studied extensively in elderly patients, particularly those with edentulous mandibles, because of the effect the absence of teeth can have on the alveolar bone. It has been established that age may play a factor in the blood supply of the IAN with elderly patients showing either a completely absent or partially absent IAA (Bradley, 1975; Polland et al., 2001). This is in opposition to the superior alveolar artery (SAA) which follows the full course of the superior alveolar nerves that shows no degeneration by age (Bradley, 1975; Polland et al., 2001). Most texts agree that the mandibular canal contains both the IAN and the IAA, but rarely contain a vein in the bundle. One goal of this study is to establish whether the nerve occupies most of the canal but will not focus explicitly on attempting to determine if a true neurovascular bundle is present.

Cellular Structures

There are no firm conclusions as to what portion of the brain has the greatest effect on masticatory movements, but it is well established that a highly complex neural network is necessary to coordinate both sets of jaw muscles to successfully masticate food. However, the motor pathway for the muscles of mastication is generally agreed upon as follows: motor commands are produced by the central pattern generator of the brainstem using sensory information from periodontal mechanoreceptors and proprioceptors in the jaw-closing muscles (Inoue, 2015; Lund & Kolta, 2006; Luschei & Goldberg, 2011; Morquette et al., 2012; Sessle et al., 2005; Singh 2019). In humans, the repetitive muscle movements in mastication are generated by motor nuclei in the brainstem (of both the facial and trigeminal nerves) but is also consciously controlled through sensory feedback (Lund & Kolta, 2006).

The trigeminal nerve has a bimodal distribution of cell size and motor axons, indicating that it contains both γ-motoneurons (gamma or fusimotor motor neurons) and α-motoneurons (alpha motor) (Appentag et al., 1980; Luschei & Goldberg, 2011; Westberg et al., 1998). Both motor neurons work together in a system to keep muscles taught and cause continuous contraction during use. Recent studies have argued that the trigeminal motor nucleus within the brain contains a third group of motoneurons referred to as primary interneurons that are both electrophysiologically distinct and different in size and shape from recognized motoneurons (Bourque & Kolta, 2001; McDavid et al., 2008; Westberg et al., 1998). These interneurons, if correctly identified, would have a crucial role in the jaw-closing muscles utilized in bite force in primate species (Bourque & Kolta, 2001). Their role in causing a reflex reaction in the mandible during chewing is also largely unexplored.

All nerves in the body have a constant feedback mechanism between the peripheral and central nervous systems. In the case of the oral cavity, each subsequent chew is programmed by the one that came before it, indicating that the sensory feedback mechanism of mammals is crucial to survival via exact chewing cycles. Lund (1991) explains that while basic mastication could be programmed by the brain stem, the result would be overall highly inefficient because the sensory feedback provided by intraoral, joint, and muscle receptors interact with the nervous system at several levels based on the characteristics of food (Lucas, 2006; Luschei & Goldberg, 2011; Morquette et al., 2012). These properties include hardness, elasticity, toughness, and other describable qualities that all show different activity levels during electromyographic studies (EMG), influencing the gape attained by the masticatory muscles and the chewing rate (Inoue et al., 1989; Lund & Kolta, 2006; Lund et al., 1998; Vinyard, 2008). When objects are placed between the molar teeth during normal masticatory cycles, there is a noted area of EMG bursts in the jaw-closing muscles that is proportional to the hardness of the object (Lavigne et al., 1987; Lund & Kolta, 2006).

Many studies have also noted the presence of an unloading reflex after a sudden closing movement of the jaw-closing muscles (Matthews, 1976). This is referred to as a feed-forward mechanism, suggesting that jaw-closing activity is preprogrammed using previous sensory information from earlier masticatory events or from the first closing activity of a chewing cycle (Komuro et al., 2001). This sudden jaw-closing, or more accurately described as jaw-stopping, reflex protects the teeth by preventing the subsequent chewing cycle to commence.

Sensory and Motor Nuclei

The central nuclei (i.e., nuclei within the central nervous system) for CNV can be functionally broken down into three sensory nuclei and one motor nucleus: 1) the mesencephalic nucleus (MesV) in the midbrain, 2) the principal (or main, or chief) sensory nucleus in the upper part of the pons, 3) the spinal nucleus in the lower part of the pons, medulla, and upper two cervical segments of the spinal cord, 4) and the motor nucleus in the dorsal portion of the pons, just medial to the principal sensory nucleus (Figure 2.5). The mesencephalic nucleus receives proprioceptive impulses from the muscles of mastication, temporomandibular joint, extraocular muscles, and sensory information from the teeth (Dubner et al., 1978; Luschei & Goldberg, 2011). The principal nucleus receives most of the touch or pressure sensation for CNV. The spinal nucleus can be further subdivided into three sub-nuclei (pars oralis, pars interpolaris, and pars caudalis) and is responsible for most of the pain and temperature sensations from the skin of the head and face, mucous membranes of the oral cavity, nasal cavity, paranasal sinuses, and meninges via sensory root fibers (Singh, 2019). Lastly, the motor nucleus supplies all the derivatives of the first pharyngeal arch, which includes all the muscles of mastication, the mylohyoid, the anterior belly of digastric, the tensor veli palatini, and the tensor tympani motor root fibers (Singh, 2019). Because the human body is organized into a series of repetitive bands or segments, the sensory and motor roots of CNV are analogous to the dorsal (sensory) and ventral (motor) roots of the spinal nerves (Martínez-Marcos & Sañudo, 2019; Singh, 2019).

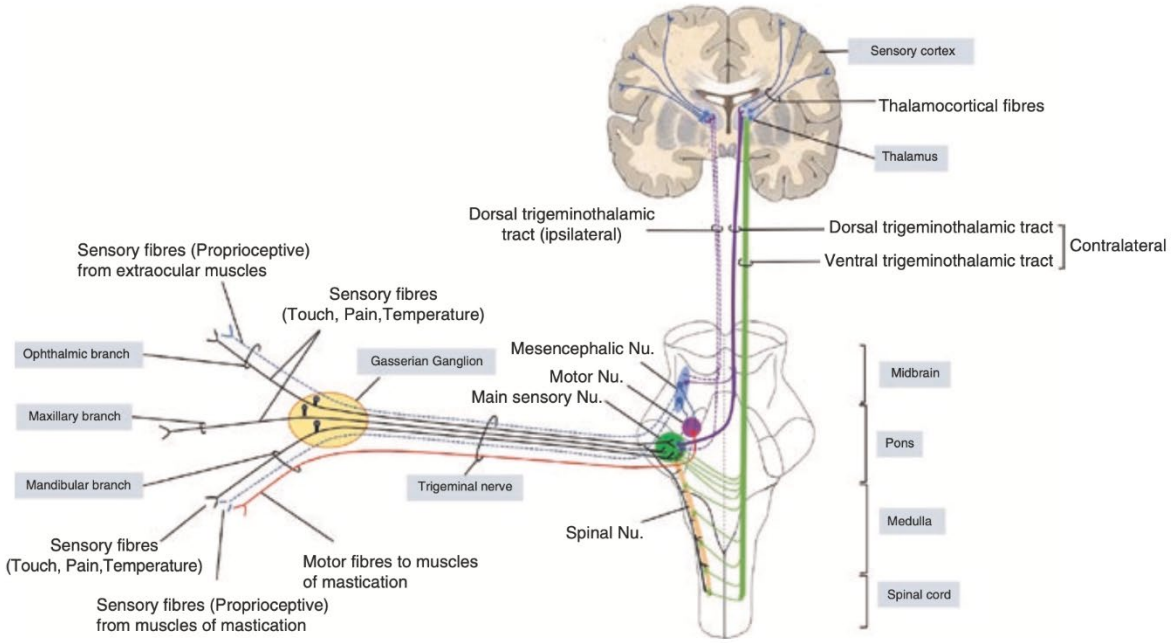

Figure 2.5. The origin and course of the trigeminal nerve and its connections to each nucleus and ganglia. Image from Singh (2019).

The MesV serves both a proprioceptive and mechanoreceptive function for mastication. Mechanoreceptive neurons supply mechanical pressure or distortion information from the teeth and have cell bodies located in the MesV (Capra & Dessem, 1992; Cody et al., 1974; Goldberg, 1971; Jerge, 1963; Luo & Dessem, 1996; Passatore et al., 1983; Van Steenberghe, 1979). It has been suggested that anterior teeth with more connections to the MesV may give greater sensory perception whereas molar afferent connections initiate complex jaw reflexes during the occlusal phase of mastication (Goldberg, 1971; Hassanali, 1997; Shigenaga et al., 1988; Van Steenberghe, 1979). However, the locations of specific neuronal receptors in parts of the ganglion and MesV has largely focused on mammals other than primates.

Additionally, the muscle spindle fibers (proprioception) relaying information to the MesV are a neuroanatomically unique structure (Anderson et al., 1970; Beaudreau & Jerge, 1968; Byers & Dong, 1989; Carpenter, 1957; Chiego et al., 1980; Hannam, 1976, 1982; Jerge, 1965; Luschei & Goldberg, 2011). Because these neurons are pseudo-unipolar (meaning a neuron

with a single process that branches into a peripheral and central process) (Figure 2.4) and first order (meaning the first neuron in a chain), they supply a direct connection from the muscles of mastication to the brain itself (rather than a series of synapses from the PNS to the CNS). This direct connection from the periphery to the brain has not been found in any other mammalian structure to date, indicating that the mammalian jaw closing reflex is integral to survival as it allows all mammals to quickly stop chewing when a foreign object is placed between the occluding surfaces (Baker & Llinás, 1971).

The Trigeminal Ganglion

All oral structures have neurons that afferent to the brainstem via the trigeminal ganglion (previously referred to as the Gasserian ganglion), the primary sensory ganglion of the trigeminal system (Beaudreau & Jerge, 1968). The trigeminal ganglion is the largest sensory ganglion in mammals and the only sensory ganglion that lies inside of the cranial cavity (Singh, 2019). The pseudo-unipolar neurons with cell bodies in the trigeminal ganglion have peripheral processes supplying information from the three main branches (V_1, V_2, and V_3) and have the central process passing into the sensory root of the overall trigeminal nerve (Singh, 2019). These first order neurons terminate in both the principal and spinal nuclei to carry touch, pain, and temperature sensations (Byers, 1985; Byers & Dong, 1989; Maeda, 1987; Singh, 2019; Van Steenberghe, 1979). Alternatively, the pseudo-unipolar neurons (and first order neurons) that carry proprioceptive impulses have cell bodies located in the mesencephalic nucleus rather than the trigeminal ganglion. The peripheral processes of these neurons receive proprioceptive information from the muscles of mastication and the teeth during occlusion while the central processes travel to the motor nucleus or synapse with second order neurons in the MesV (Beetson et al., 1974; Byers, 1985; Byers & Dong, 1989; Corbin, 1940; Dong et al., 1985; Inagaki et al., 1987; Jerge, 1963; Luschei & Goldberg, 2011; Shigenaga et al., 1988; Van Steenberghe, 1979).

All first order neurons (with cell bodies in either the trigeminal ganglion or MesV) synapse with second order neurons in the three sensory nuclei (MesV, principal sensory, or spinal nucleus) (Singh, 2019). The axons of these second order neurons cross to the opposite side and ascend into the ventral and dorsal trigeminothalamic tract (VGT and DGT, respectively) to relay information into the ventral postero-medial (VPM) nucleus of the thalamus (Singh, 2019). The VGT receives crossed fibers from the contralateral principal sensory and spinal nuclei to carry sensations for crude touch, pain, and temperature (Singh, 2019). The DGT receives both crossed fibers from the contralateral principal sensory nucleus and some uncrossed fibers from the ipsilateral principal sensory nucleus to carry fine touch and proprioceptive movements (Singh, 2019). All second order neurons then synapse with neurons in the thalamus (third order neurons), to project on to the sensory cerebral cortex posterior to the central sulcus.

In all, much is known about the cellular structure of the trigeminal nerve, but little has been done to compare these structures across species or relate it to dietary adaptations. The main function of the third branch of the trigeminal nerve is to supply both sensory and motor information to the oral cavity, two crucial functions for food consumption. When nervous tissues are mapped, it is usually tedious, in very few subjects, and in a select number of species. The bigger picture of overall nervous tissue volume and its relationship to the bony structures that surround it has rarely been questioned and thus a large gap in our knowledge of masticatory control exists.

FOOD MATERIAL PROPERTIES

All of mastication and the responses mouth movements evoke during feeding are in part controlled by the material properties of food. As diet has been studied extensively throughout many fields for hundreds of years, it has been described in a variety of ways across all primates. The largest problem in the assessment of diet in relation to the masticatory system is the

general lack of standardization as to the categories of food types in analyses. There is also a tendency to use terms such as “rough,” “harsh,” and “tough,” with little consistency in the definition (Lucas, 1994). Some authors have attempted to right this confusion by creating general definitions for others to follow, but no standard set of terms has ever been defined and truly accepted in the anthropological literature. There is also a general argument against assigning a dietary category to a given species, especially with primates who have incredibly diverse diets and do not usually consume a single group of food stuff (Boonratana, 2003; Kay, 1975). However, it is generally accepted that leaf eaters and insect eaters do not overlap in body size and that the total amount of food preparation (shearing, crushing, and grinding) is greater among primates that eat either leaves or insects in comparison to primates that primarily consume fruit (Kay, 1975).

Evaluations of food material properties in relation to primate diets are typically focused in two areas: (1) fracture toughness (*R*), an object’s ability to resist fracturing and, (2) stiffness (elastic modulus, *E*), an object’s ability to resist deformation (Kay, 1975; Lee et al., 2011; Lucas et al., 1995; Lucas, 2006; Taylor et al., 2008; Williams et al., 2005). These properties determine how food objects are fractured during the slow close phase of mastication and provide feedback to jaw-closing muscles so that the initial chew and all subsequent chews can adapt according to the specific material properties of that food item (Agrawal et al., 1997; Agrawal, et al., 1998; Taylor et al., 2008). EMG research has shown that the amount of jaw-muscle activity required during food processing is directly related to and controlled by the material properties of that food, with tougher foods requiring longer periods of chewing, without necessarily increasing the bite force (Agrawal et al., 1998; Hylander, 1979; Taylor et al., 2008; Vinyard et al., 2011; Vinyard et al., 2008). Fragmentation of food on a given occlusal surface is heavily influenced by a food’s toughness but can also be affected by a combination of toughness and stiffness (Williams et al., 2005). Primate food sources are generally evaluated by toughness, with the toughest being bark and pith, seeds, and leaves, while fruit flesh is generally categorized as

being the least tough (Taylor et al., 2008; Vinyard, 2008; Vinyard et al., 2011). Stiff foods are also assessed on a spectrum, with seeds and (some) insects categorized as the stiffest and fruit categorized as the least stiff. Those foods that fall into the non-fruit, non-leaf vegetation category such as prune pits and seed kernels have the maximum in fracture toughness and stiffness and are most likely critical determinants in the attributes selected for in tooth morphology for processing fallback foods (Williams et al., 2005).

"Soft" diets have been shown to impede mandibular and craniofacial growth, but also may affect the sensory feedback mechanism of the periodontal membrane (Beyron, 1964; Fujishita et al., 2015; Ito et al., 1988; Kiliaridis et al., 1985; Maeda, 1987; Watt & Williams, 1951). Mice fed soft diets throughout life have difficulty controlling masticatory force in response to hard-diet change, have inconsistent chewing patterns, and increase their number of chewing cycles (Fujishita et al., 2015; Luschei & Goldberg, 2011; Thexton & Hiiemae, 1997). However, mice that were fed more resistant (i.e., tougher and/or stiffer) diets from birth were better able to control the masticatory force necessary when later fed a soft diet and were better able to modify their chewing pattern based on the properties of the bolus (Fujishita et al., 2015; Watt & Williams, 1951). Chewing more and chewing tougher materials lead to a better development of the supporting bone, and a lack of chewing can lead to a replacement of fatty marrow where bone should have been formed (Watt & Williams, 1951). This research suggests that the weaning period of mammals is critical for establishing proper masticatory habits and for honing the sensory feedback mechanism necessary to properly chew foods with different properties. For example, the modern human mandible is heavily affected by masticatory movements during the early period of growth, particularly before the age of four. Without loading forces on the temporalis bone at the anterior region of the condyle, an eminence will fail to form (Nickel et al., 1997). Early actions such as suckling, teething during eruption of the incisor teeth, and incisor gnawing are all thought to be practices that naturally cause anterior loading of the condyle (Nickel et al., 1997). As weaning begins, noted changes occur in both motor and sensory

neurons within the trigeminal complex, causing an emergence in rhythmical jaw movements and trigeminal motor activity (Beecher & Coruccini, 1981; Fujishita et al., 2015; Hannam & Lund, 1981; Herring, 1985; Nickel et al., 1997; Turman, 2007). While most research in this area has been done on humans, we can extend this knowledge to other primates.

There is a suggestion that primates eating tough/stiff foods need to prioritize masticatory strength to generate larger bite force and higher load-resistance abilities, but this is contested (Teaford & Oyen, 1989; Vinyard et al., 2011). Tougher/stiffer food elicits greater EMG activity in the chewing side muscles than in the non-chewing side, and usually results in more time spent chewing (Teaford & Oyen, 1989). Because these differences are greatest at the beginning of the chewing sequence, many authors suggest that primates eating a tough/stiff diet obtain all information on the food properties in the first cycle, enabling them to make the best decision as to how to proceed with mastication (Peyron et al., 2002). However, instantaneous changes can occur in the chewing cycle if the food is not homogenous (Hiiemae et al., 1996). Relatively high occlusal pressure also supports a diet of tough materials, such as leaves or seed dispersers (Rosenberger & Kinzey, 1976). This research on both soft and tough/stiff diets implies that consuming tougher/stiffer foods is important at a young age for not only growth and development of the mandible but also for conditioning our brain to elicit proper chewing cycles.

Within the chewing cycle and because of food material properties, teeth do not necessarily come into exact occlusion with each chew. For tough/stiff foods, a primate may first use puncture crushing to break down the food before full occlusion occurs (Osburn & Lumsden, 1978). Chewing with the post-canine teeth is the second phase where teeth come into occlusion and get progressively closer throughout the cycle (Lucas, 1979). The teeth most likely to lock into occlusion are the first molars and the canines, thus giving the first molars a crucial role in food breakdown and an important component in the assessment of tooth wear (Luke & Lucas, 1983; Murphy, 1968). However, other studies show that food processing of tough/stiff objects

can occur mostly in the canine/pre-molar region, indicating that food processing is a complicated process that can be broken down into a multitude of variables (Strait et al., 2009).

Assessing Primate Diet in the Literature

Primate diets are often divided into two main groups: 1) non-resistant foods that consist mainly of fruit, and 2) resistant foods that consist of leaves, seeds, or insects (Kinzey & Norconk, 1993; Lucas & Corlett, 1991). Frugivores use sensory inputs that are outside of the oral cavity, such as sight and digit sensation when they choose fruit. Color, accessibility, weight, palatability, nutrient content, competition with other animals, morphology, pulp richness, seasonality, and seed size are all factors that have been shown to affect primate fruit choice (Gautier-Hion et al., 1985; Julliot, 1996; Strait & Overdorff, 1996). In contrast, leaf and insect eaters, rather than using external senses, often require the food to be placed into the oral cavity to help determine the toughness of a leaf or the stiffness of the insect exoskeleton (Kay, 1975; Muchlinski & Deane, 2014; Peyron et al., 2002; Scott et al., 2018; Teaford & Oyen, 1989; Vinyard, 2008; Vinyard et al., 2011). Prinz and Lucas (2000) suggest that this precise evaluation of food material properties is used in primates for the detection of tannins, as dietary tannins cause friction and may contribute significantly to increased wear rates of the premolars and molars. While tannins are often cited as a selector in foliage choice, others argue that leaf toughness and high fiber content have a more consistent negative effect on selection (Davies et al., 1988; Ganzhorn et al., 2017; Kar-Gupta & Kumar, 1994; Prinz & Lucas, 2000). Although fiber is tasteless and odorless, the amount of fiber can be estimated from the toughness of a leaf upon ingestion. Knowing the fiber content of a leaf is crucial for all primates because plant fiber is insoluble in water, and thus adds bulk to the stomach contents and stool without providing added nutrients (Ganzhorn et al., 2017; Lucas et al., 2012).

Leaves have the most nutrition before they are mature and are much harder to eat, requiring folivores to assess the toughness of the leaf in the mouth (Kar-Gupta & Kumar, 1994; Lucas, 1994; Lucas et al., 1995). Protein levels in leaves have also been shown to be

significantly correlated with a positive effect on leaf selection, leading many to believe that toughness can be correlated to protein levels (Davies et al., 1988; Ganzhorn et al., 2017; Kar-Gupta & Kumar, 1994). Mature leaves show average shear lengths that are six times greater than immature leaves, with leaf thickness contributing significantly to overall shear strength (Hill & Lucas, 1996; Lucas, 2006; Luke & Lucas, 1983; McNamara, 1974; Strait, 1997; Teaford et al., 2006; Yamashita, 1992). This is further supported by the much more uniform teeth of folivores in their morphology with small incisors, large post-canine teeth with more surface area, rigid molars to break down the leaves, and a positive correlation between number of leaves consumed regularly and the length of ridges on the second molar (Lucas, 1994; Strait, 2001; Yamashita, 1996).

In sum, while diet is not the only factor that affects the masticatory complex, it is a crucial component to its growth and overall maintenance during life. The feedback mechanism controlled by the nervous tissues is critical for protecting the teeth while any object is placed into the mouth. The different properties of food will affect this mechanism to varying degrees during individual chewing cycles and over the lifetime of an individual.

FORAGING EFFICIENCY

Although previous research has suggested that tooth morphology is directly related to what a primate predominantly eats, recent studies have suggested that tooth morphology could also be related to what a primate eats in times of resource scarcity (Constantino, 2009; Lambert et al. 2004; Marshall & Wrangham, 2007; Norconk et al., 2009; Rosenberger & Kinzey, 1976). There are two dominant (and somewhat related) theories that describe these resources: critical function foods and fallback foods. Critical function foods require a specific adaptation to consume whereas fallback foods are foods that act as fillers in a diet when a preferred food source is not available. Therefore, some fallback foods might be critical function foods, but this is not always the case. For example, while mountain gorillas consume leaves as a predominant

food source throughout the year and have tooth morphology that reflects this dietary pattern, their preferred food source are soft, pulpy fruits. For many species, it is possible to never observe the consumption of a critical function food or fallback food in long-term or short-term field studies because the animal may not be stressed sufficiently in terms of food shortages. Critical function heavily relies on understanding food material properties rather than using the standard categories of frugivore, folivore, insectivore, etc. The argument is that the material properties of food are the selective pressure driving adaptive changes to the masticatory apparatus, and particularly the teeth, with a critical function of being able to process a specific material property that is crucial for survival (Rosenberger & Kinzey, 1976; Kinzey & Norconk, 1993; Lucas et al., 2001; Marshall & Wrangham, 2007; Taylor et al., 2009).

Studies have shown a significant correlation between leaf toughness and foraging efficiency in primates, indicating that leaf toughness negatively correlates with ingestion rate and positively correlates with masticatory investment (Boonratana, 2003; Davies et al., 1988; Dunham & Lambert, 2016; Hylander, 1975a; Lucas, 1994; Lucas & Teaford, 1994; Zhou et al., 2014). While this indicates primates are using some tactile sensory information to establish the toughness of leaves prior to consumption, there are many other traits primates might have that alter their dietary choices. These include (but are not limited to) adaptations like a modified foregut that alters digestion (Boonratana, 2003; Matsuda et al., 2017; Zhou et al., 2014), food availability or seasonal differences (Hylander, 1975a; Lucas & Teaford, 1994), feeding behaviors that do not involve full consumption, like chewing seeds and then spitting them out but not swallowing (Kinzey & Norconk, 1993; Lucas, 1994), personal choice in foods based on color or learned behaviors (Chapman & Fedigan, 1990; Julliot, 1996), genetic differences such as more olfactory receptor pseudogenes that can change the way a primate perceives fragrance (Dominy, 2004; Mittermeier & van Roosmalen, 1981), a general variety in diet rather than the traditional categories (i.e., frugivore, folivore, etc.) that imply primates consume a single diet

(Chapman & Fedigan, 1990; Hanya & Bernard, 2012; Janson & Boinski, 1992; Mittermeier & van Roosmalen, 1981; Teaford, 1985), and many others.

Insectivorous feeders can be divided into “soft-bodied” and “hard-bodied” feeders dependent on the choice of prey. Species that depend on soft-bodied insects have higher shearing crests and are more restricted in feeding choice to avoid denting or fracturing the molar teeth (Strait, 1993a, b). Many primate species have been observed consuming both insects and small-bodied vertebrates, but only one genus (*Tarsier*) relies entirely on a carnivorous diet. Additionally, separating out insects and small-bodied vertebrates into different (or even the same) dietary category is difficult due to the differences in texture of the eaten materials (i.e., bone vs. muscles tissue).

In sum, primates are using tactile sensory information to choose which foods to eat by placing food objects into the oral cavity. These finite abilities to estimate the toughness/stiffness of objects has likely coevolved and been selected for based on dietary preferences and food availability. While there are many factors that determine what food primates will consume, it is clear that tactile sensory information plays a part and is an important component in understanding all primate dietary behaviors.

IMPLICATIONS FOR HUMAN EVOLUTION

The Mental Foramen as a Species Trait

While much has been said in the way of extant primate craniofacial bony morphology in the fossil record, little is said about the soft tissue structures due to their inherent lack of preservation in the fossil record. As discussed above, bony canals and foramina are thought to form around the soft-tissue structures in utero and are likely to reflect the size and shape of these tissues. This section aims to discuss the factors that can influence the size and shape of the mandibular canal, mandibular foramen, and mental foramen (MF) and the implications this has on the mandibular division of trigeminal nerve as it interacts with its bony components.

The size and location of the mental foramen has long been studied in human evolution due to the original belief that its location/size could be indicative of species traits (i.e., diet, tooth use, relatedness to other species, etc.). Having a MF directly below M_1 (as opposed to the general position below P_3 and P_4 in modern humans) was initially hypothesized to be a derived trait (Condemi, 1991; Dupont, 1866; Fraipont & Lohest, 1886; Franciscus & Trinkaus, 1995; Hublin, 1998; Quam & Smith, 1998; Stringer, 1987; Stringer et al., 1984; Williams & Krovitz, 2004). However, evidence from several Middle Pleistocene hominin populations also have more posteriorly placed MF, indicating this condition is present in ancestral populations as well (Coqueugniot, 2000; Coqueugniot & Minugh-Purvis, 2003; Rosas, 2001). Many authors have argued that the position of the MF may be a "spandrel" (Gould & Lewontin, 1979) and could be influenced by the growth of the mandibular corpus and ramus, modification of the mandibular symphysis and condyle, changes in the alveolar process and dentition, expansion of the inferior alveolar nerve and blood vessels, and/or mesial drift of the dentition (Coqueugniot & Minugh-Purvis, 2003; El-Beheri, 1985; Green & Darvell, 1988; Kjaer, 1989; Stefan & Trinkaus, 1998; Trinkaus, 1993). Multiple mental foramina are often noted as a characteristic of "prehistoric man" and have reduced in number throughout evolution (Anderson et al., 1991; Senyurek, 1946). This could indicate that a more plexus-like nature of the modern IAN arrangement in modern humans would be representative of the primitive arrangement (Anderson et al., 1991).

Mandibular Size and Tooth Form

There is a tendency for a decrease in mandibular size among modern humans in comparison to evolutionary trends seen in other primates (Liang et al., 2009b). This overall change in mandibular size should affect the positioning of the MF, as it has been shown to be more posteriorly placed in larger mandibles (Rosas, 1997, 2001; Williams & Krovitz, 2004). Recent research (Robinson & Yoakum, 2019) suggests that the overall length of the mandibular canal has a significant relationship to the size and number of mental foramina, when age, sex, and overall body size are accounted for.

Mandibular tooth form has contributed significantly to the understanding of hominin evolution, particularly that of the premolar and molar (Abbott, 1984). Growth rate of mandibular and dental traits in Neanderthals, in comparison to modern humans, is accelerated which could contribute to a more posteriorly placed foramen magnum (Williams & Krovitz, 2004). In modern humans, there has been a trend of root reduction in relation to facial shortening (Abbott, 1984). Root reduction in modern humans is more intense in the maxillary molars than in the mandibular molars. However, in all molars, there is an increase in root reduction from M_1 to M_3 (i.e., the third molar has seen the most root reduction) (Abbott, 1984; Riesenfeld, 1970). This sequence of root reduction parallels the trend seen in crown size reduction throughout human evolution (Riesenfeld, 1970). Mandibular and maxillary pre-molars have seen similar reductions culminating in the simple, single, conical pre-molar root seen today in modern humans (Abbott, 1984). All these factors: size/location of MF, the appearance of AMFs, mandibular length changes, and tooth form changes are heavily influenced by and related to the soft-tissue nervous structures, but no study to date adequately surveys extant or extinct primate nervous tissues in size or distribution.

The Craniofacial Complex Study as a Whole

While we can track changes in skeletal anatomy throughout human evolution, using the diet of extant primates to infer the diet of extinct primates through skeletal elements alone should be done with caution. There are two main reasons for this caution: 1) too much variation exists in the feeding behaviors and dietary preferences of extant primates that is not well understood even with sufficient observation periods (Ross & Iriarte-Diaz, 2014), and 2) not enough is known about the soft tissues of extinct species due to their inability to typically survive the fossilization process (Daegling & Grine, 2006). Biomechanically, the forces created along the tooth row vary dramatically when soft tissues can be considered.

There is also significant evidence that mechanical loading can result in phenotypic variation in primate craniofacial structure (Lycett & Collard, 2005). The size and shape of soft

tissues on the face will have an effect as to how much force can be generated and will thus affect the mechanical loads on the skeletal anatomy. Previous research has suggested that the hominid skull contained various homologies due to mastication related strain. However, Lycett & Collard (2005) have tested this hypothesis using extant papionines and were able to establish that mechanical loading can result in significant variation in the sections of the primate cranium that are under strain during mastication. Additionally, they were able to conclude that phenotypical plasticity is not a major cause of homoplasy in the primate skull (Lycett & Collard, 2005). This indicates that some of the variation we see in the fossil record, and particularly those fossils in the masticatory complex, should be used with caution when attempting to infer diet based on extant models. Without the ability to view both the soft and hard-tissue components of the masticatory complex, we are unable to see the full picture in both mastication and masticatory loads.

The craniofacial complex is often studied in its individual pieces, with many focusing on either the soft-tissue or hard-tissue structures separately. However, because the craniofacial complex acts a system of integrated parts that include the CNS, skeleton, and many additional soft-tissue organs, each of these parts must be addressed together before evolutionary implications can be drawn (Aldridge et al., 2005). Greer et al. (2017) addressed the observation that endocasts are often used in evolutionary science to infer both brain size and cranial capacity with no evidence to support the statement that brain size is equal to that of cranial capacity. In one study of 13 white males aged 18-21, the average distance between the brain and cranium was 4.0mm around the entirety of the brain, while individual distance between the brain and cranium ranged from 0.0mm to 24.0mm (Greer et al., 2017). The assumption that soft tissue occupies the entirety of the space in which it is contained is contested for many modern nervous structures (i.e., the hypoglossal nerve/canal) although many studies argue that changes in skull shape are often mirrored by changes in the underlying brain (Falk et al., 2005; Gault et al., 1992; Kleinman et al., 1983). This large amount of variation in such a small sample

indicates a need for further study on soft tissue in relation to bony structures before inferences can be drawn from fossil species.

In conclusion, there is a lack of study of the interaction of the soft- and hard-tissue components of the craniofacial complex. The hard-tissue components have been studied extensively by anthropologists, while the soft tissue is typically reserved for anatomists. However, tooth size and shape alone cannot be used to firmly establish the diet of a species as there are other methods the masticatory system uses to maximize the efficiency of food processing. For example, bony jaw buttressing has been suggested as a way to offset structure failure due to both repetitive loading and high force loading (Ungar, 2002). Very little research has been done to quantify the relationship between the canals/foramina/sinuses that retain nervous soft-tissue structures. However, it is often noted that hard tissue forms around the soft tissue, indicating that changes in soft tissue can affect the overall size and shape of the craniofacial complex in its entirety. This dissertation fills a gap in the literature by addressing the relationship between the mandibular tooth row, mandibular foramen, mandibular canal, mental foramen, and the inferior alveolar nerve that runs through each.

SUMMARY

In sum, a large body of knowledge exists on the separate parts of the masticatory apparatus and the selective pressures it is under, but few have addressed the connection between nervous structures in relation to tooth forms and dietary preferences. Understanding primate diet is crucial to elucidating the evolutionary processes that have shaped the primate masticatory system. Food preference is connected to food material properties in terms of physical structure as well as color and palatability. If we infer that food preference is also dependent on an individual's ability to physically consume an object during chewing, this suggests that the nervous structures within the mouth are under strong selective pressure to maximize masticatory function. The ability to quantify the volume of nervous tissue and link

these morphologies to other aspects of the masticatory apparatus has thus far not been possible without using destructive methods such as gross dissection and histology. However, precise three-dimensional quantification of these tissues, as used here, has the power to provide insights into the evolutionary trajectory of many primate species by directly linking the size and shape of dental features to the nervous tissues rather than relying solely on percentile observations of feeding behaviors, which may or may not accurately reflect the diet a given animal is adapted to. Assigned dietary categories tend to include biases in human observations because of the difficulty in observing wild species and the inaccuracies of observing species in captivity that have been affected by humans. Similar problems occur regarding tooth morphology, in that while we can observe that a trait is selected for this does not always indicate what the preferred primate food source is. There is, to date, no study showing a correlation between tooth shape, diet, and innervating neurological structures to the dentition in extant primates. This dissertation compares both tooth shape and neuroanatomy, two closely connected parts of the complicated system that is the masticatory apparatus that have yet to be closely examined together and thus stands to make a transformative impact on primate diet research.

CHAPTER 3: MATERIALS AND METHODS

INTRODUCTION

In this dissertation there are three overarching research questions that I have proposed to examine: (Q_1) does occlusal tooth morphology covary with nervous tissue size?, (Q_2) does bony canal structure track nervous tissue size in the masticatory apparatus?, and (Q_3) does the volume and cross-sectional area of the nervous tissue within the mandible correlate with feeding behavior? To address these questions, I collected both soft- and hard-tissue datasets from digital specimens. Specific materials and collection procedures are outlined below.

MATERIALS

The research questions posed in this dissertation were tested to establish whether the nervous tissues within the masticatory apparatus of the mandible are directly related to tooth form and function. Data was collected both from soft-tissue (i.e., crania with intact muscles and nerves) and hard-tissue (i.e., dry bone) specimens, with slightly different but overlapping research goals for each of these datasets. Only adult specimens were used for this study to ensure that ontogeny was not an additional variable. Adulthood was established via the eruption of all molar teeth, with crowns fully formed and erupted, and roots fully grown with only the root canal remaining open. For each specimen, data was collected from both the left and right sides of the mandible. Table 3.1 shows the specific variables collected for each specimen.

Table 3.1. Variables measured and their associated research question

Variable Name	Unit	Definition	Citation	Associated Research Question
Tooth root surface area	mm^2	Sum surface area of tooth root size	Spencer (2003)	Q1, Q3
Nervous tissue total volume	mm^3	Sum of nervous tissue volume from mental foramen to incisor	This study	Q1, Q2, Q3
Nervous tissue cross-sectional area	mm^2	Cross-sectional area measurement directly below center of tooth	This study	Q1, Q2, Q3
Enamel surface area	mm^2	Sum of surface area of crown enamel on each tooth	Kay (1975)	Q1
Mandibular canal total volume	mm^3	Total volume of the mandibular canal	This study	Q2
Orientation patch count (OPC)	n/a	A measure of surface complexity	Evans et al. (2007)	Q1
Dirichlet's Normal Energy (DNE)	n/a	Quantification of molar morphology for dietary inference	Bunn et al. (2011)	Q1
Relief index (RFI)	n/a	Ratio of the tooth crown 3D area to 2D planar area	Boyer (2008)	Q1
Occlusal slope	n/a	The average slope across the surface of the tooth	Ungar & M'Kirera (2003)	Q1
Mandible length	mm	Length from infradentale to center of mandibular condyle	McNamara (1975)	Q1, Q2, Q3

Hard-Tissue Dataset

A total of 153 microCT scans of dry bone specimens (hard-tissue samples) were obtained from online sources (i.e., morphosource.org) (Figure 3.1). Downloaded scans were required to meet the following criteria: 1) scan resolution of < 100 microns (resolution established from a previous pilot study described below), 2) no damage to the mandible or teeth, and 3) must have reached adulthood as determined by molar eruption. Further hard tissue samples were obtained from the initial microCT scans of all soft-tissue specimens (n = 129) generated in this study at the MicroCT Imaging Consortium for Research and Outreach (MICRO) at the University of Arkansas before iodine staining occurred. Combined, there were 282 hard-tissue specimens used in this study. Figure 3.1 shows the total breakdown of the

samples obtained for this study, with 72 total species spread across each of the major taxonomic groups within Primates (i.e., Strepsirrhini, Platyrrhini, Hominoidea, and Cercopithecoidea). Where possible, at least one male and one female from each species was collected (36 species) but in many instances only data for one sex was available (36 species).

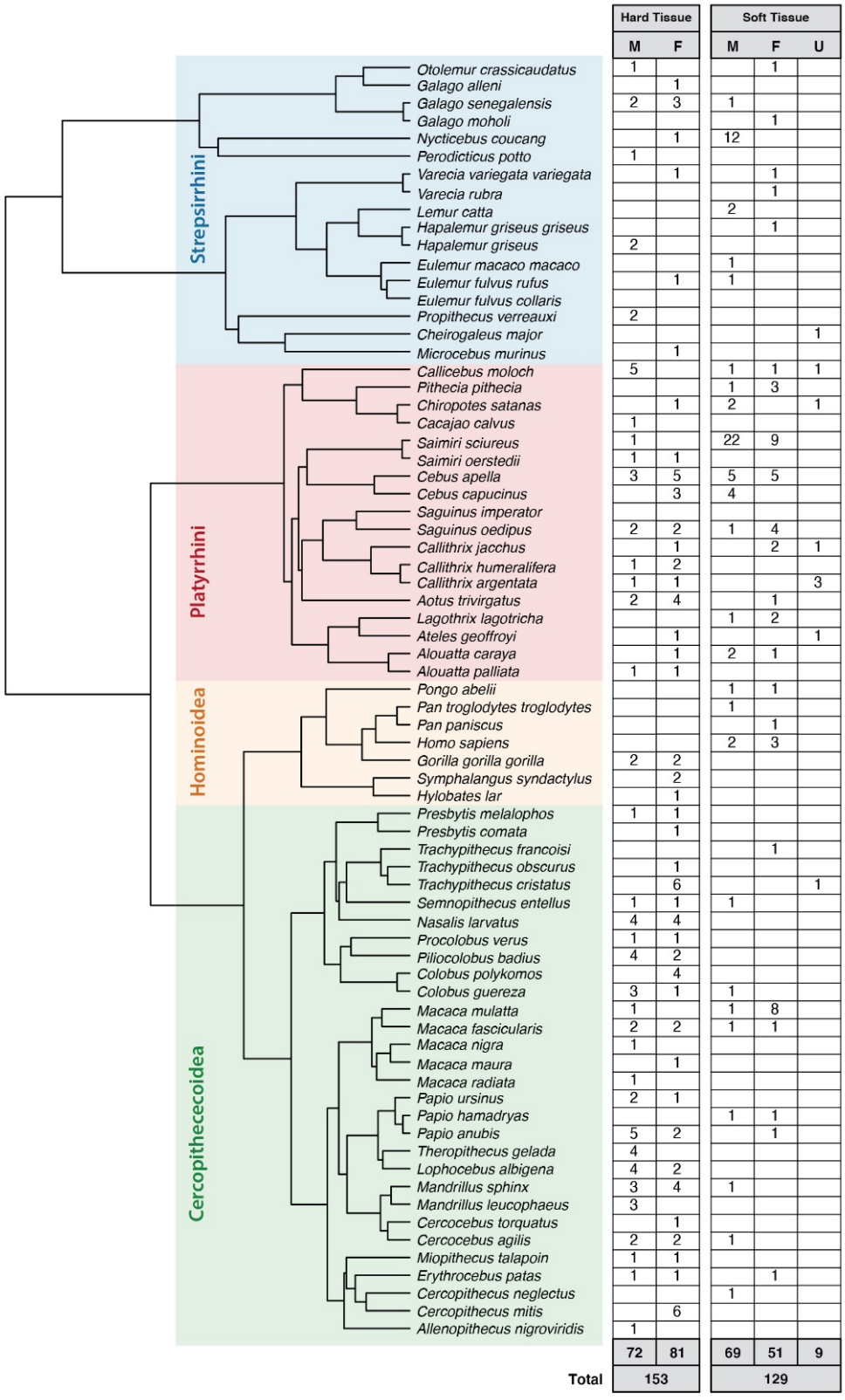

	Hard Tissue		Soft Tissue		
	M	F	M	F	U
Otolemur crassicaudatus	1			1	
Galago alleni		1			
Galago senegalensis	2	3	1		
Galago moholi				1	
Nycticebus coucang		1	12		
Perodicticus potto	1				
Varecia variegata variegata		1		1	
Varecia rubra				1	
Lemur catta			2		
Hapalemur griseus griseus				1	
Hapalemur griseus	2				
Eulemur macaco macaco			1		
Eulemur fulvus rufus		1	1		
Eulemur fulvus collaris					
Propithecus verreauxi	2				
Cheirogaleus major					1
Microcebus murinus		1			
Callicebus moloch	5		1	1	1
Pithecia pithecia			1	3	
Chiropotes satanas		1	2		1
Cacajao calvus	1				
Saimiri sciureus	1		22	9	
Saimiri oerstedii	1	1			
Cebus apella	3	5	5	5	
Cebus capucinus		3	4		
Saguinus imperator					
Saguinus oedipus	2	2	1	4	
Callithrix jacchus		1		2	1
Callithrix humeralifera	1	2			
Callithrix argentata	1	1			3
Aotus trivirgatus	2	4		1	
Lagothrix lagotricha			1	2	
Ateles geoffroyi		1			1
Alouatta caraya		1	2	1	
Alouatta palliata	1	1			
Pongo abelii			1	1	
Pan troglodytes troglodytes			1		
Pan paniscus				1	
Homo sapiens			2	3	
Gorilla gorilla gorilla	2	2			
Symphalangus syndactylus		2			
Hylobates lar		1			
Presbytis melalophos	1	1			
Presbytis comata		1			
Trachypithecus francoisi				1	
Trachypithecus obscurus		1			
Trachypithecus cristatus		6			1
Semnopithecus entellus	1	1	1		
Nasalis larvatus	4	4			
Procolobus verus	1	1			
Piliocolobus badius	4	2			
Colobus polykomos		4			
Colobus guereza	3	1	1		
Macaca mulatta	1		1	8	
Macaca fascicularis	2	2	1	1	
Macaca nigra	1				
Macaca maura		1			
Macaca radiata	1				
Papio ursinus	2	1			
Papio hamadryas			1	1	
Papio anubis	5	2		1	
Theropithecus gelada	4				
Lophocebus albigena	4	2			
Mandrillus sphinx	3	4	1		
Mandrillus leucophaeus	3				
Cercocebus torquatus		1			
Cercocebus agilis	2	2	1		
Miopithecus talapoin	1	1			
Erythrocebus patas	1	1		1	
Cercopithecus neglectus			1		
Cercopithecus mitis		6			
Allenopithecus nigroviridis	1				
	72	81	69	51	9
Total	153		129		

Figure 3.1. All specimens collected for this dissertation from either morphosource.org (hard tissue) or created by CBY (soft tissue).

Additionally, all species were given a species identifying code for data analysis figures. These species, their codes, families, and the corresponding family colors are shown in Table 3.2. These codes are either 4 or 6 letters long and are created by taking the first two letters of the genus and species names (sub-species will have 6 letters).

Table 3.2. Species code identifiers and family colors for all plots

Species	Species Code	Family
Aotus trivirgatus	AOTR	Aotidae
Alouatta caraya	ALCA	Atelidae
Alouatta palliata	ALPA	Atelidae
Ateles geoffroyi	ATGE	Atelidae
Lagothrix logotricha	LALO	Atelidae
Saguinus oedipus	SAOE	Callitrichidae
Callithrix argentata	CAAR	Callitrichidae
Callithrix humeralifera	CAHU	Callitrichidae
Callithrix jacchus	CAJA	Callitrichidae
Cebus apella	CEAP	Cebidae
Cebus capucinus	CECA	Cebidae
Saimiri oerstedii	SAIOE	Cebidae
Saimiri sciureus	SASC	Cebidae
Allenopithecus nigroviridis	ALNI	Cercopithecidae
Cercopithecus mitis	CEMI	Cercopithecidae
Cercopithecus neglectus	CENE	Cercopithecidae
Erythrocebus patas	ERPA	Cercopithecidae
Miopithecus talapoin	MITA	Cercopithecidae
Cercocebus agilis	CEAG	Cercopithecidae
Cercocebus torguatus	CETO	Cercopithecidae
Lophocebus albigena	LOAL	Cercopithecidae
Macaca fascicularis	MAFA	Cercopithecidae
Macaca maura	MAMA	Cercopithecidae
Macaca mulatta	MAMU	Cercopithecidae
Macaca nigra	MANI	Cercopithecidae
Macaca radiata	MARA	Cercopithecidae
Mandrillus leucophaeus	MALE	Cercopithecidae
Mandrillus sphinx	MASP	Cercopithecidae
Papio anubis	PAAN	Cercopithecidae
Papio ursinus	PAUR	Cercopithecidae
Theropithecus gelada	THGE	Cercopithecidae
Colobus guereza	COGU	Cercopithecidae
Colobus polykomos	COPO	Cercopithecidae

Table 3.2. (Cont.)

Species	Species Code	Family
Nasalis larvatus	NALA	Cercopithecidae
Piliocolobus badius	PIBA	Cercopithecidae
Presbytis comata	PRCO	Cercopithecidae
Presbytis melalophos	PRME	Cercopithecidae
Procolobus verus	PRVE	Cercopithecidae
Semnopithecus entellus	SEEN	Cercopithecidae
Trachypithecus cristatus	TRCR	Cercopithecidae
Trachypithecus francoisi	TRFR	Cercopithecidae
Trachypithecus obscurus	TROB	Cercopithecidae
Cheirogaleus major	CHMA	Cheirogaleidae
Microcebus murinus	MIMU	Cheirogaleidae
Galago alleni	GAAL	Galagidae
Galago senegalensis	GASE	Galagidae
Otolemur crassicaudatus	OTCR	Galagidae
Gorilla gorilla gorilla	GOGOGO	Hominidae
Homo sapiens	HOSA	Hominidae
Pan paniscus	PAPA	Hominidae
Pan troglodytes troglodytes	PATRTR	Hominidae
Pongo abelii	POAB	Hominidae
Symphalangus syndactylus	SYSY	Hominidae
Propithecus verreauxi	PRVE	Indriidae
Eulemur fulvus collaris	EUFOCO	Lemuridae
Eulemur_fulvus rufus	EUFORU	Lemuridae
Eulemur macaco macaco	EUMAMA	Lemuridae
Hapalemur griseus	HAGR	Lemuridae
Hapalemur griseus griseus	HAGRGR	Lemuridae
Lemur catta	LECA	Lemuridae
Varecia rubra	VARU	Lemuridae
Varecia variegata variegata	VAVAVA	Lemuridae
Nycticebus coucang	NYCO	Lorisidae
Perodicticus potto	PEPO	Lorisidae
Cacajao calvus	CACA	Pitheciidae
Callicebus moloch	CAMO	Pitheciidae
Chiropotes satanas	CHSA	Pitheciidae
Pithecia pithecia	PIPI	Pitheciidae

Soft-Tissue Dataset

In general, soft tissue studies are incredibly opportunistic, as samples of primate materials with soft tissue are difficult to obtain and typically do not allow destructive sampling.

While iodine staining is essentially non-destructive, it still requires a specimen to be skinned to allow the tissues to uptake the iodine. The samples obtained for this study have all been given to the project with this knowledge and many samples have been used in other research that required the removal of brain tissue, some nervous tissue, muscle tissue, and/or a variety of other tissue removal procedures. My acceptance of less than whole specimens is two-fold: 1) to ensure that these samples are used beyond what they were originally intended for in terms of research to provide all possible data and, 2) to demonstrate that using a digital replacement, like iodine-staining, allows a single specimen to be used by more than one set of researchers and research projects without damaging the morphology of the specimen using destructive methods such as gross dissections or histology. While my sampling focuses on primates, I have made it a point to collect other mammalian soft tissues to allow for phylogenetic outgroups. These outgroups include common brown rats (n = 5, *Rattus norvegicus*), European rabbits (n = 4, *Oryctolagus cuniculus*), and North American river otters (n = 1, *Lontra canadensis*).

Figure 3.1 shows the soft tissue specimens acquired for this study (n = 129). In addition to specimens already available in the Terhune Lab, specimens were obtained from the Duke Miami Collection (Duke University), Callum Ross (University of Chicago), Janine Chalk (Mercer University Medical School), Magdalena Muchlinski (University of North Texas Health Sciences Center), Andrea Taylor (Touro University), Chris Vinyard (Kent State University), the University of Arkansas Medical Sciences Center, and Stony Brook University. While obtaining specimens, my goal was to sample primates with a wide range of diets, at least two specimens within each species, and an equal number of males and females present. As shown in Figure 3.1, in the collection of soft tissues I was able to obtain 129 specimens from 40 species of primates within all major taxonomic groups (Strepsirrhini, Platyrrhini, Hominoidea, and Cercopithecoidea). Of these 40 species, 14 species had at least one male and one female present, and 26 had either one male, one female, or a specimen of unknown sex.

Although the goal was to stain all soft-tissue specimens listed in Figure 3.1, there were a variety of reasons as to why this was not possible: the COVID-19 pandemic essentially halted all data collection for a period of eight months, many specimens did not uptake the iodine stain due to prior fixatives, some of the specimens were of poor quality (i.e., had been allowed to decompose for various rates of time prior to fixation), and many of the specimens were too large to uptake stain in the amount of time given. Table 3.3 shows the specimens for which nervous tissue data was successfully collected for this study.

Table 3.3. Specimens for which nervous tissue data were collected for this study

Species	Sex		
	Male	Female	Unknown
Lontra canadensis	1		
Oryctolagus cuniculus	2	2	
Rattus norvegicus	5		
Otolemur crassicaudatus			1
Galago senegalensis	1		
Nycticebus coucang			1
Varecia variegata variegata	1	1	
Varecia rubra		1	
Lemur catta	1		
Hapalemur griseus griseus		1	
Eulemur macaco	1		
Eulemur fulvus rufus	1		
Eulemur fulvus colaris			1
Cheirogaleus major			1
Callicebus moloch	1	1	
Pithecia pithecia	1	2	
Chiropotes satanas	2		
Saimiri sciureus	7	2	
Cebus capucinus	2		
Saguinus oedipus	4	1	
Callithrix jacchus		2	1
Aotus trivirgatus			1
Lagothrix lagotricha			1
Alouatta caraya	2		
Pan paniscus		1	
Trachypithecus francoisi		1	
Trachypithecus cristatus			1
Semnopithecus entellus	1		
Colobus guereza	1		
Macaca mulatta		5	
Macaca fasicicularis		1	
Papio anubis		1	
Cercopithecus neglectus	1		
Erythrocebus patas		1	
Totals	35	23	8
	66		

METHODS

MicroCT and Iodine Staining Techniques

MicroCT was first introduced by Elliott and Dover (1982) as a novel technique for viewing high-resolution, three-dimensional (3D) data on bone density and micro-architecture. A microCT file, like a traditional CT, is composed of a stack of reconstructed cross sections of the scanned object normal to the axis of rotation (Metscher, 2009). During reconstruction, isotropic voxels (volume pixels) are automatically calculated by the imaging system's calibration software (Metscher, 2009). While at times some soft-tissue structures are visible, most soft tissue has a very low X-ray attenuation and thus requires a staining procedure to view the intricate details (Hedrick et al., 2018). For example, in traditional radiographs, the mylohyoid line and the external oblique line may be superimposed on the mandibular canal, possibly being mistook for the mandibular nerve itself (Anderson et al., 1991; Jacobs et al., 2002; Klinge et al., 1989; Liang et al., 2009b).

While CT imaging has advanced the world of hard-tissue studies, new methods like diffusible iodine-based contrast-enhanced computed tomography (diceCT) and perfusable iodine-based contrast-enhanced computed tomography (spiceCT) have made the study of individual soft tissues in detail a possibility (Gignac et al., 2016; Hedrick et al., 2018; Vickerton et al., 2013; Witmer et al., 2018). DiceCT has many challenges: large specimens are difficult to stain thoroughly, few studies have been done on tissue deformation and shrinkage, and there is generally a lack of agreed upon protocols for staining. However, this technique has made it possible to identify minute differences in tissue density *in situ* (Gignac et al., 2016). The benefits of diceCT are that the techniques are minimally destructive and visually reversible, allow for the visualization of soft-tissue structures at high resolutions, provide versatility in staining different kinds of tissues, and is time efficient for a wide variety of specimens (Gignac et al., 2016; Hedrick et al., 2018; Witmer et al., 2018). While the chemical composition of the specimen will be altered permanently, the iodine stain can be made colorless, effectively returning the

specimen to its original physical appearance (Gignac et al., 2016; Jain, 2017; O'Brien & Bourke, 2015; O'Brien & Williams, 2014; Witmer et al., 2018).

There are two established solutions that can be prepared for iodine staining: I_2E (ethanol-based) and I_2KI (aqueous-based with added potassium iodide crystals) (Li et al., 2016). Both are used to increase the solubility of molecular iodine in solutes, and neither is superior to the other for staining purposes. I_2KI (often called Lugol's iodine if the solution is 5% weight/volume) is prepared by combining one unit of elemental iodine (I_2) with two units of potassium iodide (KI) to an aqueous solution whose volume depends on the concentration required (i.e., 20% w/v). I_2E is prepared by adding elemental iodine directly to pure (>99.5%) ethanol. Because I_2KI is soluble in water, it is best used on specimens that were initially preserved in an aqueous-based solution such as 10% neutral buffered formalin. Alternatively, if a specimen was initially preserved or has been stored long-term in an ethanol-based preservative, I_2E will better bond to the tissue during staining (Li et al., 2016). Both solutions require an initial step before the specimen can be stained. The I_2E solution requires the additional step of adding the specimen to pure ethanol before staining to remove additional water, while the I_2KI approach requires that the specimen is first submerged in a sucrose (20% w/v) solution prior to staining (Li et al., 2016). Many studies choose to use I_2KI for staining likely for two reasons: it is much less costly and if research includes museum specimens it may be difficult to establish what preservative was initially used to fix the specimen.

A generally agreed upon procedure in I_2KI diceCT is formalin immersion for a period of at least 30 days prior to stain immersion, regardless of original fixative, because the formalin acts to stabilize tissue and subsequently reduce shrinkage (Hedrick et al., 2018; Li et al., 2016; Vickerton et al., 2013). If a specimen is collected fresh in the field, immediately immersed in formalin, and then transferred to I_2KI, shrinkage is minimal to non-existent (Hedrick et al., 2018). However, if a specimen is fixed and stored in ethanol, like many current museum specimens, they have likely experienced dehydration due to ethanol penetration of the tissues, which has a

known shrinkage effect (Hedrick et al., 2018; Li et al., 2016; Vervust et al., 2009; Vickerton et al., 2013). These specimens can either be immersed in formalin and stained with I_2KI or used immediately with I_2E after immersion in pure ethanol for a short period of time. While ethanol fixation does appear to cause slightly more shrinkage, I_2E staining requires lower concentrations of iodine (as low as 1% concentrations), shorter staining times, and may be more efficient at completely staining all materials than I_2KI because of the increase in the potential solubility of iodine elements within the solute phase of tissues (Li et al., 2016; Metscher, 2009).

Few studies have assessed different staining methods and their capabilities to effectively stain museum specimens that have been stored for long periods of time in ethanol-based preservatives (Hedrick et al., 2018). DiceCT has been shown to be the most effective and least toxic staining method for specimens that were either initially preserved or have been stored long-term in an ethanol-based solution (Metscher, 2009). The most agreed upon effect of diceCT staining is a minimal amount of shrinkage in some specimens, which increases directly with increasing the iodine concentration in a solution (i.e., a 5% iodine solution will cause less shrinkage than a 25% iodine concentration) (Hedrick et al., 2018). However, some tissues like the eyes and brain are affected at higher rates due to higher iodine uptake. Hedrick et al. (2018) show that in museum specimens (regardless of time immersed in stain or stored in an ethanol-based solution) the eyes and brain retain 57% and 62% of their original size, respectively. In fresh, field-collected specimens, the eyes and brain experienced significantly smaller changes in volume by maintaining 74% and 94% of their original size, respectively (Hedrick et al., 2018). One study (Fox et al., 1985) shows that shrinkage is particularly prevalent in tissue blocks but is less common in whole or partial body specimens (i.e., a head, hand, arm, etc.). All staining procedures will be affected by many variables, including but not limited to fixation method, initial steps in specimen preparation, low temperatures, and the field conditions under which they were initially collected (Hedrick et al., 2018). In general, caution should be exercised if a study hopes to compare different types of tissue when interpreting results.

DiceCT Protocols

For this dissertation, all specimens were submerged in 10% neutral buffered formalin for a period of at least 30 days prior to staining. Immediately before staining, all specimens were submerged in a 20% w/v sucrose solution for a period of 48 hours. Sucrose solutions have been shown to prevent volume loss in specimens that are stained in an aqueous-based iodine solution, although they do not appear to prevent volume loss in specimens stained in an ethanol-based iodine solution. These specimens were then stained with a 7.5% w/v aqueous-based iodine solution until all tissues had adequate iodine uptake (as determined by various check scans throughout the staining process). After the solution was added to the container with the specimen in it, it was placed on a standard laboratory orbital shaker for 24 hours to help agitate the specimen and potentially allow the iodine to penetrate faster. Staining time for these specimens varied greatly and was not necessarily dependent on size, though size has shown to be a significant factor in the length of time iodine uptake is complete (Gignac et al., 2016). All specimens were placed into stain between March 2020 – May 2020, with final post-stain scans taken of specimens between January 2021 – May 2021. Unfortunately, these staining times may not accurately represent the ideal time for staining of these specimens due to the wide range of initial fixatives (certain specimens took in iodine much easier than other) and the COVID-19 worldwide pandemic. Due to the COVID-19 pandemic, final scans of specimens were taken later than initially projected because access to the scanning facility was limited. After the final scan, all specimens were de-stained using a 2.5% w/v sodium thiosulfate solution with full submersion for 48 hours. Sodium thiosulfate does not remove the iodine molecules but rather makes them colorless, therefore returning the specimen to its original state with no apparent differences. While specimens were de-staining, they were also placed on a standard laboratory orbital shaker for 24 hours to aid in penetration.

MicroCT scans were taken of each specimen before staining (pre-stain scan) and at regular intervals during staining. All scanning was conducted at the MicroCT Imaging Center for Research and Outreach (MICRO) at the University of Arkansas.

Data Collection

For each scan (either downloaded from morphsource.org or generated for this project), image stacks (.TIF format) were imported into the program Avizo (Avizo, 2016) and the bony canals (i.e., the empty space within the bone) and nervous tissues were segmented out and surface models (.ply format) were created of each structure (Figure 3.2A-B). The mandibular canal and inferior alveolar nerve were segmented from the mandibular foramen to the mental foramen (where possible). After segmentation, these sections underwent the “grow volume” function, then the “smooth” function from all three planes, and finally the “shrink volume” function to return it back to the original size (this method helps smooth out the model where edges can be sharp) in Avizo. These segmentations were then used to create 3D surface models using the “generate surface” function with restricted smoothing in Avizo (Figure 3.2C). Surfaces were then exported from Avizo as .ply files to be used for measurements. Total volume measurements and the cross-sectional area of specific points of the sectioned canal and of the segmented nervous tissues were taken using the program Geomagic Studio (Geomagic, 2013) using the “volume measurement” and “cross-sectional area measure” features in the “Analysis” tab (Figure 3.2F). These cross-sectional area measurements were taken at the mental foramen, the mandibular foramen, and below M_1 and P_4.

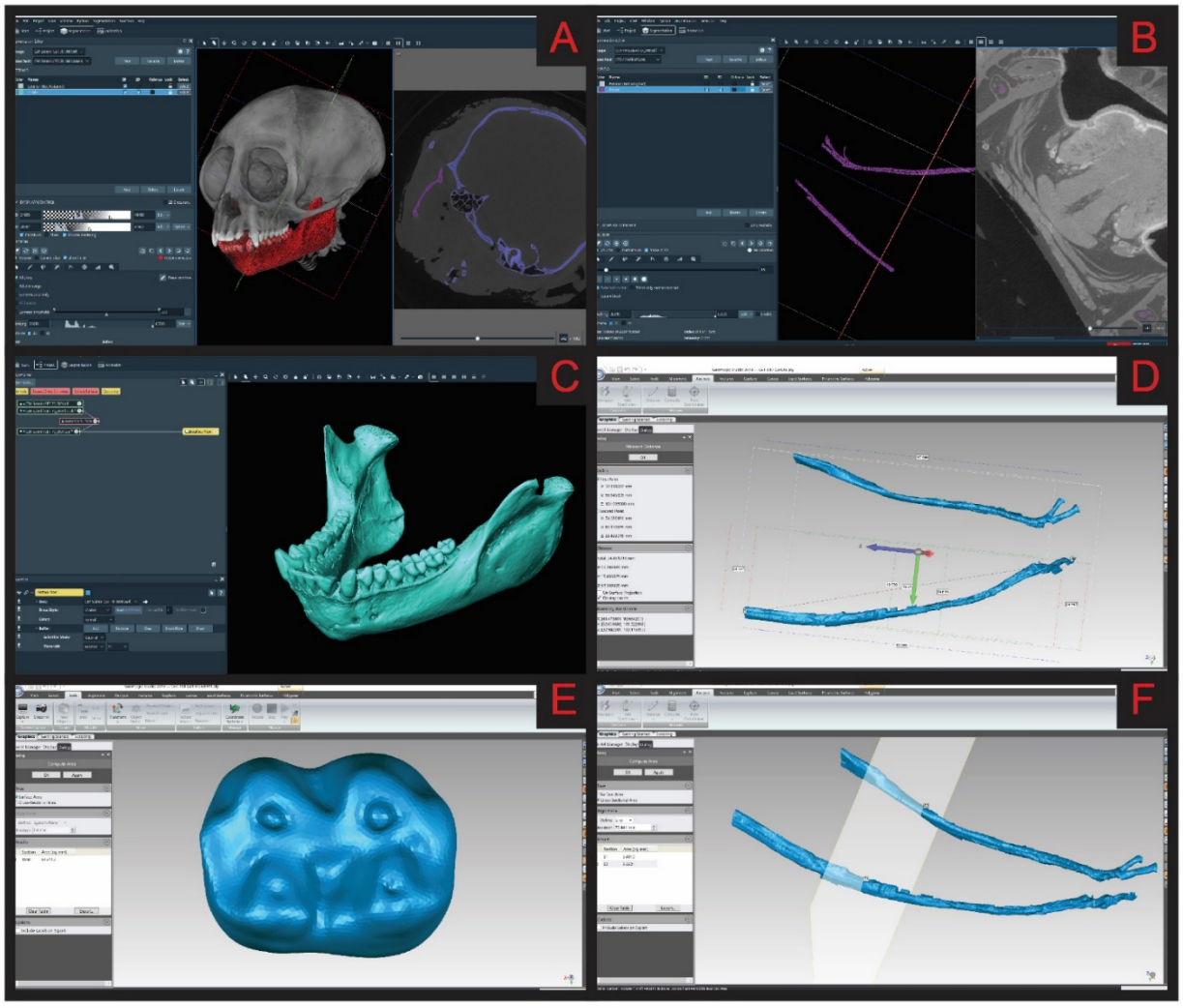

Figure 3.2. Figure showing the general workflow for data collection. First, the skeletal (A) and the soft tissue (B) are selected in the "segmentation" tab in the program Avizo. These selections are then used to generate a surface model (C), also in Avizo. After being exported from Avizo as a .ply file, they are opened in the program Geomagic so that they can be measured in a variety of ways. These examples show the "measure length" function demonstrated on nerves (D), the "measure surface area" function on a molar tooth (E), and the "Cross-sectional area measure" function on a segmented mandibular canal (F).

All teeth in both hard- and soft-tissue databases were segmented with a similar protocol, using both Avizo (Avizo, 2016) and Geomagic Studio. After sectioning out each tooth and root structure in Avizo and creating 3D surface models, surface area measurements of the enamel and tooth root were taken in Geomagic (Table 3.1; see Figure 3.2E). These measurements were recorded for four teeth on both the left and right side of the mandible: the central incisor,

the canine, the fourth premolar, and the first molar. However, cross-sectional area measurements of the canal underneath teeth could only be taken from the fourth premolar and first molar because the mental foramen (and thus the splitting of the mental and incisal nerve) typically occurs beneath the premolars in primates. If an individual was missing these teeth or the teeth were broken, measurements were taken of the remaining teeth or excluded from the dataset on an individual basis. For each individual, the mandible was segmented as an entire bone in Avizo in order to create a 3D .ply file (Figure 3.2A). Mandible length was taken from these files in Avizo by measuring the distance from infradentale to the center of the mandibular condyle using the “measure length” function in the “Analysis” tab (Figure 3.2D).

The use of R and RStudio for statistical analyses has become commonplace in research throughout the field. Packages like “molaR” have been developed for analyzing 3D surface models of teeth and can be utilized to describe the complexity of teeth. After a specimen has been scanned, a procedure defined in Pampush et al. (2016a) was used to analyze the teeth of a specimen and calculate a variety of quantitative variables describing occlusal morphology such as Dirichlet’s Normal Energy (DNE), Relief Index (RFI), Orientation Patch Count (OPC), and Occlusal Slope. All these variables assess the shape of a given tooth’s surface, rather than the size, because all teeth are scaled to the same number of “patches” during the surface generation process within Avizo.

Specifically, DNE measures the curvature (or sharpness) of a surface by detecting deviations across the planar surface (Bunn et al., 2011). When teeth are segmented digitally and represented by a mesh of triangle or “patches”, DNE is measure by calculating the normal direction for each point/triangle, the change in these directions are then established, and the sum of these changes are used to approximate the Dirichlet energy of the normal bending energy across that surface. An example of how DNE is calculated in patches is shown in Figure 3.3.

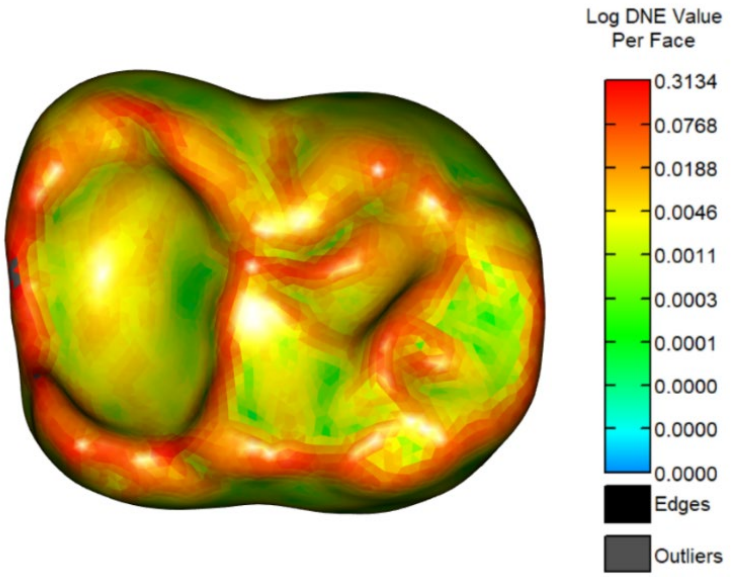

Figure 3.3. An example of the DNE calculations of specimen CET-152 (*Macaca mulatta*) on the left mandibular first molar.

OPC measures the complexity of the tooth by counting the number of patches on the tooth that have common orientations (Evans et al., 2007). OPC is estimated using the triangular "patches" on digital models of teeth by calculating the specific direction each triangle is facing and then arranging the "patches" by color into groups that face in the same direction. An example of how OPC looks after the arrangements have been calculated is shown in Figure 3.4.

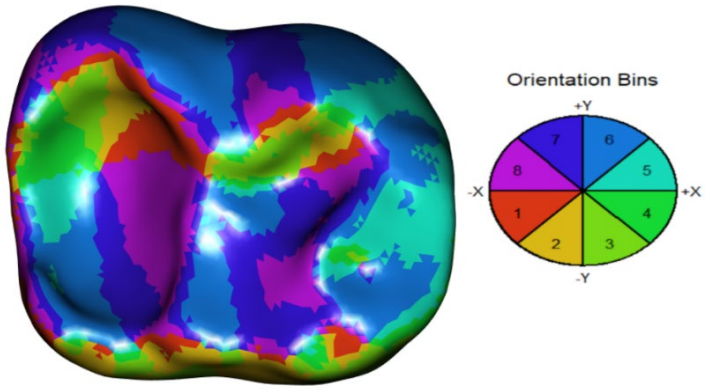

Figure 3.4. An example of the OPC calculations of specimen CET-152 (*Macaca mulatta*) on the left mandibular first molar.

RFI measures the cuspal relief on a tooth across two planes by dividing the natural log of the square root of the 3D surface area (in gray) by the natural log of the square root of the 2D surface area (in red) (Boyer, 2008). Overall, this is a measurement that assesses the relationship between the surface area of a tooth crown and its occlusal planimetric footprint. An example of the 3D plane and 2D plane are shown in Figure 3.5.

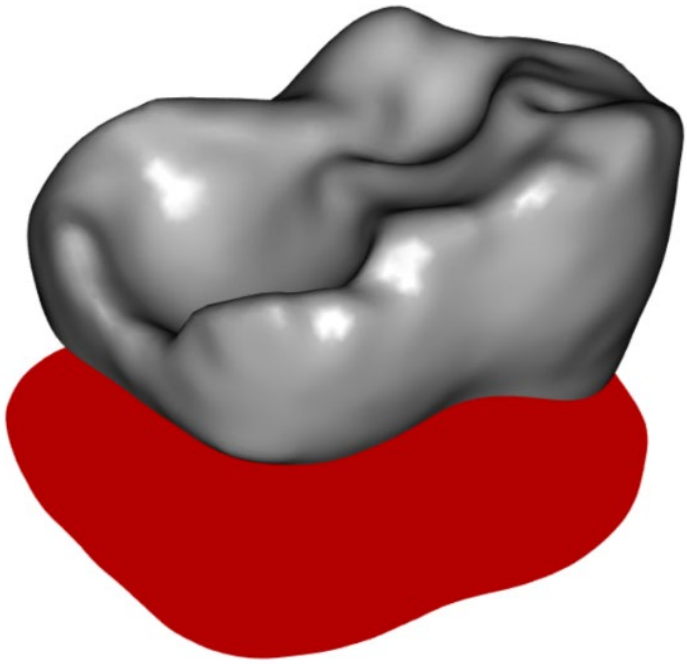

Figure 3.5. An example of the RFI calculations of specimen CET-152 (*Macaca mulatta*) on the left mandibular first molar.

Finally, occlusal slope is a measure of the average slope across the tooth surface (Ungar & M'Kirera, 2003). An example of how occlusal slope calculations are made is shown in Figure 3.6. Using these quantitative measurements of the shape of the tooth surface, as opposed to assigning individuals traditional – albeit often arbitrary – dietary categories, may give more clarity on the actual use of a tooth over that individual's lifetime and its relationship to the surrounding bony and soft-tissue structures.

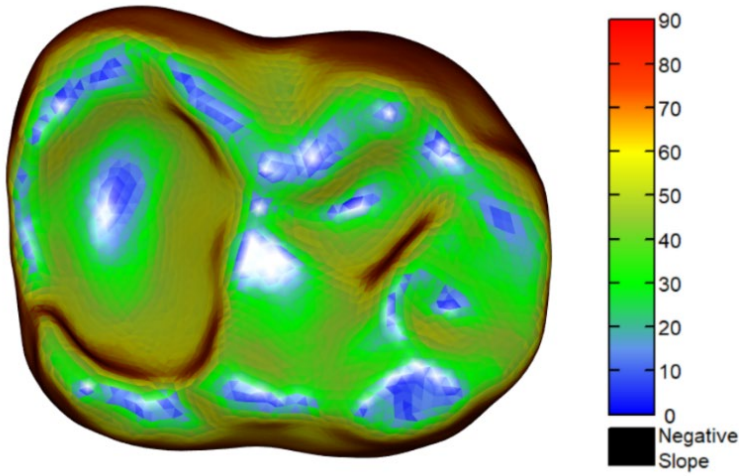

Figure 3.6. An example of the Slope calculations of specimen CET-152 (*Macaca mulatta*) on the left mandibular first molar

In general, the time spent processing data for a single individual for both soft- and hard-tissue specimens was ~12 hours (not including time for staining). Initial pre-stain scans took between 14-40 minutes and stained scans took between 2-10 hours, depending on the size of the specimen. A single canal typically took between 1-2 hours to segment, which must be done on the both the left and right side. Taking tooth surface area measurements and canal volumetric and cross-sectional measurements for a single individual required approximately one hour of work. In all, a significant portion of time was spent processing the scan data to prepare the segments or tooth sections necessary to complete all measurements and begin statistical analyses. Because of this amount of processing (~292 specimens at 12 hours each = 3,504 hours), undergraduate students were also included in the project and were trained to download/upload scans to online databases, create Avizo projects, segment large pieces of bone, segment the teeth using the aforementioned protocols, and assisted in the collection and maintenance of all soft tissue specimens.

All canal and nerve segmentations were performed by CBY. Teeth were segmented using an established protocol (taken from Pampush et al., 2016a, used in molaR) by CBY as well as undergraduate students Amber Cooper and Autumn Sanders. Surface measurements,

cross-sectional area measurements, and mandibular lengths were also measured by CBY, Amber Cooper, and Autumn Sanders. Finally, the maintenance and staining process for all soft-tissue specimens were performed by CBY and undergraduate Alice Stubbs. All specimens were de-stained and stored by Alice Stubbs or were sent back to their institution of origin.

Dietary Data

Observed feeding behavior data were established using two different methods: 1) traditional broad dietary categories (i.e., frugivore, folivore, etc.), and 2) percentages based on observed consumed foods culled from the literature. Both the traditional broad categories and the percentages can be seen in Table 3.4. The dietary categories that I focus on in my analyses include Leaf, Fruit, Gum, Seed, Animal, Grass, Stems and Bark, Roots and Tubers, Flowers, and Other. For traditional broad dietary categories, I assigned each species to primary and secondary diets based on the percentages eaten. For example, if a species consumed 60% fruit and 33% leaves, the primary diet would be recorded as “fruit” and the secondary diet would be recorded as “leaf”. I chose to use raw percentages and no arbitrary threshold for these diets (such as a primate must eat 40-50% of fruit to be considered a frugivore) to stay as close to the actual consumed food source as possible. However, many studies have shown that primate diets vary by species, environment, and even individuals (within the same species) and therefore not all primate species consume a single food source up to 40 or 50%. Because of this, I chose to analyze actual observations and not previously established categories. While not ideal, I recognize that not all primates will have been observed in the wild and thus will have little to no primary literature (i.e., direct field observations of primate ingestion) describing either their percentage of certain consumed foods or time spent feeding. Fortunately, I was able to locate primary literature on all species used in this dissertation and have recorded the percentages for foods eaten to determine the differential effects of feeding on morphology. Additionally, I subsequently divided this percentage data into non-resistant vs. resistant food categories, to determine if food material properties in differing percentages affect nervous tissue

size. For example, if a species consumed 60% fruit and 33% leaves, their primary diet would be recorded as non-resistant while their secondary diet would be recorded as resistant. Non-resistant food categories included Fruit and Gum while resistant foods included Leaf, Seed, Animal, Grass, Stems and Bark, Roots and Tubers, and Flowers. No species had the category of “Other” as either their primary or secondary diet.

Table 3.4. Breakdown of dietary data used by species (by percentage consumed)

Species	Primary diet	Secondary diet	Leaf	Fruit	Gum	Seed	Animal	Grass	Stems Bark	Roots Tuber	Flower	Other	Reference
Lontra canadensis	Animal (R)	NA	0	0	0	0	99	0	0	0	0	1	Roberts et al. 2008
Oryctolagus cuniculus	Leaf (R)	Grass (R)	48	0	0	0	0	38	0	0	0	0	Marques & Mathia 2001
Rattus norvegicus	Grass (R)	Seed (R)	0	0	0	33	0	33	0	0	0	34	NA
Otolemur crassicaudatus	Gum (NR)	Fruit (NR)	0	33	62	0	5	0	0	0	0	0	Nekaris & Bearder 2011
Galago senegalensis	Gum (NR)	Fruit (NR)	0	35	65	0	0	0	0	0	0	0	Charles-Dominique & Bearder 1979
Nycticebus coucang	Gum (NR)	Animal (R)	0	0	60	0	40	0	0	0	0	0	Streicher 2009
Varecia variegata variegata	Fruit (NR)	Leaf (R)	4.3	92	3.3	0.4	0	0	0	0	0	0	Britt 2000
Varecia rubra	Fruit (NR)	Flower (R)	4	88	0	0	0	0	0	0	6	2	Vasey 2000
Lemur catta	Fruit (NR)	Leaf (R)	42	48	0	0	0	0	0	0	2	8	Gould & Gabriel 2014
Hapalemur griseus griseus	Leaf (R)	Fruit (NR)	89.1	1.2	0	0	0	0	0	0	0.4	1.9	Overdorff et al., 1997
Eulemur macaco macaco	Fruit (NR)	Flower (R)	10	69	2	0	0	0	0	0	16	2	Simmen et al., 2007
Eulemur fulvus rufus	Fruit (NR)	Leaf (R)	12	85	0	0	2	0	0	0	0	0	Simmen et al., 2003
Eulemur fulvus collaris	Fruit (NR)	Flower (R)	3.2	74	0	0	2.6	0	0	0	14	0.7	Donati et al., 2007
Cheirogaleus major	Fruit (NR)	Flower (R)	0	69	1	0	7	0	0	0	23	0	Lahann 2006
Callicebus moloch	Fruit (NR)	Seed (R)	17.2	42.2	0	34.2	0	0	0	0	0	6.2	Müller 1996
Pithecia pithecia	Seed (R)	Fruit (NR)	5.7	25.1	0	63.2	3	0	0	0	1.8	0	Norconk et al., 2004
Chiropotes satanas	Seed (R)	Fruit (NR)	0.4	30	0	66.2	0	0	0	0	3.4	0	van Roosmalen et al., 1988
(R) indicates a resistant diet and (NR) indicates a non-resistant diet													

Table 3.4. (Cont.)

Species	Primary diet	Secondary diet	Leaf	Fruit	Gum	Seed	Animal	Grass	Stems Bark	Roots Tuber	Flower	Other	Reference
Saimiri sciureus	Fruit (NR)	Animal (R)	0	55.1	0	0	44.9	0	0	0	0	0	Lima & Ferrari 2003
Cebus capucinus	Fruit (NR)	Animal (R)	1.3	81.2	0	0	16.9	0	0	0	0.2	0	Chapman & Fedigan 1990
Saguinus oedipus	Fruit (NR)	Gum (NR)	0	38.4	14.4	0	40	0	0	0	0	0	Garber 1980
Callithrix jacchus	Gum (NR)	Fruit (NR)	0	15	68.6	0	14.6	0	0	0	0	0	Passamani & Rylands 2000
Aotus trivirgatus	Fruit (NR)	Animal (R)	4	70	0	0	15	0	0	0	10	0	Wright 1989
Lagothrix logotricha	Fruit (NR)	Leaf (R)	10	71	0	5	5	0	0	0	5	0	Dew 2005
Alouatta caraya	Leaf (R)	Fruit (NR)	60	30	0	0	0	0	8	0	2	0	Bicca-Marques et al. 1994
Pan paniscus	Fruit (NR)	Leaf (R)	21	49	0	9	0	0	15	0	6	0	Badrian et al., 1981
Trachypithecus francoisi	Leaf (R)	Fruit (NR)	51.2	34.6	0	5.5	0	0	0	0	7.8	1	Ruslin et al., 2019
Trachypithecus cristatus	Leaf (R)	Fruit (NR)	85	9	0	0	0	0	0	0	0	0	Hock & Sasekumar 1979
Semnopithecus entellus	Leaf (R)	Fruit (NR)	57.1	15.1	0	7.3	0	0	5.4	7.7	6.9	0	Sayers & Norconk 2008
Colobus guereza	Leaf (R)	Fruit (NR)	87.5	7.3	0	0.23	0	0	1.55	0	2.21	0	Harris & Chapman 2007
Macaca mulatta	Leaf (R)	Fruit (NR)	48.9	27.3	0	0.8	0	0	8.7	0	1.8	0	Tang et al., 2016
Macaca fascicularis	Fruit (NR)	Leaf (R)	17.2	66.7	0	0	4.1	0	0	0	8.9	3.2	Yeager 1996
Papio anubis	Fruit (NR)	StemsBark (R)	12	40	0	8.5	0.5	0	23.9	3.5	0	21	Okecha et al. 2006
Cercocebus agilis	Fruit (NR)	Leaf (R)	7	75	0	3	5	0	0	0	1	0	Shah 2003
(R) indicates a resistant diet and (NR) indicates a non-resistant diet													

Table 3.4. (Cont.)

Species	Primary diet	Secondary diet	Leaf	Fruit	Gum	Seed	Animal	Grass	Stems Bark	Roots Tuber	Flower	Other	Reference
Cercopithecus neglectus	Fruit (NR)	Leaf (R)	24.5	44	0	4	15	0	0	0	9	0	Cords 1986
Erythrocebus patas	Animal (R)	Fruit (NR)	0.8	24	22.3	8.7	36.2	0	0	0	1.7	0	Nakagawa 2003
(R) indicates a resistant diet and (NR) indicates a non-resistant diet													

STATISTICAL ANALYSES

Preparing Data for Analyses

All statistical analyses for this dissertation were performed in either Microsoft Excel or RStudio (version 1.3.1093). Each variable was tested for normality using the Shapiro-Wilk Normality test using package *stats* and function “shapiro.test” (version 3.6.1). All variables had non-normal data distribution (p-value < 0.001 for all variables). Because all variables had non-normal data, Bonett-Seier Tests for Equality of Variances (package *intervcomp,* function “Bonett.Seier.test”, version 0.1.2) were used to establish that the variances between the left and right side of each individual were equal. After establishing equal variance for all side variables and because the data were non-normal, I used Mann-Whitney U tests (package *stats*, function “wilcox.test”, version 3.6.1) to establish if there were significant differences between the left and right sides of each individual. No significant differences were found between the left and right sides. This process of variance tests and Mann-Whitney U tests was replicated to establish if there were significant differences between males and females, where both sexes were available for a given species. The following variables were found to be significantly different by sex: left and right mandibular canine root surface area, left and right mandibular canine enamel area, left and right canine DNE, left and right canine RFI, left and right canine OPC, left and right canine slope, and left and right dentin surface area. This was expected due to the known sexual dimorphism in most primate species (Plavcan, 1993; Plavcan & van Schaik, 1992).

Because there were no significant differences between sides, the left and right side for each individual was combined to create averages for all variables. These combined averages were again tested for normality using Shapiro-Wilk normality tests to confirm that the averaged variables were also non-normal (p-value < 0.001 for all variables). After all variables were averaged for by individual and it was established that the data was non-normal, the data needed several transformations so that it could be directly compared (i.e., power reductions and size-adjustment) and so that it would reach normality (i.e., natural log transformation). First, if a

variable was to the second or third power (i.e., a cross-sectional area), the square root or cubed root of the averaged variable was found. When all variables where in the correct power (i.e., the first), I used the mandible length measurement to create Mosimann variables (Jungers et al., 1995; Mosimann, 1970). Mosimann variables use a standard measurement (in this case mandible length) as the denominator to create ratios for each variable. By using a standard measurement in all species, and a measurement that is closely related to the other variables used, Mosimann variables can remove size as a contributing factor that may affect further analysis (Jungers et al., 1995). These ratio variables are often called the "isometric" or "geometric" size in a given dataset because while they remove overall size as a contributing factor, these variables will continue to express allometric differences across individuals (which is reflected in the dataset presented here) (Jungers et al., 1995). Finally, because the data was not normal across all variables, I took the natural log of each to normalize the dataset.

These final values, that were in the correct power, adjusted for size, and natural log transformed, were averaged by variable to create species averages. Two final datasets were created: one that averaged all individuals by species and one that averaged all individuals by both species and sex (i.e., the sexes were separated out and then averaged by species). This was because the canine variables were shown to be significantly different in the initial means tests.

To address my research questions and their corresponding hypotheses, a series of analyses were used to evaluate the data, including phylogenetic generalized least squares analysis (PGLS) (Grafen, 1989), phylogenetic regressions (a type of multiple regression that takes into account phylogeny), Pearson Correlation Coefficient analyses (Galton, 1886), and phylogenetic analysis of variance (phyANOVA) (Garland et al., 1993). Analyses incorporated phylogenetic relationships and used established phylogenetic trees (see Figure 3.1 for the tree used here) downloaded from the 10k trees website (Arnold et al., 2010). These analyses were performed in RStudio using the packages *caper* function "pgls" version 0.0-1 for PGLS analyses

and phylogenetic multiple regressions, *stats* function "cor.test" version 3.6.1 for Pearson Correlation analyses, and *phytools* function "phylANOVA" version 0.7-70 for phylANOVA analyses. For all PGLS analyses, a separate function was used (written by C. Terhune for personal use) that utilized the package *phytools*, function "phyl.RMA" to test if the slope was signficantly different from one. Specific analyses used for each research question are outlined within Chapters 4-6. For all analyses, data was visualized using a variety of techniques including box plots, scatter plots, and plotting of variables on phylogenetic trees to view the relationships between all variables.

Error Analyses

An error analysis was performed during initial data collection to determine if it was necessary to standardize voxel (micron) size across all specimen scans by resampling the data in Avizo. To do this, I resampled the voxel size of the same scan (with an original voxel size of 0.0348) to 0.025, 0.05, 0.075, and 0.1 to create four separate datasets. For each dataset, the mandibular canal was segmented using the procedure outlined above and a .ply model generated. These canals were then measured in Geomagic using the "cross-sectional area" measurement function in the "Analysis" tab at the mental foramen, halfway point along the canal, and the mandibular foramen. This study showed few differences in cross-sectional area at these points, indicating that it is not necessary to standardize voxel size across samples. Measurements taken in this error study are shown in Table 3.5. Thus, in data collection we aimed to create scans with the smallest voxel size possible so that more detail could be seen within each scan.

Table 3.5. Results from re-sampling study performed on *Rattus norvegicus*

Voxel Size	Mandibular Foramen cross-section	Halfway point cross-section	Mental Foramen cross-section
0.025	0.121	0.096	0.101
0.05	0.119	0.098	0.099
0.075	0.115	0.099	0.089
0.1	0.121	0.106	0.103

A second error analysis was performed to establish intra-observer error on three of the measurements taken by CBY: 1) mandible length, 2) cross-sectional area below M_1 (left side only), and 3) cross-sectional area of the nervous tissue at the mandibular foramen. Each measurement was taken three times (called "treatments") for 11 randomly selected specimens. Using Shapiro-Wilk Normality tests (package *stats,* function "wilcox.test", version 3.6.1) all three variables showed normal data across all measurement treatments. Because the data was normally distributed, Bartlett's Test of Homogeneity of Variances (package *stats*, function "bartlett.test" version 3.6.1) was used to establish that there were equal variances among treatments for each measurement. Finally, a repeated measures ANOVA was performed to establish if there were significant differences among treatments for each variable using package *rstatix*, function "anova_test" (version 0.7.0). There were no significant differences in mandible length (p-value = 0.999), the cross-sectional area below M_1 in the mandibular canal (p-value = 0.999), and the cross-sectional area of the nervous tissue at the mandibular foramen (p-value = 0.985).

Wear Analysis

Finally, I performed a wear analysis on a portion of my data to establish if wear had a significant effect on the dental shape variables (DNE, RFI, OPC, and occlusal slope). While teeth are adapted to eat certain diets through changes in both shape and size, teeth do not maintain a singular form throughout the lifetime of an individual (e.g., Kay, 1975; Lucas, 2006). Additionally, the primary morphology is not necessarily the form that has the highest efficiency in terms of mechanical breakdown. Rather, it has been shown that the "secondary morphology" – a tooth after it has some wear – is more efficient at mechanical breakdown than the primary morphology (Fortelius, 1985; Ungar, 2015). However, as the tooth continues to wear and becomes a flat platform, the tooth again loses efficiency in mechanical breakdown (Janis, 1990). Thus, being able to quantify wear is necessary to establish if wear is affecting the shape of a given tooth's occlusal surface and thus the efficiency of the breakdown process. Wear itself is

considered an adaptive response because it increases the tooths ability to survive and breakdown foods without damage to the tooth itself. However, the literature shows that wear is much more useful as a response in species that eat coarser diets. Other adaptive responses, such as thickening of enamel, are frequently seen in primates that focus on eating fruit and seeds (Kay, 1975; Pampush et al., 2013; Pampush et al., 2016b; Teaford, 2007; Ungar & Williamson, 2000). Therefore, even though all teeth wear down, they do not wear at the same rate between species or at the same rate within species based on diet and food preference.

In this study, I established a wear index using the dentin exposure area (Figure 3.7A) and the occlusal surface area (Figure 3.7B). Dentin exposure is calculated by highlighting the areas of exposed dentin (using Geomagic "surface area" function) and dividing that by the surface area of the entire occlusal surface. This gives a percentage of how much wear the tooth has experienced.

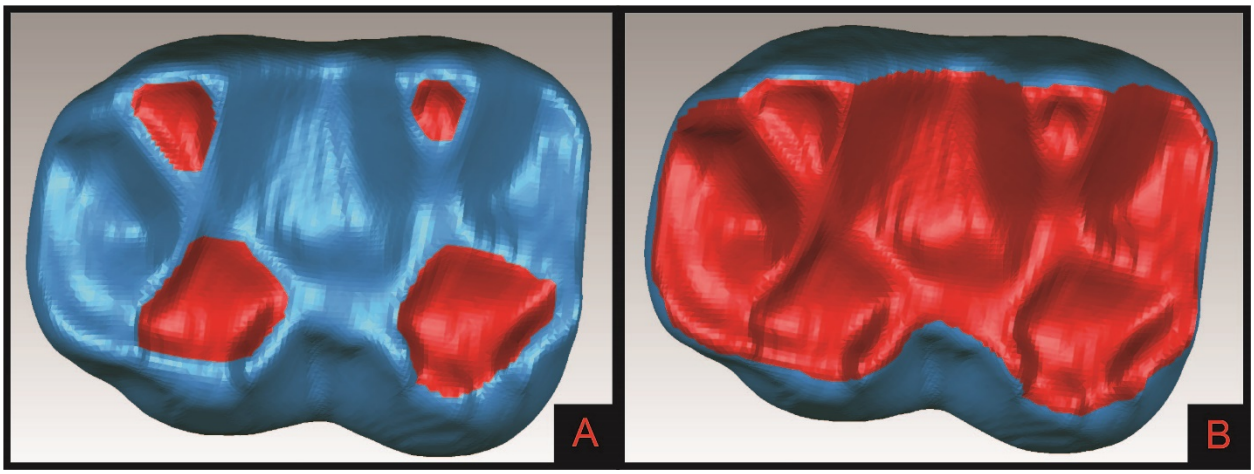

Figure 3.7. An example of how the wear index was calculated for the wear error analysis in CET-173 (*Erythrocebus patas*). First, the dentin exposure is highlighted (A) on the surface of the tooth. Second, the entire occlusal surface of the tooth is highlighted (B). Both highlighted areas then have their surface areas calculated with the "surface area" function in Geomagic. Finally, the dentin area is divided by the occlusal surface area, giving a wear index.

To assess the impact of wear on occlusal shape, four species (*Aotus trivirgatus*, *Saimiri sciureus*, *Saguinus oedipus*, and *Macaca mulatta*) were selected for analysis. Species were chosen based on two factors: 1) these four species had at least 8 specimens and, 2) individuals

came from multiple sources (i.e., while a majority of the *Saimiri sciureus* specimens were provided by the Duke Miami Collection, some also came from the Lucas and Copes project on morphosource.org). This was done so that I could establish intraspecific variation and to see if some collections showed more worn teeth than others more often. Table 3.6 shows the overall ranges and means of wear within the entire sample and each of these four species parsed out.

Table 3.6. Wear measurements for the sample

Grouping (n)	Wear Range (%)	Mean (% teeth with wear scores below mean)
Overall sample (262)	M_1: 0.45 - 72.9 P_4: 0.41 – 77.6 C_1: 0 – 59.3 I_1: 0.74 – 67.5	M_1: 14.5 (68.4) P_4: 9.20 (74.8) C_1: 5.03 (73.0) I_1: 22.4 (57.3)
Aotus trivirgatus (8)	M_1: 2.46 – 68.2 P_4: 1.42 – 41.1 C_1: 2.15 – 4.90 I_1: 17.5 – 59.2	M_1: 15.6 (75.0) P_4: 8.78 (85.7) C_1: 3.33 (75.0) I_1: 29.9 (71.4)
Saimiri sciureus (32)	M_1: 0.63 – 38.3 P_4: 4.21 – 23.9 C_1: 1.01 – 27.3 I_1: 3.92 – 53.3	M_1: 6.97 (70.4) P_4: 4.54 (79.3) C_1: 4.82 (66.7) I_1: 26.6 (53.8)
Saguinus oedipus (9)	M_1: 6.07 – 19.9 P_4: 5.04 – 15.2 C_1: 0.89 – 8.47 I_1: 6.94 – 49.9	M_1: 10.6 (66.7) P_4: 7.58 (62.5) C_1: 3.20 (66.7) I_1: 27.4 (75.0)
Macaca mulatta (10)	M_1: 11.4 – 72.9 P_4: 5.10 – 36.3 C_1: 1.76 – 36.7 I_1: 16.2 – 48.0	M_1: 31.6 (55.6) P_4: 15.9 (50.0) C_1: 10.2 (70.0) I_1: 25.6 (75.0)

Table 3.5. illustrates that some individuals show considerable wear in this sample. Across species, incisors show the most, molars second most, premolars third most, and canines show the least amount of wear, at least as measured via dentin exposure. The pattern for *Macaca mulatta* is slightly different, where this species shows the highest wear in the molars, then incisors, then premolars, and canines. However, most of the sample falls below the mean wear index with some outliers causing the mean to increase. To test if wear had a significant effect on the shape values from the occlusal surface, I ran a series of linear regressions in

RStudio (package *stats*, function “lm”) to establish if there was a significant relationship between the wear index and the shape variables. The results of this analysis are shown in Table 3.6. Results reveal that the wear index showed a significant relationship with DNE only in the premolars of *S. sciureus* (p-value = 0.004) (Table 3.7). Wear index showed significant relationships to RFI in the molars (p-value = 0.003), premolars (p-value = 0.009), and canines (p-value = 0.005) in A. *trivirgatus*, all teeth (M_1: p-value < 0.001, P_4: p-value < 0.001, C_1: p-value = 0.012, I_1: p-value = 0.002) in *S. sciureus*, and the molars (p-value = 0.007) in *M. mulatta*. Wear index showed a significant relationship to OPC only in the premolars (p-value = 0.001) and incisors (p-value < 0.001) in *S. sciureus.* Finally, wear index had a significant relationship to occlusal slope in the molars (p-value = 0.001) and incisors (p-value = 0.010) in *A. trivirgatus*, the molars (p-value < 0.001), premolars (p-value < 0.001), and the canines (p-value = 0.001) in *S. sciureus*, and the molars (p-value = 0.003) in *M. mulatta*. Interestingly, there were no significant relationships between the wear indices and the shape variables in any tooth in *S. oedipus*.

Only RFI and occlusal slope showed significant relationships in *A. trivirgatus*, with molars significant in both – indicating wear may have a significant effect on the shape of the occlusal surface in this species. Additionally, the R^2 values for these tests were relatively high (between 0.762 – 0.989) indicating that the variance in this sample is very well explained by the dependent variable. Most significant relationships were found in *S. sciureus,* which had the smallest overall wear and the largest sample size. However, the R^2 values for most of these regressions were relatively low (between 0.267 – 0.558) indicating that the variance seen in these regressions is not well explained by the dependent variables. As stated previously *S. oedipus* showed no significant relationships, indicating that wear in this sample does not significantly affect the shape of the occlusal surface in this species. Finally, *M. mulatta* only showed significant relationships again with RFI and occlusal slope in the molar teeth.

Table 3.7. Linear Regression analysis results for wear index and tooth shape variables (without size-adjustment)

***Aotus trivirgatus* (6 df)**			
Dependent variable*	**Independent variable**	**p-value**	**R^2**
DNE	Wear index	M_1: 0.196 P_4: 0.048 C_1: 0.278 I_1: 0.988	M_1: 0.261 P_4: 0.575 C_1: 0.521 I_1: < 0.001
RFI	Wear index	M_1: **0.003** P_4: **0.009** C_1: **0.005** I_1: 0.016	M_1: 0.791 P_4: 0.779 C_1: 0.989 I_1: 0.719
OPC	Wear index	M_1: 0.032 P_4: 0.020 C_1: 0.449 I_1: 0.061	M_1: 0.559 P_4: 0.696 C_1: 0.303 I_1: 0.538
Occlusal slope	Wear index	M_1: **0.001** P_4: 0.036 C_1: 0.074 I_1: **0.010**	M_1: 0.845 P_4: 0.615 C_1: 0.857 I_1: 0.762
***Saimiri sciureus* (25 df)**			
DNE	Wear index	M_1: 0.031 P_4: **0.004** C_1: 0.253 I_1: 0.214	M_1: 0.173 P_4: 0.267 C_1: 0.086 I_1: 0.064
RFI	Wear index	M_1: **< 0.001** P_4: **< 0.001** C_1: **0.012** I_1: **0.002**	M_1: 0.518 P_4: 0.470 C_1: 0.352 I_1: 0.338
OPC	Wear index	M_1: 0.247 P_4: **0.001** C_1: 0.928 I_1: **< 0.001**	M_1: 0.053 P_4: 0.322 C_1: < 0.001 I_1: 0.473
Occlusal slope	Wear index	M_1: **< 0.001** P_4: **< 0.001** C_1: **0.001** I_1: 0.016	M_1: 0.458 P_4: 0.558 C_1: 0.487 I_1: 0.219
***DNE = Dirichlet's Normal Energy, OPC = Orientation Patch Count, RFI = Relief Index** **Alpha values set at p-value < 0.0125**			

Table 3.7. (Cont.)

***Saguinus oedipus* (7 df)**			
Dependent variable*	**Independent variable**	**p-value**	**R^2**
DNE	Wear index	M_1: 0.924 P_4: 0.853 C_1: 0.518 I_1: 0.283	M_1: 0.001 P_4: 0.006 C_1: 0.062 I_1: 0.188
RFI	Wear index	M_1: 0.188 P_4: 0.532 C_1: 0.295 I_1: 0.515	M_1: 0.233 P_4: 0.068 C_1: 0.155 I_1: 0.074
OPC	Wear index	M_1: 0.068 P_4: 0.859 C_1: 0.069 I_1: 0.640	M_1: 0.397 P_4: 0.006 C_1: 0.397 I_1: 0.039
Occlusal slope	Wear index	M_1: 0.195 P_4: 0.971 C_1: 0.435 I_1: 0.112	M_1: 0.227 P_4: < 0.001 C_1: 0.089 I_1: 0.366
***Macaca mulatta* (7 df)**			
DNE	Wear index	M_1: 0.032 P_4: 0.328 C_1: 0.118 I_1: 0.503	M_1: 0.502 P_4: 0.237 C_1: 0.277 I_1: 0.078
RFI	Wear index	M_1: **0.007** P_4: 0.016 C_1: 0.071 I_1: 0.868	M_1: 0.667 P_4: 0.800 C_1: 0.350 I_1: 0.005
OPC	Wear index	M_1: 0.178 P_4: 0.145 C_1: 0.191 I_1: 0.503	M_1: 0.242 P_4: 0.449 C_1: 0.203 I_1: 0.078
Occlusal slope	Wear index	M_1: **0.003** P_4: 0.031 C_1: 0.153 I_1: 0.840	M_1: 0.738 P_4: 0.726 C_1: 0.238 I_1: 0.007
***DNE = Dirichlet's Normal Energy, OPC = Orientation Patch Count, RFI = Relief Index Alpha values set at p-value < 0.0125**			

The results in Table 3.7 show that, overall, wear index does influence the RFI and occlusal slope values in three of the four species tested, with the largest effect seen in the molars. In contrast, the results tell us that wear does not seem to have a significant effect on the OPC and DNE values in these teeth in most of the species tested. All these analyses indicate

that while wear will have a significant effect on some shape variables in some teeth it does not apply evenly across all primate species.

Figure 3.8 shows the areas of dentin exposure and occlusal surface area (raw mm^2 values collected) in molars across the four species analyzed in Table 3.6. This figure shows that some species have much more dentin exposure and larger occlusal areas than others – particularly *Macaca mulatta*. This is expected because *M. mulatta* tends to eat a much more resistant diet of leaves whereas the other three species tend to focus more on fruit as a primary diet. However, when the data are power reduced and log transformed, the variation between species decreases and the ranges begin to overlap (Figure 3.9). Figure 3.10 shows the wear index for all four species after the dentin exposure area has been divided by the occlusal surface area and then natural log transformed. While the ranges for all four species visually overlapped, I performed an ANOVA (package *stats*, function “aov”) and Tukey HSD (package *broom*, function “tidy.TukeyHSD”) in order to establish if there were significant different between the wear index means. Only two species *M. mulatta* and *S. sciureus* were shown to be significantly different (p-value < 0.001) in the means when all four species were considered. This indicates that in most interactions between species that were tested, the means of the wear index were not significantly different.

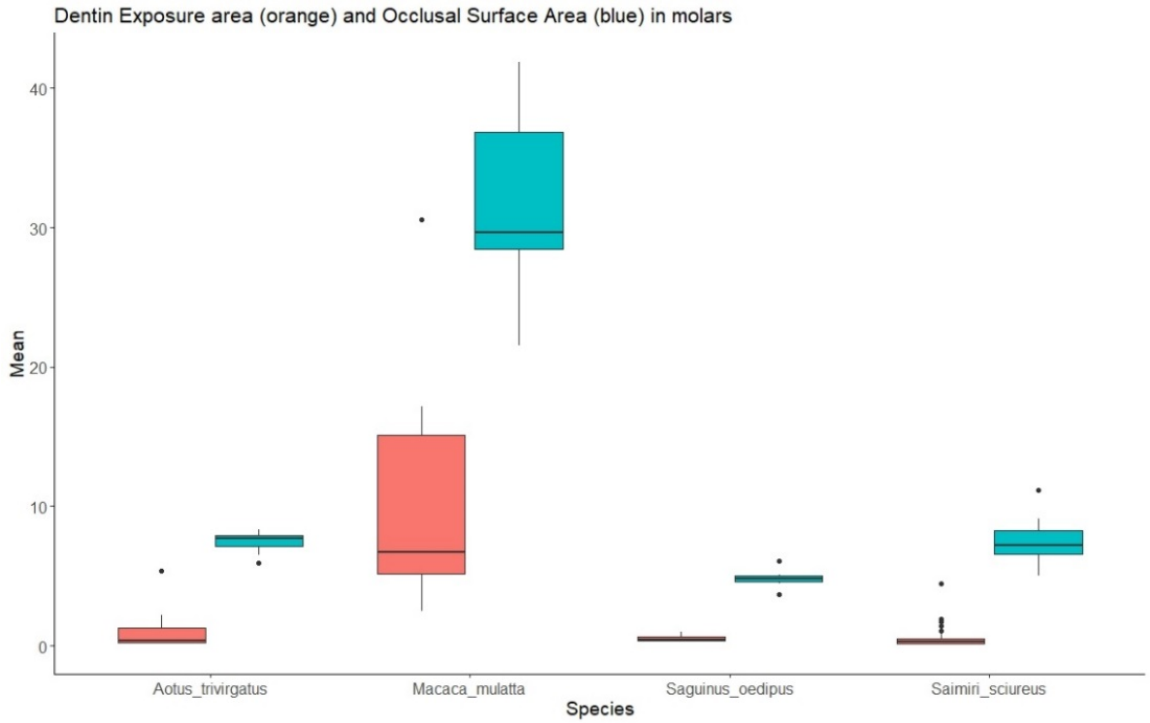

Figure 3.8. The raw values of dentin exposure area (orange) to the raw values of occlusal surface area (blue) seen in four species (*Aotus trivirgatus*, *Macaca mulatta*, *Saguinus oedipus*, and *Saimiri sciureus*). The measurements shown are in mm^2.

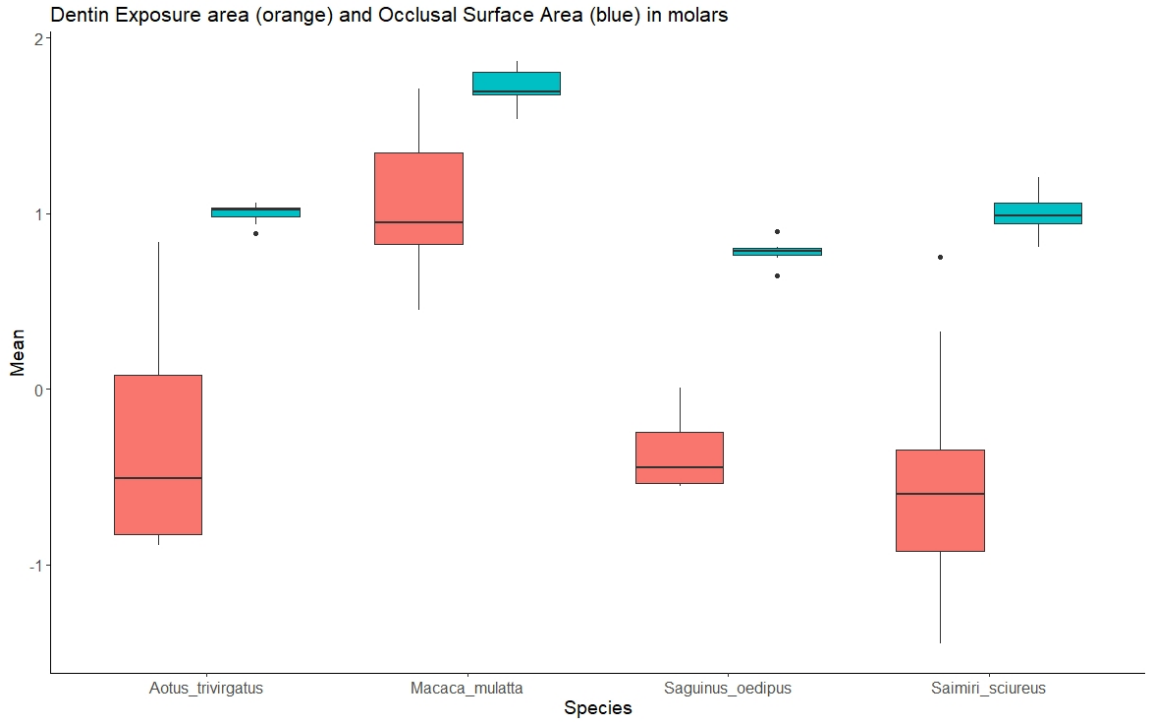

Figure 3.9. The natural log transformed data of dentin exposure area (orange) to the natural log transformed data of occlusal surface area (blue) seen in four species (*Aotus trivirgatus*, *Macaca mulatta*, *Saguinus oedipus*, and *Saimiri sciureus*). These measurements have been reduced to the first power and natural log transformed.

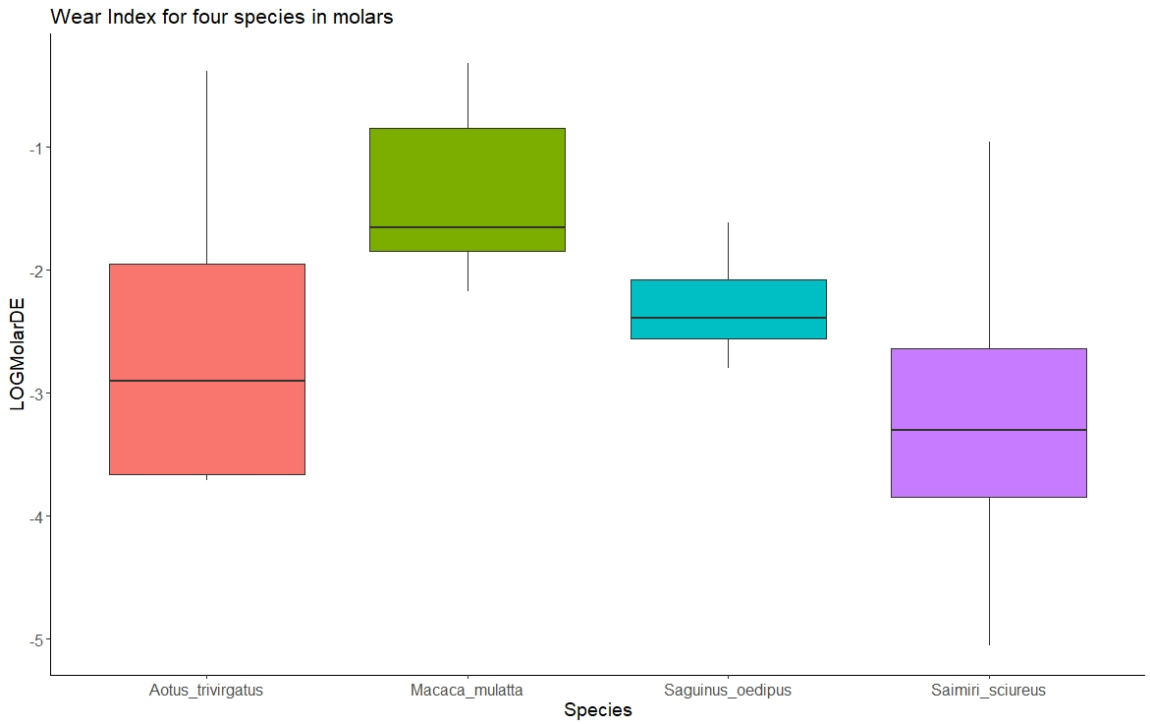

Figure 3.10. The wear index (dentin exposure/occlusal surface area) of the molars in the same four species (*Aotus trivirgatus*, *Macaca mulatta*, *Saguinus oedipus*, and *Saimiri sciureus*) using natural log transformed data. These data are dimensionless.

Because the occlusal shape variables analyzed here are adjusted for gross differences in size, they are excellent quantifiable measurements of a tooths surface that we can use to compare across all species and differently sized individuals (Pampush et al. 2016a). These measurements give us a better idea of how teeth are used *in vivo* rather than only focusing on adaptations associated with broad dietary categories. This dissertation is not aiming to discuss if wear, and thus changes in tooth shape, will affect the size of the nervous tissues. Rather, the goal was to establish if the surface of the tooth as it exists in life is related to the size of the nervous tissues. Because the results of these analyses show that there are few significant relationships between the wear index and the shape variables, wear was not used as a contributing variable for the analyses in Chapter 4 (Question 1).

CHAPTER 4: COVARIATION OF OCCLUSAL TOOTH MORPHOLOGY WITH NERVOUS TISSUE VOLUME

INTRODUCTION

Teeth are perhaps one of the most studied aspects of the skeleton in biological anthropology due to the close relationship between their shape and their food processing capabilities (Hiiemäe & Kay, 1973; Kay, 1975; Leighton, 1993; Lucas & Luke, 1980; Lucas, 1979, 2006; Lumsden & Osborn, 1977; Lund et al., 1998; Strait, 1997, 2001; Taylor, 2002). Although all mammals have the same four basic tooth types, tooth shape and size change due to selective pressures typically associated with environment and diet. The occlusal surfaces of mammalian teeth have been exhaustively studied – and to some point the roots and dentin of the teeth have also been examined – but there has been little research done on the soft tissues that innervate each tooth structure. This research is vital because we know that the teeth transmit predominately pain and pressure information to the brain to maintain accurate chewing cycles and to protect the teeth from damage (Anderson et al., 1970; Avery & Cox, 1977; Booth et al., 2013; Brashear, 1936; Crompton, 1989; Dubner et al., 1978; Luschei & Goldberg, 2011; Plaffman, 1939).

Primates (and many other mammals) use their teeth to test tough/stiff materials – such as leaves, insects, and seeds – to determine the material properties of the food (Kay, 1975; Muchlinski & Deane, 2014; Peyron et al., 2002; Teaford & Oyen, 1989; Vinyard, 2008; Vinyard et al., 2011). Often, material properties can be directly related to the nutrient content a food contains; this suggests that being able to differentiate between minute differences in material properties between food objects could be crucial for survival (Prinz & Lucas, 2000; Scott et al., 2018). While mammals need to be able to physcially consume food through chewing, the nervous impulses from the teeth are transmitting information such as the amount of force necessary to chew an object and if that object should be chewed in the first place. Thus far, no

research has examined whether there is a relationship between the size of the innervating structures of teeth and either the root surface or occlusal surfaces of the teeth, as is the goal here.

BACKGROUND AND HYPOTHESES

Teeth initiate the beginning of the mechanical breakdown process of food in the oral cavity. Through a variety of studies, it is clear that the size and shape of teeth are directly related to the amount of force necessary to break down certain food objects (e.g., Lucas, 2006; Teaford et al., 2006). However, the selective pressures on teeth that have altered tooth size/shape do not act on the tooth as a whole – rather it has been shown that the occlusal surface of teeth is under particularly strong selection to increase mechanical efficiency during food processing (e.g., Kay, 1975; Lund et al., 1998). Additionally, teeth do not maintain a single shape throughout the entirety of an individual's lifetime as they wear down through repeated use (Luke & Lucas, 1983; Murphy, 1968; Prinz & Lucas, 2000). Thus, while teeth are generally adapted to eat a certain diet in a given environment, the surface of a tooth is not static nor is the mechanical breakdown efficiency (Fortelius, 1985; Fortelius & Solounias, 2000; Janis, 1990; Ungar, 2015). Additionally, there is some evidence that teeth are even more efficient in primates that eat tough/fibrous materials in the "secondary morphology" phase where a tooth has been worn down, but to a point that is better than the original tooth morphology at breaking down fibrous foods (Pampush et al., 2016b; Ungar, 2015).

There are many arguments as to what is driving selection in tooth size/shape when it comes to diet. Some researchers argue that teeth are shaped in association with the primary diet that a primate is consuming while many others argue that diet is related to what primates must eat to survive in times of food scarcity (Constantino, 2009; Lambert et al. 2004; Marshall & Wrangham, 2007; Norconk et al., 2009; Rosenberger & Kinzey, 1976). The idea behind food scarcity is predominately looked at in two main ways: critical function foods which require a

specific adaptation to consume a particular food source, and fallback foods that are used as fillers in a diet when the preferred diet is not abundant. The critical function theory is particularly driven by food material properties in that if a food is tougher/stiffer it will require a change in the way the food is mechanically broken down (Rosenberger & Kinzey, 1976; Kinzey & Norconk, 1993; Lucas et al., 2001; Marshall & Wrangham, 2007; Taylor et al., 2009). Alternatively, fallback foods are generally described as fillers in a diet during seasons when preferred foods are not as abundant (Constantino, 2009; Marshall & Wrangham, 2007). For example, many primates prefer to consume the soft flesh of fruit when it is available but may have to eat leaves to supplement their diet.

While teeth are the direct interface with the outside environment and the main component of mechanical breakdown, information on the material properties of food do not come from the bony components themselves. Rather, all nervous impulses from the mandibular teeth and their surrounding soft- and hard-tissues comes from the inferior alveolar nerve (IAN). Teeth are typically responsible for painful impulses (Anderson et al., 1970; Avery & Cox, 1977; Brashear, 1936; Dubner et al., 1978; Luschei & Goldberg, 2011; Plaffman, 1939) while the tooth roots and periodontal ligament predominantly transmit pressure information (Bernick, 1952; Brashear, 1936; Byers et al., 1986; Capra & Wax, 1989; Kubota & Osanai, 1977; Kuzentsova & Smirnov, 1969; Linden, 1991; Loewenstein & Rathkamp, 1955; Plaffman, 1939; Trulsson et al., 1992; Yamada & Kumano, 1969). These pressure and pain impulses help primates to maximize chewing efficiency and prevent damage to the tooth row during normal mastication. Additionally, these nervous impulses transmit information on the material properties of food that may affect the nutrient levels a primate is able to consume (Davies et al., 1988; Ganzhorn et al., 2017; Kar-Gupta & Kumar, 1994).

The purpose of Question 1 (Q1) is to establish if there are relationships between the root surface structures, the enamel surface, and the nervous tissue variables. Because of the known close relationship between the size and shape of teeth and diet, it is necessary to establish if

there is a relationship between the hard- and soft-tissue structures before determining if the soft-tissue structures are under the same selection pressures as the teeth. Overall, previous work indicates that there is a relationship between the size/shape of the occlusal surface and the root structures that anchor the teeth into the maxillary bone. Two studies (Deines et al., 1993; Spencer, 2003) have demonstrated that the relative root surface area of the maxillary molar teeth is larger in species where the teeth are more heavily loaded during mastication, whether by more chewing cycles or tougher/stiffer overall diets. While this has been true in maxillary teeth, no research has been done to establish if this is the case in mandibular teeth.

Additionally, because it is understood that the teeth and periodontal membrane transmit information to the brain to improve chewing cycles and assess food material properties, there should be a relationship between these nervous tissues and the teeth that they supply (Booth et al., 2013; Crompton, 1989; Lund, 1991; Lund & Kolta, 2006; Luschei & Goldberg, 2011; Rees, 1954; Thexton et al., 1980). However, no research has been done to establish if there is relationship between the size/course of the IAN to either occlusal tooth morphology or root surface area. This chapter will establish if the hard-tissue components of teeth have significant relationships to the soft-tissue structures of the IAN throughout the mandible.

Here, I investigate this research area by asking the overarching question: “Does occlusal tooth morphology covary with nervous tissue?”. Specifically, I test three separate but related hypotheses:

H_1: There is a direct positive relationship between the size and shape of the occlusal surface of the teeth (i.e., the enamel surface area) and the size of the root structures (i.e., root surface area).

H_2: There is a direct positive relationship between the size and shape of the occlusal surface of the teeth and the nervous tissue that directly supplies the tooth.

H_3: There is a direct positive relationship between root surface area and the nervous tissues within the mandible.

MATERIALS AND METHODS

Data Collection and Preparation

To assess if there is a relationship between the occlusal surface of the teeth, root surface area, and the size of the IAN, I used the variables for "Q1" as outlined in Table 3.1 under the column header "Associated Research Question". Chapter 3 describes the data collection process for all soft- and hard-tissue variables and data preparation (i.e., size adjustment, log transformation, etc.) used for this chapter. All analyses for Q1 used a total of 261 individuals from 68 primate species for all hard-tissue variables (128 females, 125 males, 8 unknown sex) (Figure 3.1). Soft-tissue variables were collected from 56 individuals from 31 primate species (21 females, 27 males, 8 unknown sex) (see Table 3.3). Summary statistics for the raw data of all variables used in Q1 can be found in Tables A.2-8. Additionally, each species was given a species "code" to better show each species on figures. For example, *Papio anubis* would be given the code PAAN. These codes, their corresponding families, and the color identifiers from each figure can be found in Table 3.2.

Analytical Methods

For all hypotheses, and because each of these variables are numerical and continuous, I used a series of phylogenetic generalized least squares (PGLS) regressions to determine the significance of the hypothesized relationships (Grafen, 1989). Additionally, I also used phylogenetic multiple regressions to establish the interactions between each of the tooth surface variables, the root surface area, and the nervous tissue variables. These multiple regressions show the impact that the independent variables have on the outcome of the value of the dependent variable in a given model. Additionally, these tests show which of the independent variables significantly predict the outcome of the dependent variable (in this case the size of tissues), which allow me to create predictive models using only significant independent variables. All analyses were performed in RStudio using package *caper* function "pgls" version 0.0-1. To correct for type I error (false positives) in the statistical analyses, a manual alpha value

correction was used and is stated in each table reporting the test results. Additionally, all slopes were tested to establish if they were significantly different from one using a custom function (written by C. Terhune) utilizing functions from the package *phytools*. Question 1 (Q1) asks, "Does occlusal tooth morphology covary with nervous tissue" and a general overview of the analyses for Q1 are shown in Table 4.1.

Table 4.1. Tests performed in Question 1

Dependent variable	Independent variable*	Test	Hypothesis
Root surface area	Enamel surface area	PGLS	H1
Root surface area	DNE	PGLS	
Root surface area	OPC	PGLS	
Root surface area	RFI	PGLS	
Root surface area	Occlusal slope	PGLS	
Root surface area	DNE, OPC, RFI, Slope	Phylogenetic multiple regression	
Nervous tissue	Enamel surface area	PGLS	H2
Nervous tissue	DNE	PGLS	
Nervous tissue	OPC	PGLS	
Nervous tissue	RFI	PGLS	
Nervous tissue	Occlusal slope	PGLS	
Nervous tissue	DNE, OPC, RFI, Slope	Phylogenetic multiple regression	
Nervous tissue	Root surface area	PGLS	H3
Nervous tissue	Root surface area	Phylogenetic multiple regression	
***DNE = Dirichlet's Normal Energy, OPC = Orientation Patch Count, RFI = Relief Index**			

I expected to have difficulties analyzing and interpretating the data because of the vast differences in size in my sample. Within the sample, there are many examples of small-bodied primates (from both the western hemisphere and strepsirrhines) and medium bodied primates (particularly Cercopithecidae) but there are very few apes in the sample. Overall, apes are much larger than most of the primates in this sample, therefore making it difficult to directly compare across all specimens. To examine the effects of these large differences in size, I first examined my data with no size adjustment. These analyses will be presented first to discuss the allometry of the sample and some other patterns in the raw data. Next, to adjust for these large size differences, all analyses utilize Mosimann variables (Jungers et al., 1995; Mosimann, 1970) to

directly compare across all specimens. Each hypothesis will be broken down and analyzed using the size-adjusted data to understand the relationships between each component without isometric size differences acting as a conflating variable.

Specifically, for Q1-H1, I used the occlusal surface variables (enamel surface area, Dirichlet's Normal Energy (DNE), Orientation Patch Count (OPC), Relief Index (RFI), and occlusal slope) and the root surface area for each tooth class (M_1, P_4, C_1, I_1) to establish the relationship between the size and shape of the occlusal surface of the teeth and the size of the root structures.

For Q1-H2, I used the occlusal surface variables (enamel surface area, dentin exposure area, DNE, RFI, OPC, and occlusal slope), and the nervous tissue variables (total IAN volume, the nerve CSA at the mandibular and mental foramina, and the nerve CSA directly beneath the molars and premolars) to establish the relationship between the size and shape of the occlusal surface of the teeth and the nervous tissues that supply the teeth.

For Q1-H3, I used the root surface area variable and the nervous tissue variables (total volume, the nerve CSA at the mandibular and mental foramina, and the nerve CSA directly beneath the molars and premolars) to establish the relationship between the surface area of the tooth roots and the nervous tissues that supply the teeth.

In the initial data preparation (see Chapter 3) it was established that all canine variables were significantly different by sex within the dataset. This was expected based on known patterns of sexual dimorphism in primates (Plavcan, 1993). Because of this, all canine data was analyzed by first separating out all individuals by sex and then creating male and female species average data. However, the canine data was also analyzed with the males and females combined to establish if sex played a significant role in the relationships between the hard- and soft-tissue variables. Specifically, I expected males to have larger overall canines because males tend to have overall larger body sizes. Plavcan (1993) explains that although canines scale isometrically to body size, they vary significantly across primate families and subfamilies.

Additionally, studies have shown that canine size in male primates is much more closely associated with intermale competition and is less associated with variation in diet (Greenfield, 1992; Harvey et al., 1978; Kay et al., 1988; Leutenegger & Kelly, 1977; Plavcan & van Schaik, 1992; Plavcan, 1993). Therefore, I expected to find closer associations between female canines and diet because females are not often associated with using canines as weapons. Additionally, some species use canines for specialized purposes such as opening hard-objects for feeding or puncturing hard-objects prior to ingesting (Greenfield, 1992; Kinzey & Norconk, 1993). These specializations will also affect the size and shape of canine teeth but would be related to diet across both males and females.

RESULTS

Summary Statistics and Raw Data

Appendix Tables A.1 – A.8 show the summary statistics for all variables analyzed in this chapter for Q1). Because the data was non-normal, Mann-Whitney U tests were used to establish that most canine variables showed significant differences between males and females (Table 4.2), justifying the separation of sexes for all analyses involving the canines.

Table 4.2. Mann-Whitney U test results for canine occlusal variables

Occlusal surface variable	p-value
Root surface area	**0.004**
Enamel surface area	**0.014**
DNE	**< 0.001**
RFI	**< 0.001**
OPC	**0.012**
Occlusal Slope	**< 0.001**
Alpha values were set to p-value < 0.050	

Also as expected, size variation (as represented by mandible length) was considerable in this sample. In terms of mandible length, the smallest individual belonged to the species *Cheirogaleus major* (17.365 mm) while the largest individual belonged to the species *Pongo abelii* (193.732 mm). The average mandible size for the sample was 66.55 mm. Figure 4.1

shows the species average mandible lengths for the entire sample by family group. Some families, like Hominidae and Cercopithecidae show much larger ranges in variation in mandible length, while others like Cheirogaleidae and Indriidae show much less variation. This is likely due to sample size in that there were many more species within some families than others.

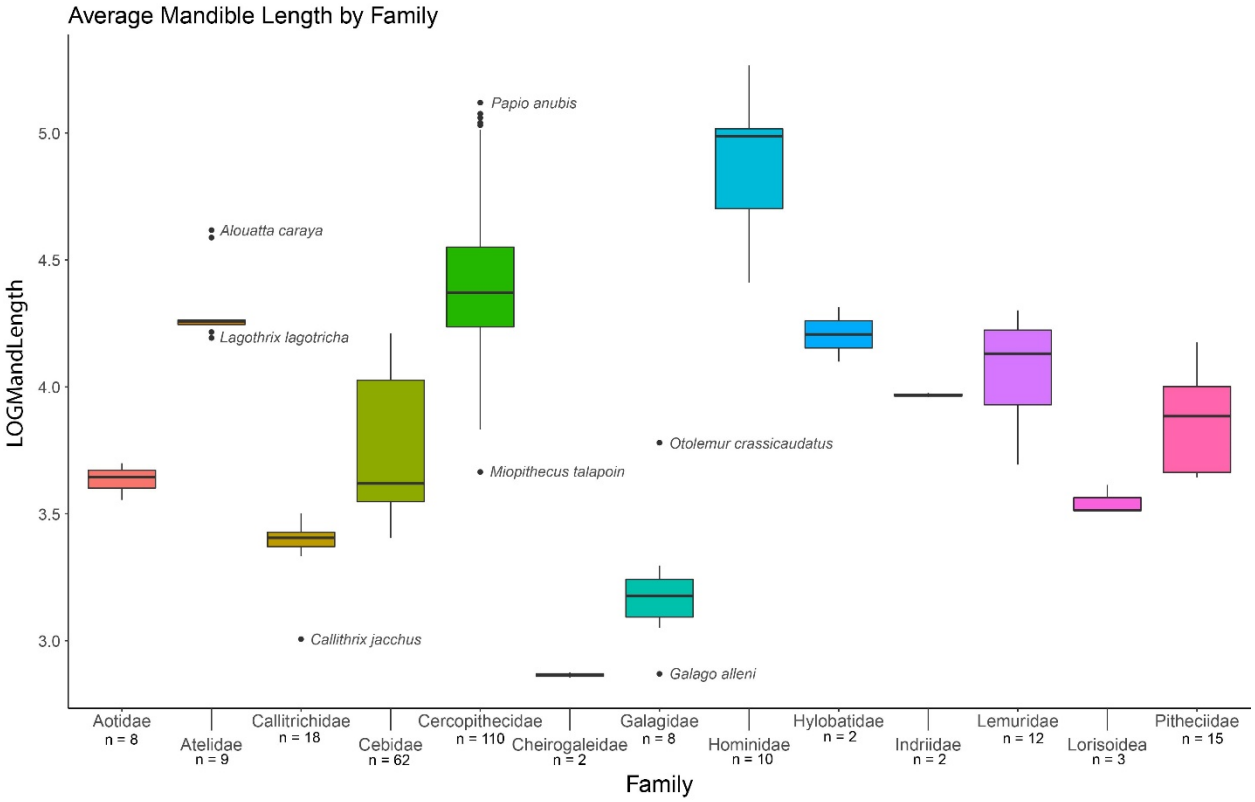

Figure 4.1. The mandible length ranges for each primate family using log transformed data.

To visualize the data, I created a series of boxplots showing variables collected for this chapter (molar data is shown here as an example). First, I wanted to see what the relationship between the enamel surface area and the root surface area for the molar teeth looked like by family. Figure 4.2 shows the power reduced and natural log transformed data comparing the enamel surface area (orange) and the root surface area (blue).

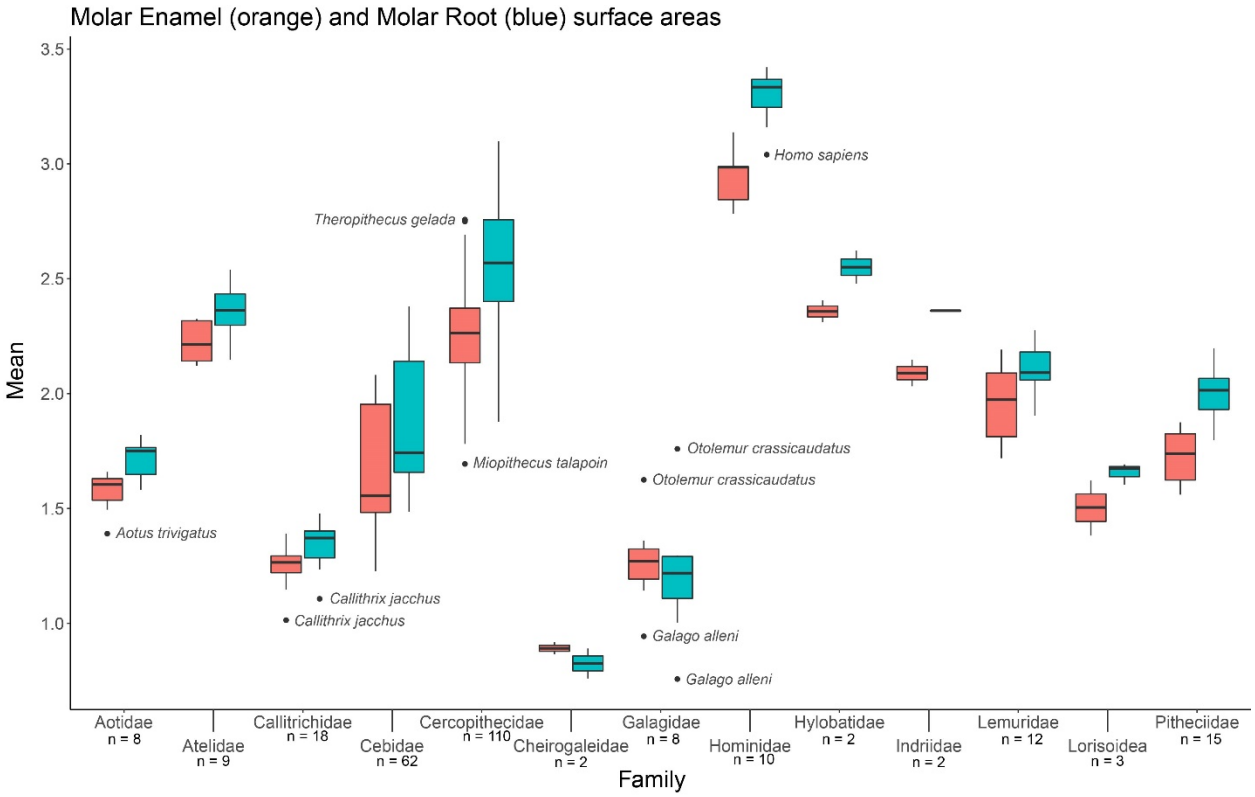

Figure 4.2. The molar root and enamel surface areas (power reduced and natural log transformed) within the sample by primate family.

In nearly all clades, root surface area was larger than the enamel surface area except for Cheirogaleidae and Galagidae, indicating that these families have smaller roots than expected when all major families within primates are assessed. While the ranges for the enamel and root surfaces for each family visually overlapped in many cases, I performed a phylogenetic ANOVA in RStudio (package *phytools*, function “phylANOVA”) to establish if there were significant differences between family groups in all hard-tissue variables in this chapter on the power reduced and natural log transformed data. The results of these phylANOVAs are shown in Table 4.3. No analysis showed significant differences between the means of any variable by family group.

Table 4.3. phylANOVA results for hard-tissue variables

Dependent variable	F-statistic	p-value
Root surface area		
Molar	38.404	0.059
Premolar	30.691	0.126
Canine	24.466	0.195
Incisor	29.462	0.135
Enamel Surface Area		
Molar	31.767	0.141
Premolar	33.245	0.097†
Canine	15.153	0.359
Incisor	17.239	0.246
DNE		
Molar	2.870	0.967
Premolar	3.807	0.936
Canine	3.254	0.942
Incisor	10.069	0.455
RFI		
Molar	2.818	0.965
Premolar	4.905	0.892
Canine	23.803	0.171
Incisor	18.527	0.139
OPC		
Molar	2.422	0.976
Premolar	2.359	0.984
Canine	2.309	0.968
Incisor	5.954	0.783
Occlusal slope		
Molar	3.739	0.931
Premolar	1.380	0.999
Canine	15.613	0.324
Incisor	7.763	0.630

Alpha values set to p-value < 0.050
***DNE = Dirichlet's Normal Energy, OPC = Orientation Patch Count, RFI = Relief Index**
†Indicates significantly different families within test

While none of the phylANOVA analyses were significant, one analysis showed pairwise differences between families: premolar enamel surface area between Atelidae and Callitrichidae (p-value = 0.045)**.** This indicates that when the data is normalized and phylogeny is considered, there are very few significant differences between primate families in terms of size and shape of the teeth.

For the occlusal surface variables, I also created boxplots of the molar data for DNE (Figure 4.3), RFI (Figure 4.4), OPC (Figure 4.5), and occlusal slope (Figure 4.6) of the natural log transformed data to give examples of how these data compare to each other across family groups. These plots visually show that there are no significant differences between the means for occlusal shape variables across all family groups. All the ranges for occlusal shape variables overlap across family groups, with very few outliers.

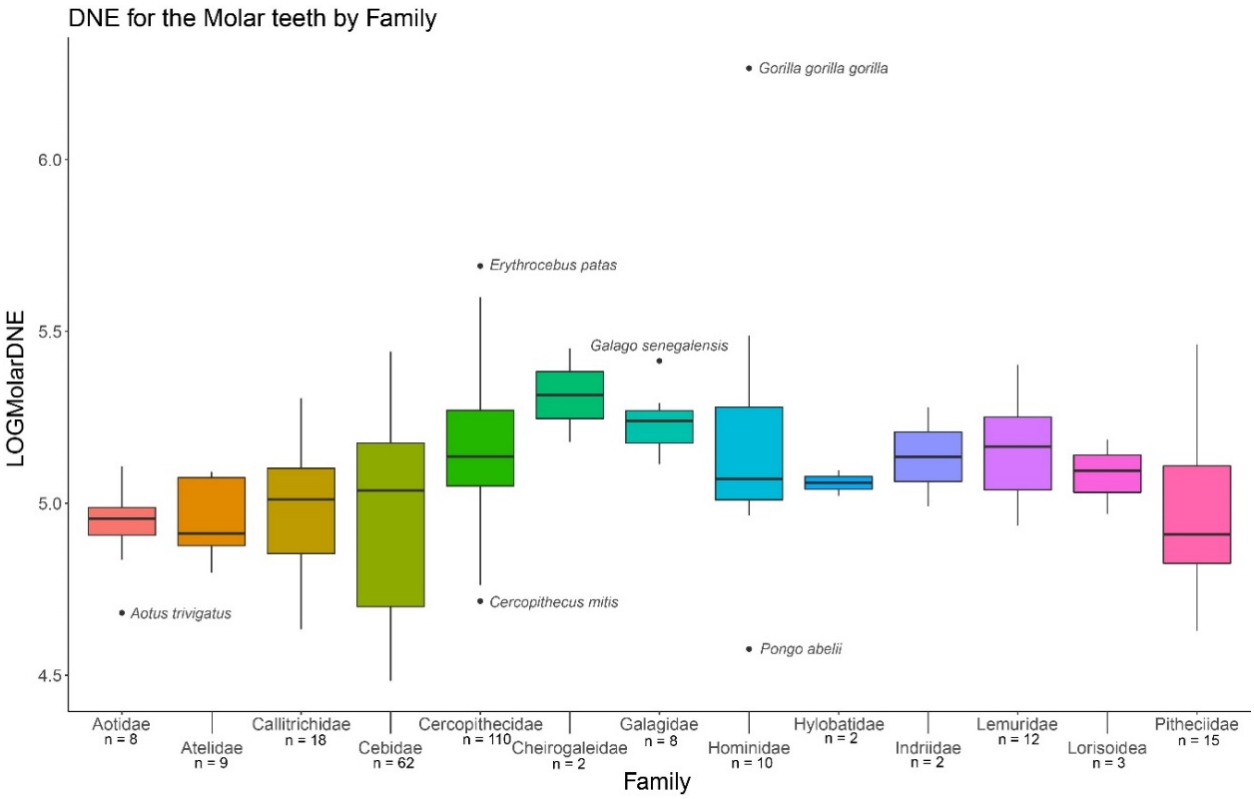

Figure 4.3. Molar DNE across the sample by family. These data are natural log transformed.

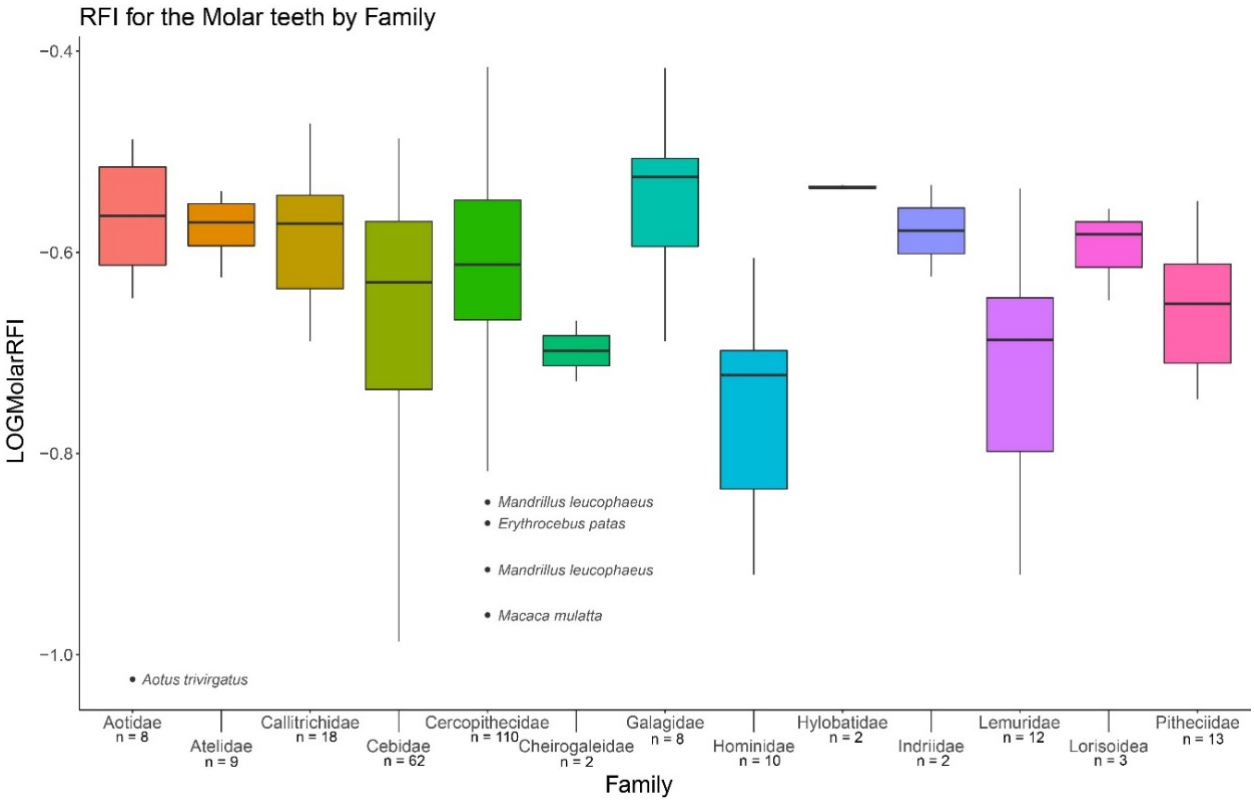

Figure 4.4. Molar RFI across the sample by family. These data are natural log transformed.

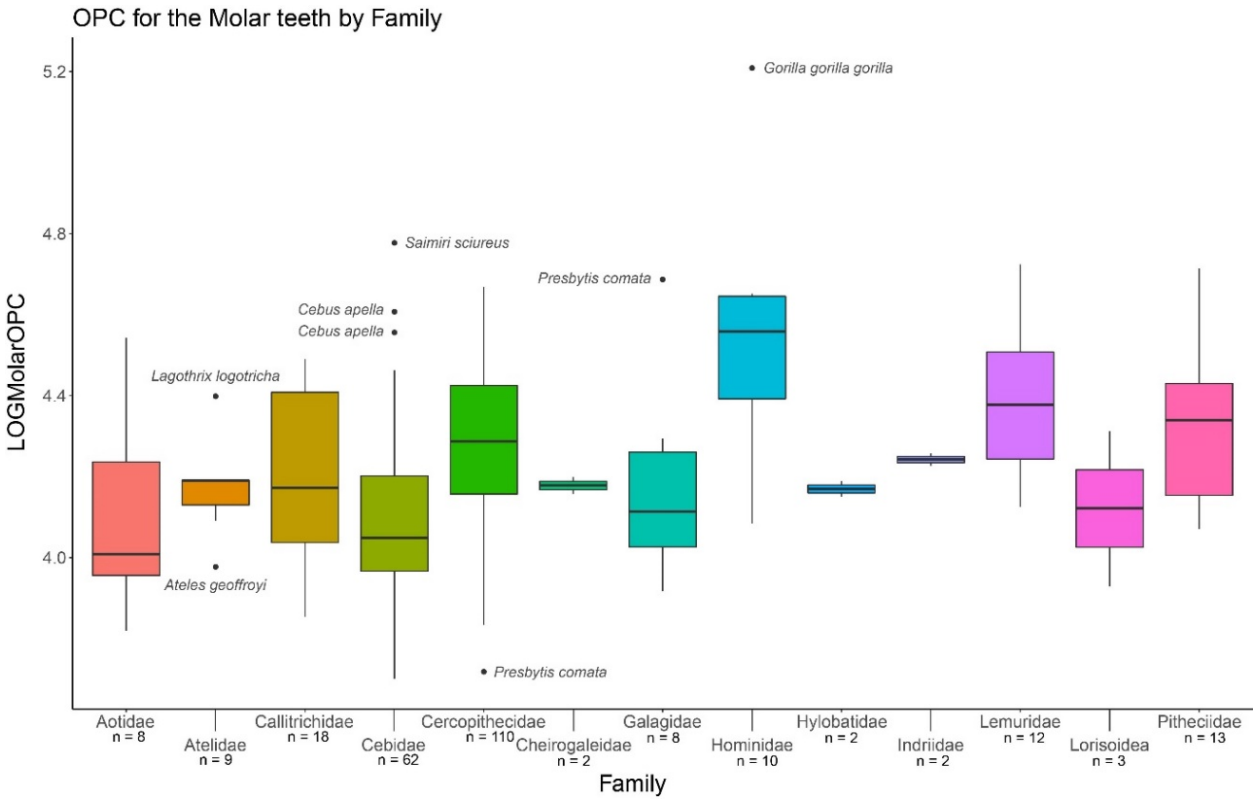

Figure 4.5. Molar OPC across the sample by family. These data are natural log transformed.

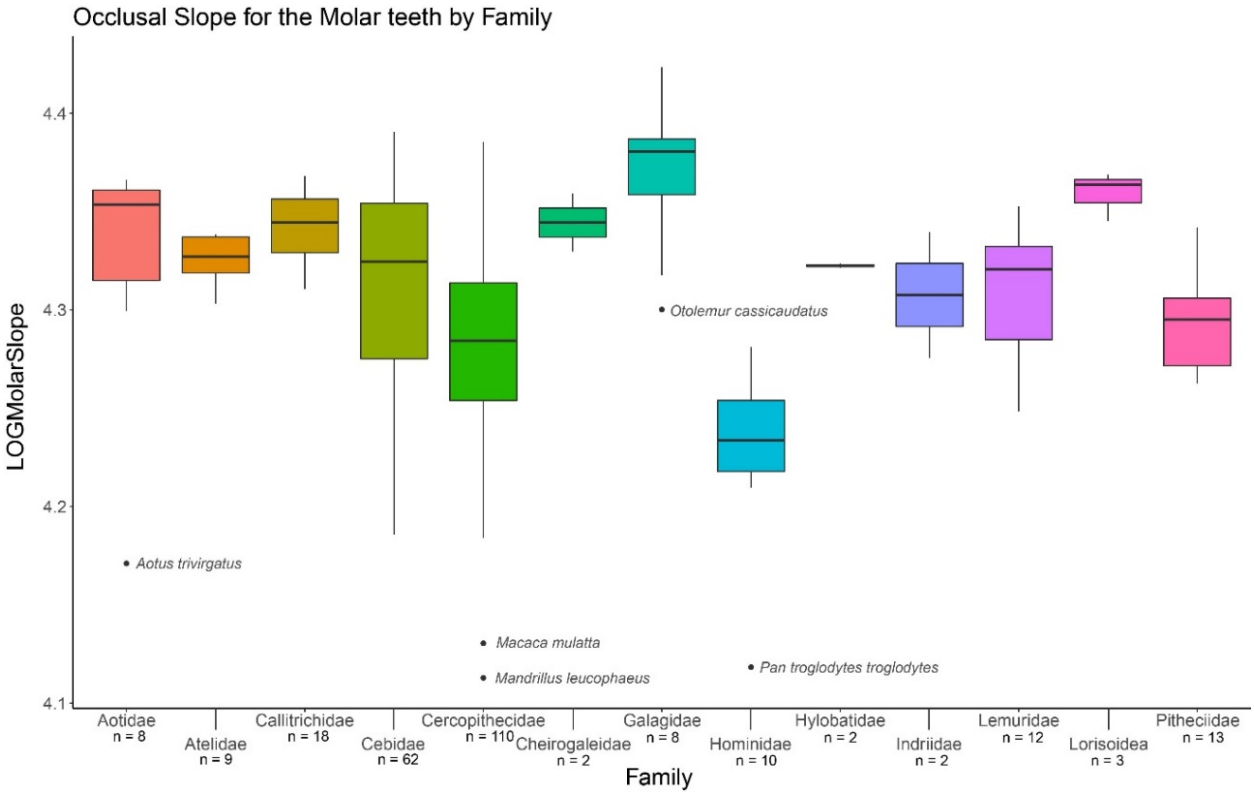

Figure 4.6. Molar occlusal slope across the sample by family. These data are natural log transformed.

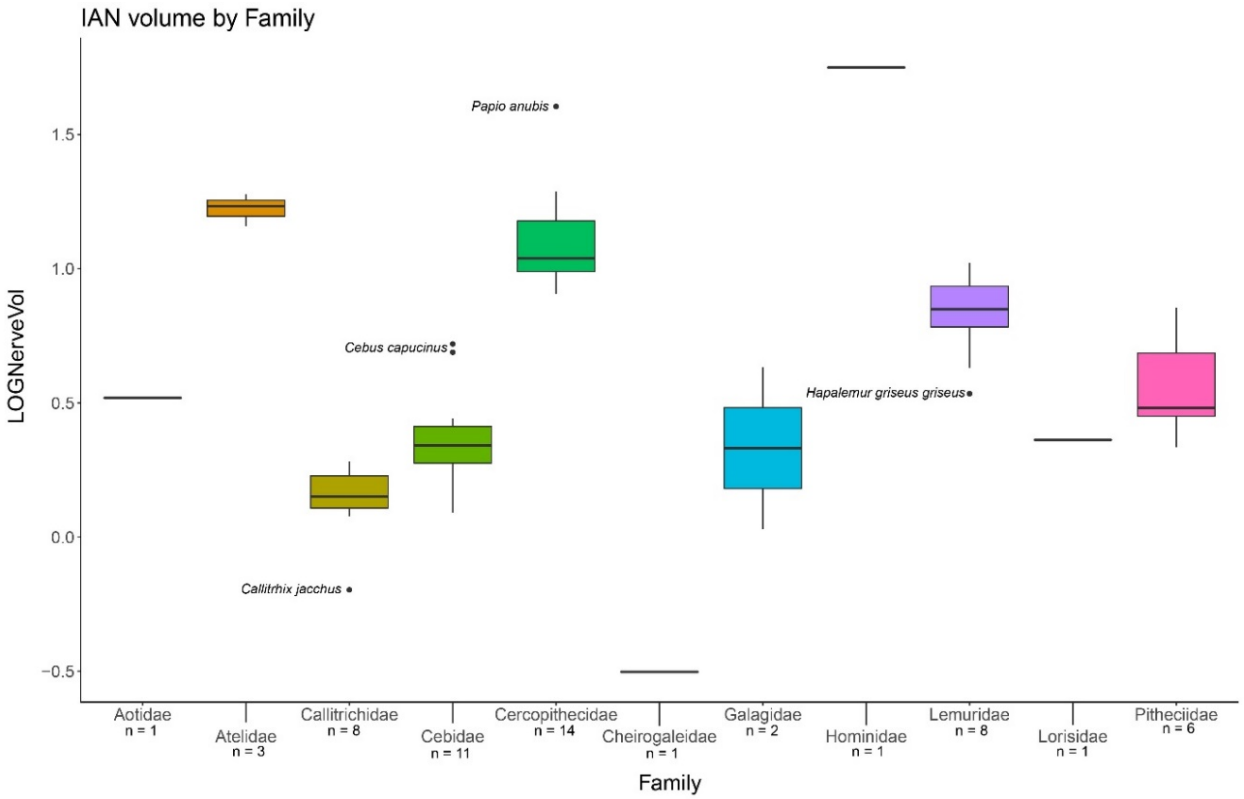

Figure 4.7. IAN volume across the sample by family. These data are natural log transformed.

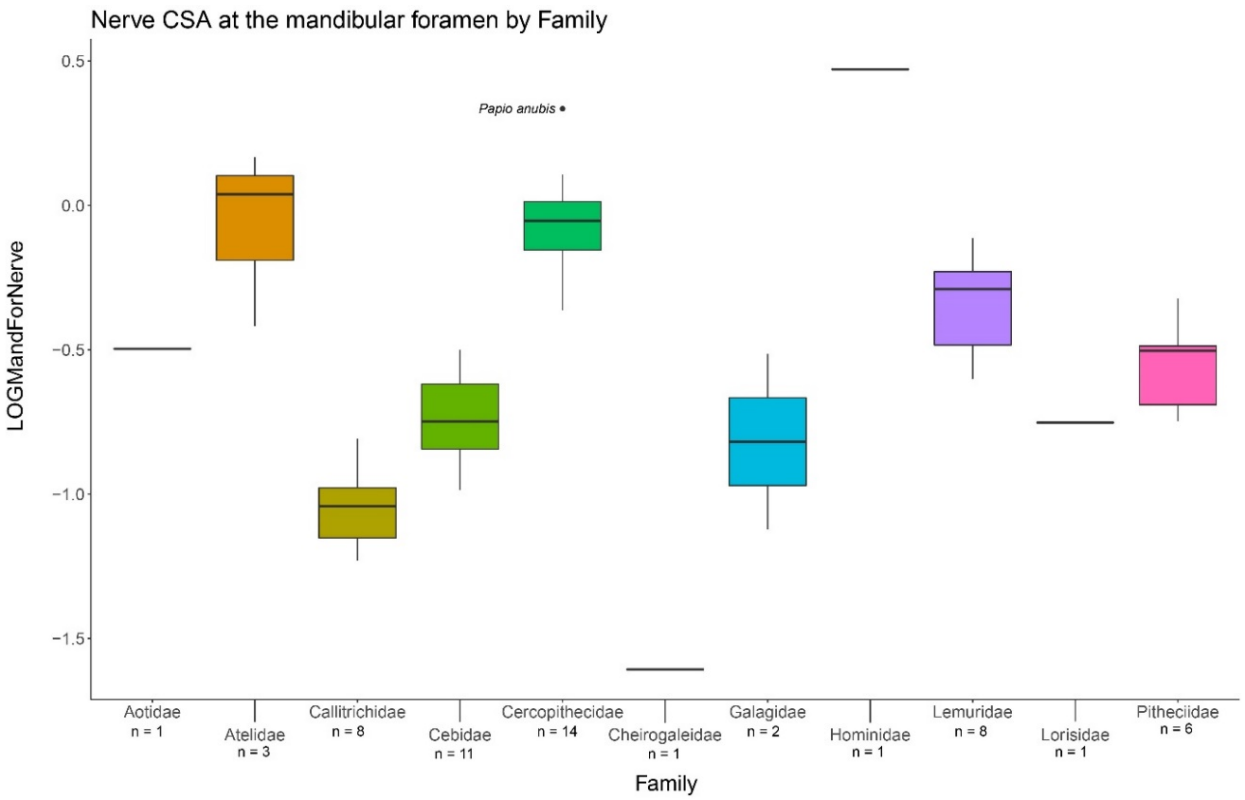

Figure 4.8. Nerve CSA at the mandibular foramen across the sample by family. These data are natural log transformed.

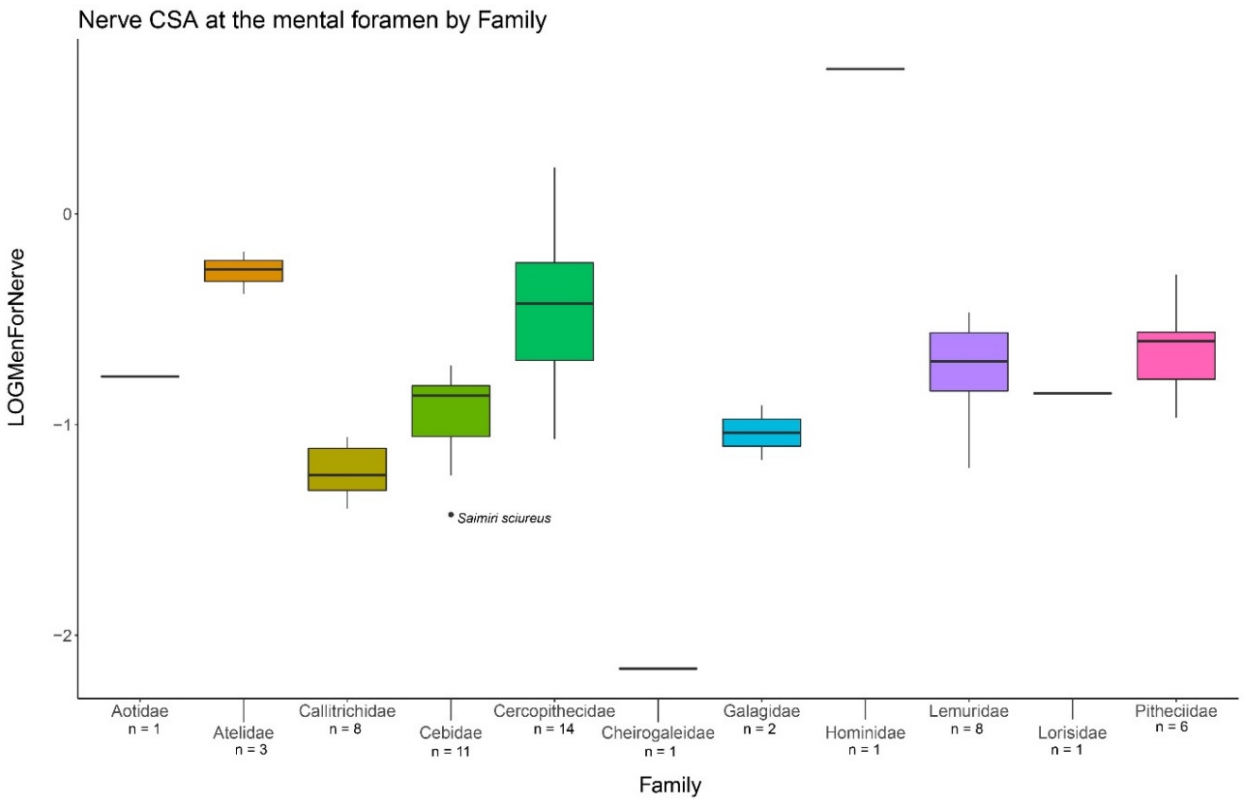

Figure 4.9. Nerve CSA at the mental foramen across the sample by family. These data are natural log transformed.

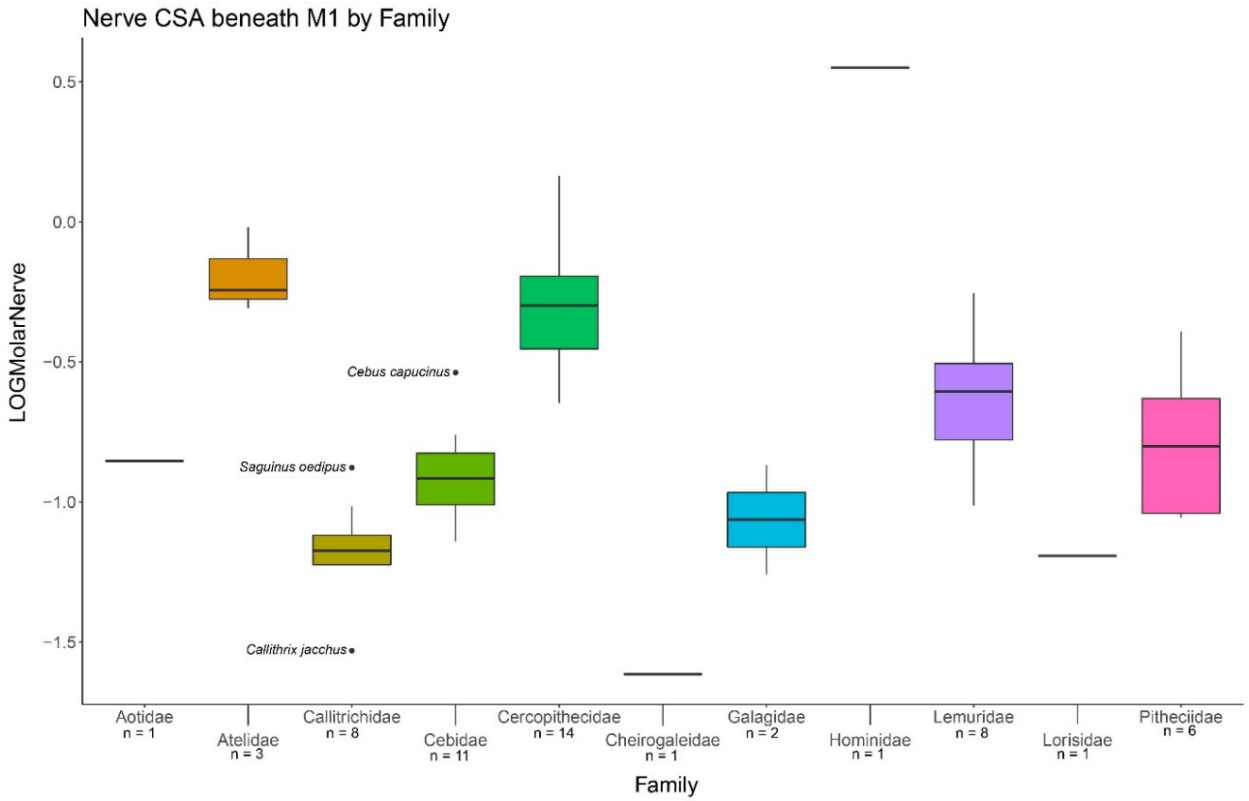

Figure 4.10. Nerve CSA beneath M_1 across the sample by family. These data are natural log transformed.

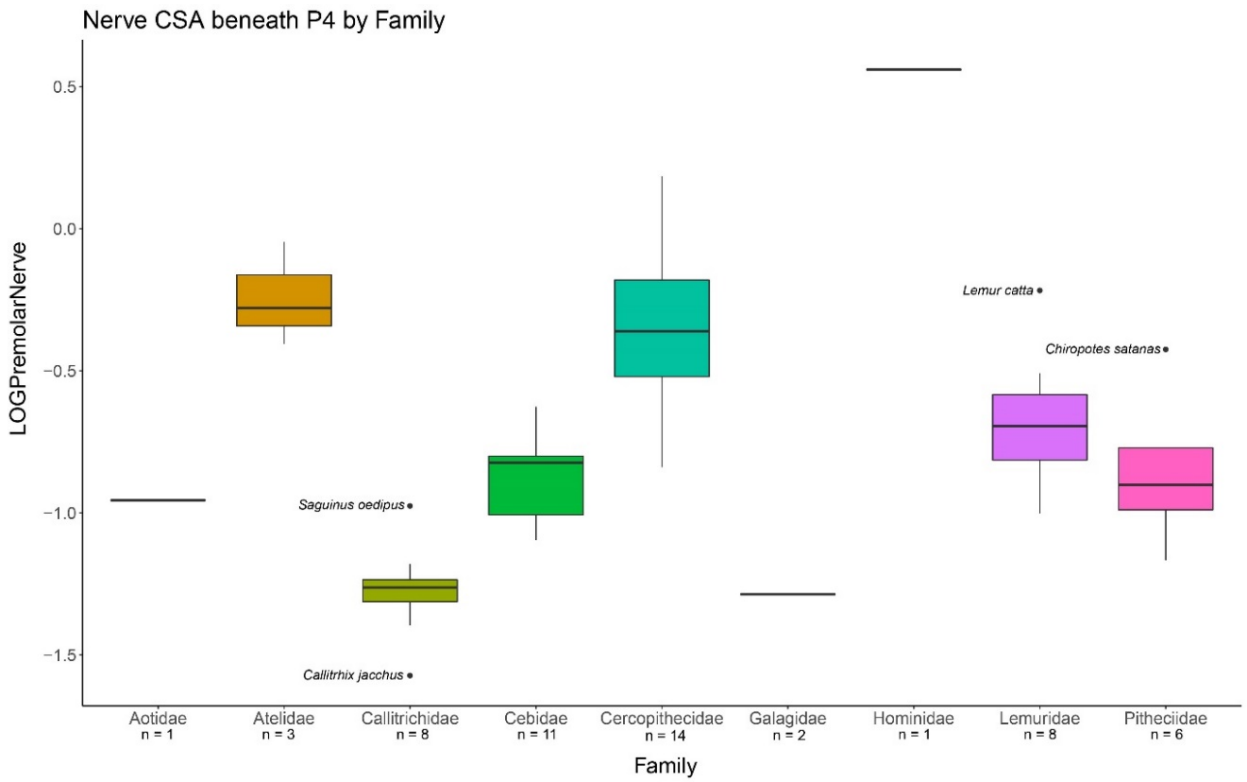

Figure 4.11. Nerve CSA beneath P_4 across the sample by family. These data are natural log transformed.

Allometric Analyses

Root surface area to enamel surface area. Allometric analyses allow us to assess if certain characteristics scale with other characteristics in an organism. The molaR variables used in this chapter (DNE, RFI, OPC, and occlusal slope) could not be analyzed for allometry in relation to other elements because they are both size-adjusted and dimensionless due to the protocol used to create these 3D surfaces. Thus, this allometric analyses only includes the root surface, enamel surface, and nervous tissue variables to determine the scaling relationships between these variables. To assess the allometry of the relationship between root surface area and the enamel surface, I ran a PGLS analysis for each tooth (Table 4.4). These results show significant relationships between the root surface area and enamel surface area (p-value < 0.001 for all teeth) (Figure 4.12A-D). Both the molar and premolar PGLS regressions showed slopes with positive allometry (>1), and further testing showed the slopes were both significantly

different from isometry (=1) (molars p-value = 0.005, premolars p-value = 0.039). Additionally, the R^2 values for these analyses are very high (molar = 0.982, premolars = 0.984), indicating that a large portion of the variance for the root surface area is explained by the enamel surface area. These analyses indicate that in relation to the enamel surface area, the root surface area is increasing at a faster rate than expected. In opposition, both the canine and incisor PGLS regressions showed slopes that were approaching isometry and further testing showed they were not significantly different from isometry (canine slope = 0.956, p-value = 0.440; incisor slope = 0.979, p-value = 0.797). These analyses also showed very high R^2 values (canine = 0.959, incisor = 0.921), indicating that a large portion of the variance for the root surface area is explained by the enamel surface area. This indicates that the root and enamel surface areas of the canines and incisors in this sample are increasing at roughly the same rates.

Table 4.4. PGLS results for Question 1, Hypothesis 1 (without size adjustment)

Dependent variable	Independent variable	p-value	R^2	slope	slope confidence interval	slope p-value
Root surface area	Enamel surface area	M_1: **<0.001** P_4: **<0.001** C_1: **<0.001** I_1: **<0.001**	M_1: 0.982 P_4: 0.984 C_1: 0.959 I_1: 0.921	M_1: 1.141* P_4: 1.086* C_1: 0.956 I_1: 0.979	M_1: 1.047 – 1.234 P_4: 1.002 – 1.169 C_1: 0.839 – 1.074 I_1: 0.808 – 1.151	M_1: **0.005** P_4: **0.039** C_1: 0.440 I_1: 0.797
All analyses used 13 degrees of freedom ***Indicates slope is significantly different from 1** **Alpha values set at p-value < 0.0125** **Slope significance tests had alpha values set to p-value < 0.05**						

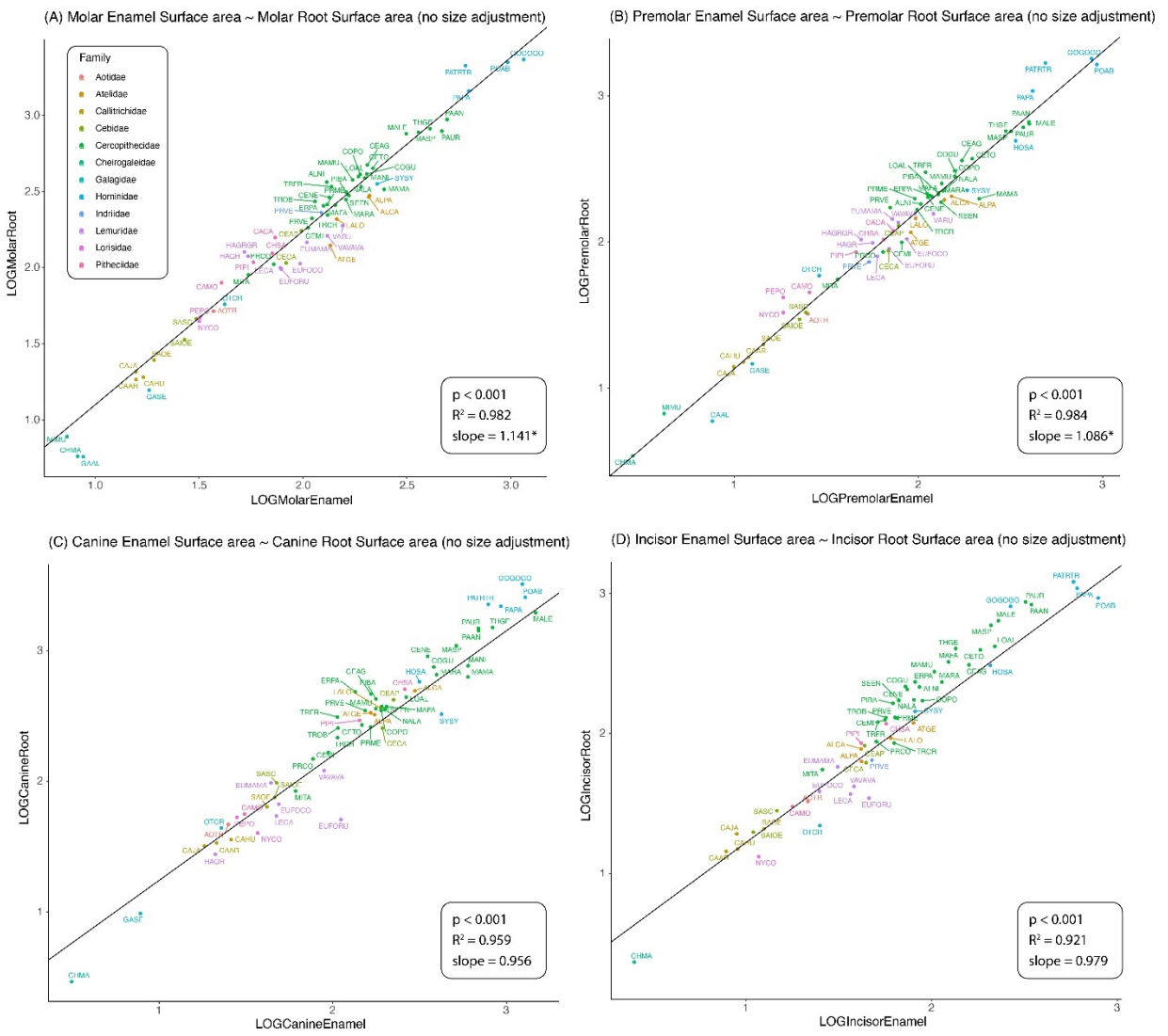

Figure 4.12. The molar (A), premolar (B), canine (C), and incisor (D) enamel surface area to root surface area PGLS. These data are power reduced and natural log transformed.

Because the canines were shown to be significantly different between males and females in the initial data preparation this same PGLS was run by sex (Table 4.5). The results showed significant relationships for both males (p-value = 0.001) and females (p-value < 0.001) when the root surface area was regressed onto the enamel surface area (Figure 4.13A-B). While females showed a slope of near isometry (1.005), males were negatively allometric (0.908), although neither slope was significantly different from isometry. These results mirror the relationships seen in the combined sexes in that this shows enamel surface area is increasing

at a relatively similar rate to root surface area. However, because males are slightly negatively allometric (although not significantly different from isometry), their root surface area is increasing at a slightly slower rate than expected in relation to the enamel surface areas. Additionally, males (0.739) had lower R^2 values than females (0.947) indicating that the variance for root surface area is not as well explained by the enamel surface area in males.

Table 4.5. PGLS Results for Question 1, Hypothesis 1 (by sex) canines (without size adjustment)

Dependent variable	Independent variable	p-value	R^2	slope	slope confidence interval	slope p-value
Root surface area	Enamel surface area	M: **0.001** F: **<0.001**	M: 0.739 F: 0.947	M: 0.908 F: 1.005	M: 0.550 – 1.267 F: 0.811 – 1.199	M: 0.547 F: 0.953
All analyses used 11 degrees of freedom ***Indicates slope is significantly different from 1** **Alpha values set at p-value < 0.025** **Slope significance tests had alpha values set to p-value < 0.05**						

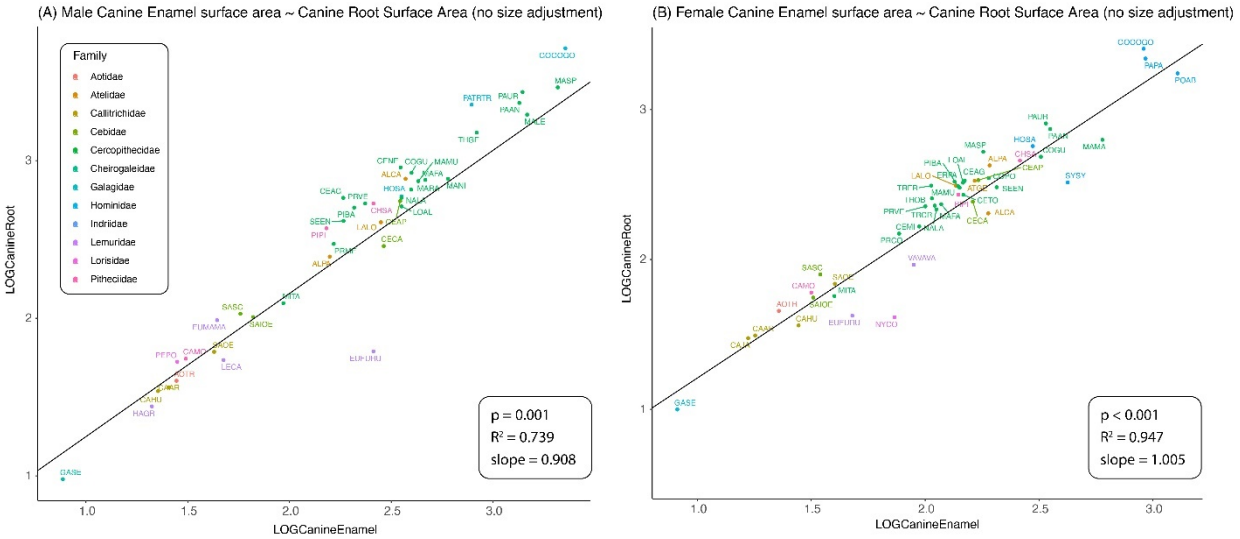

Figure 4.13. The canine enamel surface area to canine root surface area PGLS for males (A) and females (B). These data are power reduced and natural log transformed.

Enamel surface area to nervous tissue variables. To assess allometry between the enamel surface area and the nervous tissue variables, I ran a series of PGLS regressions for

each tooth type (Table 4.6). First, when the enamel surface was the independent variable, all teeth showed a significant relationship to the nervous tissue variables (p-value < 0.001). Relationships between nervous tissues variables and the enamel surface area are shown in Figure 4.14-4.18.

In the regression of total IAN volume to enamel surface area (Figure 4.14) all four teeth showed significant relationships (p-value < 0.001). However, while slopes were not significantly different from one for the molars (slope = 0.969), premolars (slope = 0.909), or incisors (slope = 0.891), the canines (slope = 0.676) did have a slope significantly different from one (p-value = 0.019). This indicates that canine IAN volume is increasing at a much slower rate than expected in relation to canine enamel surface area, while the molars, premolars, and incisor IAN volume is increasing at relatively the same rate as enamel surface area.

For the regression for the nerve CSA at the mandibular foramen to enamel surface area (Figure 4.15), both the molars (slope = 0.881) and incisors (slope = 0.809) had slopes that were not significantly different from one while the premolars (slope = 0.825, p-value = 0.047) and the canines (slope = 0.682, p-value = 0.032) were significantly different from one. Again, this indicates that while all four teeth show nerve CSA at the mandibular foramen increasing at a slower rate than expected in relation to enamel surface size, this is particularly prominent in the premolars and canines.

For the regression for nerve CSA at the mental foramen (Figure 4.16), we again see the molar slope (slope = 0.717) not significantly different from one, whereas the premolars (slope = 0.667; p-value = 0.037), canines (slope = 0.633; p-value = 0.022), and incisors (slope = 0.668; p-value = 0.039) all show slope values that were significantly different from one and were negatively allometric. This again indicates that the nervous tissue at the mental foramen is increasing at a slower rate than expected in relation to the enamel surface area in all teeth but the molars.

Finally, the nerve CSA beneath the molars (slope = 0.870) and premolars (slope = 0.0842) (Figure 4.17 and Figure 4.18) showed slopes that were negatively allometric, but neither were significantly different from isometry. Overall, this indicates that most nervous tissues are increasing in size at relatively the same rates as the enamel surface of the teeth, while many of the teeth (particularly the canines) show nervous tissues increasing in size at slower rates than expected in relation to the enamel surface area. Biologically, this means that individuals with larger canine teeth would have less nervous tissues than would be expected for their tooth size.

Table 4.6. PGLS results for Question 1, Hypothesis 2 (without size adjustment)

Dependent variable	Independent variable	p-value	R^2	slope	slope confidence interval	slope p-value
IAN Volume	Enamel surface area	M_1: **<0.001** P_4: **<0.001** C_1: **<0.001** I_1: **<0.001**	M_1: 0.961 P_4: 0.955 C_1: 0.734 I_1: 0.905	M_1: 0.969 P_4: 0.909 C_1: 0.676* I_1: 0.891	M_1: 0.851 – 1.086 P_4: 0.792 – 1.028 C_1: 0.432 – 0.919 I_1: 0.718 – 1.063	M_1: 0.577 P_4: 0.136 C_1: **0.019** I_1: 0.202
Nerve CSA at Mandibular foramen	Enamel surface area	M_1: **<0.001** P_4: **<0.001** C_1: **<0.001** I_1: **<0.001**	M_1: 0.914 P_4: 0.904 C_1: 0.679 I_1: 0.861	M_1: 0.881 P_4: 0.825* C_1: 0.682* I_1: 0.809	M_1: 0.717 – 1.043 P_4: 0.664 – 0.986 C_1: 0.401 – 0.963 I_1: 0.614 – 1.005	M_1: 0.148 P_4: **0.047** C_1: **0.032** I_1: 0.066
Nerve CSA at mental foramen	Enamel surface area	M_1: **<0.001** P_4: **<0.001** C_1: **<0.001** I_1: **0.001**	M_1: 0.623 P_4: 0.608 C_1: 0.602 I_1: 0.602	M_1: 0.717 P_4: 0.667* C_1: 0.633* I_1: 0.668*	M_1: 0.382 – 1.051 P_4: 0.346 – 0.988 C_1: 0.325 – 0.941 I_1: 0.342 – 0.993	M_1: 0.074 P_4: **0.037** C_1: **0.022** I_1: **0.039**
Nerve CSA beneath molars	Enamel surface area	M_1: **<0.001**	M_1: 0.854	M_1: 0.870	M_1: 0.654 – 1.086	M_1: 0.217
Nerve CSA beneath premolars	Enamel surface area	P_4: **<0.001**	P_4: 0.787	P_4: 0.842	P_4: 0.579 – 1.105	P_4: 0.206

All analyses used 13 degrees of freedom
***Indicates slope is significant different to 1**
Tests with all four teeth had alpha values set to p-value < 0.0125
Tests with only molar or premolar tested had alpha values set to p-value < 0.05
Slope significance tests had alpha values set to p-value < 0.05

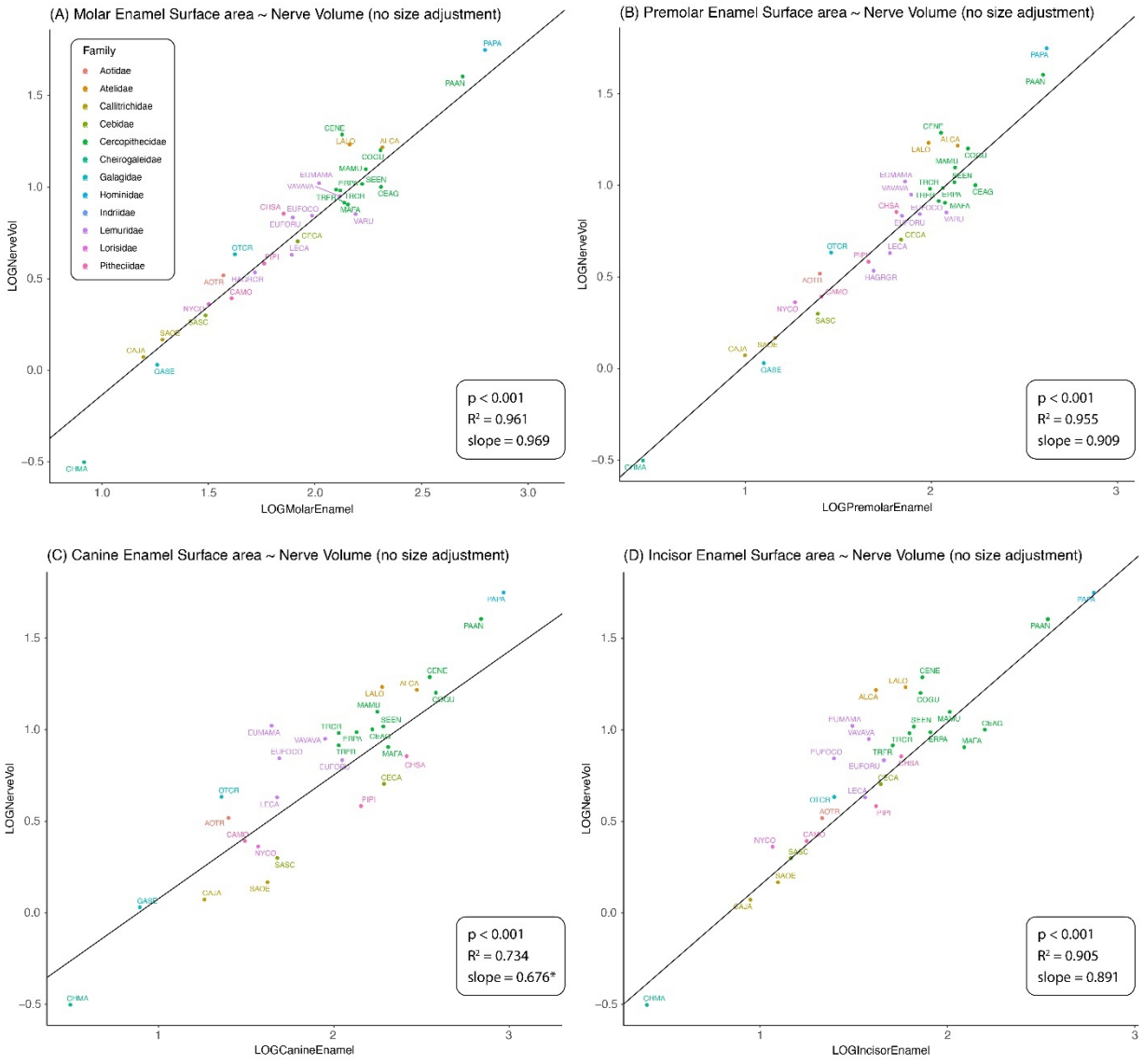

Figure 4.14. The molar (A), premolar (B), canine (C), and incisor (D) enamel surface area to <u>total IAN volume</u> PGLS analyses. These data are power reduced and natural log transformed.

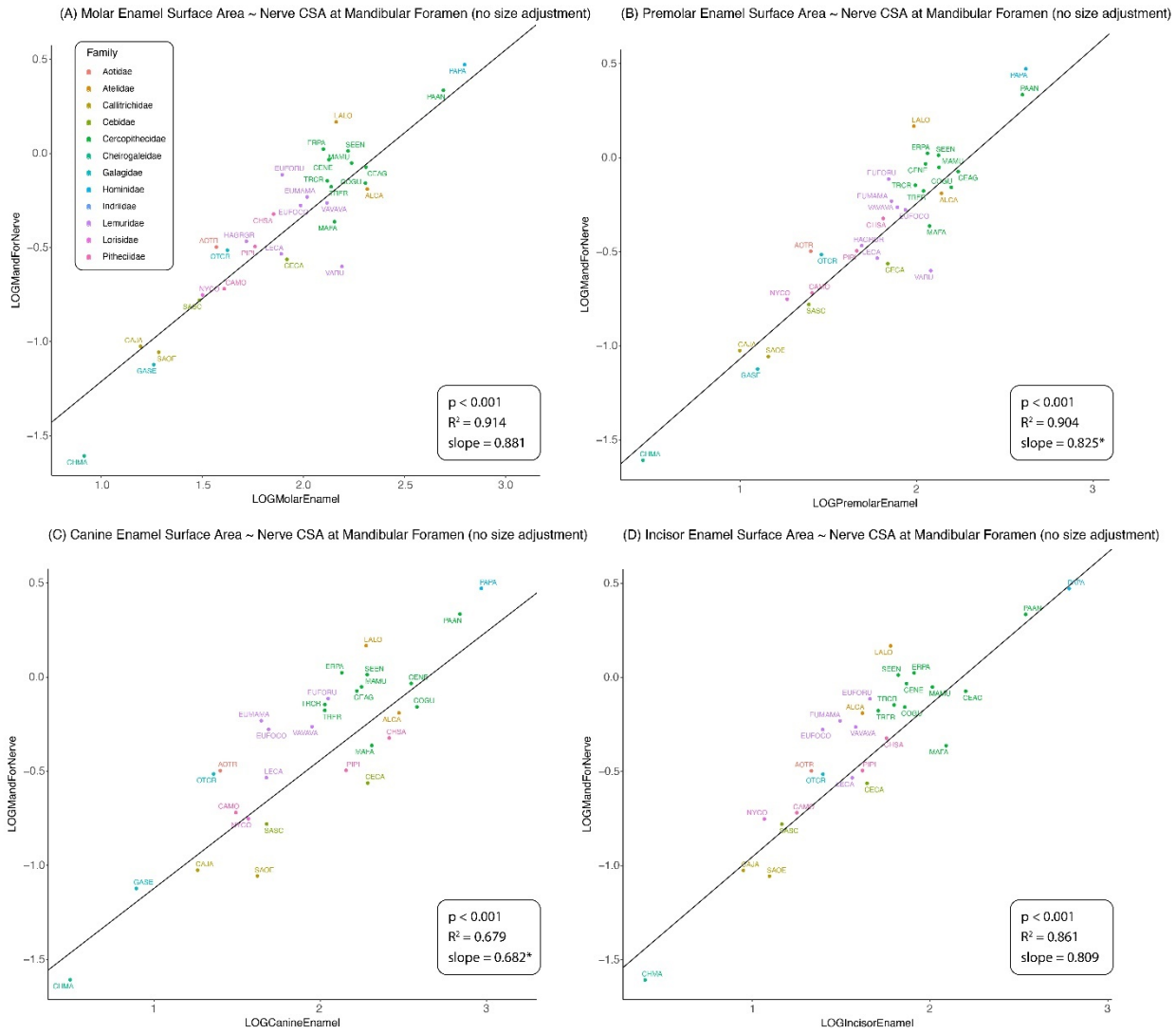

Figure 4.15. The molar (A), premolar (B), canine (C), and incisor (D) enamel surface area to nerve CSA at the mandibular foramen PGLS analyses. These data are power reduced and natural log transformed.

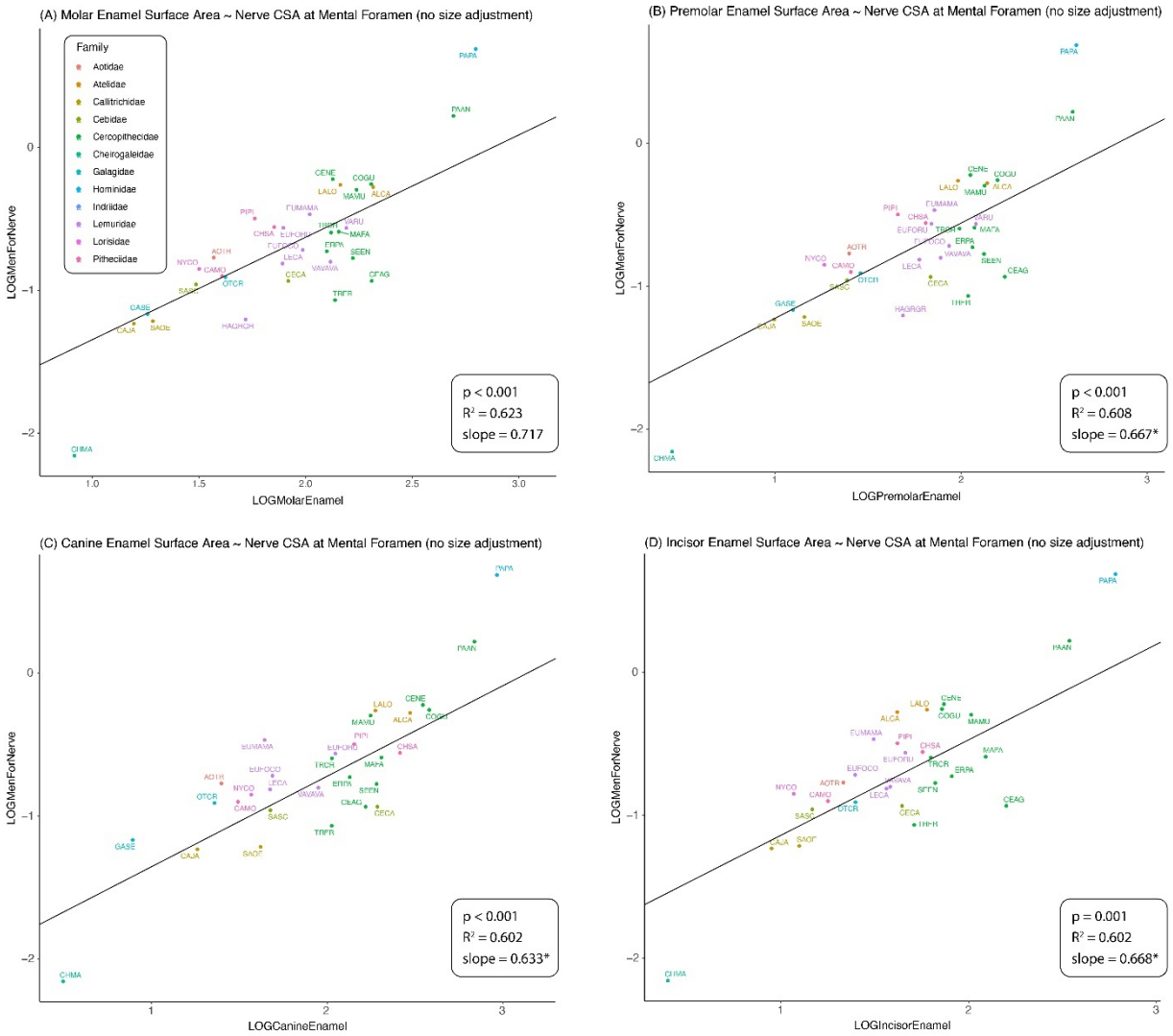

Figure 4.16. The molar (A), premolar (B), canine (C), and incisor (D) enamel surface area to nerve CSA at the mental foramen PGLS analyses. These data are power reduced and natural log transformed.

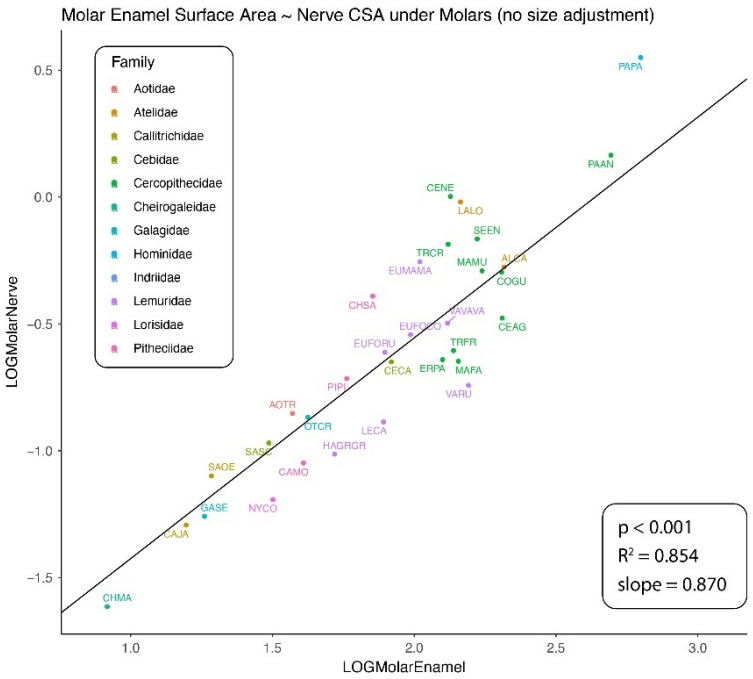

Figure 4.17. The enamel surface area to <u>nerve CSA beneath M_1</u> PGLS analyses. These data are power reduced and natural log transformed.

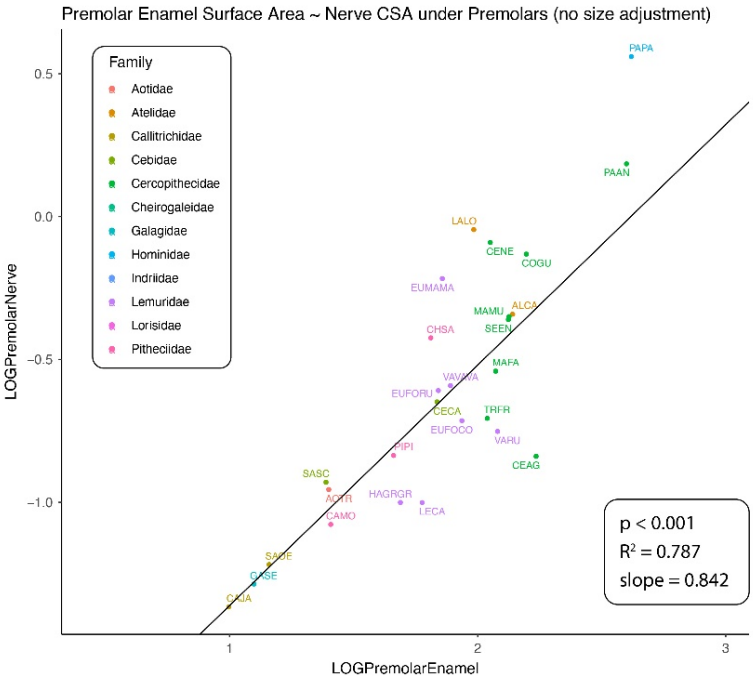

Figure 4.18. The enamel surface area to <u>nerve CSA beneath P_4</u> PGLS analyses. These data are power reduced and natural log transformed.

Because the canines were shown to be significantly different between males and females this same PGLS was run by sex (Table 4.7). These analyses showed a significant

relationship between both males and females for nervous volume to enamel surface area (males: p-value = 0.001, females: p-value = 0.001) (Figure 4.19A-B), nerve CSA at the mandibular foramen to enamel surface area (males: p-value = 0.004, females: p-value < 0.001) (Figure 4.20A-B), and nerve CSA at the mental foramen to enamel surface area (males: p-value = 0.014, females: p-value = 0.002) (Figure 4.21A-B). Interestingly, males showed negative allometry and slopes that were significantly different from isometry in all analyses (IAN volume slope = 0.565, p-value = 0.012; nerve CSA at the mandibular foramen slope = 0.459, p-value = 0.003; nerve CSA at the mental foramen slope = 0.400, p-value = 0.002). This indicates that male nervous tissue is increasing at a slower rate in relation to enamel surface area and has overall less nervous tissues in relation to tooth size than females. Biologically, this would indicate that as tooth size is increasing in males, there will be less nervous tissues overall associated with the mandible and thus potentially less sensitivity for individuals with larger teeth. While females also showed negative allometry for IAN volume (slope = 0.902) and nerve CSA at the mental foramen (slope = 0.954), neither of these slopes were significantly different from one. This indicates that in females, and potentially just individuals with overall smaller canine teeth, the nervous tissues are increasing in size at relatively the same rates at the enamel surface area.

Table 4.7. PGLS Results for Question 1, Hypothesis 2 (by sex) canines (without size adjustment)

Dependent variable	Independent variable	p-value	R^2	slope	slope confidence interval	slope p-value
IAN volume	Enamel surface area	M: **0.002** F: **0.001**	M: 0.606 F: 0.741	M: 0.565* F: 0.902	M: 0.262 – 0.867 F: 0.467 – 1.337	M: **0.012** F: 0.582
Nerve CSA at mandibular foramen	Enamel surface area	M: **0.004** F: **<0.001**	M: 0.542 F: 0.855	M: 0.459* F: 1.045	M: 0.179 – 0.739 F: 0.694 – 1.396	M: **0.003** F: 0.753
Nerve CSA at mental foramen	Enamel surface area	M: **0.015** F: **0.002**	M: 0.431 F: 0.714	M: 0.400* F: 0.954	M: 0.095 – 0.706 F: 0.462 – 1.447	M: **0.002** F: 0.811

All analyses performed on 11 degrees of freedom
***Indicates slope is significantly different from 1**
Alpha values set at p-value < 0.025
Slope significance tests had alpha values set to p-value < 0.05

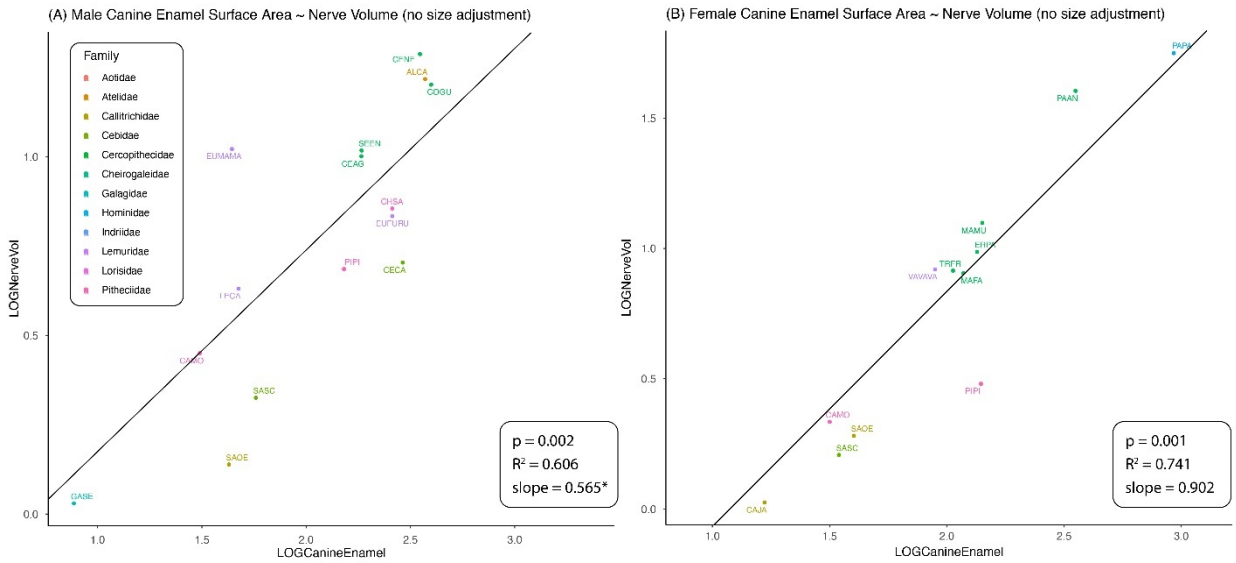

Figure 4.19. The canine enamel surface area to <u>IAN volume</u> PGLS analyses for males (A) and females (B). These data are power reduced and natural log transformed.

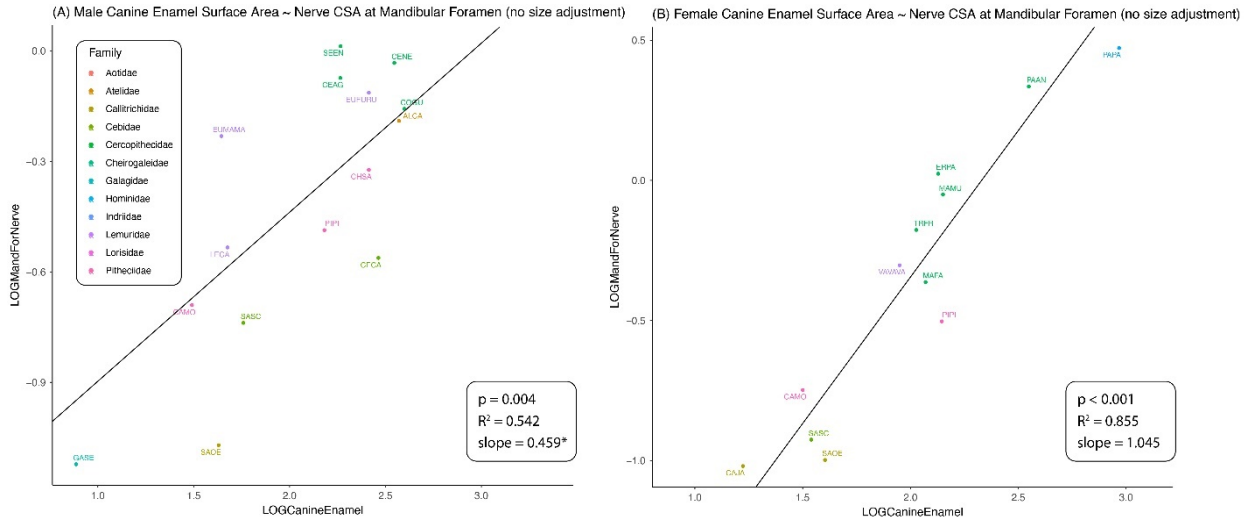

Figure 4.20. The canine enamel surface area to <u>nerve CSA at the mandibular foramen</u> PGLS analyses for males (A) and females (B). These data are power reduced and natural log transformed.

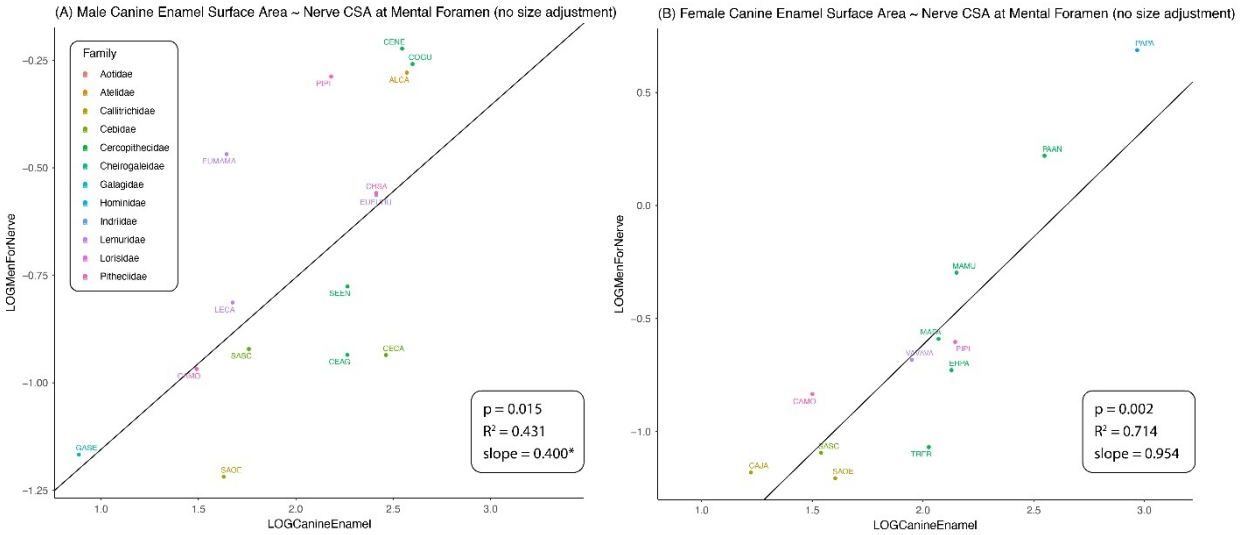

Figure 4.21. The canine enamel surface area to <u>nerve CSA at the mental foramen</u> PGLS analyses for males (A) and females (B). These data are power reduced and natural log transformed.

Root surface area to nervous tissue variables. To assess the allometry between the root surface area and the nervous tissue variables, I ran a series of PGLS regressions for each tooth type (Table 4.8). All analyses showed a significant relationship between the root surface area and the nervous tissue variables (p-value < 0.001). Relationships between nervous tissues variables and the root surface area are shown in Figures 4.21 - 4.25. While the R^2 values were

relatively high for both the IAN volume and the nerve CSA at the mandibular foramen, beneath the molars, and beneath the premolars, the nerve CSA at the mental foramen shows much lower values (R^2 = 0.597 – 0.633). This indicates that the variance within the sample cannot be explained well by the nerve CSA at the mental foramen in relation to the root surface areas

For total IAN volume, all slopes were negatively allometric (Table 4.8; M_1: 0.833, P_4: 0.823, C_1: 0.659, I_1: 0.769) and all slopes were significantly different from isometry (M_1: p-value = 0.021, P_4: p-value = 0.017, C_1: p-value = 0.013, I_1: p-value = 0.013) (Figure 4.21A-D) Similarly, the nerve CSA at the mandibular foramen also showed negative allometry (M_1: 0.765, P_4: 0.747, C_1: 0.651, I_1: 0.699) and all slopes significantly different from isometry (M_1: p-value = 0.007, P_4: p-value = 0.009, C_1: p-value = 0.013, I_1: p-value = 0.006) (Figure 4.22A-D). The nerve CSA at the mental foramen also showed all negatively allometric slopes (M_1: 0.623, P_4: 0.613, C_1: 0.585, I_1: 0.594) that were significantly different from isometry (M_1: p-value = 0.017, P_4: p-value = 0.015, C_1: p-value = 0.010, I_1: p-value = 0.009) (Figure 4.23A-D). Finally, the analysis for the nerve CSA beneath the molar (slope = 0.748) and premolar (slope = 0.752) slopes were again both negatively allometric but only the molar slope was significantly different from isometry (p-value = 0.025) (Figure 4.24 and 4.25). All of this together indicates that we again see a trend of the nervous tissues within the mandible increasing at a slower than expected rate in relation to the root surface areas.

Table 4.8. PGLS results for Question 1, Hypothesis 3 (without size adjustment)

Dependent variable	Independent variable	p-value	R^2	slope	slope confidence interval	slope p-value
IAN volume	Root surface area	M_1: **<0.001** P_4: **<0.001** C_1: **<0.001** I_1: **<0.001**	M_1: 0.941 P_4: 0.939 C_1: 0.739 I_1: 0.898	M_1: 0.833* P_4: 0.823* C_1: 0.659* I_1: 0.769*	M_1: 0.707 – 0.958 P_4: 0.697 – 0.950 C_1: 0.424 – 0.895 I_1: 0.614 – 0.925	M_1: **0.021** P_4: **0.017** C_1: **0.013** I_1: **0.013**
Nerve CSA at mandibular foramen	Root surface area	M_1: **<0.001** P_4: **<0.001** C_1: **<0.001** I_1: **<0.001**	M_1: 0.914 P_4: 0.887 C_1: 0.718 I_1: 0.853	M_1: 0.765* P_4: 0.747* C_1: 0.651* I_1: 0.699*	M_1: 0.625 – 0.906 P_4: 0.587 – 0.906 C_1: 0.407 – 0.895 I_1: 0.525 – 0.873	M_1: **0.007** P_4: **0.009** C_1: **0.013** I_1: **0.006**
Nerve CSA at mental foramen	Root surface area	M_1: **<0.001** P_4: **0.001** C_1: **0.001** I_1: **<0.001**	M_1: 0.624 P_4: 0.615 C_1: 0.597 I_1: 0.633	M_1: 0.623* P_4: 0.613* C_1: 0.585* I_1: 0.594*	M_1: 0.333 – 0.913 P_4: 0.322 – 0.903 C_1: 0.297 – 0.873 I_1: 0.323 – 0.864	M_1: **0.017** P_4: **0.015** C_1: **0.010** I_1: **0.009**
Nerve CSA underneath M_1	Root surface area (molar)	M_1: **<0.001**	M_1: 0.836	M_1: 0.748*	M_1: 0.549 – 0.947	M_1: **0.025**
Nerve CSA underneath P_4	Root surface area (premolar)	P_4: **<0.001**	P_4: 0.753	P_4: 0.752	P_4: 0.494 – 1.011	P_4: 0.062

All analyses were performed with 13 degrees of freedom
***Indicates slope is significantly different to 1**
Tests with all four teeth had alpha values set to p-value < 0.0125
Tests with only molar or premolar tested had alpha values set to p-value < 0.05
Slope significance tests had alpha values set to p-value < 0.05

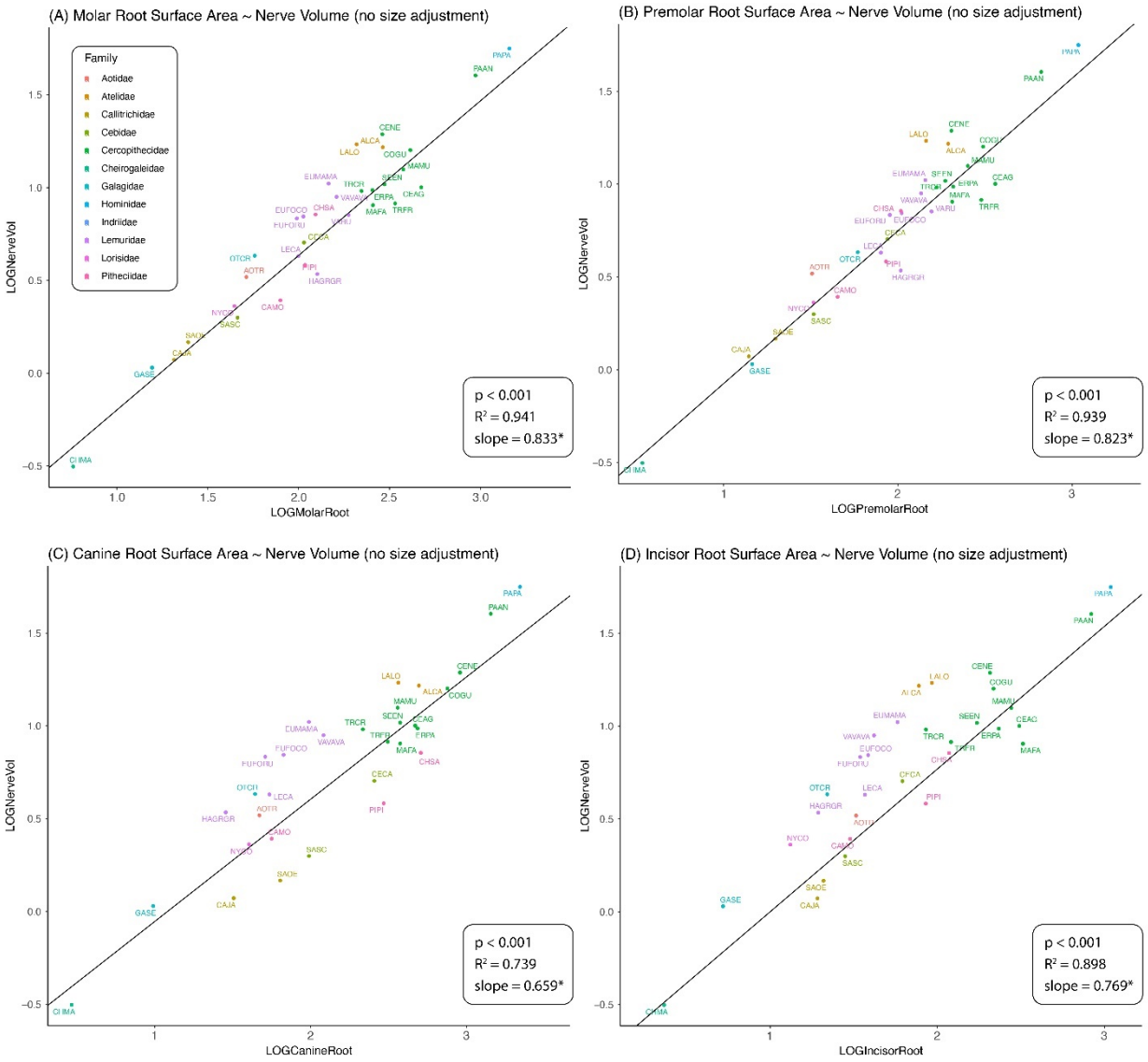

Figure 4.21. The molar (A), premolar (B), canine (C), and incisor (D) root surface area to <u>IAN volume</u> PGLS analyses. These data are power reduced and natural log transformed.

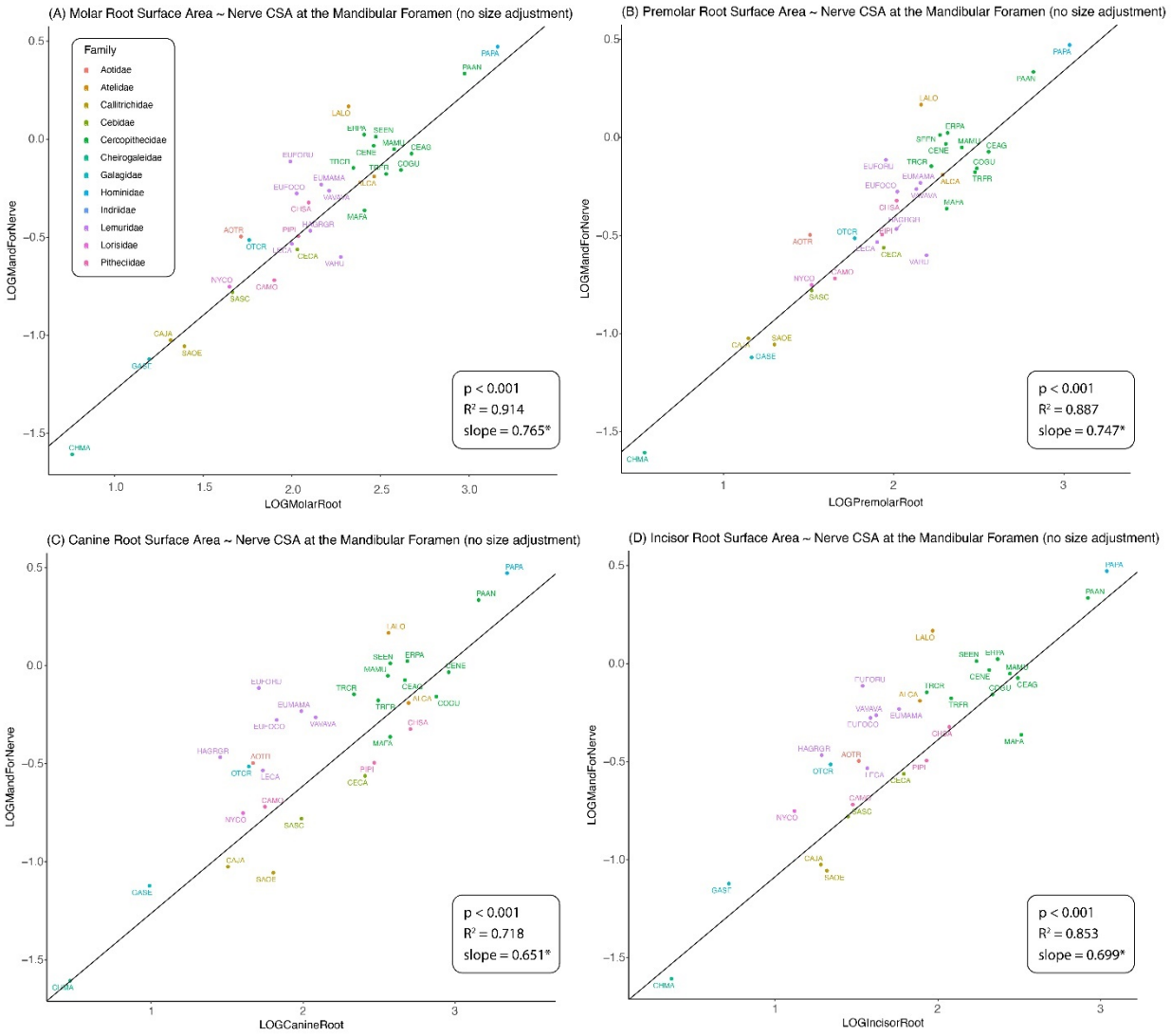

Figure 4.22. The molar (A), premolar (B), canine (C), and incisor (D) root surface area to nerve CSA at the mandibular foramen PGLS analyses. These data are power reduced and natural log transformed.

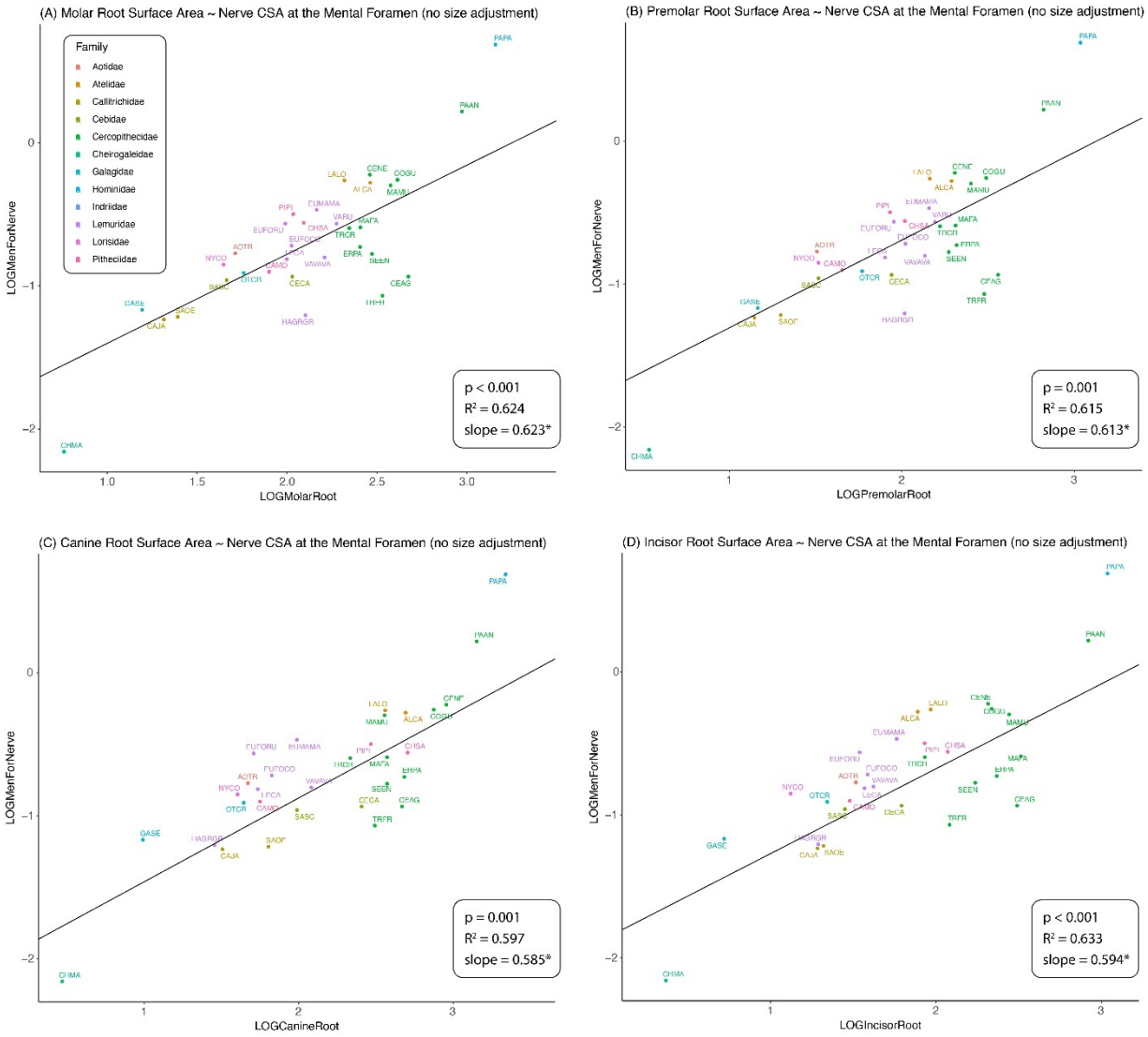

Figure 4.23. The molar (A), premolar (B), canine (C), and incisor (D) root surface area to nerve CSA at the mental foramen PGLS analyses. These data are power reduced and natural log transformed.

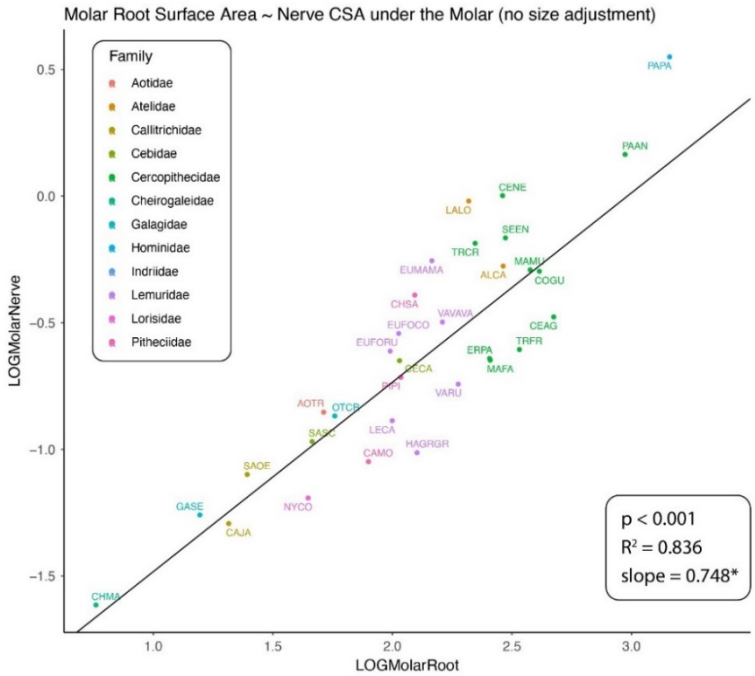

Figure 4.24. The root surface area to <u>nerve CSA beneath M_1</u> PGLS analyses. These data are power reduced and natural log transformed.

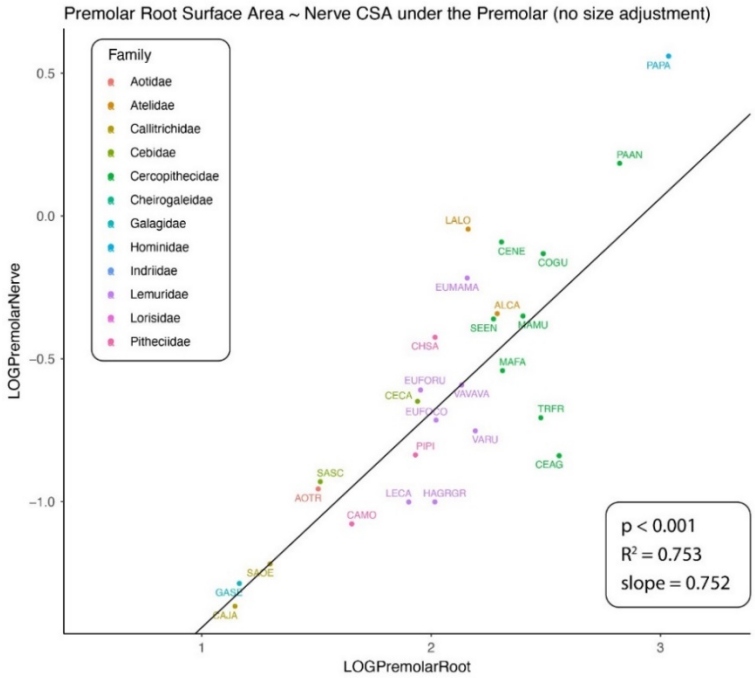

Figure 4.25. The root surface area to <u>nerve CSA beneath P_4</u> PGLS analyses. These data are power reduced and natural log transformed.

Because the canines were shown to be significantly different between males and females this same PGLS was run by sex (Table 4.9).These analyses showed a significant

relationship between both males and females for nervous volume to canine root surface area (males: p-value < 0.001, females: p-value = 0.004) (Figure 4.26A-B), nerve CSA at the mandibular foramen to canine root surface area (males: p-value = 0.002, females: p-value = 0.001) (Figure 4.27A-B), and nerve CSA at the mental foramen to canine root surface area (males: p-value = 0.011, females: p-value = 0.008) (Figure 4.28A-B).

Like the analyses seen in the enamel surface, males showed consistent negative allometry across all nervous tissue variables and had slopes that were all significantly different from one (Table 4.9; IAN volume slope = 0.652, p-value = 0.011; nerve CSA at mandibular foramen slope = 0.527, p-value = 0.007; nerve CSA at the mental foramen slope = 0.419, p-value = 0.002). Females again showed negative allometry across all nervous tissue variables to canine root surface area although these slopes were not significantly different from isometry (IAN volume slope = 0.807, p-value = 0.325; nerve CSA at mandibular foramen slope = 0.838, p-value = 0.359; nerve CSA at the mental foramen slope = 0.814, p-value = 0.381). These results again indicate that males have much higher rates of negative allometry in terms of the nervous tissues of the mandible to the root surface areas. Biologically this means that the nervous tissue structures are increasing at a much slower rate than expected in relation to the canine root surface areas.

Table 4.9. PGLS Results for Question 1, Hypothesis 3 (by sex) canines (without size adjustment)

Dependent variable	Independent variable	p-value	R^2	slope	slope confidence interval	slope p-value
IAN volume	Canine root surface area	M: **<0.001** F: **0.004**	M: 0.795 F: 0.667	M: 0.652* F: 0.807	M: 0.433 – 0.872 F: 0.342 – 1.273	M: **0.011** F: 0.325
Nerve CSA at mandibular foramen	Canine root surface area	M: **0.002** F: **0.001**	M: 0.593 F: 0.738	M: 0.527* F: 0.838	M: 0.237 – 0.817 F: 0.431 – 1.245	M: **0.007** F: 0.359
Nerve CSA at mental foramen	Canine root surface area	M: **0.011** F: **0.008**	M: 0.459 F: 0.606	M: 0.419* F: 0.814	M: 0.118 - 0.720 F: 0.279 – 1.349	M: **0.002** F: 0.381

All analyses were performed with 8 degrees of freedom
***Indicates slope is significantly different to 1**
Alpha values set at p-value < 0.025
Slope significance tests had alpha values set to p-value < 0.05

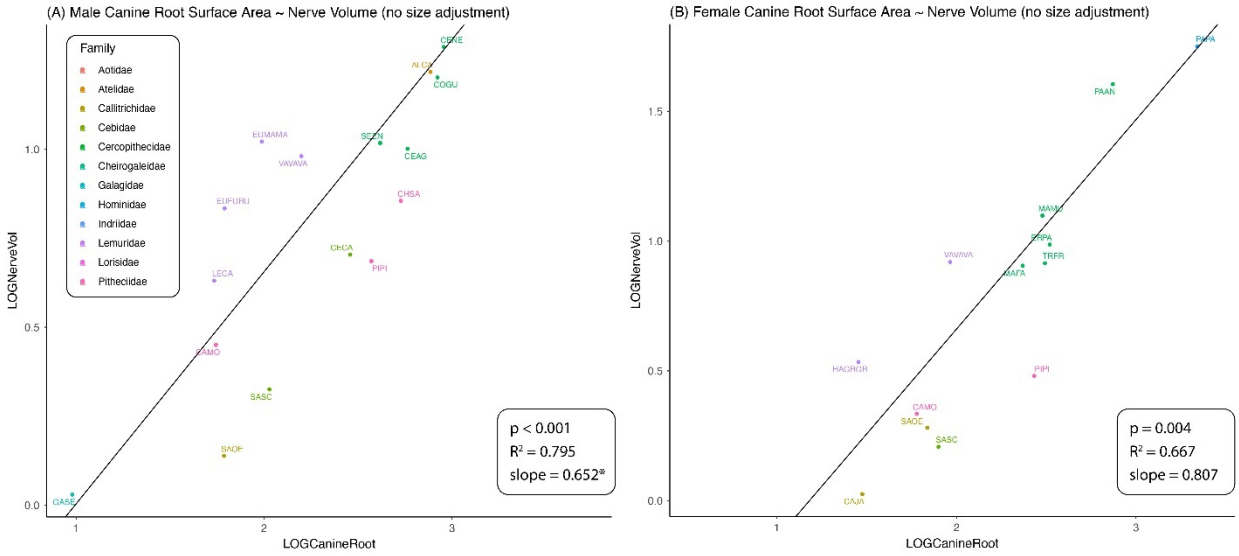

Figure 4.26 The canine root surface area to <u>IAN volume</u> PGLS analyses for males (A) and females (B). These data are power reduced and natural log transformed.

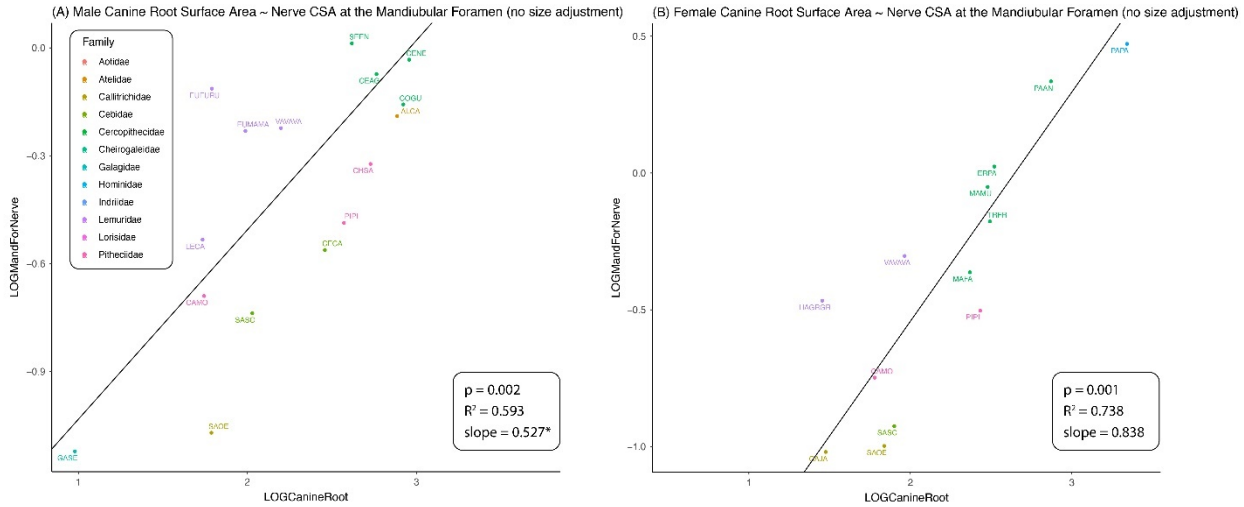

Figure 4.27. The canine root surface area to <u>nerve CSA at the mandibular foramen</u> PGLS analyses for males (A) and females (B). These data are power reduced and natural log transformed.

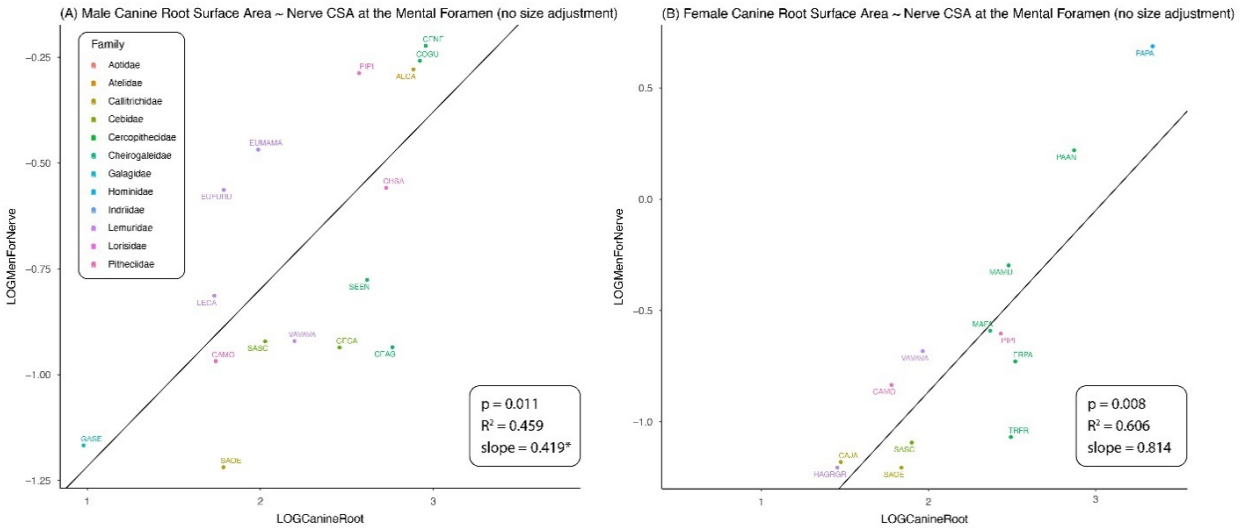

Figure 4.28. The canine root surface area to <u>nerve CSA at the mental foramen</u> PGLS analyses for males (A) and females (B). These data are power reduced and natural log transformed.

Nervous tissues and mandible length. To assess the allometric relationship between the nervous tissues and the mandible size I ran a PGLS analysis on the species averages of the nervous tissues and the mandible length because previous literature shows that brain size if negatively allometric to body size. These PGLS regressions showed these negatively allometric relationships do not hold true for nervous tissues in the mandible. Total IAN volume, the nerve

CSA at the mandibular foramen, and the nerve CSA at the mental foramen were regressed on to mandible length (Table 4.10). While all relationships were significant (volume: p-value < 0.001; mandibular foramen CSA: p-value < 0.001; and mental foramen CSA: p-value < 0.001), no slope value was shown to be significantly different to one. This indicates that the nervous tissues within the mandible show rates of isometry in terms of overall growth rather than a negatively allometric relationship.

Table 4.10. PGLS results for nervous tissues to mandible size

Dependent variable	Independent variable	p-value	R^2	slope	Slope CI	Slope p-value
IAN volume	Mandible length	**< 0.001**	0.967	0.919	0.818 -1.021	0.123
Nerve CSA at mandibular foramen	Mandible length	**< 0.001**	0.904	0.829	0.667 – 0.991	0.051
Nerve CSA at mental foramen	Mandible length	**< 0.001**	0.694	0.715	0.430 – 1.000	0.051

Hypothesis Testing

Hypothesis 1 (Q1-H1): covariation between root surface area and occlusal surface variables. To assess the relationship between the root surface areas and the occlusal surface variables, I ran a series of PGLS analyses using the power reduced, size-adjusted, and natural log transformed data (Table 4.11). These results show a significant relationship between the root surface area and the enamel surface area for all four tooth classes (M_1: p-value = 0.001, P_4: p-value <0.001, C_1: <0.001, I_1: 0.002) (Figure 4.29A-D). Interestingly, the R^2 value for the canines (R^2 = 0.883) was much higher than those seen in the molars (R^2 = 0.547), premolars (R^2 = 0.593), and incisors (R^2 = 0.539) indicating that the canine root surface area to enamel surface area relationship is tighter than other teeth in data that has been size-adjusted. There were no other significant relationships found in these analyses indicating that the shape of the tooth's surface is not directly related to the root surface area. However, wear was not used as a

contributing factor in these analyses and thus the relationships for OPC and occlusal slope may be affected by this (per the wear analysis in Chapter 3).

Table 4.11. PGLS results for Question 1, Hypothesis 1 (size-adjusted data)

Dependent variable	Independent variable*	p-value	R^2
Root surface area	Enamel surface area	M_1: **0.001** P_4: **<0.001** C_1: **<0.001** I_1: **0.002**	M_1: 0.547 P_4: 0.593 C_1: 0.883 I_1: 0.539
Root surface area	DNE	M_1: 0.773 P_4: 0.068 C_1: 0.563 I_1: 0.085	M_1: 0.006 P_4: 0.233 C_1: 0.026 I_1: 0.211
Root surface area	OPC	M_1: 0.717 P_4: 0.469 C_1: 0.024 I_1: 0.433	M_1: 0.010 P_4: 0.041 C_1: 0.334 I_1: 0.048
Root surface area	RFI	M_1: 0.761 P_4: 0.367 C_1: 0.550 I_1: 0.076	M_1: 0.007 P_4: 0.063 C_1: 0.028 I_1: 0.222
Root surface area	Occlusal slope	M_1: 0.332 P_4: 0.198 C_1: 0.661 I_1: 0.084	M_1: 0.073 P_4: 0.124 C_1: 0.015 I_1: 0.212
All analyses used 13 degrees of freedom ***DNE = Dirichlet's Normal Energy, OPC = Orientation Patch Count, RFI = Relief Index** **Alpha values set at p-value < 0.0125**			

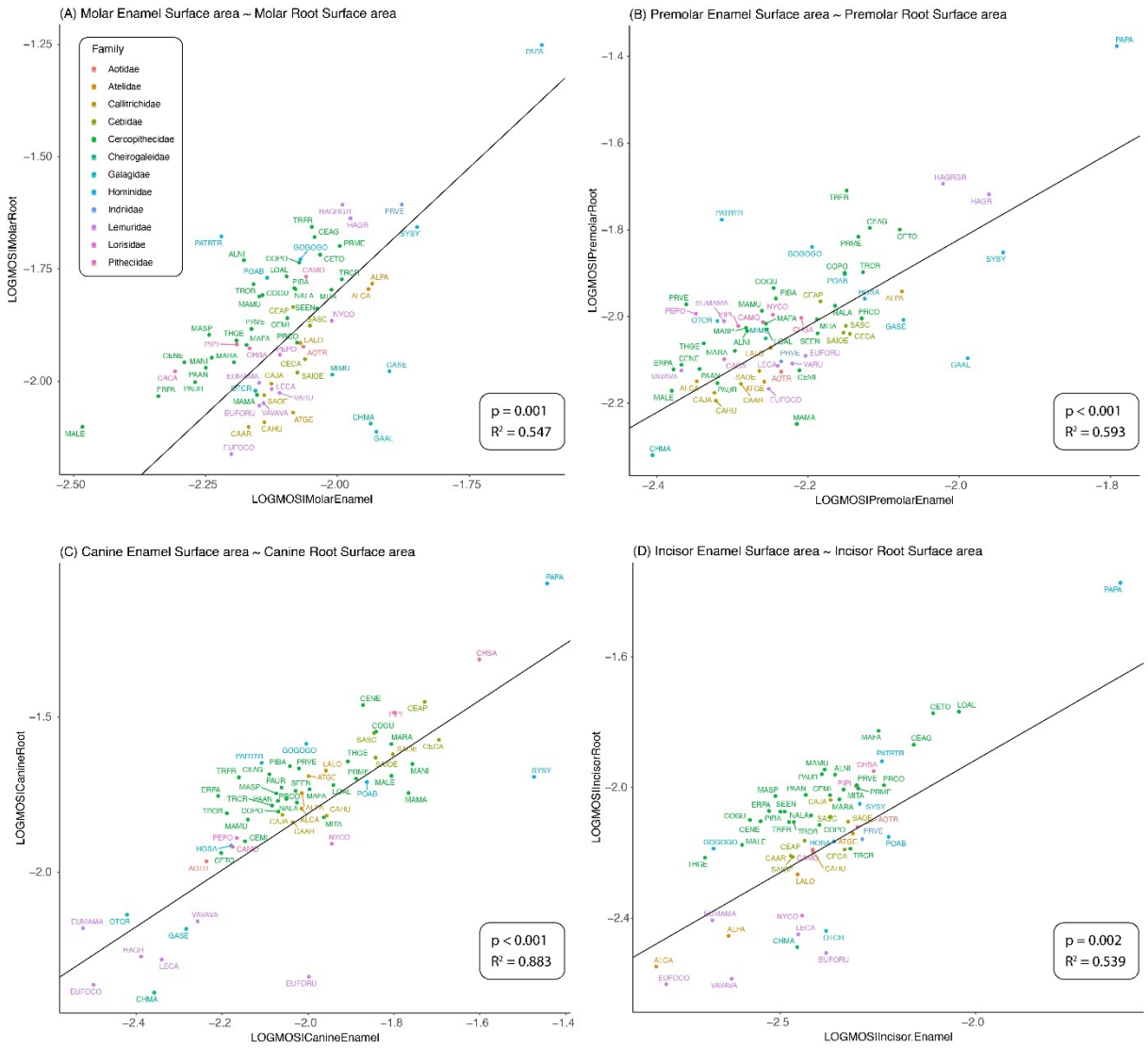

Figure 4.29. The molar (A), premolar (B), canine (C), and incisor (D) enamel surface area to root surface area PGLS analyses. These data are power reduced, size-adjusted, and natural log transformed.

Because the canines were shown to be significantly different between males and females this same PGLS was run by sex (Table 4.12). Only one analysis, root surface area to enamel surface area in females showed a significant relationship (p-value <0.001) (Figure 4.30). Additionally, the R^2 value for this relationship is relatively high ($R^2 = 0.810$), mirroring the results shown in the combined sex analyses (Table 4.2). These results were expected because primate female canines are often used for very different purposes and, as the allometric studies above showed, much more proportional in terms of root/enamel surface size. This indicates that even if

size is removed, teeth will continue to show very tight relationships between the root surface area and enamel surface area in all teeth except for male canines, which are often much larger and not used strictly for masticatory purposes.

Table 4.12. PGLS Results for Question 1, Hypothesis 1 (by sex) canines (size-adjusted)

Dependent variable	Independent variable*	p-value	R^2
Root surface area	Enamel surface area	M: 0.719 F: **<0.001**	M: 0.012 F: 0.810
Root surface area	DNE	M: 0.718 F: 0.651	M: 0.012 F: 0.027
Root surface area	OPC	M: 0.538 F: 0.087	M: 0.035 F: 0.322
Root surface area	RFI	M: 0.344 F: 0.807	M: 0.082 F: 0.008
Root surface area	Occlusal slope	M: 0.065 F: 0.695	M: 0.275 F: 0.020
All analyses used 11 degrees of freedom ***DNE = Dirichlet's Normal Energy, OPC = Orientation Patch Count, RFI = Relief Index** **Alpha values set at p-value < 0.025**			

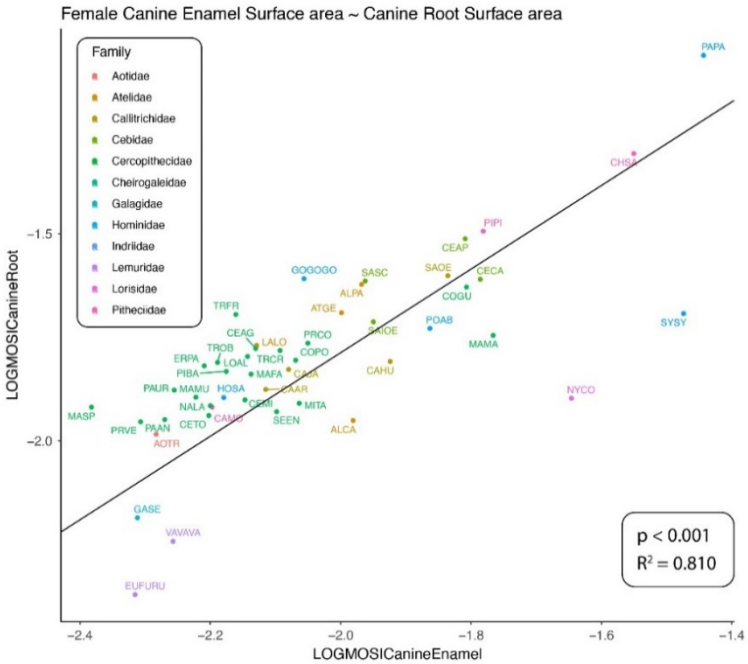

Figure 4.30. The female canine enamel surface area to root surface area PGLS analyses. These data are power reduced, size-adjusted, and natural log transformed.

Multiple regression analyses assess both the strength of the relationship between the dependent and independent variables and the interactions/contributions of each independent

variable. This allows us to estimate that if the independent variables are considered together, could they be used to predict the size of the root surface areas. In addition, phylogeny can be taken into account to ensure that phylogenetic relationships are not introduced as confounding variables. I used this phylogenetic multiple regression to assess if the tooth variables could be used as a group to predict the size of the root surface areas using the size-adjusted data. The results of this regression are shown in Table 4.13 and indicate that there was no significant relationship between the occlusal surface variables together and the root surface areas. This was expected based on the PGLS results shown in Table 4.9 as there were no significant relationships between the occlusal shape variables and the root surface areas.

Table 4.13. Phylogenetic Multiple Regression results for Question 1, Hypothesis 1 (size-adjusted data)

Dependent variable	Independent variable*	p-value	R^2
Root surface area	DNE, OPC, RFI, Slope	M_1: 0.517 P_4: 0.441 C_1: 0.202 I_1: 0.499	M_1: 0.257 P_4: 0.290 C_1: 0.421 I_1: 0.265
All analyses used 10 degrees of freedom ***DNE = Dirichlet's Normal Energy, OPC = Orientation Patch Count, RFI = Relief Index** **Alpha values set at p-value < 0.05**			

I ran the same multiple regression by sex for canines with the results shown in Table 4.14. The analysis with root surface area to the occlusal variables showed significant relationships in males (p-value = 0.013) with a relatively high R^2 value (0.763). These results were unexpected because when the occlusal shape variables were compared individually to the root surface area, no significant relationships were noted (Table 4.11). However, while the overall model was significant, no single independent variable was shown to be a significant predictor – making it very difficult to establish why these variables (when used together) could have a significant relationship to the root surface area. Additionally, because no variables were shown to be significant on their own, no further testing was run by removing the non-significant variables.

Table 4.14. Multiple Regression Results for Question 1, Hypothesis 1 (by sex) canines (size-adjusted data)

Dependent variable	Independent variable	p-value	R^2
Root surface area	DNE, OPC, RFI, Occlusal slope	M: **0.013** F: 0.418	M: 0.763 F: 0.487
All analyses used 8 degrees of freedom **DNE = Dirichlet's Normal Energy, OPC = Orientation Patch Count, RFI = Relief Index** **Alpha values set at p-value < 0.025**			

Hypothesis 2 (Q1-H2)*: *covariation of occlusal surface shape/size and nervous tissue variables. To assess the relationship between the occlusal surface shape and the nervous tissue variables, I ran a series of PGLS analyses using the power reduced, size-adjusted, and natural log transformed data. Table 4.15 shows the PGLS results for Q1-H2. Overall, these analyses showed very few significant relationships between the nervous tissue variables and the occlusal surface variables. The relationship between premolar DNE and nerve CSA at the mental foramen (p-value = 0.004) showed a significant relationship (Figure 4.31). Additionally, the relationship between nerve CSA beneath the premolars and premolar DNE also showed a significant relationship (p-value = 0.013) (Figure 4.32). DNE was relatively unaffected by wear in this sample in the wear analysis performed, meaning these analyses are likely reflecting the true relationship between these variables. However, the R^2 values for both the nerve CSA at the mental foramen (R^2 = 0.477) and the nerve CSA beneath the premolars (R^2 = 0.391) were low, indicating the relationships are not substantially close.

Table 4.15. PGLS results for Question 1, Hypothesis 2 (size-adjusted data)

Dependent variable	Independent variable*	p-value	R^2
IAN volume	Enamel surface area	M_1: 0.189 P_4: 0.125 C_1: 0.925 I_1: 0.864	M_1: 0.128 P_4: 0.171 C_1: <0.000 I_1: 0.002
IAN volume	DNE	M_1: 0.179 P_4: 0.072 C_1: 0.337 I_1: 0.520	M_1: 0.134 P_4: 0.227 C_1: 0.071 I_1: 0.033
IAN volume	OPC	M_1: 0.488 P_4: 0.769 C_1: 0.943 I_1: 0.578	M_1: 0.038 P_4: 0.006 C_1: <0.000 I_1: 0.024
IAN volume	RFI	M_1: 0.292 P_4: 0.536 C_1: 0.533 I_1: 0.452	M_1: 0.084 P_4: 0.030 C_1: 0.031 I_1: 0.044
IAN volume	Occlusal slope	M_1: 0.322 P_4: 0.285 C_1: 0.655 I_1: 0.738	M_1: 0.075 P_4: 0.087 C_1: 0.016 I_1: 0.009
Nerve CSA at Mandibular foramen	Enamel surface area	M_1: 0.057 P_4: 0.105 C_1: 0.517 I_1: 0.962	M_1: 0.251 P_4: 0.189 C_1: 0.033 I_1: <0.000
Nerve CSA at mandibular foramen	DNE	M_1: 0.173 P_4: 0.071 C_1: 0.213 I_1: 0.625	M_1: 0.138 P_4: 0.229 C_1: 0.117 I_1: 0.019
Nerve CSA at mandibular foramen	OPC	M_1: 0.755 P_4: 0.784 C_1: 0.547 I_1: 0.499	M_1: 0.008 P_4: 0.008 C_1: 0.029 I_1: 0.036
Nerve CSA at mandibular foramen	RFI	M_1: 0.448 P_4: 0.398 C_1: 0.249 I_1: 0.414	M_1: 0.045 P_4: 0.056 C_1: 0.101 I_1: 0.052
Nerve CSA at mandibular foramen	Occlusal slope	M_1: 0.525 P_4: 0.221 C_1: 0.509 I_1: 0.637	M_1: 0.032 P_4: 0.113 C_1: 0.034 I_1: 0.018

All analyses used 13 degrees of freedom
***DNE = Dirichlet's Normal Energy, OPC = Orientation Patch Count, RFI = Relief Index**
Tests with all four teeth had alpha values set to p-value < 0.0125
Tests with only molar or premolar tested had alpha values set to p-value < 0.05

Table 4.15 (Cont.)

Dependent variable	Independent variable*	p-value	R^2
Nerve CSA at mental foramen	Enamel surface area	M_1: 0.686 P_4: 0.601 C_1: 0.711 I_1: 0.169	M_1: 0.013 P_4: 0.022 C_1: 0.011 I_1: 0.141
Nerve CSA at mental foramen	DNE	M_1: 0.039 P_4: **0.004** C_1: 0.488 I_1: 0.144	M_1: 0.288 P_4: 0.477 C_1: 0.038 I_1: 0.157
Nerve CSA at mental foramen	OPC	M_1: 0.735 P_4: 0.044 C_1: 0.941 I_1: 0.372	M_1: 0.009 P_4: 0.277 C_1: <0.000 I_1: 0.062
Nerve CSA at mental foramen	RFI	M_1: 0.931 P_4: 0.968 C_1: 0.429 I_1: 0.298	M_1: <0.000 P_4: <0.000 C_1: 0.049 I_1: 0.083
Nerve CSA at mental foramen	Occlusal slope	M_1: 0.682 P_4: 0.745 C_1: 0.249 I_1: 0.375	M_1: 0.013 P_4: 0.008 C_1: 0.101 I_1: 0.061
Nerve CSA beneath molars	Enamel surface area	M_1: 0.195	M_1: 0.125
Nerve CSA beneath molars	DNE	M_1: 0.310	M_1: 0.079
Nerve CSA beneath molars	OPC	M_1: 0.560	M_1: 0.027
Nerve CSA beneath molars	RFI	M_1: 0.443	M_1: 0.046
Nerve CSA beneath molars	Occlusal slope	M_1: 0.523	M_1: 0.032
Nerve CSA beneath premolars	Enamel surface area	P_4: 0.482	P_4: 0.039
Nerve CSA beneath premolars	DNE	P_4: **0.013**	P_4: 0.391
Nerve CSA beneath premolars	OPC	P_4: 0.514	P_4: 0.034
Nerve CSA beneath premolars	RFI	P_4: 0.589	P_4: 0.023
Nerve CSA beneath premolars	Occlusal slope	P_4: 0.319	P_4: 0.076

All analyses used 13 degrees of freedom
***DNE = Dirichlet's Normal Energy, OPC = Orientation Patch Count, RFI = Relief Index**
Tests with all four teeth had alpha values set to p-value < 0.0125
Tests with only molar or premolar tested had alpha values set to p-value < 0.05

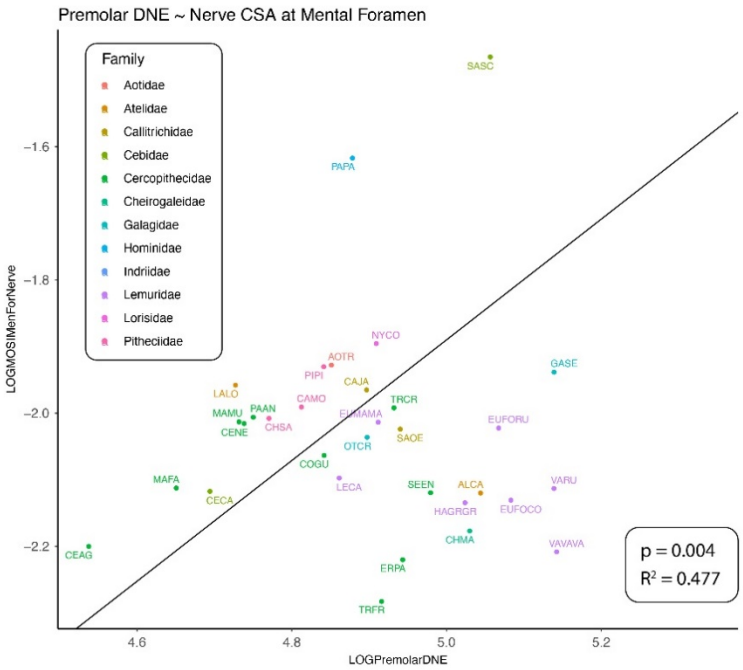

Figure 4.31. The premolar DNE to nerve CSA at the mental foramen PGLS analyses. These data are power reduced, size-adjusted, and natural log transformed.

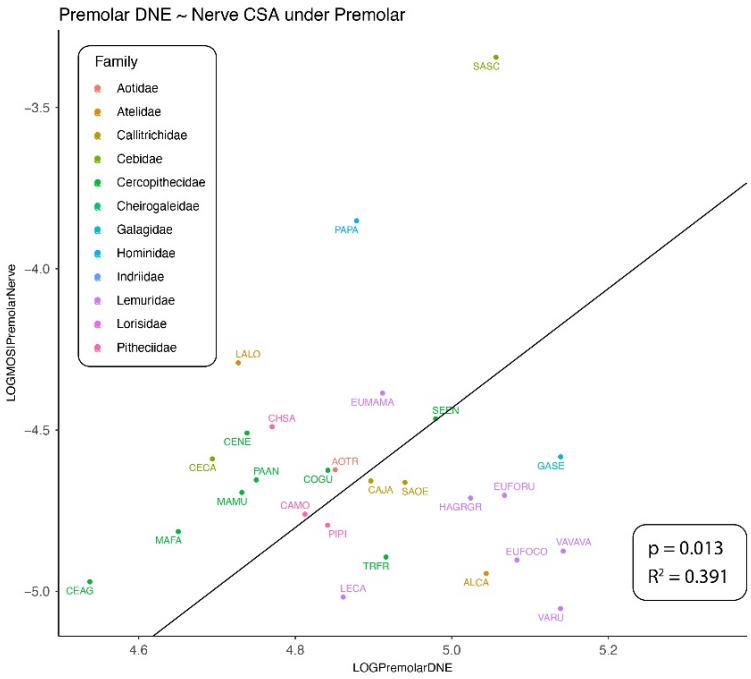

Figure 4.32. The premolar DNE to nerve CSA beneath P_4 PGLS analyses. These data are power reduced, size-adjusted, and natural log transformed.

I ran the same PGLS analyses by sex for canines with the results shown in Table 4.16.

No test showed a significant relationship between the nervous tissue variables and the occlusal

surface variables of the teeth. These analyses reflect what was shown in the data when the sexes were combined (Table 4.14). These analyses indicate that when size is removed from the data and shape is assessed, there is no significant relationship between the nervous tissues of the mandible and the occlusal surface of the tooth.

Table 4.16. PGLS Results for Question 1, Hypothesis 2 (by sex) canines (size-adjusted data)

Dependent variable	Independent variable*	p-value	R^2
IAN volume	Enamel surface area	M: 0.577 F: 0.943	M: 0.029 F: <0.000
IAN volume	DNE	M: 0.623 F: 0.129	M: 0.023 F: 0.263
IAN volume	OPC	M: 0.401 F: 0.903	M: 0.003 F: 0.002
IAN volume	RFI	M: 0.411 F: 0.316	M: 0.062 F: 0.125
IAN volume	Occlusal slope	M: 0.356 F: 0.546	M: 0.078 F: 0.047
Nerve CSA at mandibular foramen	Enamel surface area	M: 0.639 F: 0.996	M: 0.021 F: <0.000
Nerve CSA at mandibular foramen	DNE	M: 0.649 F: 0.108	M: 0.019 F: 0.290
Nerve CSA at mandibular foramen	OPC	M: 0.581 F: 0.917	M: 0.028 F: 0.001
Nerve CSA at mandibular foramen	RFI	M: 0.664 F: 0.192	M: 0.018 F: 0.202
Nerve CSA at mandibular foramen	Occlusal slope	M: 0.746 F: 0.351	M: 0.009 F: 0.109
Nerve CSA at mental foramen	Enamel surface area	M: 0.941 F: 0.937	M: 0.001 F: <0.000
Nerve CSA at mental foramen	DNE	M: 0.566 F: 0.046	M: 0.031 F: 0.411
Nerve CSA at mental foramen	OPC	M: 0.875 F: 0.921	M: 0.002 F: 0.001
Nerve CSA at mental foramen	RFI	M: 0.945 F: 0.215	M: <0.000 F: 0.185
Nerve CSA at mental foramen	Occlusal slope	M: 0.954 F: 0.338	M: <0.000 F: 0.115
All analyses used 8 degrees of freedom ***DNE = Dirichlet's Normal Energy, OPC = Orientation Patch Count, RFI = Relief Index** **Tests with all four teeth had alpha values set to p-value < 0.025**			

I ran a series of phylogenetic multiple regressions to establish if there was a significant relationship between the nervous tissue and occlusal surface variables (when used together). These results are shown in Table 4.17. In these analyses, no overall model showed significance, and therefore no further tests were run by removing the non-significant variables. These results were expected due to the occlusal surface variables showing very few significant relationships when individually tested (Table 4.15).

Table 4.17. Multiple Regression results for Question 1, Hypothesis 2 (size-adjusted data)

Dependent variable	Independent variable*	p-value	R^2
IAN volume	Enamel SA, DNE, OPC, RFI, Slope	M_1: 0.203 P_4: 0.059 C_1: 0.957 I_1: 0.674	M_1: 0.504 P_4: 0.644 C_1: 0.098 I_1: 0.263
Nerve CSA at mandibular foramen	Enamel SA, DNE, OPC, RFI, Slope	M_1: 0.185 P_4: 0.026 C_1: 0.891 I_1: 0.539	M_1: 0.517 P_4: 0.709 C_1: 0.149 I_1: 0.325
Nerve CSA at mental foramen	Enamel SA, DNE, OPC, RFI, Slope	M_1: 0.195 P_4: 0.119 C_1: 0.904 I_1: 0.704	M_1: 0.509 P_4: 0.572 C_1: 0.141 I_1: 0.249
Nerve CSA beneath molars	Enamel SA, DNE, OPC, RFI, Slope	M_1: 0.479	M_1: 0.353
Nerve CSA beneath premolars	Enamel SA, DNE, OPC, RFI, Slope	P_4: 0.089	P_4: 0.605

All analyses used 9 degrees of freedom
***DNE = Dirichlet's Normal Energy, OPC = Orientation Patch Count, RFI = Relief Index**
Tests with all four teeth had alpha values set to p-value < 0.0125
Tests with only molar or premolar tested had alpha values set to p-value < 0.05

I ran these same phylogenetic multiple regression analyses after sectioning out the data by sex for the canine teeth (Table 4.18). No test showed significance in the overall model nor were there any significant predictors within each model. Again, these results mirrored what was seen in the combined sex data analyses and was predicted based on the individual variable tests run previously (Table 4.16).

Table 4.18. Multiple Regression Results for Question 1, Hypothesis 2 (by sex) canines (size-adjusted data)

Dependent variable	Independent variable*	p-value	R^2
IAN volume	DNE, OPC, RFI, Occlusal slope, enamel SA	M: 0.839 F:0.661	M: 0.219 F: 0.461
Nerve CSA at mandibular foramen	DNE, OPC, RFI, Occlusal slope, enamel SA	M: 0.886 F: 0.672	M: 0.186 F: 0.454
Nerve CSA at mental foramen	DNE, OPC, RFI, Occlusal slope, enamel SA	M: 0.734 F: 0.588	M: 0.283 F: 0.509
All analyses were performed with 4 degrees of freedom ***DNE = Dirichlet's Normal Energy, OPC = Orientation Patch Count, RFI = Relief Index** **Alpha values set at p-value < 0.05**			

Hypothesis 3 (Q1-H3): covariation of nervous tissue and root surface area. To assess the relationship between the root surface area and the nervous tissue variables, I ran a series of PGLS analyses using the power reduced, size-adjusted, and natural log transformed data. No analysis showed a significant relationship between the nervous tissue variables and the root surface areas (Table 4.19).

Table 4.19. PGLS results for Question 1, Hypothesis 3 (size-adjusted data)

Dependent variable	Independent variable	p-value	R^2
IAN volume	Root surface area	M_1: 0.311 P_4: 0.469 C_1: 0.539 I_1: 0.928	M_1: 0.079 P_4: 0.041 C_1: 0.029 I_1: <0.000
Nerve CSA at mandibular foramen	Root surface area	M_1: 0.135 P_4: 0.405 C_1: 0.988 I_1: 0.895	M_1: 0.163 P_4: 0.054 C_1: <0.000 I_1: 0.001
Nerve CSA at mental foramen	Root surface area	M_1: 0.962 P_4: 0.584 C_1: 0.974 I_1: 0.702	M_1: <0.000 P_4: 0.024 C_1: <0.000 I_1: 0.012
Nerve CSA beneath M_1	Root surface area (molar)	M_1: 0.375	M_1: 0.061
Nerve CSA beneath P_4	Root surface area (premolar)	P_4: 0.845	P_4: 0.003
All analyses used 13 degrees of freedom **Tests with all four teeth had alpha values set to p-value < 0.0125** **Tests with only molar or premolar tested had alpha values set to p-value < 0.05**			

I ran these same analyses after sectioning out the data by sex for the canine teeth because they were shown to be significantly different during data preparation. The PGLS results

are shown below in Table 4.20. No significant relationships were established between the nervous tissue variables and the canine root surface areas. This was expected due to the combined sex data showing no significant relationships between these variables.

Table 4.20. PGLS Results for Question 1, Hypothesis 3 (by sex) canines (size-adjusted data)

Dependent variable	Independent variable	p-value	R^2
IAN volume	Canine root surface area	M: 0.588 F: 0.593	M: 0.028 F: 0.037
Nerve CSA at mandibular foramen	Canine root surface area	M: 0.773 F: 0.584	M: 0.007 F: 0.039
Nerve CSA at mental foramen	Canine root surface area	M: 0.675 F: 0.798	M: 0.016 F: 0.009
All analyses were performed with 11 degrees of freedom Alpha values set at p-value < 0.025			

I ran a series of phylogenetic multiple regressions to establish if there was a significant relationship between the occlusal surface variables and the nervous tissue variables. These results are shown in Table 4.21. No analysis showed significance in the overall model, nor were there any significant predictors within the model. Therefore, no further analyses were performed by removing the non-significant variables. Again, these relationships were expected due to previous analyses where the variables were assessed individually (Table 4.19).

Table 4.21. Phylogenetic multiple regression results for Question 1, Hypothesis 3 (size-adjusted data)

Dependent variable	Independent variable	p-value	R^2
IAN volume	All root surface areas (M_1, P_4, C_1, I_1)	0.616	0.216
Nerve CSA at mandibular foramen	All root surface areas (M_1, P_4, C_1, I_1)	0.579	0.231
Nerve CSA at mental foramen	All root surface areas (M_1, P_4, C_1, I_1)	0.441	0.291
All analyses were performed with 10 degrees of freedom Alpha values set at p-value < 0.0125			

The last analyses for Q1-H3 were phylogenetic multiple regression analyses by sex to establish if there were significant relationships between the root surface areas and the nervous tissue by sex. The results for these analyses are shown in Table 4.22. Of the three analyses,

none showed significant relationships between the nervous tissue variables and the root surface areas. Again, this was expected due to the individual variable analyses.

Table 4.22. Multiple Regression Results for Question 1, Hypothesis 3 (by sex) canines (size-adjusted data)

Dependent variable	Independent variable	p-value	R^2
IAN volume	All root surface areas (M_1, P_4, C_1, I_1)	M: 0.872 F: 0.905	M: 0.129 F: 0.160
Nerve CSA at mandibular foramen	All root surface areas (M_1, P_4, C_1, I_1)	M: 0.909 F: 0.827	M: 0.107 F: 0.224
Nerve CSA at mental foramen	All root surface areas (M_1, P_4, C_1, I_1)	M: 0.712 F: 0.784	M: 0.213 F: 0.254
All analyses were performed with 8 degrees of freedom Alpha values set at p-value < 0.025			

DISCUSSION

Brief Overview

The goal of this chapter was to examine whether there were relationships between tooth occlusal morphology, nervous tissue variables, and root surface area. Because teeth are the direct interface to the outside environment and the beginning of the mechanical breakdown process for any food consumed, they are under strong selective pressures to adapt to diet. However, while the teeth are the beginning of this breakdown process, the chewing cycle, the force we use to chew with, and the decision to consume certain objects does not necessarily come from the surface of the teeth – it is instead deeply intertwined with the nervous sensations that inform the brain on how to proceed with all these processes. Therefore, the nervous structures and root structures should be under the same evolutionary pressures that the surface of the teeth are to maximize the chewing efficiency of the tooth's surface.

My first hypothesis (Q1-H1) was that there would be a direct, positive relationship between the size and shape of the occlusal surface of the teeth and the size of the root structures. This hypothesis was only supported in the relationships between the enamel surface area and the root surface area – in both the allometric analyses and the size-adjusted data. No

significant relationships between the shape of the occlusal surface and relative root surface area were noted – indicating that the overall size of the enamel surface has a much larger effect on the root surface area than the shape of the tooth surface.

My second hypothesis (Q1-H2) was that there would be a direct, positive relationship between the size and shape of the occlusal surface and the nervous tissues variables. This hypothesis was supported in the allometric analyses, but there were very few significant relationships between these variables when the data were size adjusted. This indicates that size – not shape – is much more influential on the nervous tissues of the mandible.

Finally, my third hypothesis (Q1-H3) was that there would be a direct, positive relationship between the root surface area and the nervous tissue variables of the mandible. Again, this hypothesis was only supported in the allometric analyses. There were no significant relationships between the root surface areas and the size/shape of the occlusal surface when the data were size adjusted. This further supports previous evidence that the size of the occlusal surface is more closely related to the size of the nervous tissues and that the shape has very little effect on how these tissues vary.

Allometric Analyses

When the raw data were analyzed to examine allometric patterns, some very interesting trends appeared. First, in both the combined sex data and the separated canine data, there were significant relationships between the root surface area and the enamel surface area for all tooth types. In all these relationships, the slopes approached isometry, although the molars and premolars presented slopes that were positively allometric and significantly different from isometry. Additionally, in all these relationships, the R^2 values were very high – indicating that these relationships are particularly tight and consistent across the tooth row. This is unsurprising in that as the enamel surface increases, the root surface would need to increase at a relatively similar rate to support forces generated on the surface of the tooth. It is interesting, but not surprising, that the molars and premolars showed positive allometry in these tests indicating that

these roots would be increasing at a faster rate than expected in relation to the enamel surface area.

Because previous research has shown that a more resistant diet may have selected for larger post-canine root surface areas (Deines et al., 1993; Spencer, 2003), these results show this is the case for many species, but not all. In this analyses, 19 species had a primary resistant diet and of these 19, 11 fell above the regression line in the molar PGLS analysis for root to enamel surface areas (See Chapter 3 for a full table of all species used and the assigned dietary categories). The species that had primary resistant diets that fell below the regression line for the molar regression were *Nasalis larvatus*, *Presbytis comata*, *Propithecus verreauxi, Semnopithecus entellus*, *Theropithecus gelada*, and *Trachypithecus cristatus*. Of these 19, premolars showed 12 species with positive allometry in the PGLS analysis for root to enamel surface area. The species that fell below the regression line (but had resistant diets) were *Macaca mulatta*, *Nasalis larvatus*, *Presbytis comata*, *Semnopithecus entellus*, and *Trachypithecus cristatus*. Interestingly, of the species that had a resistant primary and secondary diet (*Colobus polykomos*, *Piliocolobus badius*, *Presbytis melaphos*, and *Theropithecus gelada*), only *Theropithecus gelada* did not show positive allometry across both post-canine teeth. This could indicate that the more resistant a diet is overall, the larger the molar roots need to be in relation to the enamel surface to withstand those forces. These dietary relationships will be discussed in greater detail in Chapter 7 (Discussion and Conclusions) to synthesize results from this chapter and chapter 6 – a chapter devoted entirely to dietary analyses.

Biologically, roots are the anchor points for the teeth and are part of the vital system that keep the tooth embedded within the body of the mandible. Roots for all teeth would need to be similar in size to the crown that they anchor to withstand any force on the tooth's surface, either through diet or other oral manipulations. Additionally, the larger a tooth root is, the more attachment sites that are required for the periodontal ligament to keep the tooth in place. The

periodontal ligament is a vital component in the feedback mechanism that prompts a mammal to stop chewing when the teeth detect a foreign object within the bolus (Byers & Dong, 1989; Crompton, 1995; Falin, 1958; Inoue et al., 1989; Linden, 1991; Ross et al., 2010). These results indicate that as root surface area is increasing in the post canine teeth, more attachment sites would be present, and thus there would be a higher potential for greater touch sensitivity in the molars and premolars when compared with the incisors and canines.

Second, in both the combined sex data and the separated canine data, there is an overall all trend of nervous tissue variables increasing at slower than expected rates in relation to the enamel surface area. Because no study like this – with quantified nervous tissue measurements across primates – has ever been performed, these results were unexpected. Most slopes in these analyses show negative allometry between the nervous tissue variables and the enamel surface area of all tooth types (molars, premolars, canines, and incisors) although only male slopes were shown to be significantly different from isometry. The only exception to this was in the analysis for the nerve CSA at the mandibular foramen to the enamel surface area (slope = 1.045) in female canines (although the slope was not significantly different from isometry).

All these results reach the general conclusion that the nervous tissues are increasing in size at a slower than expected rate in relation to the enamel surface of the tooth. This is particularly true in the canines when males and females were analyzed separately. Males consistently showed negative allometry, with slopes that were significantly different from isometry, throughout the analyses. This is likely because males use their canine teeth for purposes other than dietary process (i.e., intermale competition), which do not necessarily require greater touch sensitivity (Pickford, 1986; Plavcan, 1993). Male canines are under strong selective pressures to increase in enamel surface area (and overall tooth size) due to different habitats and group sizes (Plavcan, 1993). The data presented here supports the previous literature in that species like *Saimiri osteridii* – which show moderate rates of canine dimorphism

– fall below the regression line for canine enamel to root enamel and fall below the regression line (and are negatively allometric) in the analysis for canine enamel to IAN volume. This shows that species with higher levels of canine dimorphism have larger enamel surfaces in relation to root surfaces and much larger enamel surfaces in relation to overall nervous volume. As stated, these results were unexpected as my hypotheses estimated that there would be a direct and positive relationship between these tissues and the teeth. Teeth serve the important function of pain and pressure sensation during mastication and chewing, all of which is transmitted via the inferior alveolar nerve (Anderson et al., 1970; Avery & Cox, 1977; Brashear, 1936; Dubner et al., 1978; Luschei & Goldberg, 2011; Plaffman, 1939). However, these analyses show that as teeth increase in size, the nervous tissues that surround and support these teeth are increasing at just under the same rate (negatively allometric but not significantly different from isometry) or at a much slower rate than expected (this is true for male canines in all cases).

Finally, in both the combined and the separate canine data, the trend of all analyses showing significant relationships and negative allometry between the nervous tissues and the hard tissues continued with the root surface areas. All slopes for these analyses were negatively allometric and the majority were significantly different from one. In the combined data, only one test was not significantly different to one: nerve CSA beneath P_4 and premolar root surface area (slope = 0.752). However, this analysis was approaching significance with a p-value of 0.062. One interesting trend in these analyses is that the canines repeatedly showed lower R^2 values than any other tooth indicating that these relationships are less close than those seen in the molars, premolars, and incisors. Conversely, when the canines were separated by sex, all analyses were again significant and negatively allometric, but only male slopes showed values that were significantly different from isometry. In these sex-specific analyses, we again see lower R^2 values (0.459 - 0.795) although males were much lower in the analyses for nerve CSA at the mandibular foramen (0.593) and nerve CSA at the mental foramen (0.459).

Altogether, these allometric analyses show that while the root surface area and enamel surface area are relatively proportional in size across all tooth types (M_1, P_4, C_1, and I_1) the nervous tissues are not increasing at the same rates throughout the mandible. This is particularly evident in male canines when sexes are analyzed separately and is likely due to sexual dimorphism in male canines (Pickford, 1986; Plavcan, 1993). Although I expected to find direct and positive relationships between the enamel and root surfaces of the teeth and the nervous tissues, these negatively allometric relationships indicate that nervous tissue in the mandible is consistently increasing at a slower rate (although nearly isometric) than expected in relation to the hard tissues. However, these studies do show that there is a direct relationship between the size of the teeth and the nervous tissues, indicating that tooth size will likely determine how much nervous tissue is necessary for innervation and a properly functioning masticatory apparatus.

Many allometric studies on brain size have been done to assess the evolution of the primate brain (Clutton-Brock & Harvey, 1980; Deacon, 1990; Rilling, 2006; Stephan et al., 1981, 1988). While primates have a relatively large brain to body size ratio in relation to other mammals, the evolutionary trajectories of brain growth have been different for all major clades of primates. For example, while all primate species have a cerebellum, humans exhibit a cerebellum far larger in relative and absolute size (Rilling, 2006). Additionally, all parts of the brain have been shown to either increase or decrease in size independently from each other throughout various evolutionary trajectories in animals. Rilling (2006) explains that while body size can explain 94% of the variation seen in brain size across a wide variety of primate species, the overall relationship between brain and body size is negatively allometric. This indicates that as body size increases, the nervous tissues within the brain increase at a slower rate than expected.

Hypothesis Testing

Occlusal surface covariation with root structures (H1). The results for Q1-H1 show a clear relationship between the root surface areas and enamel surface areas of all tooth classes in both the size-adjusted data and in the allometric analyses. This was expected, based on previous research that showed not only a significant relationship between the root surface and the enamel surface, but also to the root surface area and the diet certain primates consume (Deines et al., 1993; Spencer, 2003). Roots are the anchor points for the teeth into the mandible and therefore must resist and effectively dissipate any forces that are occurring on the occlusal surface of the teeth during chewing. Spencer (2003) specifically showed that primates that with tougher/stiffer diets (and therefore larger bite force or more chewing cycles) had adapted larger maxillary molar root surface areas to account for the increased forces. Q1-H1 supports this data in that even when size is adjusted for, there is still a significant relationship between all tooth types (M_1, P_4, C_1, and I_1) enamel surface and root surface area.

Interestingly, when the canine data was separated by sex, females continued to show a significant relationship between the enamel surface area and the root surface area in the size-adjusted data. These results suggest that female canines may have been selected to serve similar functions (such as diet) to other teeth on the mandibular tooth row whereas male teeth have adaptations that are much more closely associated with male-male competitions (Greenfield, 1992; Harvey et al., 1978; Kay et al., 1988; Leutenegger & Kelly, 1977; Plavcan & van Schaik, 1992; Plavcan, 1993). These results support this previous literature in that males do not show a significant relationship between the enamel surface and the root surface area when adjusted for overall differences in size.

Occlusal surface covariation with nervous tissue structures (H2). The results for Q1-H2 show very few relationships between the nervous tissues and the occlusal surface of the teeth in the size-adjusted data. Only two analyses (nerve CSA at the mental foramen and the nerve CSA beneath the premolar) showed a significant relationship to P_4 DNE. DNE is a

measure of the sharpness of the tooth's surface and will thus increase as the complexity of the surface increases. My hypotheses anticipated that, as the complexity of the tooths surface increased, nervous tissue size would also increase to allow for greater touch sensitivity. These results show that premolars may play a vital role in the touch sensitivity of the mouth because of their significant relationship to the nervous tissues that directly supply (nerve CSA beneath P_4) and are near in location to the teeth (nerve CSA at the mental foramen). Previous research has suggested that the P_4 (at least in humans) has the largest canal (in diameter) leaving from the mandibular canal to the tooth root – indicating that this tooth has the potential to have the most nervous tissue connecting it to the IAN (Erisen et al., 1989; Kress et al., 2004). Additionally, an increase in premolar size has often been directly associated with diet – particularly in species that utilize hard-object feeding and species that use the premolars in the first step of food processing (Daegling et al., 2011; Delezene et al., 2013; Fleagle & McGraw, 2002; Kinzey, 1992; Lucas et al., 1994; Singleton, 2004; Spencer, 2003; Wright, 2005). Scott et al. (2018) were able to show that premolar size is evolutionarily sensitive to changes in loading – directly relating the pressure response in premolar teeth to the tooths surface. With the results found here - premolar DNE showing significant relationships to closely associated nervous structures – this further supports the argument that the occlusal surface of the premolar teeth is vital in initiating and maintaining the masticatory cycle.

Nervous tissue structure covariation with root surface areas (H3). The results for Q1-H3 showed no significant relationships between the nervous tissue variables and the root surface areas in the size-adjusted data. This data was relatively expected based on the results from the previous hypotheses. Although there was a significant relationship between the root surface area and the enamel surface area (in the allometric studies and Q1-H1) there were very few relationships between the nervous structures and the occlusal surface in Q1-H2. Because the relationship between the enamel surface area and root surface area was so close, it would be expected that they would have similar relationships to the soft tissues. I expected the roots

and nervous tissues to be very closely related because it is the roots that relay the nervous tissues into the dentin and enamel of the tooth. Additionally, the roots are held in place by the periodontal ligament – a large component of the periodontal membrane that is also supplied by nervous structures from the IAN. However, these data show that when size is adjusted for, there are no significant relationships between the nervous tissues of the mandible and the root surface areas of the mandibular tooth row.

CONCLUSION

Overall, there were three main conclusions drawn from the data here:

1. There is a clear relationship between the root surface area and enamel surface area and little to no relationship between root surface area and shape of the occlusal surface.
2. The shape (particularly the sharpness) of the mandibular premolar occlusal surface is related to the nervous structures that directly supply or are very near to P_4.
3. There are no clear relationships between the root surface areas of the mandibular tooth row to the nervous tissues of the mandible.

In sum, there are some clear relationships between the hard- and soft-tissue components analyzed here. However, most of these relationships appear to be size-dependent and show a negatively allometric relationship between most of the hard- and soft-tissue components. When size is adjusted for, only the relationship between the hard-tissue variables (enamel surface and root surface area) remains and only one occlusal surface variable (premolar DNE) has a relationship to the soft-tissue components. This indicates that the size of nervous tissues is scaling with (but slightly slower than) the hard-tissue components that surround the soft tissues and are likely unaffected by the shape of a tooth's surface.

CHAPTER 5: CORRELATION ANALYSIS BETWEEN THE INFERIOR ALVEOLAR NERVE, THE MANDIBULAR CANAL, AND ASSOCIATED FORAMINA

INTRODUCTION

An extensive amount of morphological variation has been noted in the mandibular canal, the mental foramen, and the mandibular foramen (Anderson et al., 1991; Angelopoulos, 1966; Barclay, 1971; Blackmore & Jennett, 2001; Booth et al., 2013, Wyman & Stoia, 2013; Edwards & Gaughran, 1971; Gershenson et al., 1986; Mardinger et al., 2000; Morris & Jackson, 1933; Murphy & Grundy, 1969; Olivier, 1927, 1928; Starkie & Stewart, 1931; Sutton, 1974; Wadu et al., 1997). Often, this research is performed only on humans and other non-primate mammals (with small sample sizes), but little has been done to investigate the mandibular canal and the inferior alveolar nerve (IAN) across primates (Edin & Trulsson, 1992; Holland, 1978; Rood, 1978). Typically, this research requires gross dissection or other methods, such as the x-ray, that either destroys the specimen itself or gives a two-dimensional picture of the canal and soft-tissue structures. While soft tissues can be seen in 3D in a magnetic resonance image (MRI), these scans are typically long, expensive, only done on specific areas of the body, and are used primarily in a medical capacity (Burian et al., 2020). However, it is important to understand the relationship between the IAN and the mandibular canal due to the IAN's close relationship to the teeth and mastication, and thus dietary capabilities. While it is assumed (e.g., Jamniczky & Russell, 2004) that most bony canals within the skull grow around and form to pre-existing nervous structures, this has never been shown to represent the relationship between the IAN and the mandibular canal. Using diceCT and digital segmentation methods, I was able to create high resolution microCT scans with radiopaque soft-tissue structures without damage to the specimens to assess the relationship between the mandibular canal and the IAN.

BACKGROUND AND HYPOTHESES

Bony canals and foramina often form around soft-tissue structures that appear first in growth and development, thus allowing us to study the bony components rather than the nervous or vascular structures themselves (Albrecht, 1967; Aldridge et al., 2005; Benoit et al., 2018; Chávez-Lomeli et al., 1996; Greer et al., 2017; Jamniczky & Russell, 2004). However, recent research has shown that while canals/foramina may form initially around soft-tissue structures, they may not always represent the size and shape of those soft tissues throughout all points in an individual's life. For example, the hypoglossal nerve does not take up a majority of space in the hypoglossal canal, where as both the optic and infraorbital nerve accurately represent the size and shape of their corresponding canals (Jamniczky & Russell, 2004; Jonas et al., 1992; Mackinnon & Dellon, 1995). This discrepency should force researchers that are studying the interactions between the soft- and hard-tissue components of the skull to look much more closely at the validity of studying the hard tissue in place of the soft tissue.

The mandibular canal and its associated formaina (mental and mandibular) have been studied extensivly throughout the 20th century and well into the modern day. An enormous body of literature exists on its location in humans and other mammals because of its close assocation to the teeth, face, and oral caivty (Anderson et al., 1991; Cryer, 1901; Gowgiel, 1992; Mardinger et al., 2000; Olivier, 1927; Starkie & Stewert, 1931; Wadu et al., 1997). Often, it is described as a bony tube with a posterior opening at the mandibular foramen and an anterior opening at the mental foramen (Anderson et al., 1991; Cryer, 1901; Olivier, 1927). However the mental foramen is not a termination of the canal, as it splits medially into a cribriform opening that houses the incisal nerve plexus (Cryer, 1901; Gowgiel, 1992; Mardinger et al., 2000; Olivier, 1928; Starkie & Stewart, 1931; Wadu et al., 1997). It is generally agreed upon that the mandibular foramen is the posterior termination of the canal, that the canal walls are thickest at the posterior portion, and that the canal walls begin to thin out at the posterior aspect of the tooth row and continue to get progressively thinner (and at some points disappearing all

together) until there is a clear division at the anterior-most portion at the mental foramen (Gowgiel, 1992; Mardinger et al., 2000; Wadu et al., 1997). Throughout the canal, there are small lateral tubes (or canals) that connect the mandibular canal to the roots of each tooth, with the last premolar and first molar typically having the largest of all canals in diameter, suggesting larger soft-tissue structures innervating these posterior teeth (Anderson et al., 1991; Cryer, 1901; Erisen et al., 1989; Kress et al., 2004; Littner et al., 1986; Polland et al., 2001; Wadu et al., 1997). However, little research has actually been done to assess the variation that we see in the size of these lateral canals.

The variation seen in the mandibular foramen was first discussed in the literature by Olivier (1928) who established that is a “slit” rather than an oval foramen. Later publications (Anderson et al., 1991) would establish that, contrary to published literature, it is not consistently placed at an equal distance from the sigmoid notch and the lower border of the mandible. Most research (Ashkenazi et al., 2011; Feuerstein et al., 2019; Hayward et al., 1977; Nicholson, 1985; Prado et al., 2010; Thangavelu et al., 2012) on the mandibular foramen has been done for dentistry studies with very small human sample sizes – usually to establish a method on using numbing agents to block somatic sensation via the IAN from the mandibular tooth row. Thus, there is very little literature on the mandibular foramen variation seen in non-human primates and non-primate mammals. These studies typically agree that the mandibular foramen is near the midpoint of the ramus and, in humans, is inferior to the tooth row (Hayward et al., 1977; Nicholson, 1985; Thangavelu et al., 2012). Additional studies have shown that the mandibular foramen placement can be affected by age (Ashkenazi et al., 2011; Prado et al., 2010) and growth and development (Feuerstein et al., 2019). No published research has shown the presence of multiple mandibular foramina and this dissertation showed only a single mandibular foramina on each side for all individuals in this sample.

While there is little research that focuses on variation in the mandibular foramen on mammals other than humans, a significant body of research exists on the mental foramen with a

particular emphasis on factors that affect its placement, size, and number. Although earlier studies argued that the mental foramen was uniform across humans in its placement and size, factors such as growth and development (Anderson et al., 1991, Salah El-Beheri, 1985; Williams & Krovitz, 2004), differences in feeding behaviors and side preference during mastication (Agarwal & Gupta, 2011; Amorim et al., 2008; Voljevica et al., 2015; Yesilyurt et al., 2008), diet (Moore et al., 1968), age (Charalampakis et al., 2017; Gabriel, 1958; Gershenson et al., 1986; Heasmen, 1984; Iwanaga et al., 2019; Wadu et al., 1997; Xie et al., 1997), and number of mental foramina (Kramer, 1989; Montagu, 1954; Risenfeld, 1956; Robinson & Yoakum, 2019; Simonton, 1923) have shown that there is substantial variation within humans and few non-human primates (with a primary focus on apes). There is no general consensus as to which of these factors, if any, play a signficant role in the size, shape and number of the foramen in primates.

Because it has been shown (Brashear, 1936; Byers, 1985; De Lange et al., 1969; Hannam, 1982; Nuwer & Pouratian, 2017; Van Steenberghe, 1979; Young, 1977) that the size of a nervous structure directly correlates to the speed information can be sent to the brain and the type of information (i.e., pain, pressure, etc.) a specific nervous structure can transmit, knowing the size of a nerve and its structure can help determine the amount of information it can convey from the periphery to the central nervous system. This indicates that knowing the size of the mental nerve could give more information on its touch sensitivity capabilities and somatic sensation abilities. However, only one study has addressed if the mental foramen can be used as a proxy for touch sensitivity (Muchlinski & Deane, 2016) and found that it cannot be although these results were based on the assumption that the nerve and foramina were equal or proportional in size to each other. No study has addressed if the mental foramen can be used as a proxy for the mental nerve, which does not allow us to comment on the touch sensitivity capabilites of the mental nerve itself.

Although the bony components of the mandible have been studied extensively due to their ability to persist far longer than soft tissues, there is a body of literature on the nerve within the mandibular canal, the inferior alveolar nerve (IAN) (Anderson et al., 1970; Avery & Cox, 1977; Bernick, 1966; Brashear, 1936; Blackmore & Jennett, 2001; Byers, 1977; Byers & Dong, 1983; Cash & Linden, 1980; Edin & Trulsson, 1992; Edwards & Gaughran, 1971; Falin, 1958; Frank, 1968; Kubota & Osanai, 1977; Lewinsky & Steward, 1937; Lund et al., 1971; Luschei & Goldberg, 2011; Morris & Jackson, 1933; Plaffman, 1939; Rood, 1978; Sandring, 2015; Seto, 1972). In general, most researchers agree that the mandibular canal houses the IAN and the inferior alveolar artery (IAA), but there is a substantial argument as to whether it contains a vein as well (making it a true neurovascular bundle) (Anderson et al., 1991; Blackmore & Jennett, 2001; Booth et al., 2013; Edwards & Gaughran, 1971; Frank, 1966; Gowgiel, 1992; Lindh et al., 1995; Littner et al., 1986; Morris & Jackson, 1933; Rosenquist, 1996; Shadad et al., 2019). To date, a majority of the research describing the variation of the IAN has been done on humans primirily in the dentistry literature (Bradley, 1975; Buria, et al., 2020; Heasman, 1984; Kress et al., 2004; Nortje et al., 1977; Rosenquist; 1996; Starkie & Stewart, 1931; Stockdale, 1959; Wadu et al., 1997). This is because the IAN supplies sensation to the mandibular tooth row and is often at risk for damage during standard dental procedures. No study to date has described the variation of the IAN in primates other than humans, and no analyses have examined whether the IAN has a signficant relationship to the mandibular canal.

It is well understood (Anderson et al., 1970; Avery & Cox, 1977; Brashear, 1936; Dubner et al., 1978; Luschei & Goldberg, 2011; Plaffman, 1939; Shadad et al., 2019) that the IAN provides somatic sensory innervation to the gums and teeth as it begins anteriorly at the mental foramen, passes underneath the posterior tooth row, and exits towards the brain at the mandibular foramen. Both pressure and pain signals are sent from the teeth/gums to the brain via the IAN in order to assess food matieral properties and to adjust the chewing cycle according to those properties (Booth et al., 2013; Crompton, 1989; Hiiemae, 1974; Luschei &

Goldberg, 2011; Rees, 1954; Thexton et al., 1980). Being able to chew foods – and not damage the teeth – are integral parts of the mammalian life, indicating that the ability to assess the material properties of food is a key component of mammalian survival.

Based on the vast majority of medical textbooks and other scientific literature describing the size/course of the mandibular canal and nerve, I expected to find that the nerve would be equal to or very close in size to the diameter of the mandibular canal (Anderson et al., 1991; Angelopoulos, 1966; Barclay, 1971; Blackmore & Jennett, 2001; Booth et al., 2013, Wyman & Stoia, 2013; Edwards & Gaughran, 1971; Gershenson et al., 1986; Mardinger et al., 2000; Morris & Jackson, 1933; Murphy & Grundy, 1969; Olivier, 1927, 1928; Starkie & Stewart, 1931; Sutton, 1974; Wadu et al., 1997). This expectation is further supported by the fact that in many cases, the bony canals and foramina of the skull form around, and are thus equal in size to, the soft tissue that runs through them (Albrecht, 1967; Aldridge et al., 2005; Benoit et al., 2018; Chávez-Lomeli et al., 1996; Greer et al., 2017; Jamniczky & Russell, 2004).

The purpose of this chapter is to assess whether the mandibular canal and its foramina can be used as proxies to study the soft tissues contained within them. If the relationship between the soft- and hard-tissues is not well understood, any studies using the hard tissue to comment on the innervating capabilites of the IAN will have questionable results. While the teeth have evolved to sustain certain forces during chewing, the sensation along the tooth row enables us to adjust chewing in order to further protect the teeth – indicating that the IAN is deeply integrated with its surrounding hard tissues and should be studied as a system rather than as separate parts.

For Question 2 (Q2), I invesitage this research area by asking the overarching question: “Does bony canal structure track nervous tissue structure in the masticatory apparatus?”. Specifically, I test one hypothesis:

> **H_1**: The mandibular canal, when it can be identified as a single bony canal, is equal and/or proportional in cross-sectional area and volume to the inferior alveolar nerve.

MATERIALS AND METHODS

Data Collection and Preparation

To assess if there is a relationship between the mandibular canal, its associated foramina, and the size of the IAN, I used the variables for "Q2" as outlined in Table 3.1 under the column header "Associated Research Question". Chapter 3 describes the data collection process for all soft- and hard-tissue variables and data preparation (i.e., size adjustment, natural log transformation, etc.) used for this chapter. All analyses for Q2 used a total of 273 individuals (131 females, 134 males, and 8 unknown sex) from 68 primate species and three mammalian outgroups (*Lontra canadensis* (n = 1)*, Rattus norvegicus* (n = 5)*,* and *Oryctolagus cuniculus* (n = 4)) for all hard-tissue variables (Figure 3.1). Soft-tissue variables were collected from 66 individuals from 33 primate species and the same three mammalian outgroups (see Table 3.3). Summary statistics for the raw data of all variables used in Q2 can be found in Tables A.8 and A.9. Additionally, each species was given a species "code" to better show each species on figures. Codes are either 4 or 6 letters long and are the first two letters of the genus and species (sub-species will have 6 letters). For example*, Papio anubis* uses the code PAAN. These codes, their corresponding families, and the color identifiers from each figure can be found in Table 3.2.

Analytical Methods

To qualitatively assess the data, I started by looking at a variety of factors in the raw data. In this assessment I looked at how often the canal can be segmented as a "true canal" (i.e., a tube that is surrounded by bone and is continuous from the mandibular to mental foramina), if this is more prevalent by species or sex, and a variety of ratios to test if the canal volume, mandibular foramen, mental foramen, and cross-sectional areas of the canal are similar in size to the corresponding nervous tissue. These ratios were used because they are relative measurements and do not require a size-adjustment or a natural log transformation. Each of these ratios represent the soft tissue (i.e., either the CSA or volume of the IAN) as the numerator divided by the hard tissue (i.e., either the CSA or volume of the mandibular canal) as

the denominator to show how much of the nerve is occupying the canal space or foramen in question. Specifically, I look at the ratio of the nerve CSA at the mandibular foramen to the mandibular foramen CSA, the nerve CSA at the mental foramen to the CSA at the mental foramen, the CSA at the mental foramen to the CSA at the mandibular foramen, the nerve CSA beneath M_1 and the CSA of the mandibular canal beneath M_1, the nerve CSA beneath P_4 to the CSA of the mandibular canal beneath P_4, and the total IAN volume to total mandibular canal volume. Because previous literature suggests that the mental foramen should be smaller than the mandibular foramen, I also established a ratio of the mental foramen CSA divided by the mandibular foramen CSA. These values are sometimes > 100%, indicating that in some species/individuals, the mental foramen is larger than the mandibular foramen. These values were not multiplied by 100 in the data analysis phase and are thus shown on graphs as 0 – 1 (or higher than one if the numerator was larger than the denominator) but will be discussed in text as percentages.

To visualize this data, I first created a series of boxplots showing the distributions of each ratio. For some plots (e.g., the mental nerve CSA/mental foramen CSA ratio) there was more data available because all specimens used provided retained these anatomical features (i.e., the nerve and foramen were able to be segmented in all specimens). However, in some plots (e.g., the nerve CSA beneath the premolar/mandibular canal CSA beneath the premolar) there are fewer individuals/families represented because this ratio required that individuals had both a true canal and nerve as well as having a mental foramen that was anterior to P_4 (this was not the case in a majority of strepsirrhines). I performed a phylogenetic ANOVA for each nervous tissue variable to establish if there were significant differences between primate families (Garland, 1993). I next used a series of PGLS regression analyses to determine the significance of the relationships between the cross-sectional area (CSA) and volume of the mandibular canal to the CSA and volume of the IAN (Grafen, 1989). All slopes from the PGLS analyses were tested to establish if they were significantly different from one (i.e., isometry)

using a custom function (written by C. Terhune) utilizing functions from the RStudio package *phytools.*

All analyses were performed in RStudio using package *phytools* function “phylANOVA” version 0.7-80 for phylogenetic ANOVA analyses and package caper function “pgls” version 0.0-1 for PGLS analyses. Both the phylANOVA and PGLS analyses only include primates although the mammalian outgroups are included in all visual plots for comparison purposes. To correct for Type I Error (false positives) in the statistical analyses, a manual alpha value correction was used and is stated in each table reporting the test results. Question 2 (Q2) asks, “Does bony canal structure track nervous tissue structure in the masticatory apparatus” and a general overview of the analyses for Q2 are shown in Table 5.1.

Table 5.1. Tests performed in Question 2

Dependent variable	Independent variable	Test
Mandibular foramen (bone)	Mandibular foramen (nerve)	PGLS
Mental foramen (bone)	Mental foramen (nerve)	PGLS
Mandibular canal CSA	Mandibular nerve CSA	PGLS
Mandibular canal volume	Mandibular nerve volume	PGLS

In this chapter, each analysis was performed on data that was not size adjusted (i.e., Mosimann variables). However, all data was power reduced and natural log transformed prior to any statistical analysis. Size adjustments effectively remove isometric size differences in any analysis and therefore would not allow me to comment on the allometry of the sample. The purpose of this chapter is to assess the relationships between the size of the nerve and the size of the canal, thus making size an important variable to discuss without removing it. Specifically, for Q2-H1, I used a series of ratios to discuss the differences in size and/or proportion between the IAN and the mandibular canal. These ratios effectively allow me to control for gross differences in species size in the sample.

Leading into these analyses, I expected to find certain trends in the data based on previously published literature. First, I expected to find very little – if any – sexual dimorphism in

the analyses. Although there will be an overall size difference between males and females in most primate species, these data are looked at in ratios – which are relative and do not require a size adjustment. Previous works suggests that the course and size of the mandibular canal is not affected by sex (Anderson et al., 1991; Nortje et al., 1977). Additionally, in the data preparation stage for this question, there were no signficant differences found between the sexes for any variable used in Q2. This justified the use of combined sex data in the species average dataset.

Second, I expected there to be low levels of asymmetry between the left and right sides of the mandibular canal in individuals. For the mandible to be able to efficiently break down food during mastication, the left and right side must be near symmetry. While there may be slight differences in the canal shape, there is little evidence to support mandibular canal asymmetry (Littner et al., 1986; Matsuda, 1929; Nortje et al., 1977), but there have been no studies to assess the asymmetry of the IAN itself. To assess asymmetry in canals, I first segmented the canals on both sides of the mandible to establish how many individuals had a canal on one side but not the other (n = 4 in this sample). In the initial data preparation, no variables used in Q2 were shown to be significantly different between the left and right sides for any individual. This again justifies the use of averaging the left and right sides of each individual prior to analyses.

Third, accessory mental foramina (AMF's) are present in some primate species and most often appear in individuals with overall larger mandible lengths (Robinson & Yoakum, 2019). AMFs are defined as any foramina near the mental foramen that is smaller in diameter than the main mental foramen. When specimens in this sample presented with AMFs, all mental foramina were measured for their cross-sectional area and then added together for one total CSA. The same procedure was followed when multiple mental nerves were entering the mandible through multiple mental foramina.

RESULTS

Summary Statistics and Raw Data

Appendix Tables A.8 – A.9 show the summary statistics for all variables analyzed in this chapter for Q2. In the initial steps of data preparation, no significant differences were found between either the left or right sides of each individual nor were there significant differences between the sexes in the mandibular canal, its associated foramina, and corresponding nervous structures. Because of this, the data were averaged first by individual (left and right sides) and then averaged by species for all analyses.

Qualitative Analysis of the Mandibular Canal and Associated Foramina

Out of 263 primate individuals, a total of 66 (25.1%) had canals on both the left and right sides or one side that could be digitally segmented. Four out of 263 individuals (1.5%) had a true canal on one side (50% right, 50% left) and no canal on the other. Because so many specimens lacked a true canal only the foramina (mandibular and mental) could be segmented for 197 of 263 individuals (74.9%). In the mammalian outgroups, *Lontra canadensis* (n = 1) had a defined canal, *Rattus norvegicus* (n = 5) showed defined canals in all five individuals, and *Oryctolagus cuniculus* (n = 4) showed no defined canals (only foramina could be identified) in all four specimens. Figure 5.1 shows the course of the mandibular canal (beginning at the mandibular foramen and proceeding anteriorly) in a *Saimiri sciureus* specimen (CET-079) with a canal (Figure 5.1, A-D) and a different *S. sciureus* specimen (CET-082) without an identifiable canal (Figure 5.1, E-H). Both specimens are female and adults with all permanent dentition fully erupted and in occlusion.

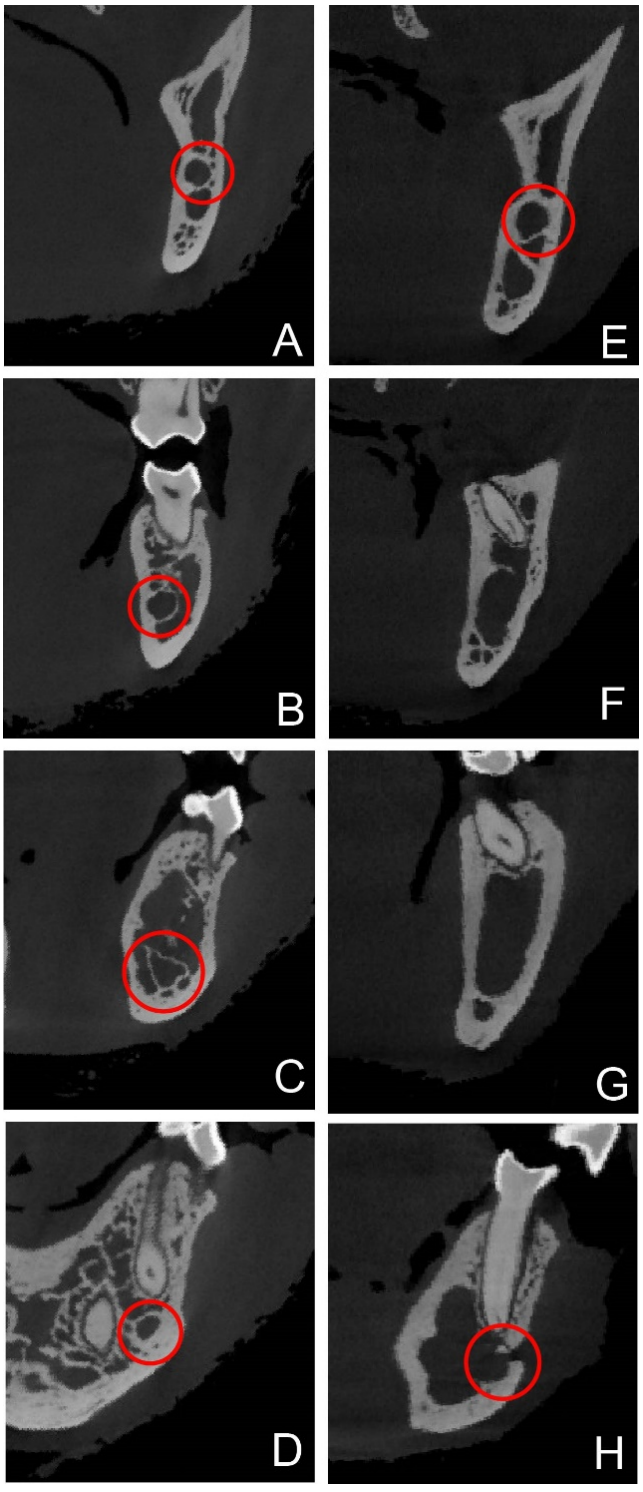

Figure 5.1. An example pre-stain scan of two *Saimiri sciureus* specimens, tracing the mandibular canal from the mandibular foramen (posterior) to the mental foramen (anterior). The images A-D show CET-079 with a clearly defined canal and the images E-H show CET-082 with clearly defined foramina, but no canal within the body of the mandible. Both specimens are female and adults with all permanent dentition fully erupted and in occlusion.

By species, the four individuals that had a canal on one side but not the other were *Macaca mulatta* (right side only), *Saimiri sciureus* (right side only), *Galago senegalensis* (left side only), and *Homo sapiens* (left side only). In this sample, 33 of 72 (45.8%) total species had individuals with true canals that could be segmented. Table 5.2 shows the species where a canal could be segmented, with 0.5 measurements indicating a canal on only one side of a single individual could be segmented.

Table 5.2. A breakdown of segmented canals by species (.5 measurements indicate a canal on one side but not the other in a single specimen)		
Species	**Number of individuals**	**Individuals with canals**
*Lontra canadensis**	1	1
*Rattus norvegicus**	5	5
*Otolemur crassicaudatus**	1	1
Galago senegalensis	6	3.5
*Nycticebus coucang**	2	2
*Perodicticus potto**	1	1
Varecia variegata vareigata	3	1
*Hapalemur griseus griseus**	1	1
*Hapalemur griseus**	2	2
Eulemur fulvus rufus	2	1
*Microcebus murinus**	1	1
Callicebus moloch	7	6
Saimiri sciureus	31	3.5
Saguinus oedipus	9	2
Callithrix jacchus	4	1
*Lagothrix lagotricha**	3	3
Alouatta caraya	3	2
*Pongo abelii**	2	2
Homo sapiens	5	.5
Presbytis melalophos	2	1
Semnopithecus entellus	3	1
Nasalis larvatus	8	1
Piliocolobus badius	6	1
Colobus guereza	5	1
Macaca mulatta	10	1.5
*Macaca radiata**	1	1
*Papio ursinus**	4	4
Papio anubis	8	3
Theropithecus geleda	4	3
Lophocebus albigena	6	1
*Mandrillus sphinx**	7	7
Mandrillus leucophaeus	3	1
Cercocebus agilis	5	3
Erythrocebus patas	3	2
*Allenopithecus nigroviridis**	1	1
***Indicates 100% of individuals in that species had true canals**		

When the data is broken down by sex, 26 of 130 (20%) females had true canals that could be segmented. Of those 26, 3 individuals had only one canal (*Homo sapiens, Macaca mulatta*, and *Saimiri sciureus*) on either the left or right side. Out of 125 males, 37 (29.6%) individuals had true canals that could be segmented. Only one male individual (*Galago senegalensis*) had a canal on the left side only. Additionally, eight individuals were of unknown

sex and three of those had true canals (*Lagothrix lagotricha, Otolemur crassicaudatus*, and *Nycticebus coucang*).

Ratios describing the relationship between the nerve and canal size showed that in all variables, the nerve does not occupy most of the space of the mandibular canal, mandibular foramen, or mental foramen. Table 5.3 shows the ratios used, the average percentage across all specimens for each ratio, and the range of percentages across all specimens.

Table 5.3. Ratio averages and ranges across all variables

Numerator	Denominator	N	Average Ratio	Ratio range	SD
Nerve CSA at mandibular foramen	Mandibular foramen CSA	65	23.84%	11.71 – 35.65%	0.059
Nerve CSA at mental foramen	Mental foramen CSA	65	22.35%	4.13 – 72.61%	0.139
Mental foramen	Mandibular foramen	274	68.46%	5.89 – 187.2%	0.386
Nerve CSA beneath M_1	Mandibular Canal CSA beneath M_1	21	25.86%	8.01 – 66.67%	0.173
Nerve CSA beneath P_4	Mandibular canal CSA beneath P_4	13	19.72%	10.51 - 35.09%	0.072
IAN volume	Mandibular canal volume	21	21.64%	10.39 – 33.82%	0.073

The individual with the smallest ratio of nerve CSA at the mandibular foramen to mandibular foramen CSA (11.7%) belonged to the species *Alouatta caraya* and was a male, while the largest of this ratio (35.7%) belonged to the species *Trachypithecus cristatus* of an undetermined sex (Table 5.3). While the only other (female) individual in *T. cristatus* had the second largest ratio (35.1%), a second (male) *A. caraya* had an above average ratio (28.5%). Figure 5.2 shows the boxplots for this ratio by family. A phylogenetic ANOVA (for primate families only) established there are no significant differences between the means of each family (F-statistic = 0.973, p-value = 0.993).

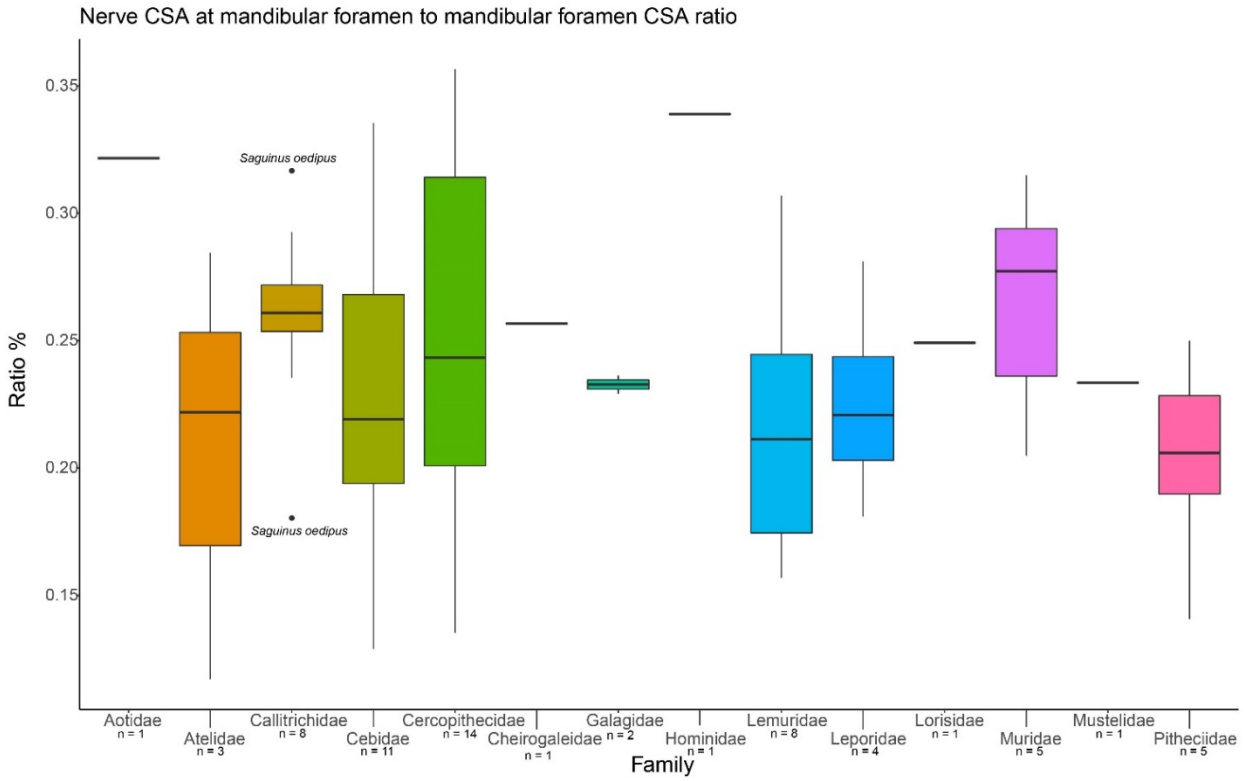

Figure 5.2. Boxplots for the nerve CSA at the mandibular foramen to mandibular foramen CSA ratio.

The individual with the smallest ratio of nerve CSA at the mental foramen to mental foramen CSA (4.1%) belonged to the species *Oryctolagus cuniculus* (a European rabbit used as a mammalian outgroup in the study), while the largest of this ratio (72.6%) belonged to the species *Rattus norvegicus* (Table 5.3). The smallest of this ratio in primates was 4.4% in the species *Varecia variegata* (male) while the largest of this ratio in primates was 67.3% in the species *Pan paniscus* (female). Figure 5.3 shows the boxplots for this ratio by family. The phylogenetic ANOVA found no significant differences (F-statistic = 3.484, p-value = 0.789) in this measure between primate families.

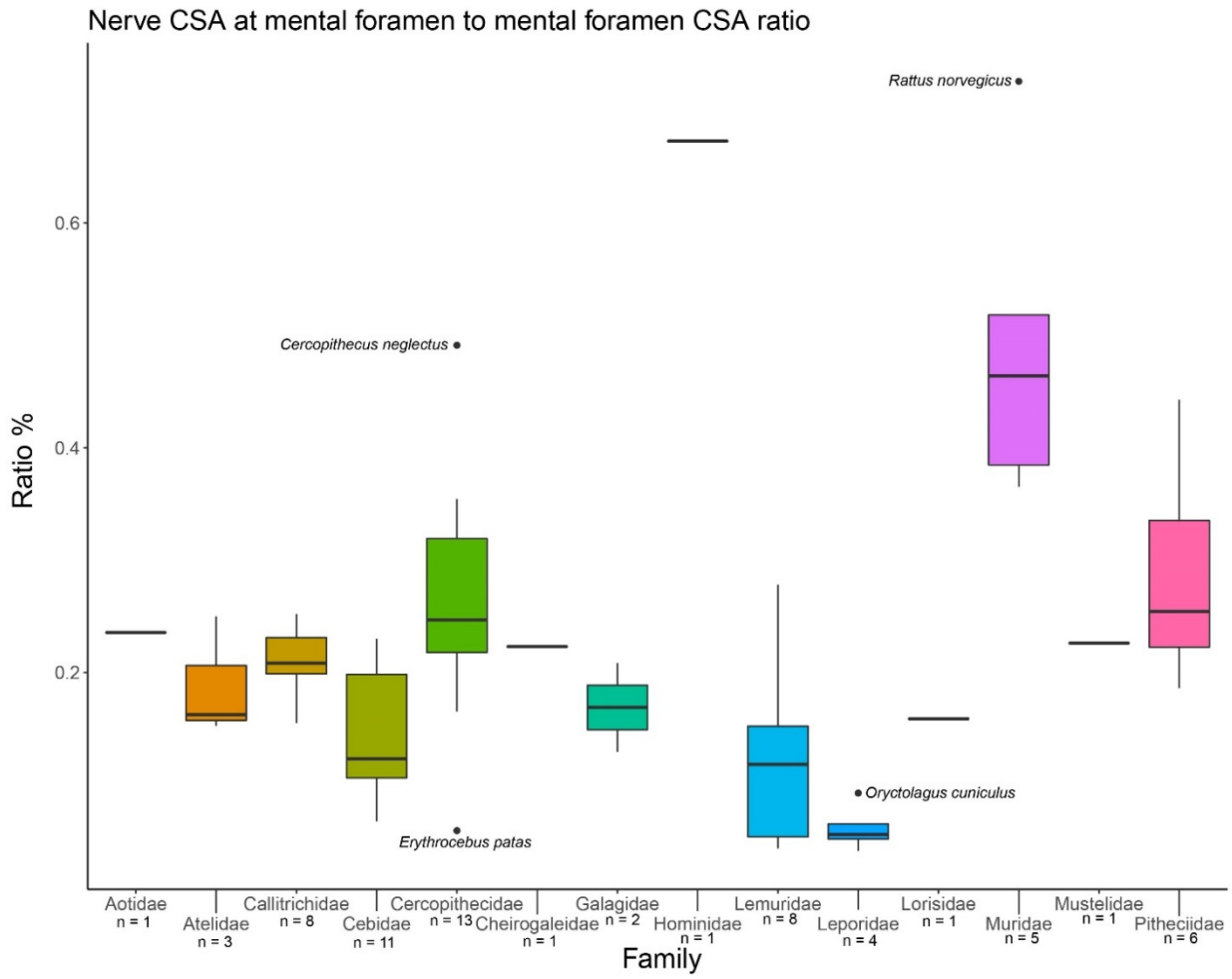

Figure 5.3. Boxplots for the nerve CSA at the mental foramen to mental foramen CSA ratio.

Out of 273 specimens (mammalian outgroups included), 214 had mental foramina that were smaller in size when compared to the mandibular foramina. This ratio is the mental foramen CSA divided by the mandibular foramen CSA, with values < 100% indicating a smaller mental foramen than mandibular foramen and values > 100% indicating a larger mental foramen than mandibular foramen. The individual with the smallest ratio (5.9%) belonged to the species *Macaca nigra*, whereas the individual with the largest ratio (187.2%) belonged to the species *Saimiri sciureus*. Interestingly, the species *S. sciureus* clustered at the larger end of this ratio with a range of 71.9 – 187.2%. Figure 5.4 shows the boxplots for this ratio by family. A

phylogenetic ANOVA showed no significant differences between families (F-statistic = 3.454, p-value = 0.948).

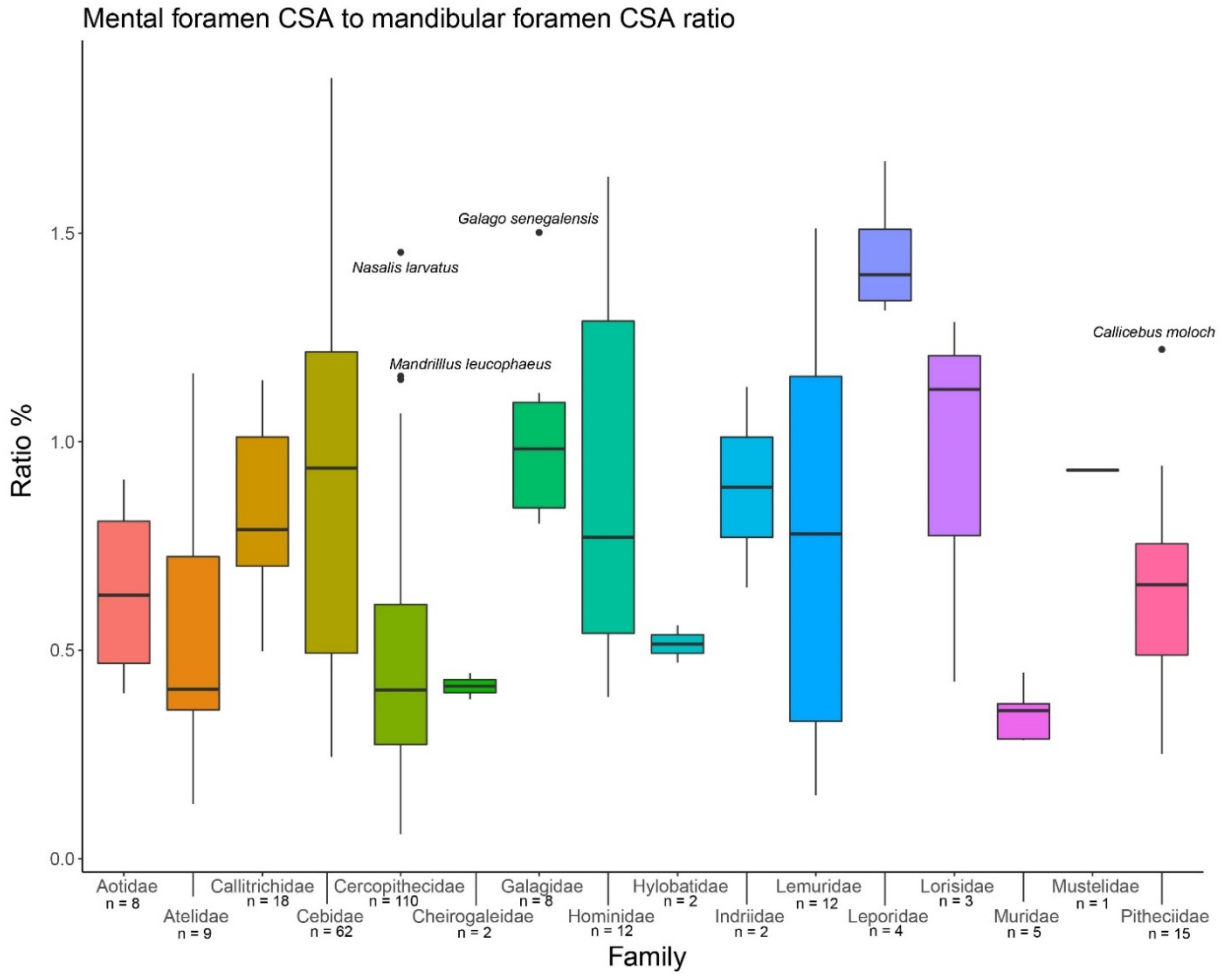

Figure 5.4. Boxplots for the mental foramen to mandibular foramen ratio.

The individual with the smallest nerve under M_1 to canal under M_1 ratio belonged to the species *Erythrocebus patas* (female) at 8.01%, while the individual with the largest of this ratio belonged to *Rattus norvegicus* (male) at 66.7%. All rats clustered at the highest end of this ratio with a range of 42.6 – 66.7%. Primates had a range of 8.01 – 38.6%, with the species *Lagothrix lagotricha* having the highest ratio at 38.6%. The strepsirrhine families (Lemuridae, Lorisidae, and Galagidae) clustered at the lower end of the ratios with a range of 8.0 – 13.5%. Additionally, Cebidae, Atelidae, and Cercopithecidae clustered at the higher end of this ratio (19.7 – 38.6%)

and did not overlap in ratios with the strepsirrhines. Figure 5.5 shows the boxplots for this ratio by family. A phylogenetic ANOVA showed no significant differences between families in the overall model (F-statistic = 1.96, p-value = 0.863).

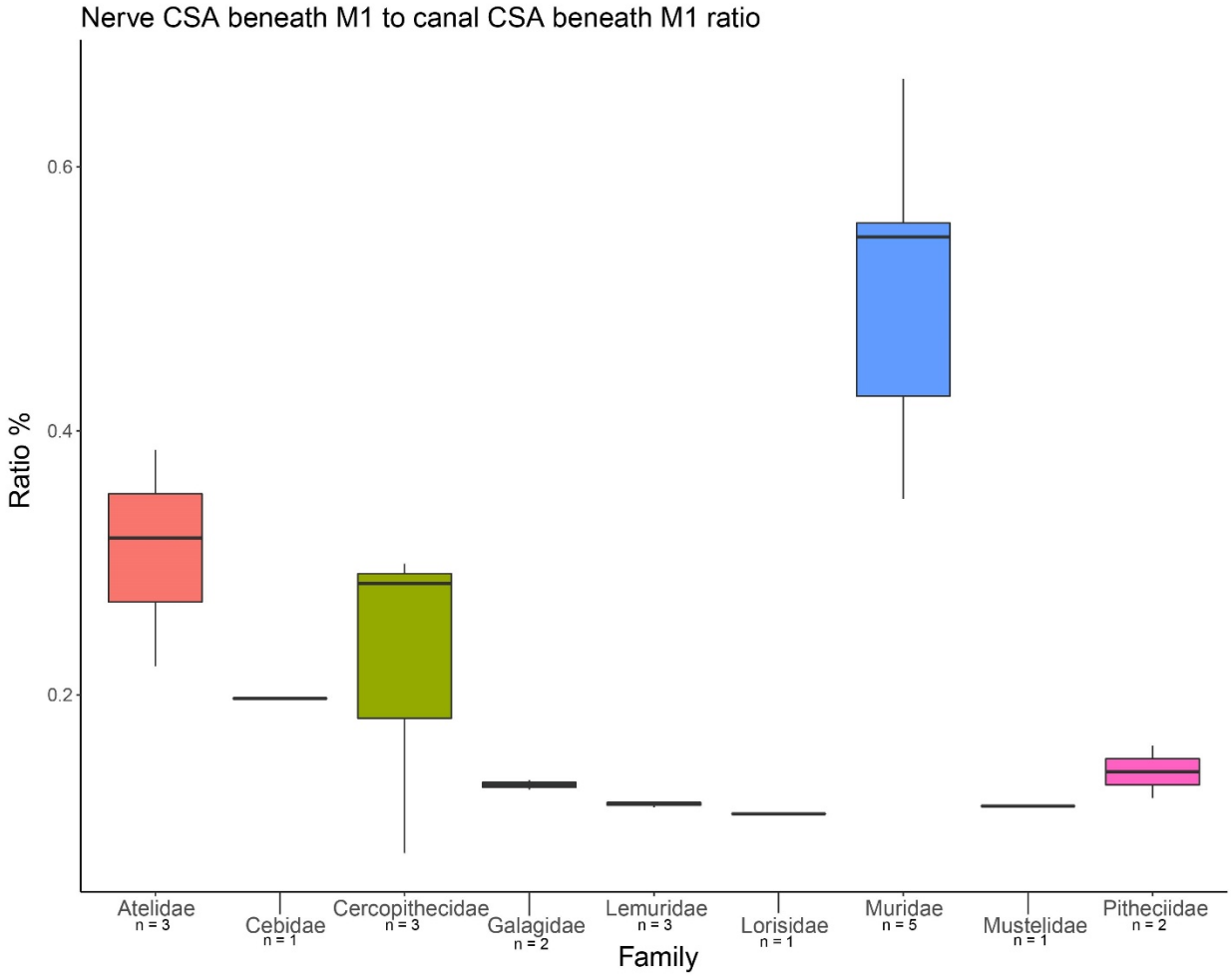

Figure 5.5. Boxplots for the nerve CSA beneath M_1 to the mandibular canal CSA beneath M_1.

The individual with the smallest nerve CSA under P_4 to canal CSA under P_4 ratio belonged to the species *Eulemur fulvus rufus* (male) at 10.5%, while the individual with the largest ratio belonged to the species *Lagothrix lagotricha* (undetermined sex) at 35.1%. Additionally, Lemuridae and Pitheciidae clustered at the lowest end of this ratio with a range of 10.5 – 22.4%. The same individual (CET-160) from *Lagothrix lagotricha* had the largest ratio at both P_4 and M_1. Unfortunately, this is the only individual from that species that had a true

mandibular canal and nerve, and thus I could not determine the variation within the species of the ratio between the canal and nerve underneath the tooth row. Figure 5.6 shows the boxplots for this ratio by family. A phylogenetic ANOVA showed there were no significant differences between families (F-statistic = 2.178, p-value = 0.743).

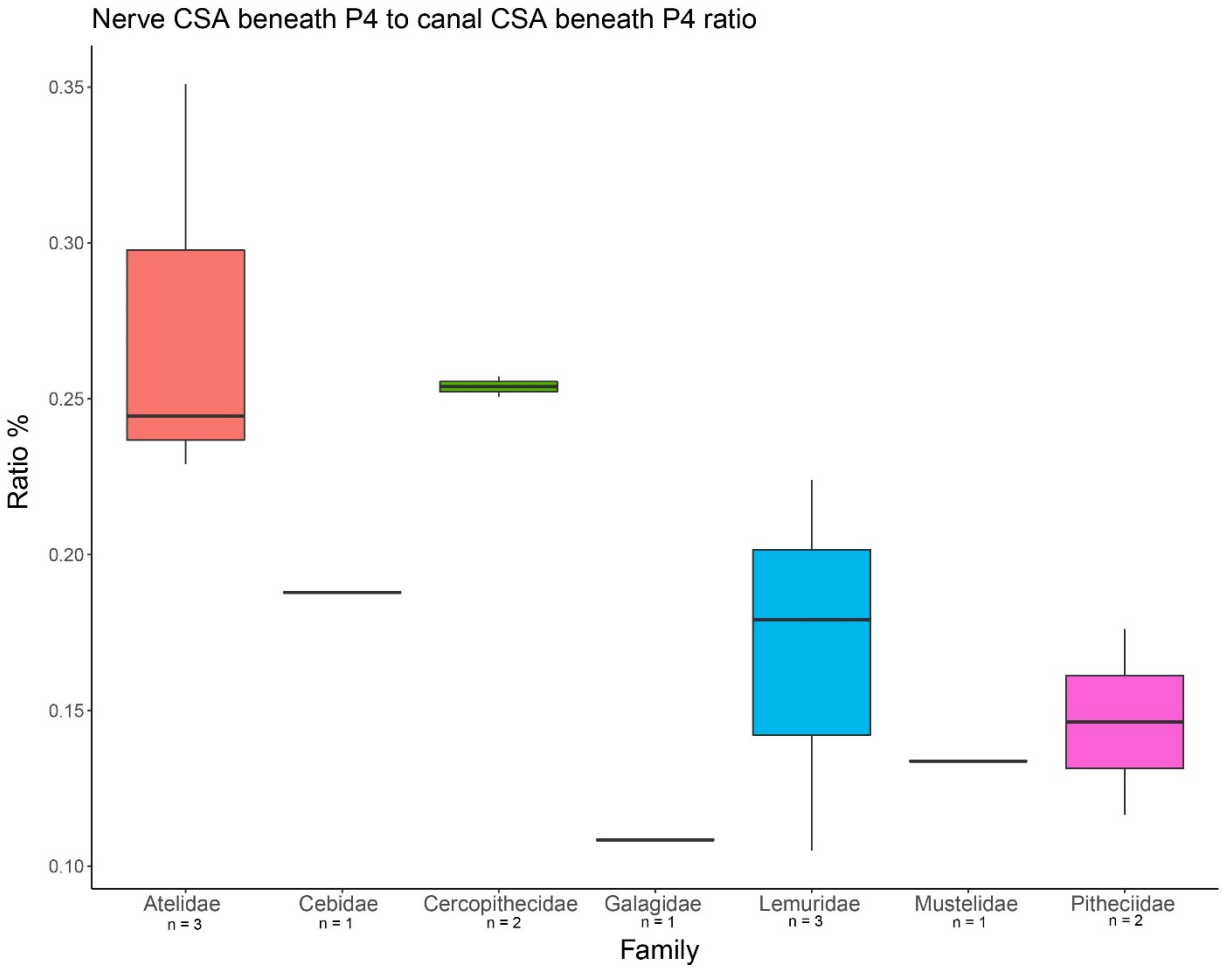

Figure 5.6. Boxplots for the nerve CSA beneath P_4 to the mandibular canal CSA beneath P_4.

Finally, the individual with the smallest total IAN volume to total mandibular canal volume ratio belonged to the species *Eulemur fulvus rufus* (male) at 10.39%, while the individual with the largest ratio belonged to the species *Rattus norvegicus* (male) at 33.82%. The largest primate ratio belonged to the species *Macaca mulatta* (female) at 28.69% with primates clustering at the lower end of the scale. Only one specimen of *Rattus norvegicus* had a smaller

ratio at 27.31% than two primate individuals (one unknown *Lagothrix lagotricha* and one female *Macaca mulatta*) while all other brown rats (n = 4) were larger than all primates. Figure 5.7 shows the boxplots for this ratio by family. A phylogenetic ANOVA found no significant differences between primate families (F-statistic = 1.056, p-value = 0.951).

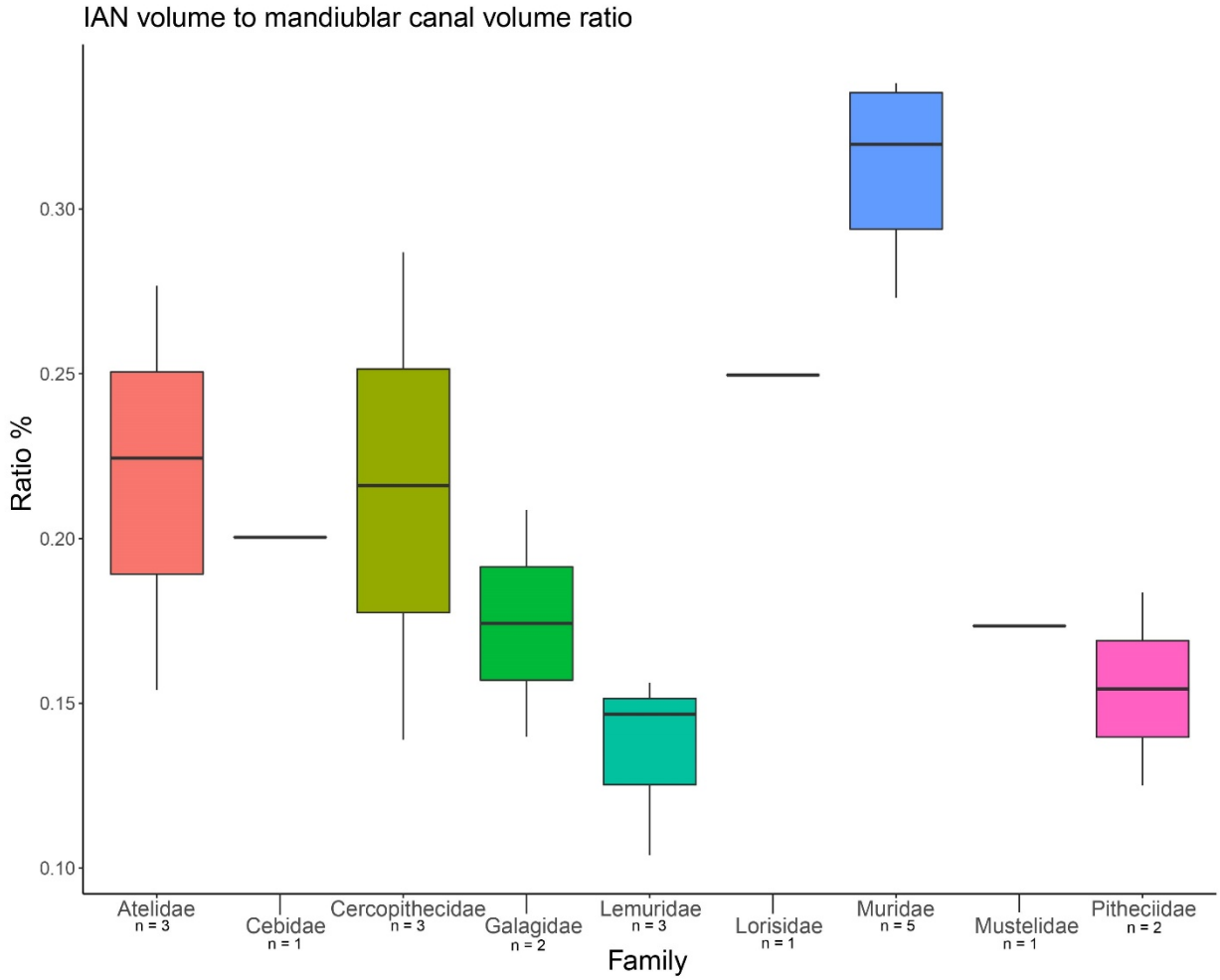

Figure 5.7. Boxplots for the IAN volume to the mandibular canal volume ratio.

Allometric Analyses: Mandibular Canal Size to IAN Size

I ran a series of PGLS analyses on the primate data that was not size-adjusted, and all analyses showed significant relationships between the canal measurements and corresponding nervous tissues (p-value < 0.001 for all) (Table 5.4; Figure 5.8A-E). Additionally, all R^2 values are relatively high in these analyses (0.759 - 0.954), indicating that the relationships seen here

are not only significantly related but also close. While the mandibular nerve/foramen analysis and IAN volume/canal analysis both showed slopes > 1, the slopes were not significantly different from isometry (=1). The remaining analyses all showed slopes < 1 but again, were not significantly different from isometry. This indicates that as the nerve size is increasing, the canal size is increasing at similar rates.

Table 5.4. PGLS results (with no size adjustment)

PGLS analyses results						
Dependent variable	**Independent variable**	**p-value**	**R^2**	**Slope**	**Slope CI**	**Slope p-value**
Mandibular foramen CSA	Nerve CSA at mandibular foramen	**< 0.001**	0.950	1.159	0.982 ± 1.336	0.056
Mental foramen CSA	Nerve CSA at mental foramen	**< 0.001**	0.759	0.798	0.500± 1.097	0.160
CSA of canal beneath M_1	CSA of nerve beneath M_1	**< 0.001**	0.865	0.917	0.675± 1.157	0.451
CSA of canal beneath P_4	CSA of nerve beneath P_4	**< 0.001**	0.841	0.809	0.575± 1.043	0.109
Mandibular canal volume	Mandibular nerve volume	**< 0.001**	0.954	1.039	0.887± 1.190	0.563
All analyses used 11 degrees of freedom **Alpha values set to p-value < 0.0125 for CSA analyses** **Alpha values set to p-value < 0.050 for volume analyses**						

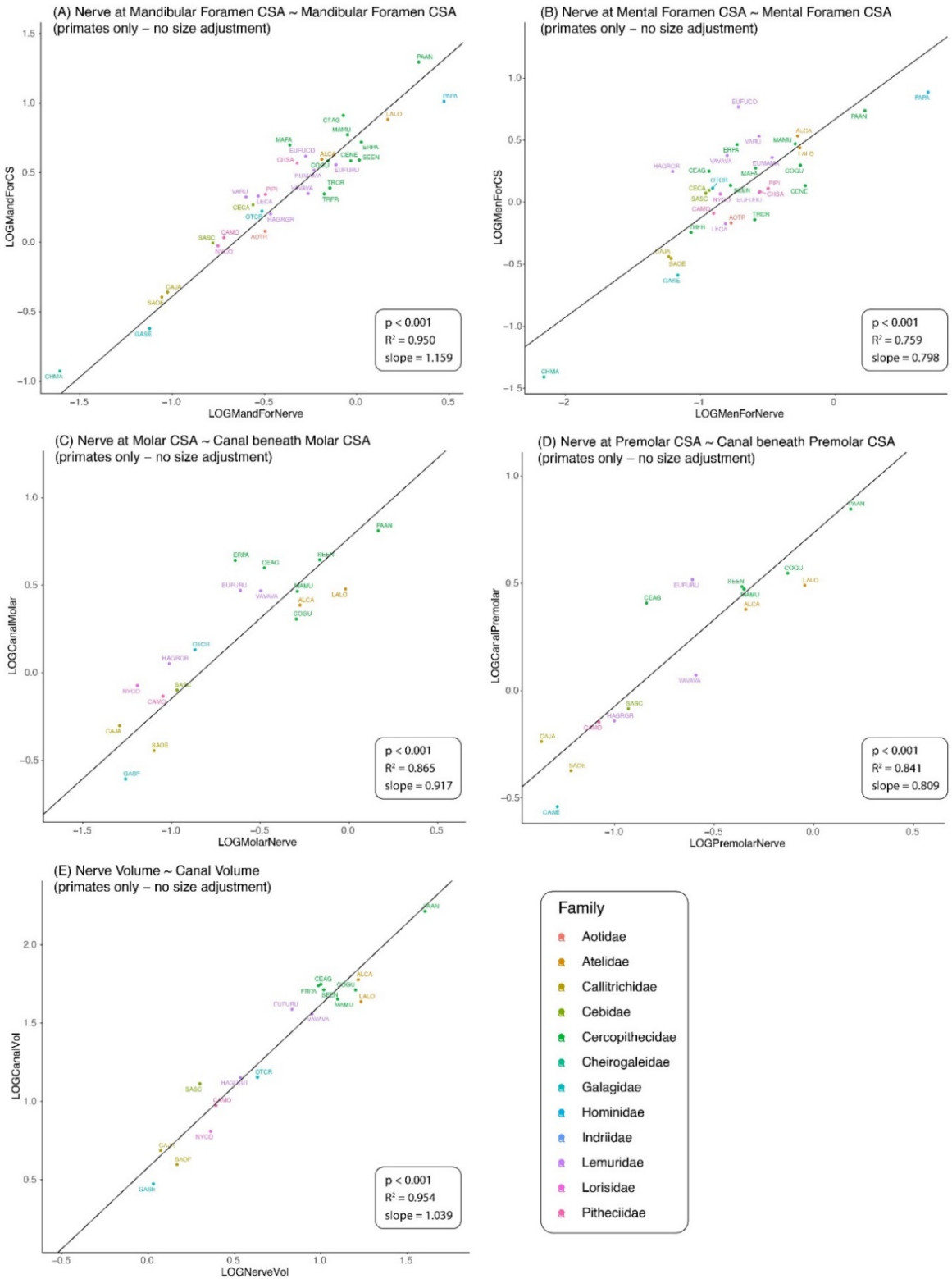

Figure 5.8. Regression plots showing the significant PGLS results for the mandibular foramen variables (A), the mental foramen variables (B), the M_1 variables (C), the P_4 variables (D), and the volume variables (E).

DISSCUSSION

Brief Overview

The purpose of this chapter was to establish the relationship between the bony components of the mandibular canal to the IAN. While the mandibular canal and its corresponding foramina have been studied extensively in both the medical and scientific literature, no study has definitively shown that the bony components can be used as a proxy for the soft-tissue structures (Anderson et al., 1991; Angelopoulos, 1966; Barclay, 1971; Blackmore & Jennett, 2001; Booth et al., 2013; Wyman & Stoia, 2013; Edwards & Gaughran, 1971; Gershenson et al., 1986; Mardinger et al., 2000; Morris & Jackson, 1933; Murphy & Grundy, 1969; Olivier, 1927, 1928; Starkie & Stewart, 1931; Sutton, 1974; Wadu et al., 1997). Understanding the relationship between the soft- and hard-tissue components is important for two main reasons: 1) many researchers have attempted to use the bony components to discuss the capabilities (particularly touch sensitivity) of the soft-tissue components, and 2) the IAN relays important information to the brain during chewing to maintain the chewing cycle and protect the teeth from damage. While we understand that the IAN relays this information, there is no understanding of its variation across primates or how it relates to the bony components that surround and protect it.

The qualitative data provided here do not support the hypothesis (Q2-H1) that the mandibular canal, when it can be identified as a bony canal, is equal and/or proportional in cross-sectional area to the mandibular nerve (IAN). The largest takeaway from these analyses is that the neural tissues do not comprise most of the mandibular canal, the mental foramen, or the mandibular foramen across all primate species. Second, the mandibular canal is often not even a canal at all. In most primate specimens (74.9%) the canal could not be identified and rather the neural tissues simply run through a large open space within the body of the mandibular bone.

Hypothesis Testing: Relationships Between the Soft- and Hard-Tissues of the Mandibular Canal

Qualitative analysis of the mandibular canal and corresponding nervous structures. Because only four primate individuals out of 263 had a true canal on one side of the mandible and no true canal on the other, this indicates that levels of asymmetry in terms of presence/absence of the mandibular canal are relatively low. This reflects what is already known in the body of literature on the mandibular canal (Littner et al., 1986; Matsuda, 1929; Norje et al., 1977). Similarly, since the majority (74.9%) of individuals did not have the presence of a true canal, and thus only the foramina were segmented, the presence of a true canal is not common across primates. This is in opposition to the majority of literature, written primarily on humans, that the mandibular canal is a true canal that holds a neurovascular bundle (Anderson et al., 1991; Angelopoulos, 1966; Barclay, 1971; Blackmore & Jennett, 2001; Booth et al., 2013; Wyman & Stoia, 2013; Edwards & Gaughran, 1971; Gershenson et al., 1986; Mardinger et al., 2000; Morris & Jackson, 1933; Murphy & Grundy, 1969; Olivier, 1927, 1928; Starkie & Stewart, 1931; Sutton, 1974; Wadu et al., 1997). In this sample, I had five human individuals, only one of which had a single canal that could be segmented from the right side. However, each of these individuals would be considered elderly, which complicates my interpretation of these data for several reasons: 1) the IAN has been shown to atrophy in edentulous individuals (two of these individuals were completely edentulous) or those with decreased tooth use (Bradley, 1975; Polland et al., 2001), and 2) of the three individuals that had remaining teeth, there was extensive dental work performed on all posterior teeth. The absence of some teeth and extensive dental work on the mandibular tooth row could cause changes to the IAN and mandibular canal through damage or bone resorption.

The four species where only one side of the canal could be segmented (*Macaca mulatta*, *Saimiri sciureus*, *Galago senegalensis*, and *Homo sapiens*) are not closely phylogenetically related – indicating that the presence or absence of a canal on one side but not the other (i.e.,

asymmetry) is likely not directly related to phylogeny. Additionally, three of these species (*M. mulatta*, *S. sciureus*, and *G. senegalensis*) had other individuals within the species where either canals could be segmented on both sides or only the foramina were segmented. For example, *G. senegalensis* had six total individuals, three of which had true canals on both sides (two females, one male), two had only the foramina and no true canal (one female, one male), and one individual had only one side with a true canal (male). *M. mulatta* was represented by ten individuals in the sample; one had true canals on both sides (female), eight had the foramina and no true canal (two males, six females), and one had only one side with a true canal (female). Finally, *S. sciureus* had a total of 32 individuals represented in the sample, with three individuals having true canals on both sides (one male, two females), 28 individuals having only the foramina and no true canal (21 males, seven females), and one individual having a true canal on only one side (female). This indicates that the presence/absence of having a defined canal on only one side is rare and could indicate asymmetry at the individual level rather than the species level or due to sex. Again, this supports the previous literature that sexual dimorphism or species designation does not play a significant role in the asymmetry of the mandibular canal in primates (Anderson et al., 1992; Nortje et al., 1977).

Overall, the ratios analyzed from this sample tell a very different story from what is typically presented in the literature: the mandibular canal does not have a uniform path or size across primates and the neural tissue that runs through it does not occupy most of the canal space. In terms of averages, the nerve at both the mental and mandibular foramina occupies a relatively similar (22-24%) ratio of the cross-sectional area at the foramina. However, the range for the mental nerve CSA to mental foramen CSA (4.12 – 72.6%) is much larger than that seen at the mandibular foramen (11.71 – 35.65%).

When the nerve CSA at the mental foramen to the mental foramen CSA ratio was used, common brown rats showed an overall larger ratio – except in comparison to Hominidae. However, only one specimen (*Pan paniscus*) represents Hominidae in the sample, thus

suggesting more data is needed from this family before firm conclusions can be drawn. All other primate groups clustered together at the lower end of the range (< 50%) with no significant differences between the means. These data do not support using the mental foramen as a proxy for the mental nerve and thus touch sensitivity (as was done in Muchlinski & Deane, 2016) on the lower face because no family/species showed that the mental nerve occupies most of the foramen.

There was far less variation in the range for the nerve CSA at the mandibular foramen to the mandibular foramen CSA than that seen in the ratio established at the mental foramen. Even Hominidae, which had a nerve that occupied 67.3% of the mental foramen, had a much smaller ratio at the mandibular foramen (< 35%). This indicates that the nerve size at the mandibular foramen is much more conserved across all families measured – even the mammalian outgroups. However, these results mirror those seen at the mental foramen in that the mandibular foramen cannot be used as a proxy for the nerve at this location as no species showed nerves that occupied more than 35% of the foramen.

It is often cited in the literature that the mandibular foramen is larger than the mental foramen, however this showed to not be true in all cases in the sample here (Anderson et al., 1991; Olivier, 1927; Starkie & Stewart, 1931; Wadu et al., 1997). In some species, the mental foramen was almost twice the size of the mandibular foramen, like in *S. sciureus*, but there is extensive variation in that size within species in this sample. Again, the ratio of the CSA of the mental foramen to mandibular foramen appears to vary across and within species, with little to no correlation with phylogeny or sex. Although no quantitative analyses were performed on the number of mental foramina in the dataset here, all specimens in this sample had between one and nine mental foramina. This was relatively consistent with the literature (Robinson & Yoakum, 2019) in that the larger specimens did have more AMFs than smaller specimens, with the exception of *S. sciureus*. Many of the *S. sciureus* specimens had between 3-4 AMFs. This is

interesting because *S. sciureus* showed a very high ratio (many over 100%) in terms of the size of the mental foramen to the mandibular foramen.

When I examined the space beneath M_1 and P_4 of the CSA of the nerve to canal ratio, the strepsirrhines again clustered at the smallest end of the range. This indicates that the mandibular canal, from the mental foramen until at least under the molars is a much larger space than necessary in terms of containing the neural tissues in this group of primates. Additionally, Atelidae, Cebidae, and Cercopithecidae clustered at the higher end of this ratio (19.73 – 38.56% for M_1; 22.91 - 35.09% for P_4), indicating that all monkeys have larger nerves in relation to the strepsirrhines (10.9 - 13.5% for M_1; 10.5 - 22.4 for P_4) in the mandibular canal beneath the tooth row. While these ranges do not overlap, the sample size here is very small (n = 21 individuals) and this could change if sample sizes were increased. It is important to note that strepsirrhines have increased touch sensitivity on their upper lip/nasal region that helps them to identify a variety of materials, including food, in their environment (Muchlinski & Deane, 2015). It has also been shown that there is a significant relationship between the infraorbital foramen (IOF) and the diet of strepsirrhines although there is no known relationship between the mental foramen (the mandibular correlate of the IOF) and diet (Muchlinski, 2008; Muchlinski & Deane, 2016; Spriggs et al., 2016). The analyses above have shown that strepsirrhines appear to have smaller nerves in relation to the bones that surround them within the mandibular canal and surrounding foramina, indicating that while strepsirrhines may have increased touch sensitivity on their faces, they may have decreased sensitivity along the bottom tooth row, at least in comparison to other primate species.

Finally, when I compared the IAN volume to the volume of the mandibular canal, there were no significant differences between any primate family groups. However, visually, the brown rats had much higher volumes and had a range that only overlapped with Cercopithecidae. Only two species, *Macaca mulatta* and *Lagothrix lagotricha*, had ratios that fell within the range of brown rats. Again, both Lemuridae and Galagidae clustered at the lower end of the ratios,

although both overlapped in range with Pitheciidae and Cercopithecidae. Overall, these results show that in mammals, the IAN volume occupies less than half of the mandibular canal (when it can be identified as a true canal) and primates show overall lower volumes when compared to non-primate mammals such as common brown rats.

Allometric analyses. In the PGLS analyses, all bony components had significant relationships to their soft-tissue structures. This indicates that the size of the nervous tissues has a particularly close relationship to the corresponding bony structures. Two of these analyses – the PGLS for mandibular foramen/nerve CSA (slope = 1.159) and mandibular canal to IAN volume (slope = 1.039) – showed slopes that were > 1, although neither slope was significantly different from isometry. This indicates that as the nervous tissues increase in size, the bony correlates are increasing at relatively the same rate.

Interestingly, the remaining three analyses show slopes that were < 1 between the nervous tissues and the bony correlates. First, the mandibular canal and nerve CSA beneath M_1 had a slope of near isometry (0.917) that was not significantly different from isometry. This indicates that as the nervous tissues beneath M_1 are increasing in size, the bony correlates are increasing in size at nearly the same rate. Both the mental foramen/nerve CSA and the canal/nerve CSA beneath P_4 also have slopes < 1 but again, neither slope is significantly different from isometry. This again indicates that as these nervous structures are increasing in size, the bony correlates are increasing at nearly the same (or slightly less) rate than expected. Because no data like those collected here have been researched or published, it is difficult to ascertain why we see these relationships over others. I would expect, based on previous literature, that the nervous tissues would consistently show negative allometry in relation to the hard-tissue structures that surround them due to overall body size having a relationship to mandible size (Rilling, 2006). However, these data show that throughout the mandibular canal, the nervous tissues and hard-tissue components are increasing roughly isometrically.

CONCLUSION

Overall, there were three main conclusions drawn from the data here:

1. In primates, the mandibular canal is often not easily defined as a canal and would more accurately be described as an open space of trabecular bone within the body of the mandible in most cases.
2. Unlike other nervous tissues such as the brain, the IAN shows relationships of near isometry for the nervous tissues and the surrounding bony components
3. There are significant relationships between the size of the IAN and the size of the mandibular canal, but no clear differences in the IAN tissue between primate family groups.

In sum, there are some clear relationships between the hard- and soft-tissue components analyzed here. However, most of these relationships appear to be size dependent and show isometric relationships between the soft- and hard-tissues. This indicates that the size of nervous tissues within the mandible are scaling isometrically with the hard-tissue components.

CHAPTER 6: AN ANALYSIS BETWEEN THE INFERIOR ALVEOLAR NERVE AND FEEDING BEHAVIORS IN PRIMATES

INTRODUCTION

Data suggest that tooth shape is generally correlated with feeding behavior and food material properties (Kay, 1975; Lucas, 2006; Lund et al., 1998; Luschei & Goldberg, 2011; Teaford et al., 2006). This has led many researchers to divide primate diets into two primary groups: 1) non-resistant foods such as fruit or gum, and 2) resistant foods such as leaves, seeds, grass, flowers and insects (Kinzey & Norconk, 1993; Lucas & Corlett, 1991). These groups each require different tooth shapes to efficiently break down food. Although teeth are the interface with all foodstuffs, all food material property testing that is performed in the oral cavity requires nervous sensation. It has been well-established that primates often use their posterior dentition to test the properties of foods prior to ingestion of certain leaves and other stiff or tough objects (Kay, 1975; Muchlinski & Deane, 2014; Peyron et al., 2002; Teaford & Oyen, 1989; Vinyard, 2008; Vinyard et al., 2011). This extensive oral testing is indicative of higher quantities of nervous tissue supplying the posterior dentition for primates that rely on tough and/or stiff foods. Similarly, many primates use their anterior dentition extensively to process fruits before ingestion and should thus have higher quantities of nervous tissues innervating the anterior dentition (Gautier-Hion et al., 1985; Julliot, 1996; Strait & Overdorff, 1996). Insects and seeds fall into separate categories as they can be either tough and/or stiff but would require extensive processing with the posterior dentition regardless. Because the speed and sensitivity of nervous relays is directly related to the size of the nervous structures themselves (Nuwer & Pouratian, 2017), diets that require more sensitivity (i.e., resistant diets) should have larger nervous structures for better relay. However, no study has addressed whether there is a relationship between the size of the nervous tissues and the diet that a primate actually eats. The purpose of

this chapter is to determine if there is a relationship between the size of the nervous tissues and the diet that a primate is consuming.

BACKGROUND AND HYPOTHESES

While all mammals have the same four basic tooth types, they vary significantly in size and shape as a response to diet and environment. This is because teeth are the first step in the mechanical breakdown of food and are therefore vital for life. Many studies have shown that tooth form and size are directly related to the amount of force necessary to breakdown certain food objects (Hiiemäe & Kay, 1973; Kay, 1975; Leighton, 1993; Lucas, 2006; Strait, 1997, 2001; Taylor, 2002; Teaford et al., 2006). Specifically, the contact areas on teeth (i.e., the occlusal surface) have a direct relationship to the diet that primates are consuming (Lucas & Luke, 1980; Lucas, 2006; Strait, 1997). However, because of their differences in size and shape, the teeth in the anterior portion of the mouth have different uses than the teeth in the posterior aspect of the mouth. Anterior teeth are more involved in the manipulation (incison) of food as it enters the mouth and are the teeth that we use to take an initial bite of a foodstuff (Lucas, 2006; Highlander, 2006; Murphy, 1968; Ungar, 1998, 2002). The posterior teeth – particularly the molars – are much more involved in the processing (mastication) of food after it has entered the oral cavity and as a bolus begins to form (Kleiber, 1961; Lucas, 2012).

The morphology of the post-canine teeth is often much more closely related to diet due to their role in the processing of food. Molar tooth size is directly related to body size and metabolism which often allows research to estimate the diets of extinct populations using data from the molars of modern species (Kay, 1975; Lund et al., 1998). However, our understanding of diet and particularly how we break it down into categories in the scientific literature is not standardized. Often, researchers break down diet based on the toughness or stiffness of an object, but these are not necessarily continuous values, nor are there agreed upon thresholds. For example, the toughness of a leaf species can be tested, but it is likely that other leaves

belonging to the same species will show variation in the toughness based on whether they are young or old leaves. Because diet is most often broken down into these resistant vs. non-resistant categories, researchers often put molars into two categories as well: mortar and pestle like teeth that process non-resistant foods, and blade-like teeth which are used to process resistant foods (Lucas, 1979, 2006; Lucas & Luke, 1980; Lumsden & Osborn, 1977; Strait, 1997). Further, some researchers (i.e, Gautier, 1985; Nekaris & Bearder, 2011; etc.) choose to break food categories down into percentages eaten that are based on direct field observations of single individuals or groups of the same species. These percentages are then used to assign a standard category, like fruigivore or folivore, to a species at large based on the observations of a few individuals. Essentially, there is still no agreed upon and standardized way to measure and estimate the specific diet that a species is consuming, although we understand that tooth shape/size has a direct relationship to diet in some capacity.

Although teeth are necessary to process the food that a primate eats, the teeth themselves do not sense the food material properties. For the mandibular teeth, all somatic sensation comes from the inferior alveolar nerve (IAN). The IAN sends constant feedback to the brain during each chewing cycle to establish how much force the next chewing cycle should use and to detect any changes in food material properties that may harm the occlusal surface of the tooth (Beyron, 1964; Fujishita et al., 2015; Luschei & Goldberg, 2011; Thexton & Hiiemae, 1997; Watt & Williams, 1951). The IAN additionally transmits innervation from the periodontal membrane, which is a system of tissues (the gingiva, periodontal membrane, and the periosteum) that surround the teeth and keep them anchored in place in the mandibular bone (Hannam, 1976, 1982). Both the teeth and the periodontal membrane send constant feedback information to the brain during tooth use for both pain and pressure sentations (Anderson et al., 1970; Avery & Cox, 1977; Brashear, 1936; Plaffman, 1939).

Although this sensation from the IAN is crucial for maintaining the proper chewing cycles, primates do not always complete a full chewing cycle with all food materials placed in

the oral cavity. For example, some primates use puncture crushing (i.e., vertical movements where the teeth puncture food items but do not come into full occlusion) when they are chewing tougher/stiffer objects to break down the food initially before the teeth come into occlusion (Osburn & Lumsden, 1978). Additionally, some field studies have shown that primates will “test” certain objects by placing them between the teeth (usually the premolars or molars) to establish the toughness/stiffness of the object (Kay, 1975; Muchlinski & Deane, 2014; Peyron et al., 2002; Scott et al., 2018; Teaford & Oyen, 1989; Vinyard, 2008; Vinyard et al., 2011). This has been particularly shown in primates that eat leaves in that they will choose certain leaves over others (usually younger leaves over older leaves) seemingly due to the toughness of the leaf (Davies et al., 1988; Ganzhorn et al., 2017; Kar-Gupta & Kumar, 1994; Lucas et al., 2012; Prinz & Lucas, 2000). Some reasearchers argue that this is due to tannin content in leaves (Prinz & Lucas, 2000) while others argue that this is more related to the fiber content (Ganzhorn et al., 2017; Lucas et al., 2012). Fiber in particular appears to have a consistently negative effect on food consumption in that foods with high fiber content are chosen less often and tend to be tougher/stiffer (Ganzhorn et al., 2017; Lucas et al., 2012). Primates would likely avoid high fiber foods because fiber is insoluble in water and adds unneccesary bulk to the stomach contents and stool without providing added nutrients. All of this oral testing would be done on the mandibular tooth row through the IAN (or the maxiilary tooth row via the superior alvolar nerve, SAN), indicating that the sensory capabilities of this nerve should have an intricate relationship to the food a primate is able to consume.

Research has shown, particularly during growth and development, that having a diet with no resistance will cause inconsistent chewing patterns, difficulty controlling masticatory forces, and issues with bone development (Fujishita et al., 2015; Luschei & Goldberg, 2011; Thexton & Hiiemae, 1997; Watt & Williams, 1951). During adulthood, impulses from the IAN show higher EMG activity, higher rates of saliva production, and better maintenance of chewing cycles when consuming more resistant objects (Anderson et al., 1985; Hector, 1985; Hiiemae et al., 1996;

Rosenberger & Kinzey, 1976; Teaford & Oyen, 1989; Watanabe & Dawes, 1988). All of this research indicates that chewing reistant foods is vital for the proper growth and maintenance of the masticatory system even though more resistant foods are much more likley to damage the tooth row. Because of this potential for damage, it is likely that the nervous tissues at the back of the oral cavity (where the majority of food processing is done) are larger and thus better able to send more information at faster rates to the central nervous system (Nuwer & Pouratian, 2017).

While the post-canine teeth and their corresponding nervous tissues are responsible for protecting the teeth while consuming resistant objects, the anterior teeth play the crucial role of food incision. Fruit is often chosen for consumption prior to ingestion due to a variety of factors: color, accessibility, weight, palatability, nutrient content, competition with other animals, morphology, pulp richness, seasonality, and seed size (Gautier-Hion et al., 1985; Julliot, 1996; Strait & Overdorff, 1996). Primates will often use the lips and lower face to smell and feel a fruit prior to ingestion, indicating that the exterior aspect of the mandible and oral cavity are heavily involved in fruit selection (Muchlinski & Deane, 2016). Thus, the anterior portion of the IAN (i.e., the termination of the mental nerve) should play a role in the food selection process.

However, as discussed throughout this dissertation, studying the soft tissue of primates (and particularly non-human primates) is incredibly difficult and opportunistic. To date, no study has assessed the variation seen in the IAN in non-human primates and those studies that have been done on human individuals usually involve very small sample sizes. Because no study has addressed this variation or established the relationship between the soft- and hard-tissue components of the mandible, no assessment has been made as to whether the IAN has a direct relationship to primate diet and/or feeding behavior.

Because the scientific body of literature has shown that there is a close association between the occlusal surface of the tooth and diet, we might expect to see a relationship between the IAN and the diet a primate species is consuming. Additionally, I expect to find

tighter relationships between the anterior aspect of the mouth in primates that manipulate food extensively before ingestion (i.e., fruit) and tighter relationships between the posterior dentition in primates that masticate food extensively on their post-canine teeth (i.e., leaves, insects, etc.)

Here, I investigate this research area by asking the overarching question: “Does the actual and relative volume and cross-sectional area of the nervous tissue within the mandible correlate with feeding behavior?”. Specifically, I test two separate but related hypotheses:

> **H_1:** Primates that use the posterior dentition for extensive processing of leaves, seeds, and insects will have more nervous tissue concentrated in and around the posterior dentition.
>
> **H_2:** Primates that use the anterior dentition for extensive processing of fruit (e.g., peeling fruit skins away from pulp) will have more nervous tissue concentrated in and around the anterior dentition.

MATERIALS AND METHODS

Data Collection and Preparation

To assess if there is a relationship between the IAN and feeding behavior, I used the variables for “Q3” as outlined in Table 3.1 under the column header “Associated Research Question”. Chapter 3 describes the data collection process for all soft- and hard-tissue variables and data preparation (i.e., size adjustment, natural log transformation, etc.) used for this chapter. All analyses for Q3 used a total of 66 individuals (23 females, 33 males, 8 of unknown sex) from 31 primate species and 3 mammalian outgroups (*Lontra canadensis* (n = 1), *Rattus norvegicus* (n = 5), and *Oryctolagus cuniculus* (n=4)) for all soft-tissue variables (Figure 3.1). Summary statistics for the raw data of all variables used in Q3 can be found in Table A.8 and all dietary information can be found in Table 3.4. Dietary data for this chapter was first culled from the literature using primary observations for each species that were recorded by percentage eaten. Then, the highest percentage eaten was assigned as the primary diet (i.e., if a primate

ate 66% fruit, they would be assigned a primary diet of “fruit”) and the second highest percentage was assigned as the secondary diet. Finally, these primary and secondary diets were assigned as either “resistant” (i.e., fruit, gum, etc.) or “non-resistant” (i.e., leaves, insects, seeds, etc.). All these categories – the raw percentages, primary standard categories, and resistant vs. non-resistant categories are used in this chapter to assess if nervous tissues have a relationship to the diet a primate is consuming. Additionally, each species was given a species “code” to better show each species on figures using the first two letters of the genus and species. For example, *Papio anubis* would be given the code PAAN. These codes, their corresponding families, and the color identifiers from each figure can be found in Table 3.2.

Analytical Methods

For Q3, and because each of the variables are numerical and continuous, I used a series of phylogenetic ANOVAs (phylANOVA) and phylogenetic multiple regression analyses to determine the significance of the relationships between the IAN and the feeding behaviors of primates (with some mammalian outgroups included) (Grafen, 1989). To qualitatively assess the data, I looked at a variety of factors in the raw data. In this assessment, I looked at the average size of the nerve cross-sectional area (CSA) at the mental foramen, the average size of the nerve CSA at the mandibular foramen, the average nerve CSA at P_4 and M_1, and a ratio (thus making the data dimensionless and allowing for direct comparisons) of these numbers to establish if there are large differences in CSA size. This ratio assessed the relationship between the nerve CSA of the mental foramen (as the numerator) to the nerve CSA at the mandibular foramen (as the denominator). Additionally, I used boxplots to show the power reduced, natural log-transformed data for feeding behaviors across all species by family to establish the size differences in nervous tissues in relation to diet. All analyses were performed in RStudio using package *caper* function “pgls” version 0.0-1 and the package *phytools* function “phylANOVA”. To correct for type I error (false positives) in the statistical analyses, a manual alpha value correction was used and is stated in each table reporting the test results. Question 3 asks,

“Does the volume and cross-sectional area of the nervous tissue within the mandible correlate with feeding behavior?” and a general overview of the analyses for Q3 are shown in Table 6.1.

Table 6.1. Tests performed in Question 3

Dependent variable	Independent variable	Test	Hypothesis
Nerve CSA at the Mandibular foramen	Categorical diets	Phylogenetic ANOVA	H1
Nerve CSA at the Mandibular foramen	Resistant/non-resistant diet	Phylogenetic ANOVA	
IAN nerve CSA (under M_1 and P_4)	Categorical diets	Phylogenetic ANOVA	
IAN nerve CSA (under M_1 and P_4)	Resistant/non-resistant diet	Phylogenetic ANOVA	
Nerve CSA at the Mandibular foramen	Diet percentages	Phylogenetic regression	
IAN nerve CSA (under M_1 and P_4)	Diet percentages	Phylogenetic regression	
Nerve CSA at the Mental foramen	Categorical diets	Phylogenetic ANOVA	H2
Nerve CSA at the Mental foramen	Resistant/non-resistant diet	Phylogenetic ANOVA	
Nerve CSA Mental foramen nerve CSA	Diet percentages	Phylogenetic regression	
IAN volume	Categorical diets	Phylogenetic ANOVA	
IAN volume	Diet percentages	Phylogenetic regression	

Specifically, for Q3-H1, I used the posterior nervous tissue variables (nerve CSA beneath M_1, nerve CSA beneath P_4, and nerve CSA at the mandibular foramen) and the dietary categories (both categorical and resistant/non-resistant) to establish if there is a relationship between the posterior IAN and feeding behaviors. I also used the averages of the nerve CSA at the mandibular foramen, M_1, and P_4 tissues to establish if there is more nervous tissue at certain points along the posterior IAN by species.

For Q3-H2, I used the anterior nervous tissues variable (nerve CSA at mental foramen) and the dietary categories (both categorical and resistant/non-resistant) to establish if there is a relationship between the anterior IAN and feeding behaviors. I also established the averages of the nerve CSA at the mental foramen to determine if there is more nervous tissue at the anterior IAN by species.

Finally, to tie both hypotheses together, I established the average IAN volumes across species to determine which species have overall larger nervous tissues. Additionally, I used a ratio of the nerve CSA at the mental foramen and mandibular foramen to establish the differences in nervous tissues size as the IAN enters and exits the mandibular canal.

RESULTS

Summary Statistics and Raw Data

Table A.8 shows the summary statistics for all variables used in Q3 (found in Appendix A). Because this chapter focuses on differences in nervous tissue in both the anterior and posterior aspects of the mandible, I first compared the average nerve CSA at the mental foramen to the average nerve CSA at the mandibular foramen by family to assess if there are major differences. This means that values < 1 indicate there are more nervous tissues at the mandibular foramen and values > 1 indicate that there are more nervous tissues at the mental foramen. These numbers were not multiplied by 100 to create an actual percentage in the figures, therefore “1” indicates 100% for all figures in this chapter. However, percentages (out of 100%) will be used for discussion throughout this chapter.

Figure 6.1 shows the boxplots for this ratio by family. This ratio ranged from 16.8% in *Trachypithecus francoisi* to 161.3% in *Alouatta caraya*. Atelidae displays the greatest range in this ratio, followed by Cebidae, and Cercopithecidae. However, families like Aotidae, Cheirogaleidae, Hominidae, Lorisidae, and Mustelidae show no range because only one individual represents that family. The average ratio across all specimens is 64.6% indicating that, on average, the mental foramen has roughly half the amount of nervous tissue running through it than the mandibular foramen.

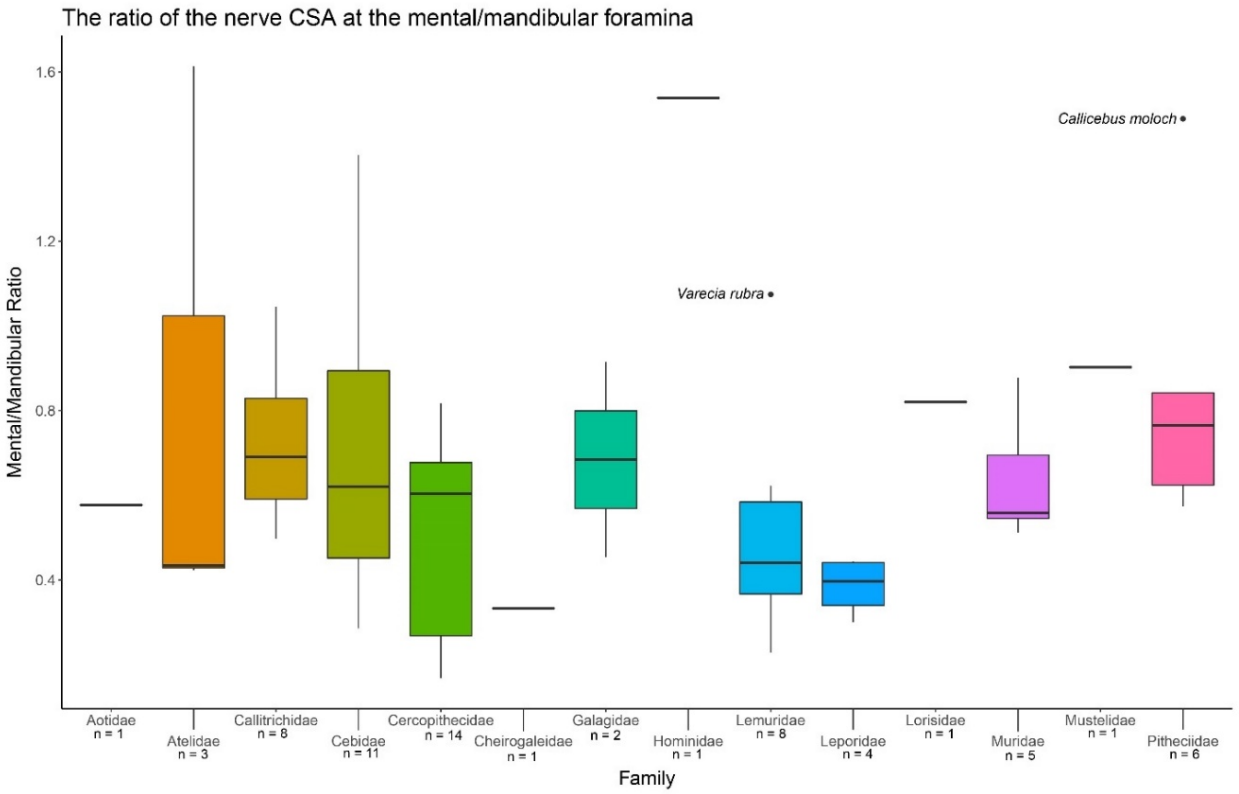

Figure 6.1. Boxplots showing the ratio of the nerve CSA at the mental foramen to the nerve CSA at the mandibular foramen.

After examining the nerve CSA at the mental foramen to the nerve CSA at the mandibular foramen ratio by family, I also examined this ratio by dietary category. The boxplots showing nerve ratio size by primary and secondary diet are shown in Figure 6.2A-B. Figure 6.2A shows that this ratio is relatively standard across all groups by dietary category in that all ranges overlap for the primary diet. The secondary diet (Figure 6.2B) also shows substantial overlap between most food groups for this ratio. However, *Pan paniscus* is a clear outlier in this ratio (and all future data analyses) indicating much more nervous tissue within this species than any other examined.

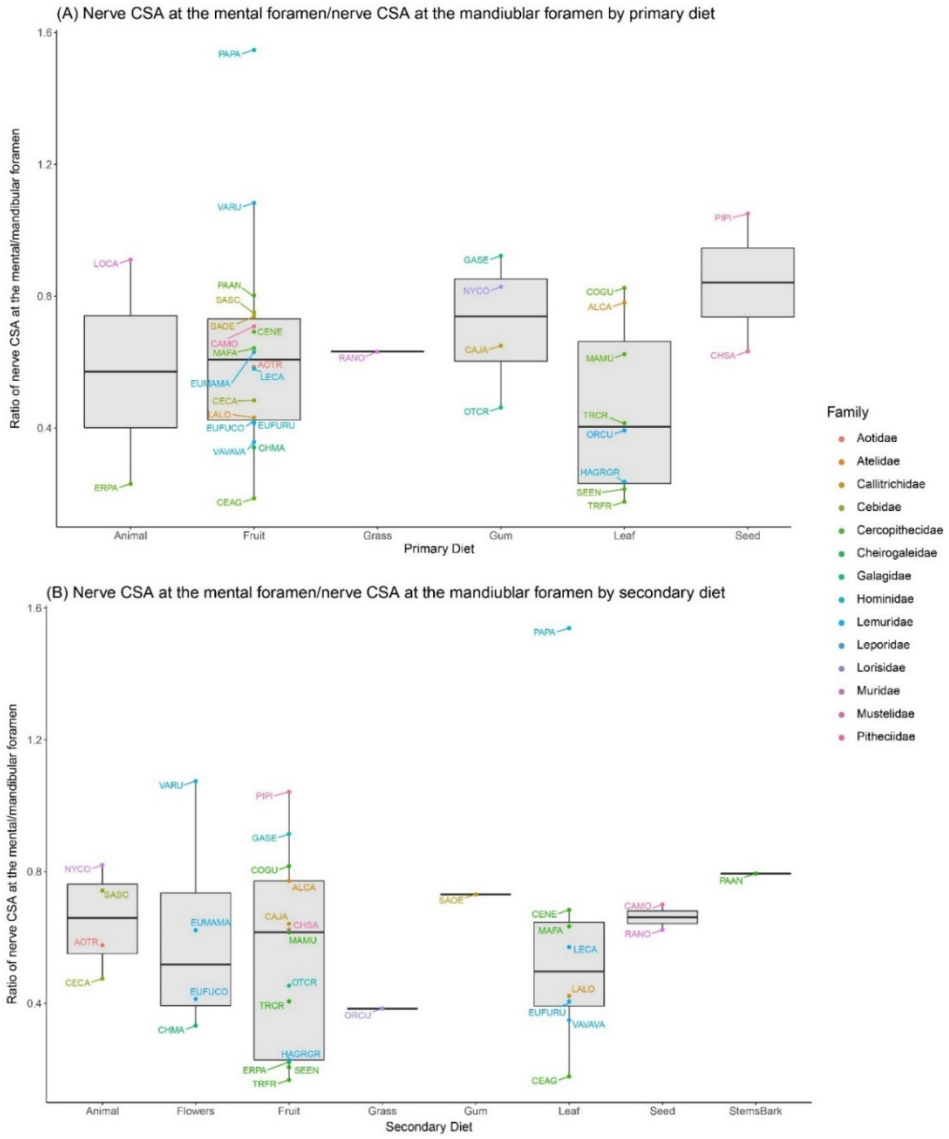

Figure 6.2A-B. Boxplots showing the ratio of the nerve CSA at the mental foramen to the nerve CSA at the mandibular foramen by primary (A) and secondary (B) category.

Additionally, I examined this data by resistant vs. non-resistant primary and secondary categories. Boxplots for these analyses are show in Figure 6.3A-B. There is substantial range overlap again when the diets are examined as just resistant or non-resistant in both primary and secondary diet for this ratio as well.

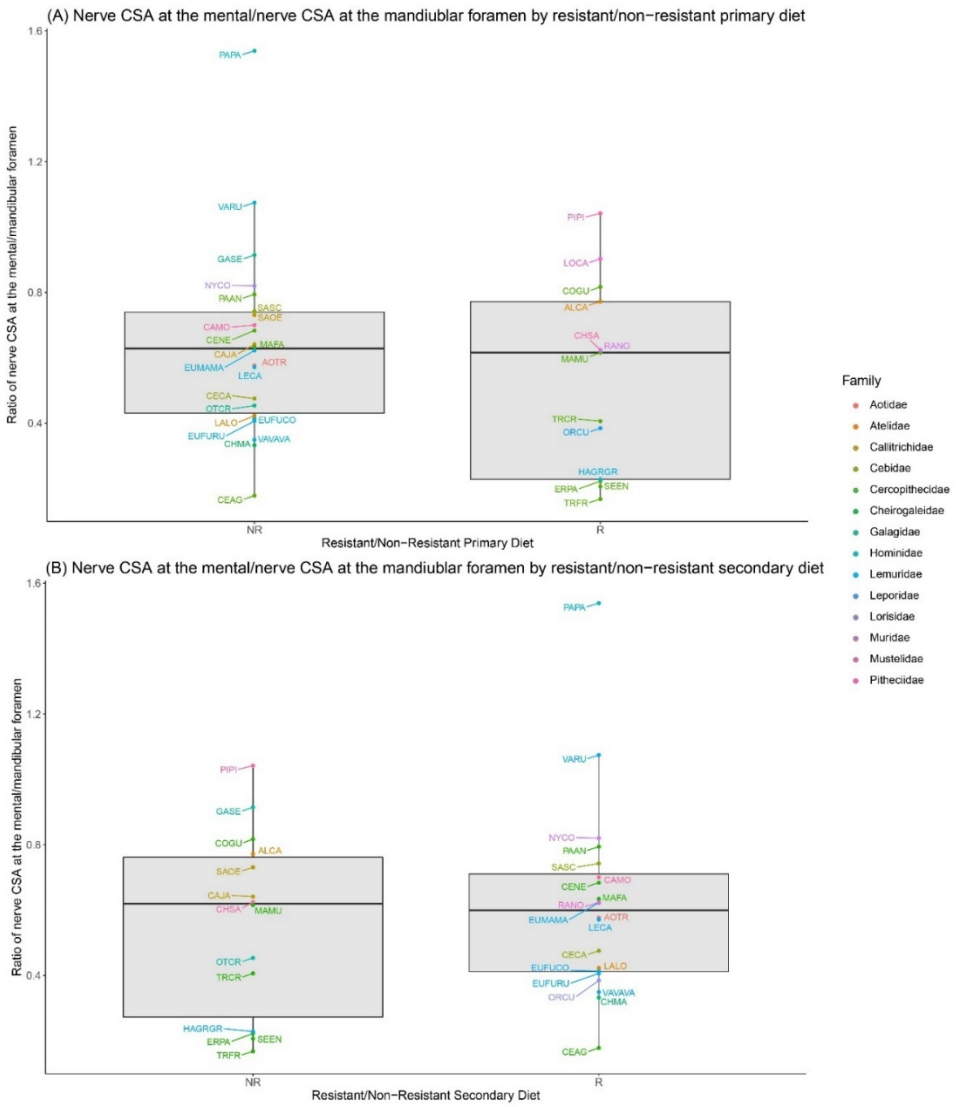

Figure 6.3A-B. Boxplots showing the ratio of the nerve CSA at the mental foramen to the nerve CSA at the mandibular foramen by primary resistant/non-resistant (A) and secondary resistant/non-resistant (B) category.

Quantitative Analyses

To assess relationships between the nervous tissues and dietary categories, I ran a series of phylogenetic ANOVAs on the primary, secondary, and resistant vs. non-resistant primary and secondary dietary categories against each of the measured nervous tissues. Each of these tests only included the primate sample but the mammalian outgroups will be shown on the corresponding boxplots for each test for comparison purposes. The first of these tests were performed on data that was power reduced and natural log transformed (but not size adjusted).

This allows me to discuss how the size of the nerve may affect the relationship to diet. The results of these analyses are shown below in Table 6.2. No analysis showed a significant relationship between primary or secondary diet and any nervous tissue variable in the non-size adjusted data.

Table 6.2. Phylogenetic ANOVA results of the IAN variables and categorical variables (no size-adjustment to data)

Dependent variable	Independent variable	F-statistic	p-value
Posterior Dentition			
Primary diet	IAN CSA at mandibular foramen	2.017	0.378
Primary diet	IAN CSA at M_1	1.950	0.393
Primary diet	IAN CSA at P_4	2.071	0.262
Secondary diet	IAN CSA at mandibular foramen	2.304	0.176
Secondary diet	IAN CSA at M_1	1.647	0.377
Secondary diet	IAN CSA at P_4	1.392	0.475
Anterior Aspect of Oral Cavity			
Primary diet	IAN CSA at mental foramen	0.554	0.886
Secondary diet	IAN CSA at mental foramen	1.595	0.379
Total IAN Volume			
Primary diet	IAN volume	1.784	0.445
Secondary diet	IAN volume	2.157	0.215
Alpha values were set to p-value < 0.025			

Second, I performed the same analyses on the data that was power reduced, size adjusted, and natural log transformed to assess the relative relationships between the IAN and diet. These results are shown in Table 6.3. Like the data with no size-adjustment, there were no significant differences between the primary or secondary diet and any nervous tissue variable in the size-adjusted data.

Table 6.3. Phylogenetic ANOVA results of the IAN variables and categorical variables (size-adjusted data)

Dependent variable	Independent variable	F-statistic	p-value
Posterior Dentition			
Primary diet	IAN CSA at mandibular foramen	0.127	0.994
Primary diet	IAN CSA at M_1	0.711	0.827
Primary diet	IAN CSA at P_4	0.207	0.932
Secondary diet	IAN CSA at mandibular foramen	1.272	0.506
Secondary diet	IAN CSA at M_1	0.533	0.904
Secondary diet	IAN CSA at P_4	0.391	0.912
Anterior Aspect of Oral Cavity			
Primary diet	IAN CSA at mental foramen	1.712	0.477
Secondary diet	IAN CSA at mental foramen	0.384	0.960
Total IAN Volume			
Primary diet	IAN volume	0.451	0.925
Secondary diet	IAN volume	0.608	0.877
Alpha values were set to p-value < 0.025			

To assess if food material properties – rather than standard dietary categories – showed a relationship to the IAN, I performed these same phylANOVAs on both size-adjusted data and data with no size-adjustment. The results for the data with no size adjustment are shown in Table 6.4 and the results for the data with a size-adjustment are shown in Table 6.5. There were no significant differences in primary or secondary resistance in diet for either the non-size adjusted data (Table 6.4) or the size adjusted data (Table 6.5).

Table 6.4. Phylogenetic ANOVA results of the IAN and resistant/non-resistant variables (no size-adjustment to data)

Dependent variable	Independent variable	F-statistic	p-value
Posterior Dentition			
Primary diet R/NR	IAN CSA at mandibular foramen	2.620	0.258
Primary diet R/NR	IAN CSA at M_1	1.480	0.448
Primary diet R/NR	IAN CSA at P_4	0.374	0.606
Secondary diet R/NR	IAN CSA at mandibular foramen	0.095	0.820
Secondary diet R/NR	IAN CSA at M_1	0.216	0.747
Secondary diet R/NR	IAN CSA at P_4	1.412	0.336
Anterior Aspect of Oral Cavity			
Primary diet R/NR	IAN CSA at mental foramen	0.317	0.717
Secondary diet R/NR	IAN CSA at mental foramen	0.506	0.619
Total IAN Volume			
Primary diet R/NR	IAN volume	1.719	0.414
Secondary diet R/NR	IAN volume	0.230	0.743
Alpha values were set to p-value < 0.025			

Table 6.5. Phylogenetic ANOVA results of the IAN and resistant/non-resistant variables (size-adjusted data)

Dependent variable	Independent variable	F-statistic	p-value
Posterior Dentition			
Primary diet R/NR	IAN CSA at mandibular foramen	0.008	0.954
Primary diet R/NR	IAN CSA at M_1	0.194	0.796
Primary diet R/NR	IAN CSA at P_4	0.220	0.688
Secondary diet R/NR	IAN CSA at mandibular foramen	0.010	0.948
Secondary diet R/NR	IAN CSA at M_1	0.059	0.883
Secondary diet R/NR	IAN CSA at P_4	0.084	0.828
Anterior Aspect of Oral Cavity			
Primary diet R/NR	IAN CSA at mental foramen	1.925	0.369
Secondary diet R/NR	IAN CSA at mental foramen	0.442	0.627
Total IAN Volume			
Primary diet R/NR	IAN volume	0.212	0.777
Secondary diet R/NR	IAN volume	0.198	0.762
Alpha values were set to p-value < 0.025			

Nerve CSA of the mandibular foramen. Figure 6.4 shows the primary diet for the nerve CSA of the mandibular foramen data with no size adjustment (A) and with size-adjustment (B). There were no differences between the means for each primary food group for the data with no size-adjustment (Table 6.2; F-statistic = 2.017, p-value = 0.378) or with a size-adjustment (Table 6.3; F-statistic = 0.127, p-value = 0.994).

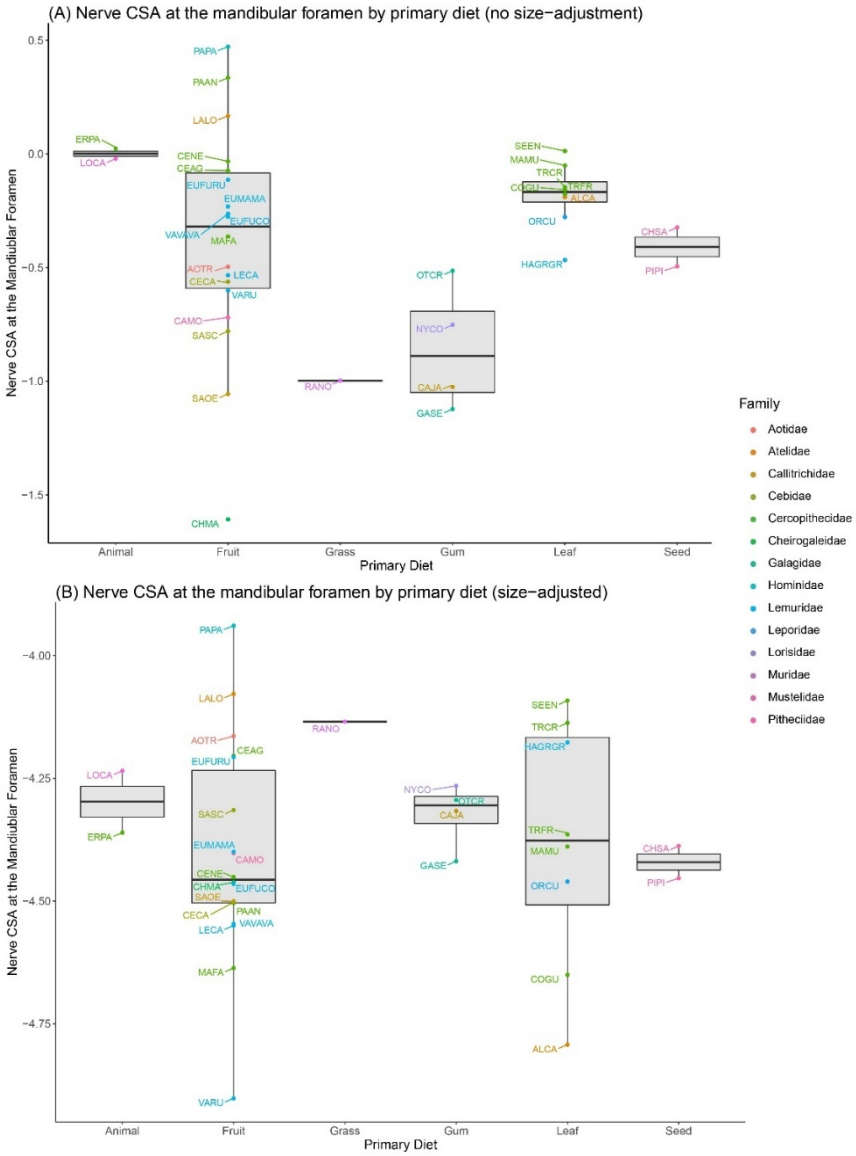

Figure 6.4A-B. The nerve CSA at the mandibular foramen by primary diet in data that is not size-adjusted (A) and size-adjusted (B). These data are also power reduced and natural log transformed.

Figure 6.5 shows the primary resistant vs. non-resistant diet for the data with no size adjustment (A) and with a size-adjustment (B) for nerve CSA at the mandibular foramen. Similarly, the data with no size-adjustment (Table 6.4; F-statistic = 2.620, p-value = 0.258) and the size-adjusted data (Table 6.5; F-statistic = 0.008, p-value = 0.954) showed no significant differences between the means for a primary diet that is either resistant or non-resistant.

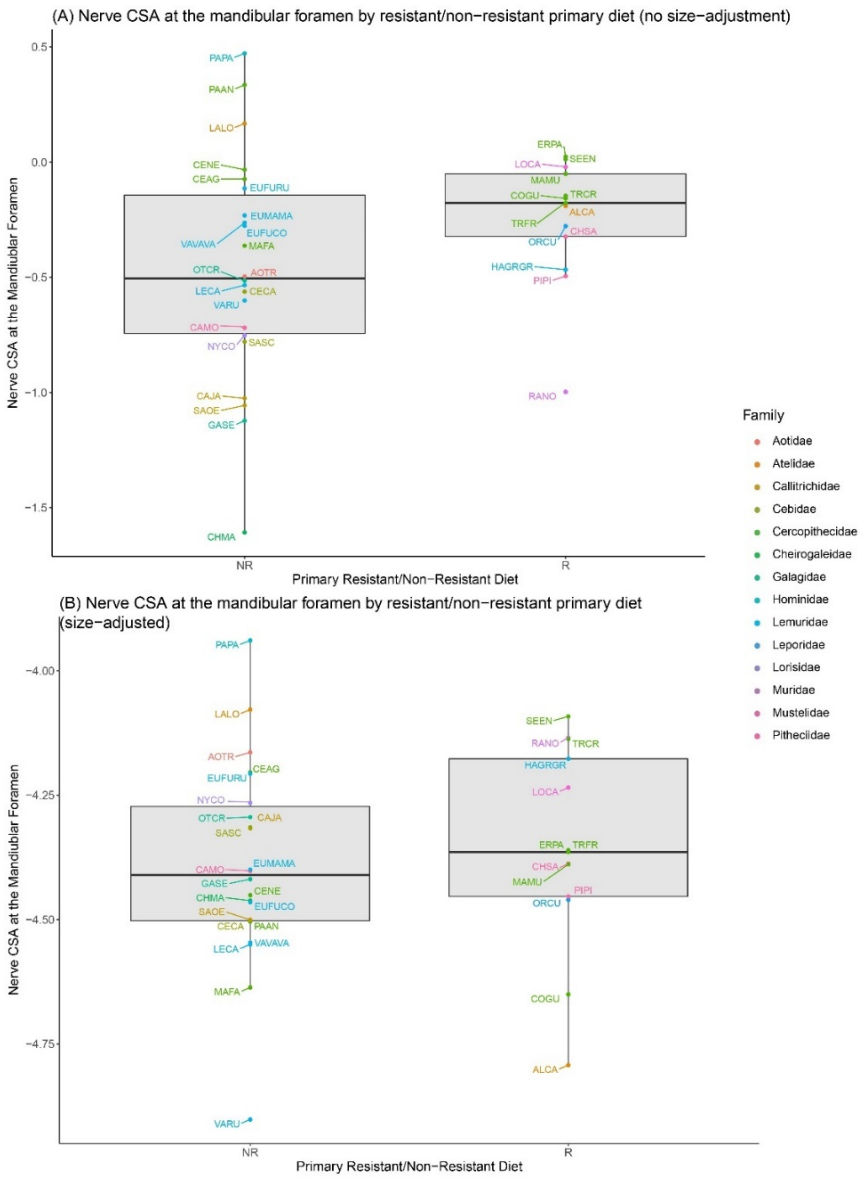

Figure 6.5A-B. The nerve CSA at the mandibular foramen by primary resistant vs. non-resistant diet in data that is not size-adjusted (A) and size-adjusted (B). These data are also power reduced and natural log transformed.

Figure 6.6A-B shows the secondary diet for the data with no size adjustment (A) and with a size-adjustment (B) for nerve CSA at the mandibular foramen. There were no significant differences between primate families for the data with no size-adjustment (Table 6.2; F-statistic = 2.304, p-value = 0.176) or the data with a size-adjustment (F-statistic = 1.272, p-value = 0.506).

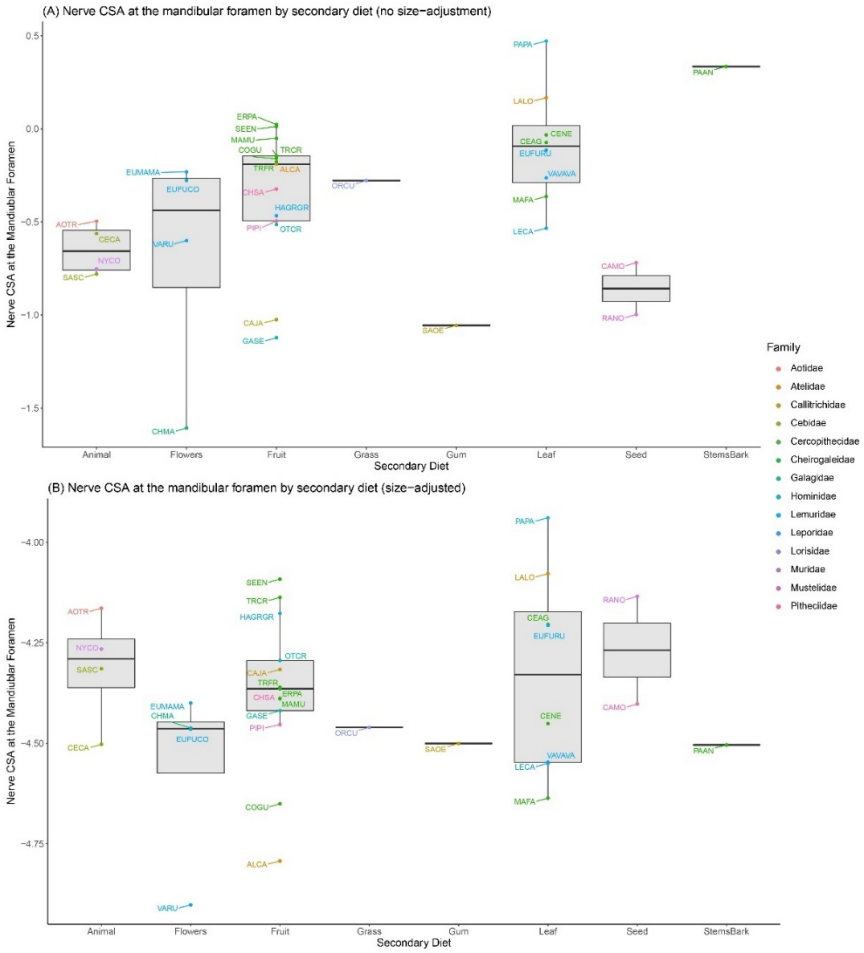

Figure 6.6A-B. The nerve CSA at the mandibular foramen by secondary diet in data that is not size-adjusted (A) and size-adjusted (B). These data are also power reduced and natural log transformed.

Figure 6.7A-B shows the secondary resistant vs. non-resistant diet for the data with no size adjustment (A) and with a size-adjustment (B) for the nerve CSA at the mandibular foramen. These results again show no significant differences between dietary groups for the data with no size-adjustment (Table 6.4; F-statistic = 0.095, p-value = 0.820) or for the size-adjusted data (Table 6.5; F-statistic = 0.010, p-value = 0.948).

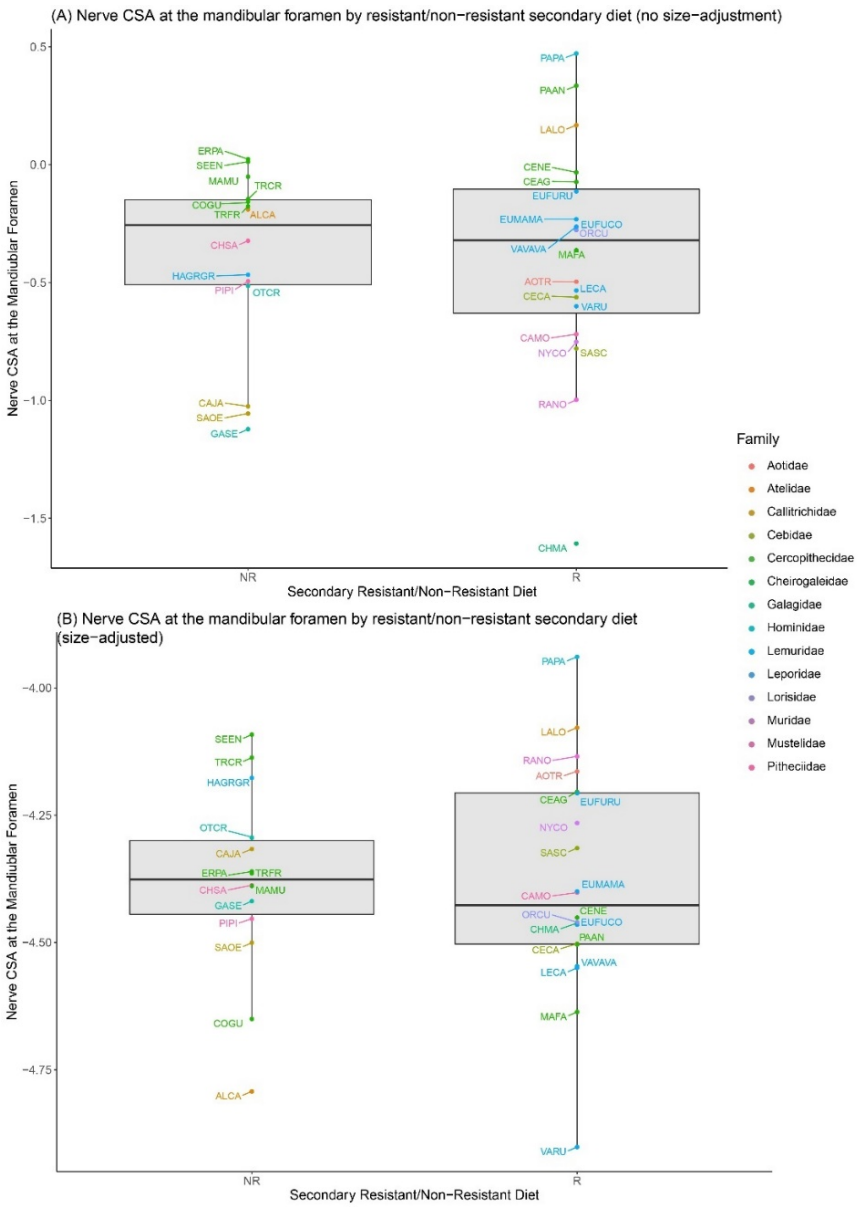

Figure 6.7A-B. The nerve CSA at the mandibular foramen by secondary resistant vs. non-resistant diet in data that is not size-adjusted (A) and size-adjusted (B). These data are also power reduced and natural log transformed.

Nerve CSA beneath M_1. Figure 6.8 shows the primary diet for the nerve CSA beneath M_1 data with no size adjustment (A) and with a size-adjustment (B). The results for the molar nerve CSA closely mirrors that seen at the mandibular foramen. There were no significant differences between primate feeding groups when the data is not size adjusted (Table 6.2; F-

statistic = 1.950, p-value = 0.393) or when size is adjusted for (Table 6.3; F-statistic = 0.711, p-value = 0.827).

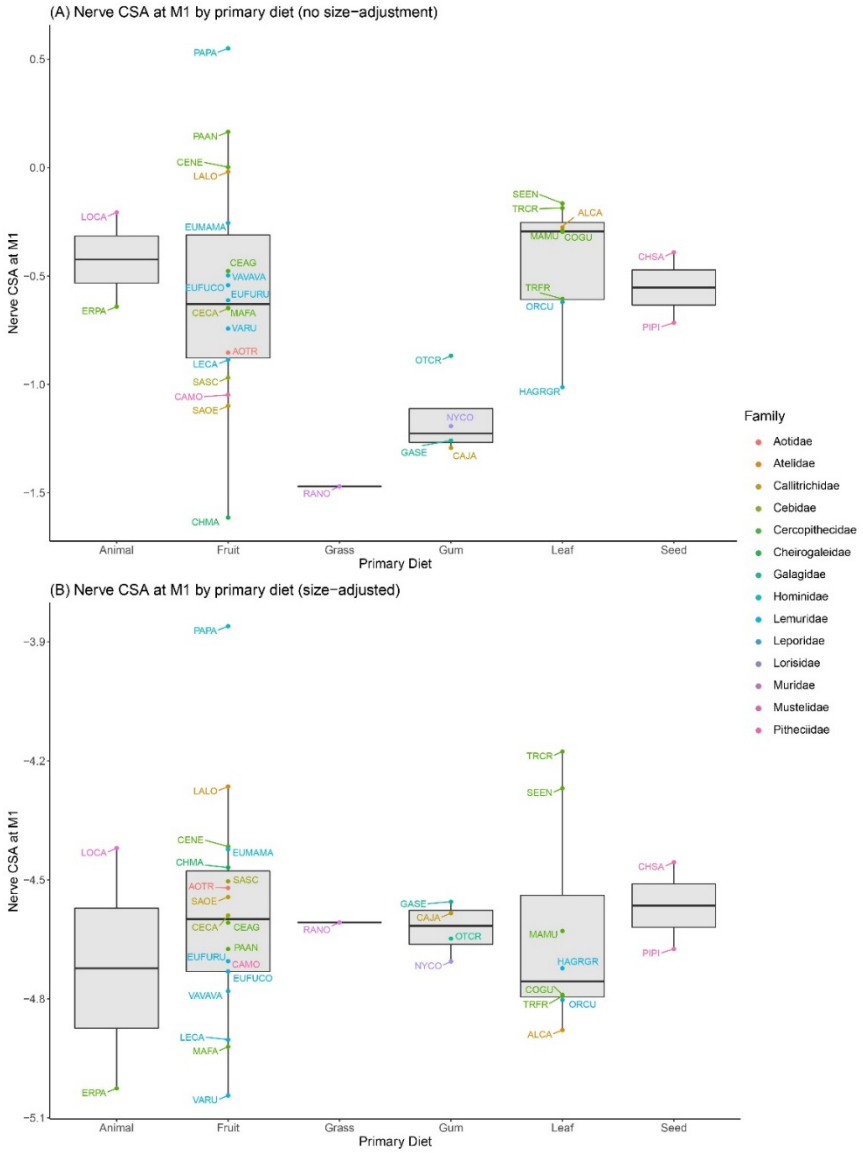

Figure 6.8A-B. The nerve CSA beneath M_1 by primary diet in data that is not size-adjusted (A) and size-adjusted (B). These data are also power reduced and natural log transformed.

Figure 6.9A-B shows the primary resistant vs. non-resistant diet for the data with no size adjustment (A) and with a size-adjustment (B) for the nerve CSA beneath M_1. These data again show very few differences in the means or ranges for both the size-adjusted data (Table 6.4; F-

statistic = 0.194, p-value = 0.796) and data with no size-adjustment (Table 6.5; F-statistic = 1.480, p-value = 0.448) and no significant differences in the phylANOVAs.

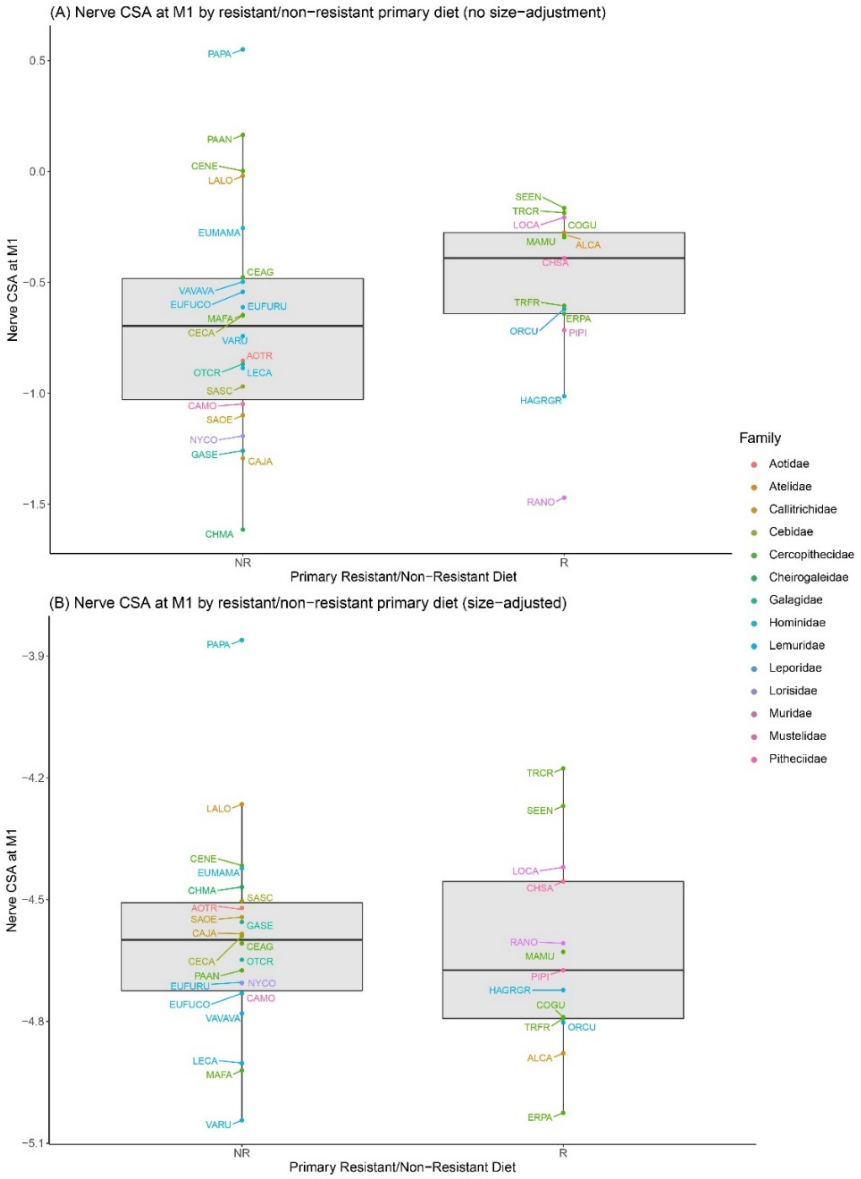

Figure 6.9A-B. The nerve CSA beneath M_1 by primary resistant vs. non-resistant diet in data that is not size-adjusted (A) and size-adjusted (B). These data are also power reduced and natural log transformed.

Figure 6.10A-B shows the secondary diet for the data with no size adjustment (A) and with a size-adjustment (B) for nerve CSA beneath M_1. These data mirror the primary diet results in that there were no significant differences among feeding groups by nerve size in either the

non-size adjusted data (Table 6.2; F-statistic = 1.647, p-value = 0.377) or the size-adjusted data (Table 6.3; F-statistic = 0.533, p-value = 0.904).

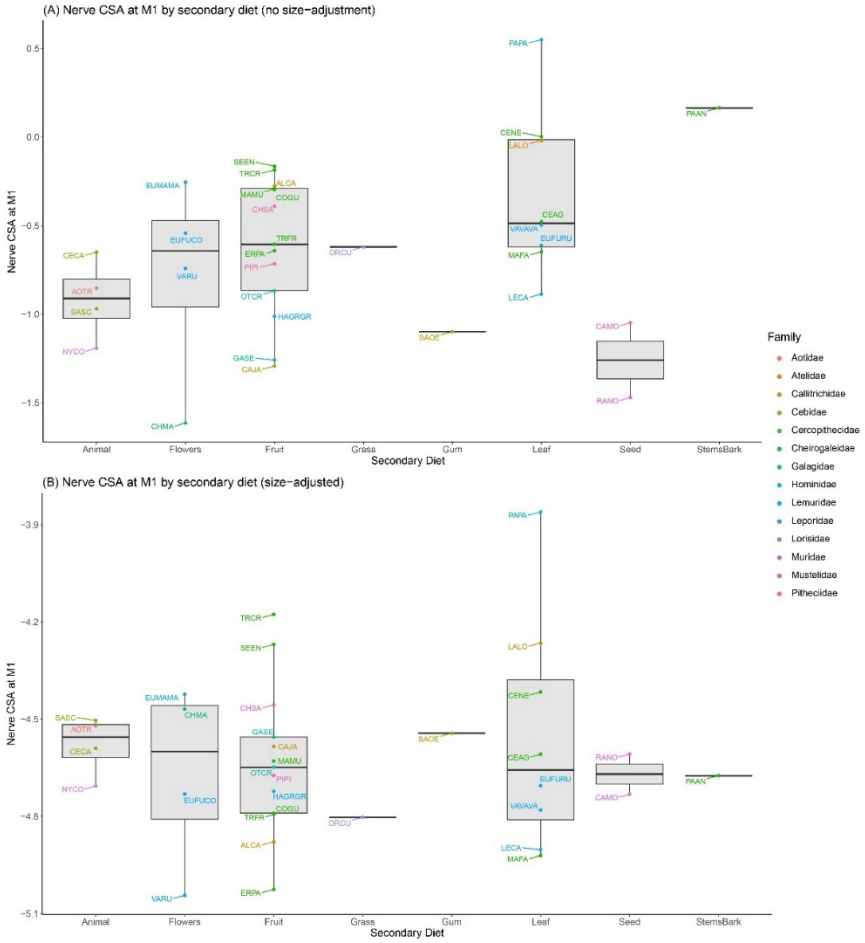

Figure 6.10A-B. The nerve CSA beneath M_1 by secondary diet in data that is not size-adjusted (A) and size-adjusted (B). These data are also power reduced and natural log transformed.

Figure 6.11A-B shows the secondary resistant vs. non-resistant diet for the nerve CSA beneath M_1 data with no size adjustment (A) and with a size-adjustment (B). Again, these data showed no significant differences in the non-size adjusted data (Table 6.4; F-statistic = 0.216, p-value = 0.747) and the size-adjusted data (Table 6.5; F-statistic = 0.059, p-value = 0.883) when the dietary categories are divided into resistant or non-resistant.

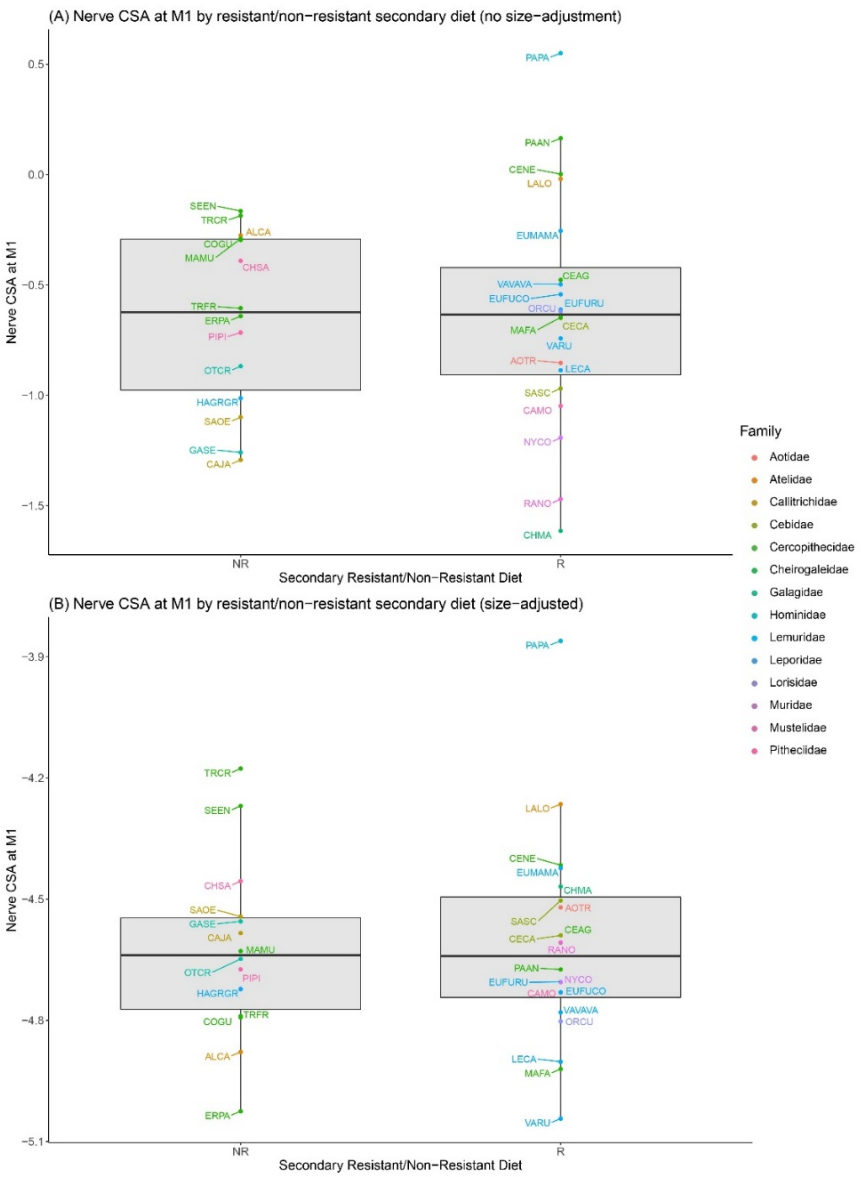

Figure 6.11A-B. The nerve CSA beneath M_1 by secondary resistant vs. non-resistant diet in data that is not size-adjusted (A) and size-adjusted (B). These data are also power reduced and natural log transformed.

Nerve CSA beneath P_4. Figure 6.12 shows the primary diet for the nerve CSA beneath P_4 data with no size adjustment (A) and with a size-adjustment (B). These figures show that, like the nerve size at the mandibular foramen and M_1, there is substantial overlap in the ranges of nerve CSA beneath P_4 in both the size-adjusted and non-size adjusted data. The phlylANOVA results support these visual similarities in that there were no significant differences in the data

with no size-adjustment (Table 6.2; F-statistic = 2.071, p-value = 0.262) and the data with a size-adjustment (Table 6.3; F-statistic = 0.207, p-value = 0.932).

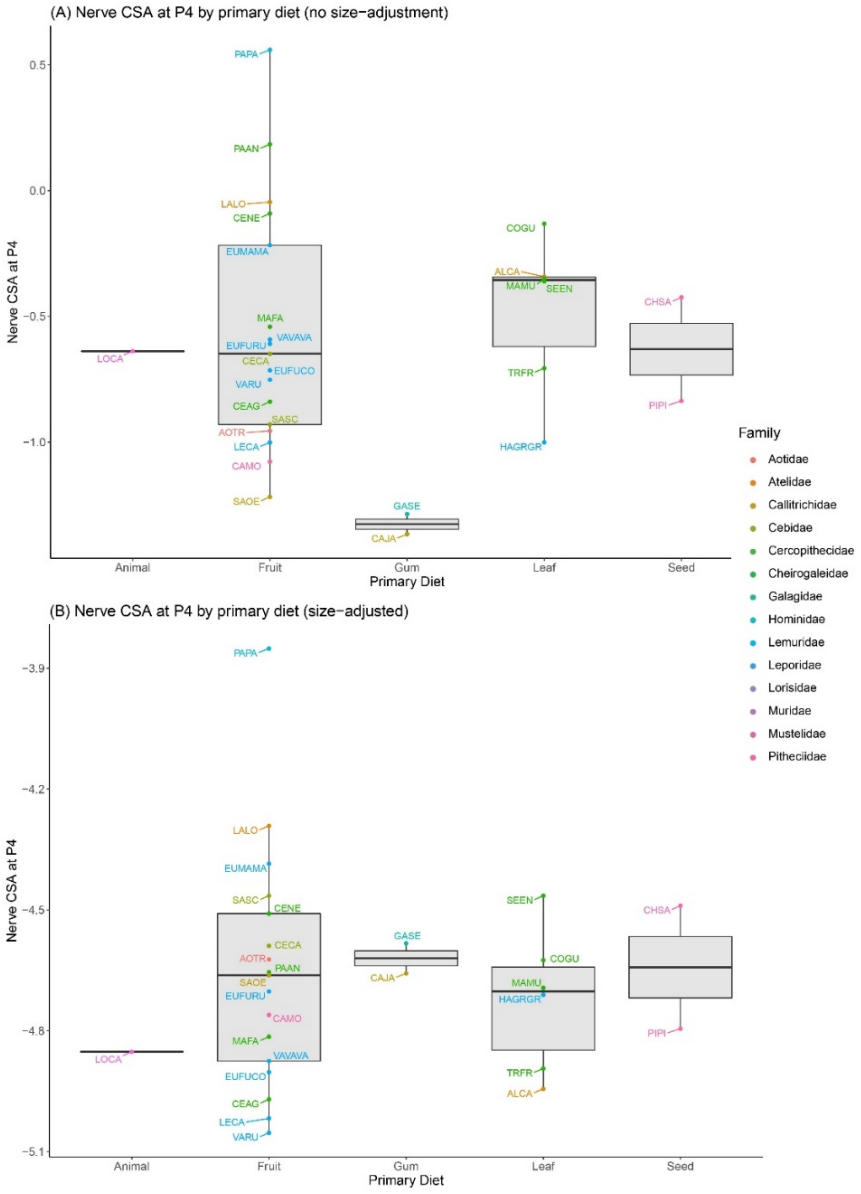

Figure 6.12A-B. The nerve CSA beneath P_4 by primary diet in data that is not size-adjusted (A) and size-adjusted (B). These data are also power reduced and natural log transformed.

Figure 6.13 shows the primary resistant vs. non-resistant diet for the data with no size adjustment (A) and with a size-adjustment (B) for the nerve CSA beneath P_4. There were again

no significant differences in the non-size adjusted data (Table 6.4; F-statistic = 0.374, p-value = 0.606) or the size-adjusted data (Table 6.5; F-statistic = 0.220, p-value = 0.688).

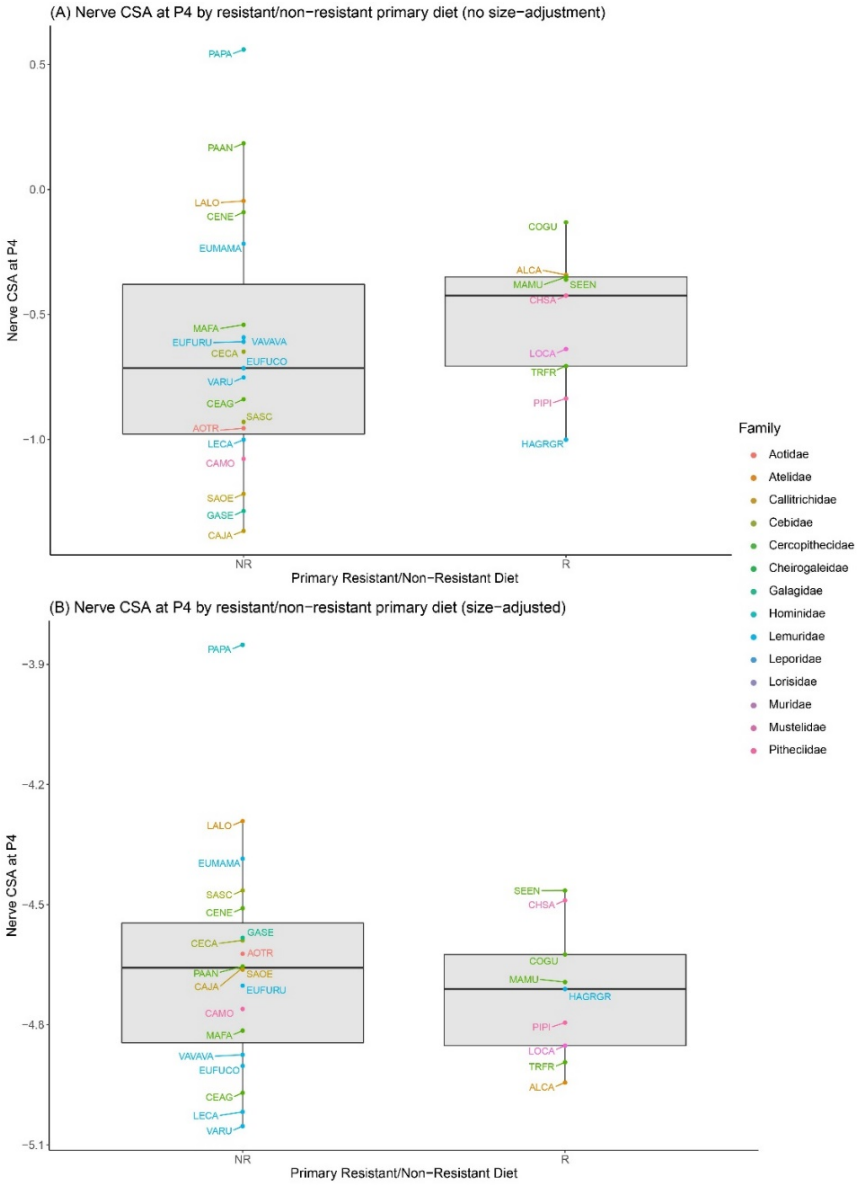

Figure 6.13A-B. The nerve CSA beneath P_4 by primary resistant vs. non-resistant diet in data that is not size-adjusted (A) and size-adjusted (B). These data are also power reduced and natural log transformed.

Figure 6.14 shows the secondary diet for the nerve CSA beneath P_4 data with no size adjustment (A) and with a size-adjustment (B). There were again no significant differences by feeding behavior in either the non-size adjusted data (Table 6.2; F-statistic = 1.392, p-value = 0.475) or the size-adjusted data (Table 6.3; F-statistic = 0.391, p-value = 0.912).

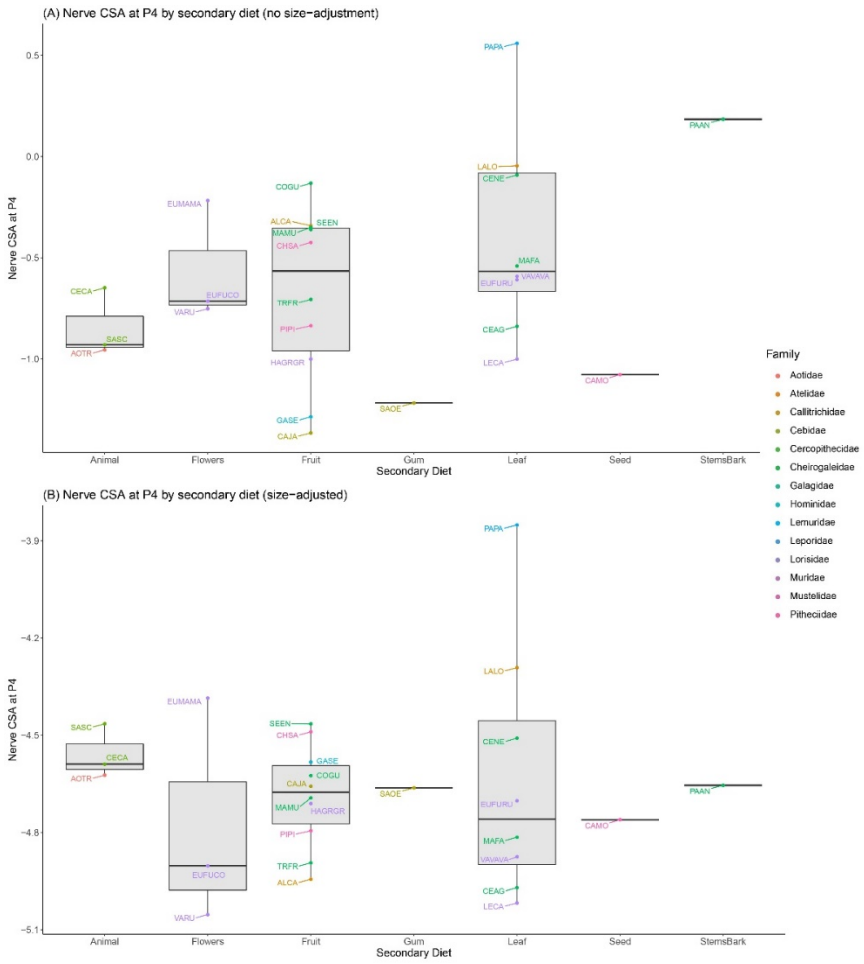

Figure 6.14A-B. The nerve CSA beneath P_4 by secondary diet in data that is not size-adjusted (A) and size-adjusted (B). These data are also power reduced and natural log transformed.

Figure 6.15 shows the secondary resistant vs. non-resistant diet for the data with no size adjustment (A) and with a size-adjustment (B) for nerve CSA beneath P_4. These results mirror the primary diet in that there are no significant differences in resistant vs. non-resistant feeding behaviors in relation to nerve size in either the non-size adjusted data (Table 6.4; F-statistic = 1.412, p-value = 0.336) or the size-adjusted data (Table 6.5; F-statistic = 0.084, p-value = 0.828).

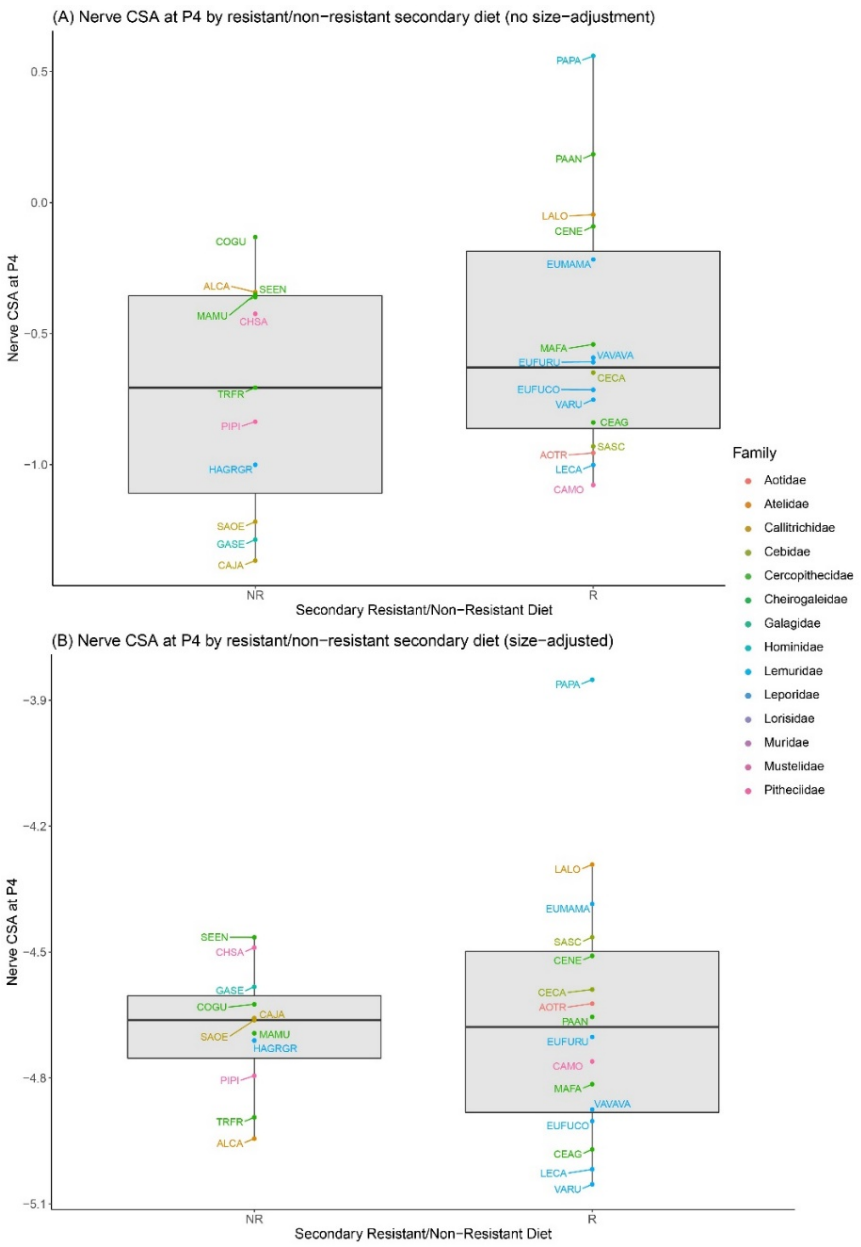

Figure 6.15A-B. The nerve CSA beneath P_4 by secondary resistant vs. non-resistant diet in data that is not size-adjusted (A) and size-adjusted (B). These data are also power reduced and natural log transformed.

Nerve CSA at the mental foramen. Figure 6.16 shows the primary diet for the nerve CSA at the mental foramen data with no size adjustment (A) and with a size-adjustment (B). The anterior aspect of the oral cavity showed similar results to what was seen in the posterior aspect of the tooth row in that there were no significant differences between feeding groups by

nerve size for the non-size adjusted data (Table 6.2; F-statistic = 0.554, p-value = 0.886) or size-adjusted data (Table 6.3; F-statistic = 1.712, p-value = 0.447).

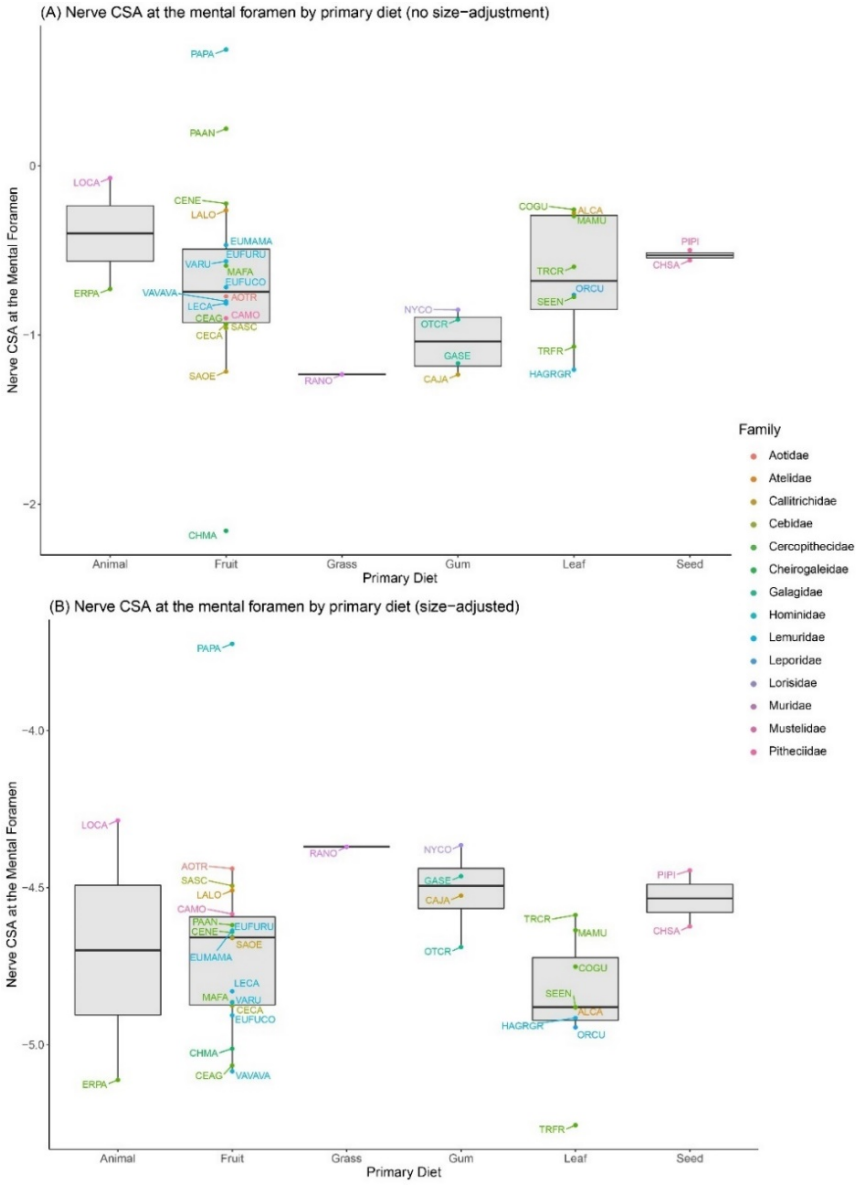

Figure 6.16A-B. The nerve CSA at the mental foramen by primary diet in data that is not size-adjusted (A) and size-adjusted (B). These data are also power reduced and natural log transformed.

Figure 6.17 shows the primary resistant vs. non-resistant diet for the data with no size adjustment (A) and with a size-adjustment (B) for nerve CSA at the mental foramen. There were again no significant differences between resistant and non-resistant primary feeders and nerve

size in the non-size adjusted data (Table 6.4; F-statistic = 0.317, p-value = 0.717) or the size-adjusted data (Table 6.5; F-statistic = 1.925, p-value = 0.369).

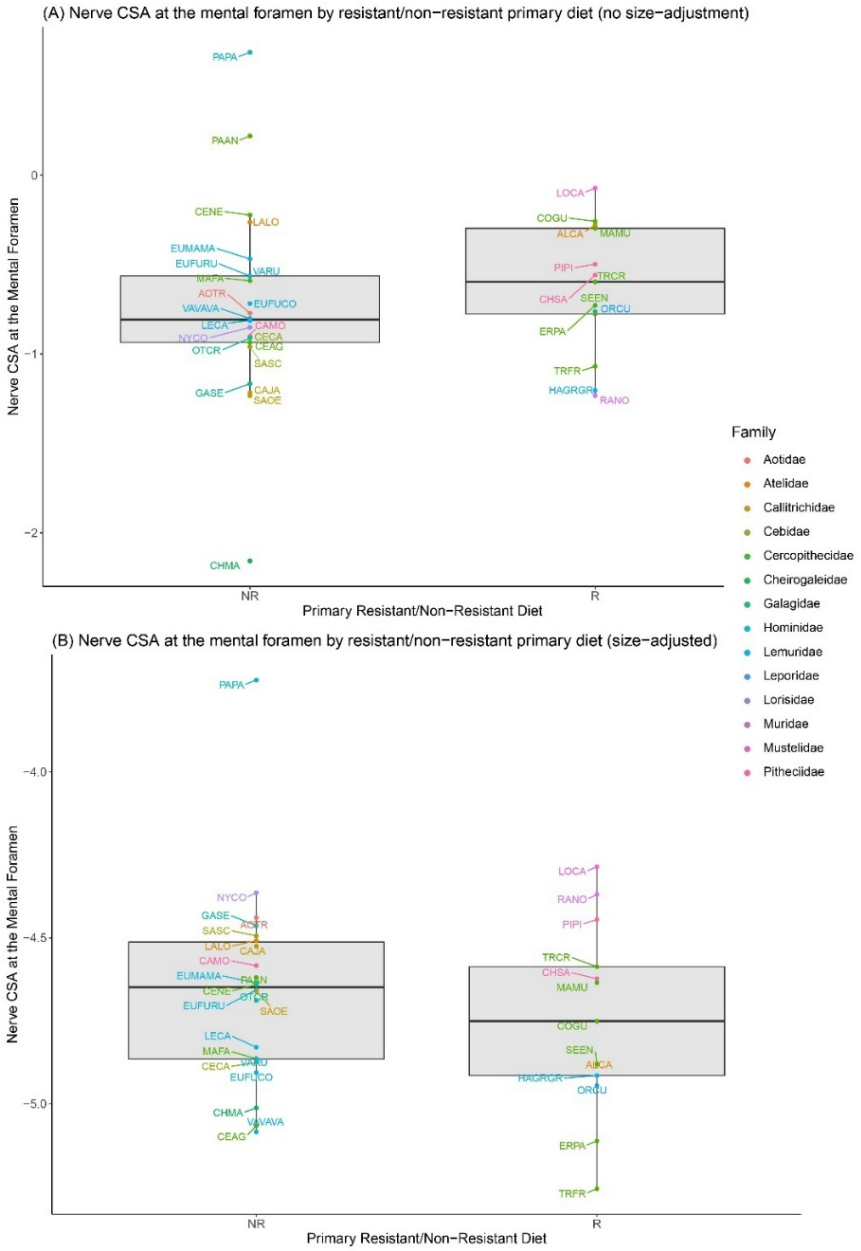

Figure 6.17A-B. The nerve CSA at the mental foramen by primary resistant vs. non-resistant diet in data that is not size-adjusted (A) and size-adjusted (B). These data are also power reduced and natural log transformed.

Figure 6.18 shows the secondary diet for the data with no size adjustment (A) and with a size-adjustment (B). There were again no significant differences in feeding behavior for

secondary diet at the mental foramen for either the non-size adjusted data (Table 6.2; F-statistic = 1.595, p-value = 0.379) or size-adjusted data (Table 6.3; F-statistic = 0.384, p-value = 0.960).

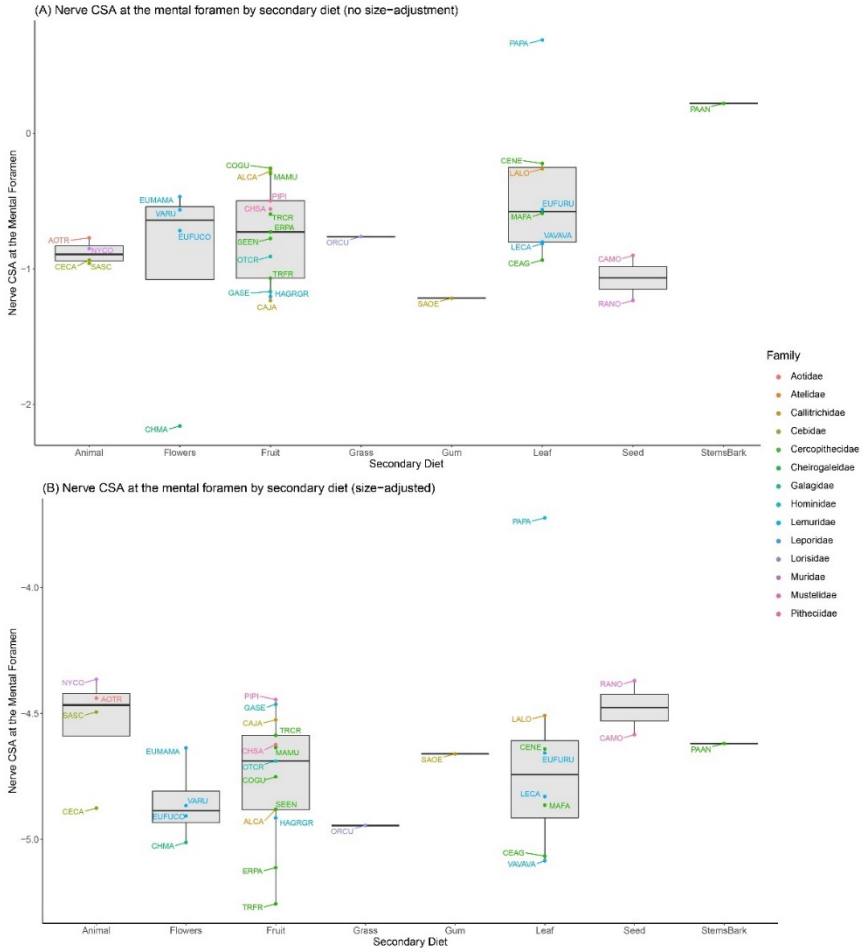

Figure 6.18A-B. The nerve CSA at the mental foramen by secondary diet in data that is not size-adjusted (A) and size-adjusted (B). These data are also power reduced and natural log transformed.

Figure 6.19 shows the secondary resistant vs. non-resistant diet for the data with no size adjustment (A) and with a size-adjustment (B). There were no significant differences in resistant vs. non-resistant feeding behavior and nerve CSA at the mental foramen for either the non-size adjusted data (Table 6.4; F-statistic = 0.506, p-value = 0.619) or the size-adjusted data (Table 6.5; F-statistic = 0.442, p-value = 0.627).

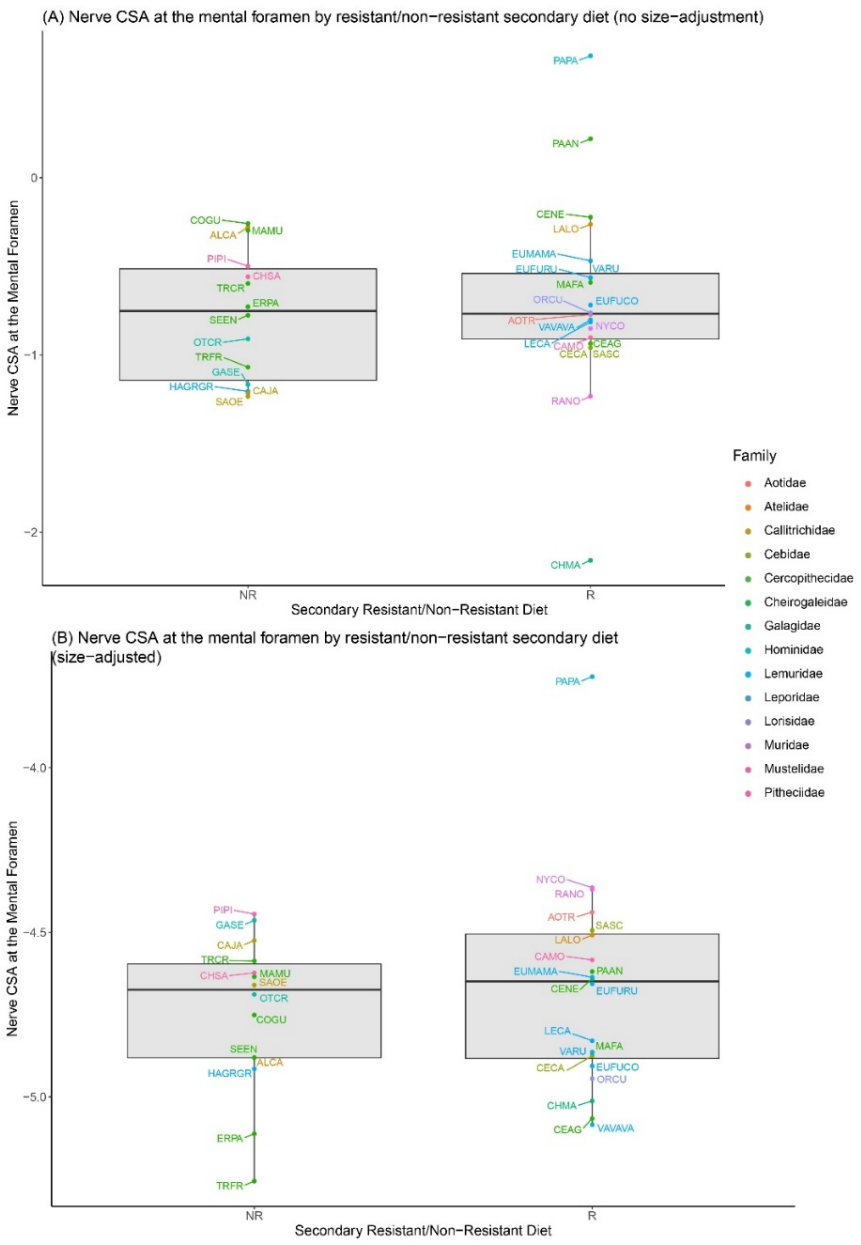

Figure 6.19A-B. The nerve CSA at the mental foramen by secondary resistant vs. non-resistant diet in data that is not size-adjusted (A) and size-adjusted (B). These data are also power reduced and natural log transformed.

Total IAN volume. Figure 6.20 shows the primary diet for the IAN volume data with no size adjustment (A) and with a size-adjustment (B). These results mirrored those seen in the cross-sectional area analyses in that there were no significant differences between primary feeding groups by IAN volume in the non-size-adjusted data (Table 6.2; F-statistic = 1.784, p-value = 0.445) or the size-adjusted data (Table 6.3; F-statistic = 0.451, p-value = 0.925).

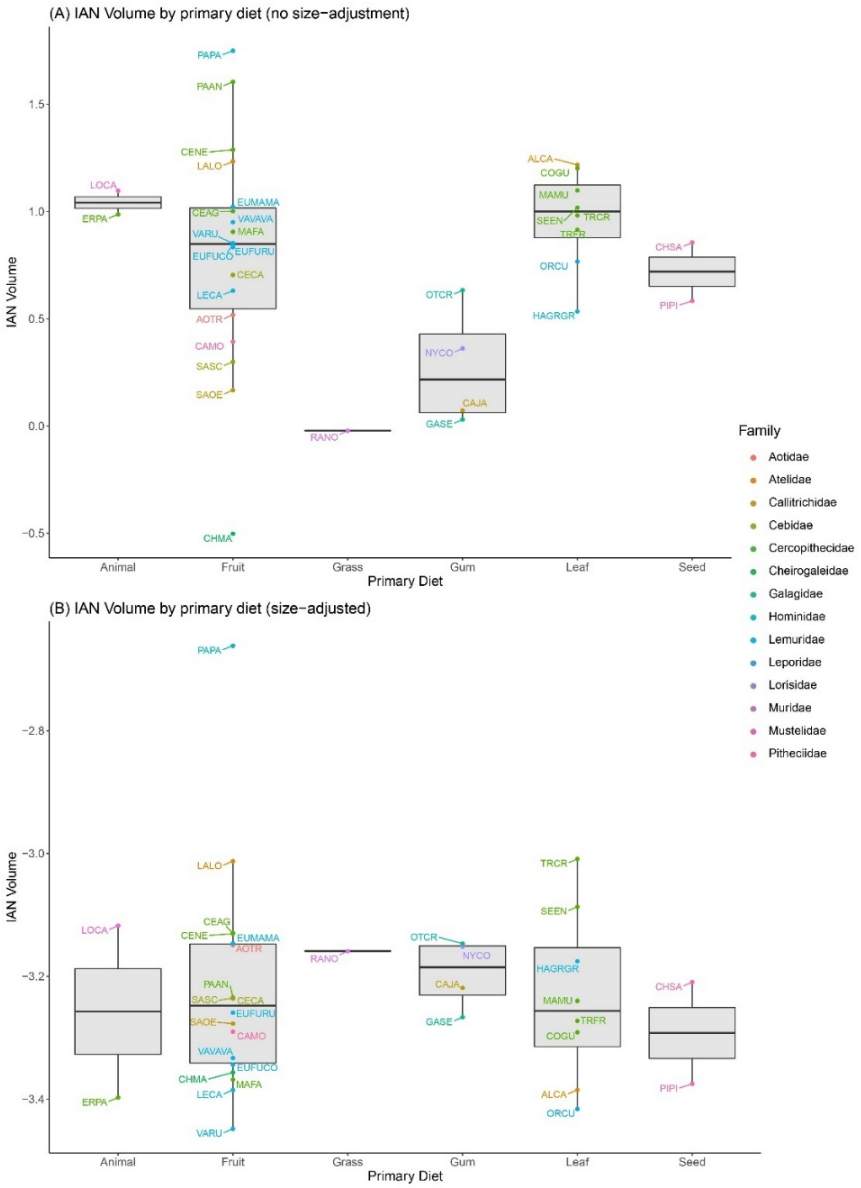

Figure 6.20A-B. The IAN volume by primary diet in data that is not size-adjusted (A) and size-adjusted (B). These data are also power reduced and natural log transformed.

Figure 6.21 shows the primary resistant vs. non-resistant diet for the data with no size adjustment (A) and with a size-adjustment (B) for IAN volume. These data again showed no significant differences between resistant and non-resistant primary feeding behaviors by IAN volume for the non-size adjusted data (Table 6.4; F-statistic = 1.719, p-value = 0.414) and the size-adjusted data (Table 6.5; F-statistic = 0.212, p-value = 0.777).

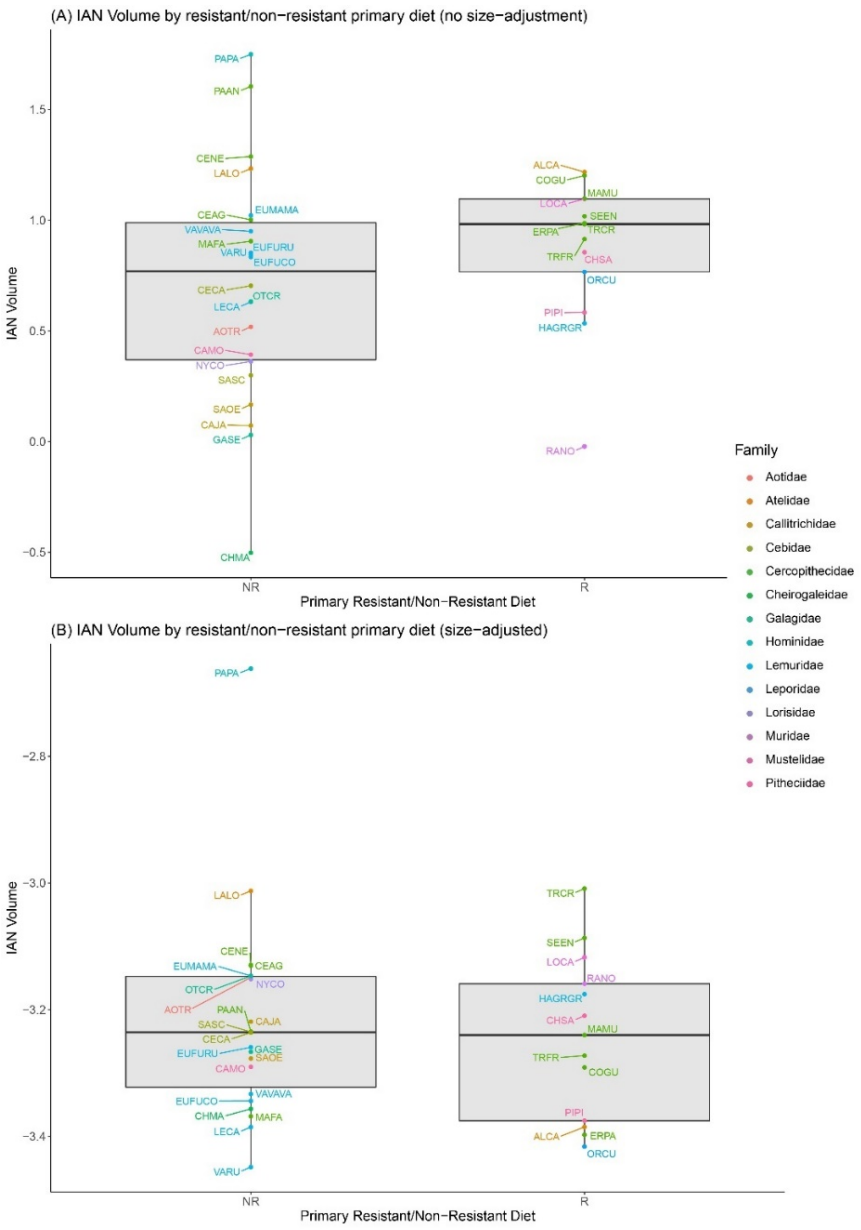

Figure 6.21A-B. The IAN volume by primary resistant vs. non-resistant diet in data that is not size-adjusted (A) and size-adjusted (B). These data are also power reduced and natural log transformed.

Figure 6.22 shows the secondary diet for the data with no size adjustment (A) and with a size-adjustment (B). Again, there were no significant differences in secondary feeding behaviors by IAN volume in either the non-size adjusted data (Table 6.2; F-statistic = 2.157, p-value = 0.215) or the size-adjusted data (Table 6.3; F-statistic = 0.608, p-value = 0.877).

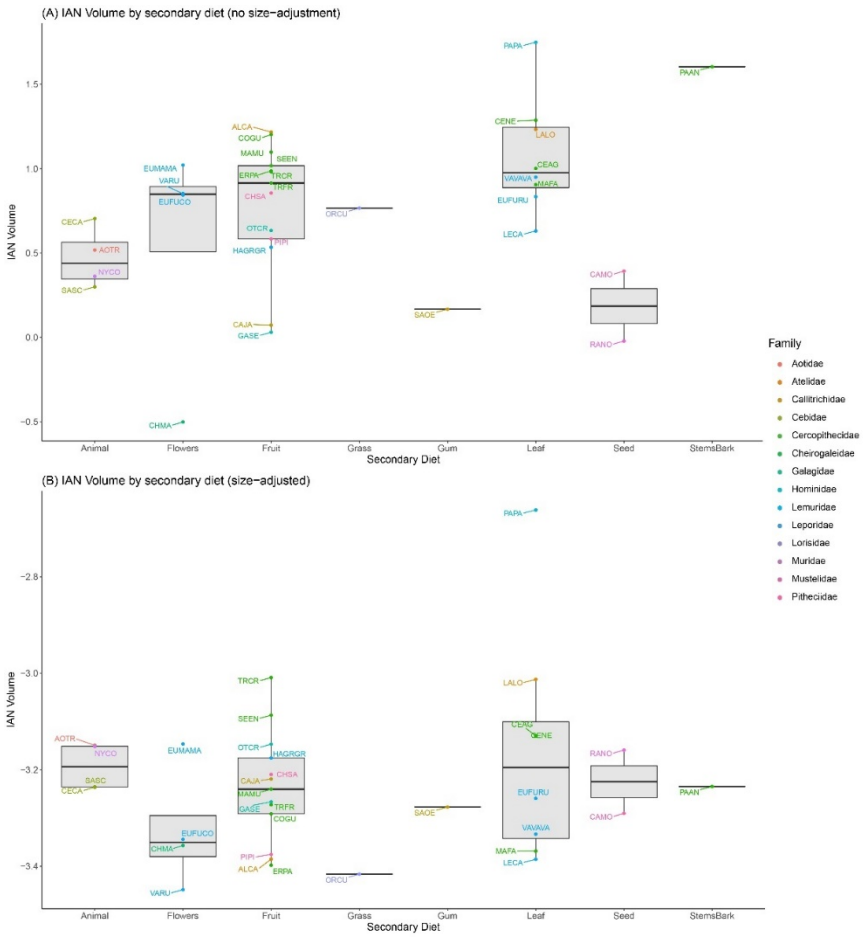

Figure 6.22A-B. The IAN volume by secondary diet in data that is not size-adjusted (A) and size-adjusted (B). These data are also power reduced and natural log transformed.

Figure 6.23 shows the secondary resistant vs. non-resistant diet for the data with no size adjustment (A) and with a size-adjustment (B). There were no significant differences in resistant vs. non-resistant feeding behavior by IAN volume in either the non-size adjusted data (Table 6.4; F-statistic = 0.230, p-value = 0.743) or the size-adjusted data (Table 6.5; F-statistic = 0.198, p-value = 0.762).

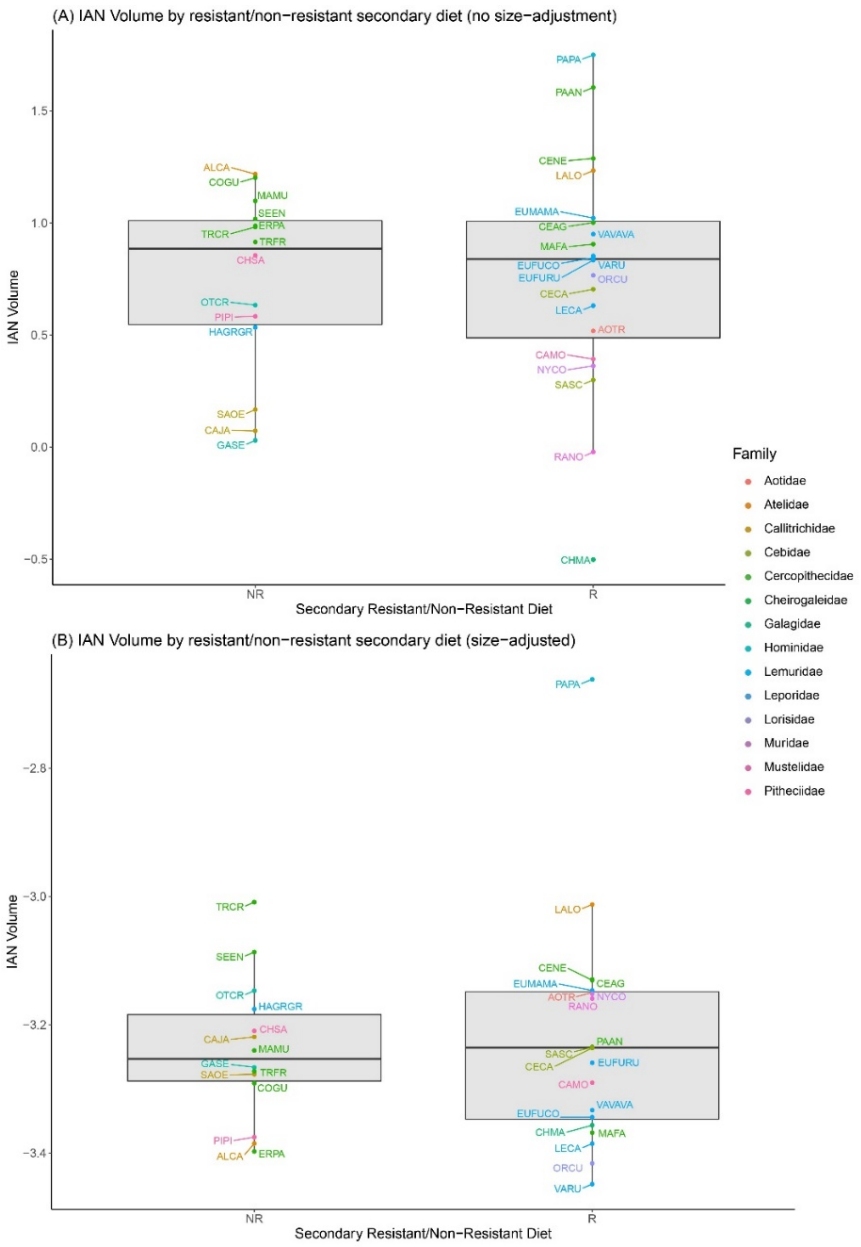

Figure 6.23A-B. The IAN volume by secondary resistant vs. non-resistant diet in data that is not size-adjusted (A) and size-adjusted (B). These data are also power reduced and natural log transformed.

Phylogenetic multiple regression analyses. To view the interactions between all food categories and to incorporate the raw percentage data collected, I ran a series of phylogenetic multiple regressions to establish the relationship between the IAN and diet. These multiple regressions show the impact that the independent variables have on the outcome of the value of the dependent variable in a given model. These analyses were only performed on data that was

power-reduced, size-adjusted, and natural log-transformed to assess the relative relationship between IAN and all dietary percentages. These results are seen in Table 6.6. There were no significant relationships seen in any overall analysis although two analyses – the nerve CSA at the mandibular foramen and beneath M_1 – had "seed" as a significant predictor within the models.

Table 6.6. Phylogenetic multiple regression results for the IAN and dietary percentages (size-adjusted data)

Dependent variable	Independent variable	p-value	R^2
Posterior Dentition			
Nerve CSA at mandibular foramen	All dietary percentages	0.037*	0.547
Nerve CSA at M_1	All dietary percentages	0.038*	0.545
Nerve CSA at P_4	All dietary percentages	0.496	0.339
Anterior Aspect of Oral Cavity			
Nerve CSA at mental foramen	All dietary percentages	0.667	0.244
Total IAN Volume			
IAN volume	All dietary percentages	0.416	0.325
All analyses used 18 degrees of freedom **Alpha values were set to p-value < 0.025** ***Indicates significant interaction within model**			

Because the phylogenetic multiple regression models showed seeds to be significant predictors within the models for nerve CSA at the mandibular foramen and beneath M_1, I removed the non-significant variables and re-ran each of these analyses (i.e., only seed was used as an independent variable). Both tests were significant (p-value ≤ 0.001) but had relatively low R^2 values (nerve CSA at mandibular foramen = 0.425; nerve CSA beneath M_1 = 0.368) indicating that seed eating explains very little variance within the model and therefore the relationship is not particularly close.

There were no significant relationships in the overall model or significant predictors within the models for nerve CSA beneath P_4 (p-value = 0.496), the nerve CSA at the mental foramen (p-value = 0.667), or the IAN volume (p-value = 0.416) (Table 6.6).

DISCUSSION

Brief Overview

The goal of this chapter was to examine if there were relationships between the size of the nervous tissues within the mandible and diet. Because previous research indicates that size and shape of the teeth and diet are significantly and tightly related to one another (e.g., Hiiemäe & Kay, 1973; Kay, 1975; Leighton, 1993; Lucas & Luke, 1980; Lucas, 1979, 2006; Lumsden & Osborn, 1977; Lund et al., 1998; Strait, 1997, 2001; Taylor, 2002), I expected to find that the nervous tissues were also significantly related to diet. This is because the nervous tissues of the mandible (and maxilla) send information to the brain to control chewing cycles and growth and development of the mandible – indicating that these tissues are incredibly important for maintenance of the mammalian tooth row.

My first hypothesis (Q3-H1) was that primates that used the posterior dentition for extensive processing (i.e., leaf or seed eating) would have higher concentrations of nervous tissues in the posterior aspect of the mandibular tooth row. This hypothesis was not supported in either the non-size adjusted or size-adjusted data. There were no clear distinctions between resistant food categories and nervous tissue size nor were there any significant differences seen in the phylogenetic ANOVAs or significant relationships seen in the phylogenetic multiple regressions.

My second hypothesis (Q3-H2) was that primates that used the anterior dentition for extensive food manipulation (i.e., fruit eating) would have higher concentrations of nervous tissues in the anterior aspect of the mandible. Like H1, this hypothesis was also not supported in either the non-size adjusted or size-adjusted data. There were again no clear distinctions between the non-resistant food categories and nervous tissue size nor were there any significant differences seen in the phylogenetic ANOVAs or significant relationships in the phylogenetic multiple regressions.

Finally, IAN volume was also not related to any dietary category (traditional categories and resistant/non-resistant) or to the dietary percentages. This mirrors the results seen from nervous tissues along the IAN within the mandible in that overall nervous tissue size has no direct relationship to the dietary capabilities of primates.

The analyses performed on data that was not size-adjusted show that the size of nervous structures is very closely related to mandible size – and likely body size by extension. This continues to support the data and analyses from Chapter 4 of this dissertation in that while the root surface areas and enamel surface areas are significantly and closely related, there are few relationships between the shape of the teeth and the nervous tissues that supply them. The phylogenetic ANOVAs and multiple regressions presented here show that nervous tissues also have no significant relationship to dietary capabilities – which we know are tightly related to the shape of the tooths surface (Kay, 1975; Lucas, 2006; Lund et al., 1998; Luschei & Goldberg, 2011; Teaford et al., 2006). Thus, the data here do not support the hypotheses presented but do continue to show that nervous tissues are not significantly related to their corresponding hard tissues when size is adjusted for.

Posterior Nervous Tissues and Diet

As shown in Table 6.2 and 6.3, there were no significant differences between the posterior nervous structures (nerve CSA at the mandibular foramen, nerve CSA at M_1, and nerve CSA at P_4) and standard dietary categories. There were also no significant differences between these nervous structures when primary and secondary diets were divided into resistant or non-resistant. This indicates that the size of the nervous structures in the posterior aspect of the mandible do not change in relation to the primary or secondary diet that a primate is consuming. As we have learned more about primate diets, it is understood and accepted that primate diets vary widely – even amongst individuals in the same species (Boonratana, 2003; Gautier-Hion et al., 1985; Julliot, 1996; Kay, 1975; Strait & Overdorff, 1996). The nervous

structures therefore would need to be capable of testing various foods for certain material properties.

All primary dietary categories with non-size adjusted data showed the same relationships across all posterior nervous tissues in that grass eaters (unfortunately only *Rattus norvegicus*) were consistently the smallest, followed by gum eaters. Fruit, leaf, and seed eaters clustered together at slightly higher values with all ranges overlapping. In both the nerve CSA beneath M_1 and nerve CSA at the mandibular foramen “animal” eaters clustered at the high end of the range while the nerve CSA beneath P_4 was on par with fruit, leaf and seed eaters and did not appear substantially larger. Primary dietary categories in the size-adjusted data showed less variation across these variables. All ranges overlapped in the nerve CSA beneath M_1, whereas most ranges overlapped at both the nerve CSA at the mandibular foramen and beneath P_4. In both, animal eaters and gum eaters did not overlap, although very few individuals represented these dietary categories within the sample.

When primary diets were divided into resistant vs. non-resistant categories, there were again some patterns in the posterior nervous data. There was far less variation in nervous size (in all three variables) when the primary diet was resistant, and the data had no size-adjustment. These data again clustered by mandible size, with smaller bodied primates having the smallest nervous tissues and larger primates have the largest tissues. When the data were size-adjusted, resistant primary feeders again show slightly less variation in nervous tissue size, but the ranges again substantially overlap.

For secondary dietary categories, similar patterns were seen in the posterior nervous tissues when there was no size adjustment to the data. Seed and gum eaters showed the smallest nervous tissues, followed by animal eaters. Flower eaters had the largest range in terms of nerve size, but overlapped with fruit, grass, and leaf eaters. Stems and bark eaters were at the highest end of the values but overlapped with the range for leaf eating. Again, when

the data was size adjusted, there were very few differences in the ranges across dietary categories.

Secondary resistant/non-resistant diets showed the opposite results to the primary diets in the non-size adjusted data in that the resistant secondary feeders showed a larger range in nerve size. When the data were size adjusted, there were no significant differences between the two groups nor were there substantial differences in the ranges.

Although the overall phylogenetic multiple regression models were not significant, seed eating was shown to be a significant predictor in the nerve CSA at the mandibular foramen and beneath M_1. However, this was not a close relationship, as shown by the relatively small R^2 values. However, these analyses do show there is a significant relationship to consuming seeds in some capacity within a diet and the most posterior aspect of the mandibular tooth row. Seed eating ranged between 0.25% in *Colobus guereza* to 66.2% in *Chiropotes satanas* as a component of diet. Out of 35 species, 15 species ate seeds in some capacity although most species used seeds as less than 10% of their overall diet. Seeds are one of the hardest substances consumed by primates, indicating that the size of the posterior nervous tissues (where most food processing is done) would need to be large enough to send fast signals to the brain to preserve the tooth row (Nuwer & Pouratian, 2017). However, these results should be assessed further as no other tough/stiff food (i.e., leaves, animal, etc.) showed significant relationships to the nervous tissues indicating the relationship with seeds may not be entirely influenced by the food material properties.

These data do not support Q3-H1 in that there are no clear distinctions between the posterior nervous tissues when the raw data is assessed nor are there any significant relationships between the overall dietary categories or the percentage of certain foods eaten. This indicates that the amount of nervous tissue needed to test various foods is much more closely related to mandible size rather than dietary capabilities.

Anterior Nervous Tissues and Diet

The results from both the phylogenetic ANOVA analyses and the phylogenetic multiple regression analyses show no relationships with the anterior nervous tissue to traditional dietary categories, resistant/non-resistant food groups or the percentage data of specific foods consumed. This indicates that the anterior nervous tissues (the IAN as it enters the mental foramen) is not related to the diet consumed by primates. This is supported in the literature that discusses the mental foramen in that there is no connection between the size, location, or presence/absence of foramina and the diet a primate consumes (Agarwal & Gupta, 2011; Amorim et al., 2008; Moore et al., 1968; Muchlinski, 2008; Muchlinski & Dean, 2016; Voljevica et al., 2015; Yesilyurt et al., 2008). The nervous tissues mirroring these results lends further support for the argument that the mental foramen and the IAN at the mental foramen should not be used to estimate diet in extinct species (Muchlinski & Deane, 2016).

The primary dietary categories for variables with no size adjustment show similar relationships to those seen in the posterior nervous tissues in that they appear to cluster by body size. Grass eaters are smallest, followed by gum eaters although they overlap in range with both leaf and fruit eaters. Animal and seed eaters show the largest nervous tissues although they again overlap in range with leaf and fruit eaters. When these same data are size adjusted, all ranges overlap (except grass and leaf eaters) and there are no significant differences between categories. When the primary diet data is broken down by resistant/non-resistant, there is no visual or significant differences between the size of the nervous tissue and dietary groups in both non-size adjusted and size adjusted data.

The secondary dietary categories for variables with no size adjustment showed that gum eaters again had the smallest nervous tissues, but overlapped with flower, fruit, and seed eaters. These data again appeared to cluster much more by mandible size rather than differences in nervous tissues based on primary diet. When these data were size adjusted, animal and seed eaters clustered at the highest end of the values, although other resistant

groups such as leaves, grass, and flowers had the lowest values in their ranges. These data show that secondary diet does not influence the size of the nervous tissues nor are there significant relationships to the nervous tissues due to dietary category. The secondary resistant/non-resistant ranges showed very similar results to the primary data in that there was substantial overlap in range and no significant differences by group in either the non-size adjusted or size-adjusted data.

These data do not support Q3-H2 in that primates that use the anterior dentition for extensive processing of fruit (e.g., peeling fruit skins away from pulp) do not have more nervous tissue concentrated in and around the anterior dentition. There are no relationships with the anterior IAN and the dietary categories, the resistance of food, or the dietary percentages. This indicates that the size of the anterior IAN cannot be predicted by the foods a primate is consuming.

IAN Volume

The results from both the phylogenetic ANOVA analyses and the phylogenetic multiple regression analyses showed no relationships between the IAN volume and traditional dietary categories, resistant/non-resistant food groups, or the percentage data of specific foods consumed. This again shows that there is no relationship between the amount of nervous tissue a primate has and the diet that it consumes.

The primary dietary categories for the data with no size adjustment again appeared to cluster by body size. Grass eaters (*Rattus norvegicus*) show the smallest nervous tissues, followed by gum eaters. However, gum eaters overlapped with both fruit, leaf, and seed eaters – indicating there are no clear differences between diet and nervous tissue size. The size-adjusted variables showed even fewer differences with all dietary ranges overlapping except for grass and seed eaters. For primary resistant/non-resistant diets in the non-size adjusted data, the non-resistant eaters showed a much larger range in nervous tissue volume in relation to

resistant eaters. However, when the data were size adjusted there was very little differences in the ranges and no significant differences in the means.

Finally, IAN volume showed very similar relationships to both the posterior and anterior nervous tissues in secondary diets with no size adjustment to the data. Gum, seed, and flower eaters showed the smallest volumes while animal, fruit, grass, leaf, and stems and bark eaters had the largest values. However, there is substantial overlap in the ranges and no significant differences in the means. The variation is reduced when there is a size adjustment to the data with grass showing the smallest values and all other dietary groups overlapping in range. Secondary resistant/non-resistant diet showed that the range for resistant feeders was larger in non-size adjusted data but very similar when the data was size adjusted.

Throughout all nervous tissues, *Pan paniscus* was the consistent outlier and always had the largest values for nervous tissues in both the actual and relative data. This potentially indicates that Hominidae has more nervous tissue than expected in the mandible than all other primate groups and thus greater touch sensitivity along the mandibular tooth row. However, only one specimen represents this species (and all of Hominidae for soft-tissue variables by extension) indicating that this needs further testing before strong conclusions can be drawn.

CONCLUSION

Overall, there were three main conclusions drawn from the data here:

1. Nerve size is much more closely related to mandible size (and likely overall body size) than it is to dietary capabilities.
2. Primates that perform extensive oral processing with their posterior dentition do not have more nervous structures in the posterior aspect of the oral cavity.
3. Primates that perform extensive oral manipulation with their anterior dentition and lower face do not have more nervous structures in the anterior aspect of the oral cavity.

In sum, there are no clear relationships between the size of the nervous tissues and the dietary capabilities of primates. In general, nervous size appears to be much more closely related to mandible size (also shown in chapter 5) and not related to the shape of the tooth and by proxy the dietary capabilities of that tooth (also shown in chapter 4). This indicates that the size of nervous tissues is not directly related to dietary capabilities and thus cannot be used to establish diet in primates.

CHAPTER 7: DISCUSSION AND CONCLUSIONS

INTRODUCTION

This dissertation examined how the inferior alveolar nerve (IAN) relates to 1) the size of surrounding bones, and 2) the diet of primates (in both dietary observational data and the shape of the tooth surface). Chapter 4 established that the IAN is related to the size of the root and enamel surfaces, but not necessarily to the shape of the teeth. Chapter 5 established that the IAN is related to the size of the mandibular canal but does not equal the canal in size. Finally, Chapter 6 established that there are no relationships between the size of the IAN and diet in primates. The purpose of this final chapter is to discuss the main results seen in the data and how this compares to other studies on similar topics.

THE RELATIONSHIP BETWEEN THE IAN AND ITS BONY CORRELATES

The IAN and Its Relationship to Tooth Size

Previous work suggests that bony structures and their surrounding soft tissues will share a strong relationship due to both the proximity of the structures and their shared function(s) (i.e., the form function relationship). For example, it is known that there are close relationships between the size of the muscles of mastication, the size of certain aspects of the mandible, and the development of craniofacial morphology (e.g., Hylander, 1975b, 1985; Kiliaridis, 1995; Kiliaridis et al., 1985; Lycett & Collard, 2005; Proffit et al., 1983; Sella-Tunis et al., 2018; Vinyard, 2008; Vinyard et al., 2011). The plasticity of bones and their ability to adapt to repeated mechanical loading over time (Wolff's Law or bone functional adaptation; Wolff, 1892) has led many researchers to believe that while hard tissues are formed initially in a specific shape, they may change over time in response to soft tissue stimulation (e.g., Cowin, 2001; Lanyon & Skerry, 2001; Ruff et al., 2006). While it has been established that an increase or decrease in muscle strain can lead to more deposition or resorption (respectively) of bone tissue, few studies have assessed the variation seen in the effects of nervous stimulation on the

surrounding bony structures in species other than humans. However, it is known that in human individuals that are edentulous, bone resorption has been noted as a result of lack of stimulation via chewing due to tooth loss (Bradley, 1975; Charalampakis et al., 2017; Edwards & Gaughran, 1971; Gabriel, 1958; Gershenson et al., 1986; Iwanaga et al., 2019; Polland et al., 2001; Wadu et al., 1997). This suggests that the presence or absence of stimulation via nervous tissues could affect bone deposition and resorption in similar ways to muscles. Thus, it is imperative to understand if soft tissues other than muscles – particularly nervous tissues that supply somatic sensation – have a relationship to their surrounding bony structures.

The occlusal surface and roots of teeth have been studied extensively as separate parts of the masticatory apparatus but are rarely discussed as a single system in the literature (e.g., Deines et al., 1993; Fortelius, 1985; Fortelius & Solounias, 2000; Janis, 1990; Kay, 1975; Lucas, 2006; Lund et al., 1998; Spencer, 2003; Teaford et al., 2006; Ungar, 2015). However, some studies have shown that the roots of the teeth are directly related to the occlusal surface either due to overall body size or because of the material properties of the diet that a primate species is adapted to eat (Deines et al., 1993; Spencer, 2003). Because of this, I hypothesized that there would be direct and positive relationships between the roots and occlusal surfaces of I_1, C_1, P_4, and M_1 in the primate mandibular tooth row. Additionally, and because of their close relationship to the IAN, I expected these roots and occlusal surfaces to have a direct and positive relationship to the nervous structures that supply each of these teeth. My findings suggest that while the roots and occlusal surfaces of these teeth have a significant and positive relationship, there are few significant relationships between the nervous structures of the mandible and the teeth they innervate.

It is generally agreed upon that teeth are responsible for the majority of pain sensation (Anderson et al., 1970; Avery & Cox, 1977; Brashear, 1936; Dubner et al., 1978; Luschei & Goldberg, 2011; Plaffman, 1939), while the periodontal membrane is responsible for the majority of pressure sensation (Byers & Dong, 1989; Crompton, 1995; Falin, 1958; Inoue et al.,

1989; Linden, 1991; Ross et al., 2010) although both can transmit each type of information. Studies have shown that in teeth with finite growth, the anterior dentition have more nerve endings than the posterior dentition, while the periodontal membrane has more innervating structures surrounding the posterior dentition (Byers & Dong, 1989; Cash & Linden, 1980; Kubota & Osanai, 1977; Lewinsky & Steward, 1937; Hassanali, 1997; Maeda, 1987). This may suggest that the anterior teeth are more responsible for food acquisition and the initial determination of food material properties (Jacobs et al., 2007; Lucas, 2006; Lucas et al., 2012; Highlander, 2006; Murphy, 1968; Trulsson, 2006; Trulsson & Johansson, 1996; Ungar, 1998, 2002) while the posterior teeth are more invovled in the maintenance of the chewing cycle (Byers & Dong, 1989; Crompton, 1995; Falin, 1958; Inoue et al., 1989; Linden, 1991; Ross et al., 2010).

There is very little research on tooth-root to enamel surface relationships, but Kovaks (1979) explains the three basic strain relationships between the roots and enamel surfaces: 1) force is transmitted when the surfaces are equal, 2) force is distributed when the roots are larger than the enamel surface, and 3) force is concentrated on the root when it is smaller than the enamel surface (although he notes that this relationship is typically only seen in pathological individuals). Further, it has been concluded that a tooth's ability to resist a force is directly related to the surface area of the tooth root (Kovacs, 1979; Spencer, 2003). The results in this dissertation indicate that incisor and canine root/enamel surfaces may have evolved to transmit large forces down to the tooth roots due to their isometric relationships while the positive allometry in the post-canine teeth may have evolved to distribute large forces across the post-canine teeth.

The anterior teeth are responsible for the initial assessment of food material properties, peeling tough-skinned fruits, and utilizing large bite force to incise food objects. Incisor size is known to increase with tough skinned fruit eating (Hylander, 1975a), such as in *Pan* or *Papio*, but incisors size remains relatively small in species that prioritize eating foods that do not

require incisal preparation. An increase in enamel surface area implies an increase in the tooth root surface area to either withstand or dissipate larger forces applied to the anterior teeth. Hogg et al. (2011) tested this hypothesis and were able to show that as the enamel surface area of *Callithrix* gets larger, the roots also increase in size, likely to account for the increased forces on these teeth as *Callithrix* utilizes tree gouging for exudates as a large percentage of their diet. Although the data presented here show overall isometry in the relationship between the roots and the enamel surface of the incisors, the raw data shows that root surface areas are typically slightly – but not significantly – larger than the enamel surface areas. However, in these analyses, Galagidae show enamel surface areas that are larger overall than the root surface areas. These data would indicate that this family does not use their anterior teeth for specialized feeding, yet the two Galagidae species in this sample (*Otolemur crassicaudatus* and *Galago senegalensis*) primarily feed on exudates by using their lower dentition to gouge or scrape trees (Bearder & Martin, 1980; Burrows & Smith, 2004). This data disagrees with the literature in that, if primates are using their anterior teeth extensively for larger bite forces, the roots should be larger to withstand these forces.

Canines also showed isometric relationships between the roots and enamel surfaces, again indicating that as the enamel surface increases, the roots must also increase at a proportional rate. In this dataset, root surface areas were always slightly – but not significantly – larger than the enamel surfaces. Families like Pitheciidae and Atelidae that are known for utilizing puncture crushing as a dietary specialization did show overall larger canine root to enamel surface area although they were not significantly different from other families. The ranges for these root sizes overlapped with Cebidae, Cercopithecidae, Hominidae, and Lemuridae – families that have a wide range of dietary capabilities (Kinzey & Norconk, 1993; Kinzey, 1992; Mittermeier & van Roosmalen, 1981; Spencer, 2003). However, as with the incisors, the data collected here show that these relationships are isometric, and the roots of the canines are not larger in relation to the enamel surface area and are thus not selected to

dissipate large bite forces along the tooth row. There is evidence that large forces generated in the anterior teeth transmit forces into the mandible itself, with species that do this often-showing increased size of the mandibular symphysis to accommodate these behaviors (Hylander, 1985; Scott & Hogue, 2012).

The post-canine teeth are responsible for the majority of mastication and would thus have sustained forces applied regularly, regardless of diet (Deines et al., 1993; Spencer, 2003). Additionally, teeth wear down throughout the life of an individual through repeated use – particularly in the post-canine teeth – which will change the overall size of the tooths surface over time (Fortelius, 1985; Janis, 1990; Ungar, 2015). In this sample, the premolars showed average root surface area sizes that were slightly larger overall than the enamel surface areas and analyses showed a positively allometric relationship. This supports what is known in the literature in that the post-canine teeth are most involved in sustained forces that are dissipated along the tooth row during normal mastication, indicating that the post-canine roots need to be larger than their corresponding enamel surfaces (Kovaks, 1979; Spencer, 2003). However, while the molars also showed positive allometry throughout this sample, two families – Cheirogaleidae and Galagidae – showed roots that were substantially smaller than their enamel surface areas. The species represented by these two families in this sample both specialize in exudate feeding or soft fruit eating and would thus not be generating large forces along the post-canine teeth during mastication.

In the allometric analyses for IAN to root and enamel surfaces, there was a general trend of either isometry or negative allometry. This indicates that the IAN is increasing at the same or a slightly slower rate than the surfaces (both root and enamel) of the teeth. This trend is seen in other nervous tissues as evidenced by Rilling (2006) who argues that brain size scales with negative allometry in relation to body size. This indication – that nerve size does not increase at a proportional rate with body size – is shown to an extreme in these data with male canines. Male IAN size was significantly negatively allometric in relation to both the enamel and root

surfaces. This could indicate less sensitivity in male canines, a useful trait if canines are being used as weapons with large forces being applied irregularly (Cash & Linden, 1980; Pickford, 1986; Plavcan, 1993). Spencer (1999) argues that overall mammals have adapted to have more specialized anterior dentition for intensive force production at the incisors and canines (rather than the post-canine teeth) because this would favor safety during diverse and dynamic loading to decrease the chance of joint distraction. Altogether this shows that male canines, while able to generate large forces, are not necessarily more sensitive than other teeth and that they have overall less nervous tissues in relation to the root/enamel surfaces.

In the size-adjusted data, there were no significant relationships between the nervous tissue variables and either the enamel surface area or the root surface area. This was particularly surprising for the root surface area because the roots are very closely associated with the periodontal membrane (the periodontal ligament, gingiva, and periosteum) which is supplied with nervous sensation via the IAN (Anderson et al., 1970; Avery & Cox, 1977; Beertsen et al., 2000; Brashear, 1936; Byers & Dong, 1989; Cromption, 1995; Falin, 1958; Fearnhead, 1967; Hannam, 1976, 1982; Inoue et al., 1989; Linden, 1991; Plaffman, 1939; Ross et al., 2010). More attachment sites for the periodontal membrane would allow these teeth to resist masticatory stress more efficiently, particularly when the roots are larger than the enamel surfaces (Kovaks, 1979; Lucas, 2012). Additionally, many authors have argued that the periodontal tissues are responsible for the tactile perception of pressure and may be an important factor in the protection mechanism of occlusion (Adler, 1949; Gordon, 1979; Kennett & Linden, 1987; Kubota & Osanai, 1977; Loewenstein & Rathkamp, 1955; Plaffman, 1939). However, the results here show that there are no relationships between the roots and nervous tissues at any cross-sectional point along the IAN, indicating that the amount of nervous tissues directly supplying the teeth is not related to the relative size of teeth. Additionally – and because of the known relationship between the root surface and enamel surface areas – it is unsurprising that there were also no relationships between the enamel surface and the IAN. While the

enamel surface does not contain nerve endings, the forces (and particularly pain sensation) generated on the enamel surface are sensed by the tooth pulp, which does contain nerve endings.

Overall, these results mirror what has been seen in previous studies in that nerve size tends to increase with body size in either an isometric or negatively allometric pattern (Rilling, 2006; Lietch et al., 2014). The results shown here in terms of root to enamel ratio support what is known in the literature in that, while the anterior teeth are more likely to generate large forces, these forces do not dissipate along the tooth row and are more often transmitted to the mandibular bone (Jacobs et al., 2007; Lucas, 2006; Lucas et al., 2012; Highlander, 2006; Murphy, 1968; Trulsson, 2006; Trulsson & Johansson, 1996; Ungar, 1998, 2002). Additionally, the post-canine teeth continue to show that dissipation of forces is much more likely during mastication, thus supporting what is known in the somatic sensation literature in that the post-canine teeth work together as a unit to continually assess food material properties (Edin & Trulsson, 1992; Hannah, 1982; Johnsen & Trulsson, 2003; Linden, 1991; Matthews, 1977; Trulsson et al., 1992).

The Path of the IAN Through the Mandible

Chapter 5 demonstrated that there while there are significant and positive relationships between the IAN and the mandibular canal, the IAN does not take up most of the canal space nor is there a true canal (i.e., a tube that is surrounded by bone from mandibular to mental foramina) in 75% of specimens assessed here. Although there is a body of literature on the mental (e.g., Agarwal & Gupta, 2011; Amorim et al., 2008; Anderson et al., 1991; Charalampakis et al., 2017; Salah El-Beheri, 1985; Williams & Krovitz, 2004) and mandibular foramina (e.g., Ashkenazi et al., 2011; Feuerstein et al., 2019; Hayward et al., 1977; Nicholson, 1985; Prado et al., 2010; Thangavelu et al., 2012) separately, no study has addressed the variation seen in size comparisons of these two openings. Many specimens within Cercopithecidae, Cebidae, Galagidae, Hominidae, Indriidae, Lemuridae, Leporidae, Lorisidae,

and Pitheciidae showed mental foramina that were larger than their mandibular foramen counterpart. These results indicate that further study is needed to determine how much variation exists in the size of the mental and mandibular foramina and if larger mental foramina are more prevalent within particular primate species and/or families.

One important caveat of this study is the potential for the soft tissues being analyzed to shrink during iodine staining. Shrinkage is a known factor is both preservation studies and iodine staining studies (Gignac et al., 2016; Hedrick et al., 2018; Li et al., 2016; Vickerton et al., 2013). Many of the specimens used here came from collections that likely used alcohol-based preservatives, which can lead to volume loss due to dehydration. Additionally, diceCT staining has been shown to affect brain tissues by shrinking 6-38%, typically dependent on how fresh the specimen is and if the specimen is isolated soft tissue (Fox et al., 1985; Hedrick et al., 2018). If shrinkage occurred in the specimens here, this could affect the size of the nerve at the corresponding canal. However, these shrinkage rates are not consistent across all specimens and are less likely to effect specimens that are whole or partial body specimens (Fox et al., 1985). All of this indicates that even if these specimens shrunk during fixation and/or staining, the IAN would continue to occupy < 60% of the mandibular canal space and thus would continue to show that the canal or its foramina are not viable proxies for nerve size.

The nerve CSA at the mandibular foramen to CSA of the mandibular foramen ratio showed the most consistent percentages across the sample with substantial overlap between most ranges, with no significant differences shown between family groups in the phylANOVA. This indicates within this sample of primates, there are very similar amounts of nervous tissues exiting the mandible to take information to the brain. No other study has addressed the amount of nervous tissues exiting the mandibular foramen and thus it is unknown how these results in primates compare to other clades. This is in opposition to the nerve CSA at the mental foramen to the mental foramen CSA in that while there was some overlap between families (Aotidae, Atelidae, Callitrichidae, Cebidae, Cercopithecidae, Cheirogaleidae, Galagidae, Lemuridae,

Leporidae, Lorisidae, and Mustelidae), others were outliers within the data (Hominidae and Muridae). This indicates that these two species - *Pan paniscus* and *Rattus norvegicus* - have more nervous tissue entering the mandible at the mental foramen to innervate the lower tooth row.

While primate nerve size at the mental foramen has not been explored in the literature, there are some analyses performed on the nerve size of *Rattus norvegicus* that could shed light on rats having relatively large amounts of nervous tissues entering the mandible at the mental foramen. Rats have been shown to have a relatively mature trigeminal sensory nucleus development (a portion of the trigeminal CNS) at birth and similar amounts of nervous tissues in relation to metatherians and monotremes (Ashwell, 2015) – two groups that are considered much more altricial at birth. Ashwell (2015) hoped to establish that rats, due to their vibrissae and precocial development, would have larger nervous tissues or more advanced trigeminal systems at birth in relation to the other mammalian groups but ultimately concluded that there were very similar amounts of nervous tissues across all three groups surveyed. This dissertation shows that rats – relative to body size – have some of the largest nervous tissues, potentially due to their vibrissae and extensive snouts. However, all non-human primates have snouts with whiskers or small vibrissae, which should indicate some level of somatosensation along the top and side lip. The data presented here show that primates have very similar relative amounts of nerves to each other along the bottom lip. The large increase in rat nervous tissues entering the mental foramen could mean more somatosensation in rodents along the lower lip – potentially due to locomotion or foraging strategies – that primates lack.

The nerve CSA beneath M_1 to canal CSA beneath M_1 ratio was again much more constrained across primates. Only Muridae (*Rattus norvegicus*) was a substantial outlier, although their ratio ranges overlapped slightly with the higher end of Atelidae. Atelidae, Cebidae, and Cercopithecidae showed higher ratios than those seen in Galagidae, Lemuridae, Lorisidae, and Pitheciidae. This was mirrored in the results for the nerve CSA beneath P_4 to the

canal CSA beneath P_4 ratio. This indicates that primates in Atelidae, Cebidae, and Cercopithecidae have larger amounts of nervous tissues feeding these post-canine teeth while the strepsirrhines and Pitheciidae have less nervous tissues within the canal. This is interesting because Pitheciidae, Cebidae, and Atelidae (particularly some species in *Chiropotes*, *Cebus,* and *Ateles*) are specialized seed eaters that utilize puncture crushing – with high magnitude canine bite-force production (Spencer, 2003). Many species from these families use their anterior teeth to peel fruit from seeds, consume the fruit, crush the seed with the canine teeth, and then continue to masticate the seeds on the post-canine dentition (Kinzey & Norconk, 1993; Kinzey, 1992; Mittermeier & van Roosmalen, 1981; Spencer, 2003). Phylogenetically, Cebidae and Atelidae are more closely related to each other, but both are closer to Pitheciidae than Cercopithecidae. Thus, these results indicate that the amount of nervous tissues a primate has is not dependent on dietary composition or phylogeny.

There was significant variation seen in the sample and in many cases there were few individuals representing entire species or families, therefore these conclusions on phylogenetic signals should be assessed with caution. For example, *Alouatta caraya* (n = 2) and *Lagothrix lagotricha* (n = 1) are the only two species that represented Atelidae. Within this family, *Lagothrix* had a nerve volume of 37.05 mm^3, while *Alouatta* had nerve volumes of 31.86 mm^3 and 46.35 mm^3 (both male specimens). *Lagothrix* is slightly larger in body size than *Alouatta* on average but has relatively similar nervous tissue volumes. Cebidae was represented by 38 individuals from two species (*Cebus capucinus* and *Saimiri sciureus*) with nervous volumes that ranged from 1.34 – 3.56 mm^3 (*Saimiri sciureus*) to 6.88 - 9.08 mm^3 (*Cebus capucinus*). Although *Cebus* has higher volumes of nervous tissues than *Saimiri* in the raw data, when body size is accounted for, they have near identical volumes of nervous tissue. Finally, Pithiciidae was represented by three species that had a wide range of nervous volumes: 2.80 – 3.62 mm^3 (*Callicebus moloch*), 13.73 mm^3 (*Chiropotes satanas*, only one specimen), and 4.23 – 7.46 mm^3 (*Pithecia pithecia*). However, when body size is accounted for, *Callicebus* falls between

Chiropotes and *Pithecia* in average nervous volume. While these families have substantially different nervous tissue cross-sectional areas beneath the posterior dentition, overall, they have very similar (and overlapping) total amounts of nervous tissue volume. Collectively, these findings of similar nervous volumes but substantial differences in CSA beneath M_1 and P_4 corroborate strong, positive relationships between the volume of nervous tissue and body size, as well as suggest that the amount of nervous tissues may not be evenly spread throughout the mandible.

Throughout the analyses in this dissertation, one species – *Pan paniscus* – consistently showed the largest values for all nervous tissues. However, these results should be assessed with caution because only one specimen represented this species, the specimen was of unknown origin (i.e., wild or zoo), and the specimen had been necropsied prior to staining. These factors, along with some others (like the general state of the specimen appearing to be elderly) indicate that the results shown here should be supported with further data before any strong conclusions about the IAN in Hominidae are drawn.

While there are few studies that assess canal to nerve relationships, there are others (e.g., DeGusta et al., 1999; Jungers et al., 2003; Kay et al., 1998) that have studied the soft- and hard- tissues separately. For example, Jungers et al. (2003) measured the hypoglossal canal and hypoglossal nerve (in separate specimens) and came to similar conclusions seen here. The canal and nerve cross-sectional areas amongst modern humans, fossil hominids, and modern apes have significant overlap in their ranges and cannot be used to differentiate amongst species or to establish speech capabilities. However, Jungers did note that in humans, “bundles of nerve XII occupied a small percentage of the canal’s cross-sectional area” but did not give the specific measurements of how much nervous and vasculature tissue occupied the canal (Jungers et al., 2003:479). The results here, along with the current literature, indicate that canals used to house peripheral nervous tissues should be used with caution as proxies for soft tissues.

This work adds to the growing body of literature on scaling analyses within the masticatory apparatus. For example, Hylander (1985) explains that as body size increases symphyseal thickness shows positive allometry, jaw length shows positive allometry, while the mandibular arch width shows negative allometry (Scott & Hogue, 2012). Additionally, there is an indication that the balancing side muscles (during chewing) must use increased force with increases in body size due to overall dietary changes (Hylander, 1985). While the hard-tissues of the mandible have different scaling relationships based on the forces being applied to them by soft-tissues, there is a consistent negatively allometric relationship between brain mass and body size across both primates and other mammals (Leitch et al., 2014; Rilling, 2006; Burger et al. 2019). The results here show an isometric relationship between the IAN and its hard tissue components and demonstrate that the IAN is not equal in size to the mandibular canal. Thus, more research is needed to understand why the central nervous system shows negative allometry to body size, while the peripheral nerve studied here shows near isometry to the surrounding hard tissues.

THE RELATIONSHIP BETWEEN THE IAN AND DIET IN PRIMATES

It has been well established that teeth are under strong selective pressure to adapt to diet due to their integral role in the mechanical breakdown of food (Hiiemäe & Kay, 1973; Kay, 1975; Leighton, 1993; Lucas & Luke, 1980; Lucas, 1979, 2006; Lumsden & Osborn, 1977; Lund et al., 1998; Strait, 1997, 2001; Taylor, 2002). However, while teeth are the interface to food objects, all chewing and mandibular movements are controlled in part by the IAN via both somatic sensation and motor movements (Anderson et al., 1970; Avery & Cox, 1977; Booth et al., 2013; Brashear, 1936; Crompton, 1989; Dubner et al., 1978; Luschei & Goldberg, 2011; Plaffman, 1939). Because of the close relationship between the mandibular tooth row and the IAN, I hypothesized that the IAN would be under similar selective pressures to the teeth and thus would also adapt to diet. However, the analyses in this dissertation have shown that the

IAN is not related to the shape of the teeth (barring one result) or the diet that a primate is consuming.

One tooth – P_4 – did show some significant relationships between the enamel surface shape and the nervous tissues (although the R^2 values did not indicate a particularly close relationship). The nerve CSA at the mental foramen and beneath P_4 showed a significant relationship to the DNE (Dirichlet's Normal Energy) of the premolars. DNE is most often described as the "sharpness" of the tooth and are considered dimensionless values, thus giving some insight into the working surface of the tooth's shape. These relationships do suggest that premolars may play a role in touch sensitivity within the mandibular tooth row and previous research has suggested that P_4 has the potential to have the largest amount of nervous tissue directly supplying it (Erisen et al., 1989; Kress et al., 2004). Premolar teeth have been shown to have a direct relationship between the size of the enamel surface and diet – specifically they increase in size with stiffer diets and higher loading (Daegling et al., 2011; Delezene et al., 2013; Fleagle & McGraw, 2002; Kinzey, 1992; Lucas et al., 1994; Scott et al., 2018; Singleton, 2004; Spencer, 2003; Wright, 2005). Further, DNE has been shown as one of the most useful topographic measurements of the tooth surface to use in diet reconstructions of both extant and extinct primate species (Bunn et al., 2011). This indicates that premolar teeth may be under strong selective pressure to change the size and shape of the tooths surface with changes in dietary stiffness, which would require the ability to detect minute differences in the food material properties. The wear analysis performed for this dissertation (see Chapter 3) indicated only one significant relationship between wear index and the premolar DNE in *Saimiri sciureus*. There were no significant relationships between DNE variables in the other three species surveyed, indicating that within this sample, wear does not particularly influence DNE values. This lends further support to the hypothesis that premolar teeth – particularly the sharpness of the tooth's surface – play a role in food material property detection and thus a vital role in the maintenance of the masticatory apparatus.

While DNE and premolar tooth shape has been linked to diet and some of the nervous tissues linked to these values/teeth, there were no relationships established between dietary categories and the nervous tissues themselves. It is known and well understood that body size influences the diet that a primate eats and what they supplement their main diet with (Kay, 1975; Ungar, 1998). For primary diets across all nervous tissues, there were clear differentiations by overall body size before the data were adjusted for gross differences in size. When size is adjusted for, the ranges for each primary dietary category overlap for all nervous tissue variables (except in cases when one species represented the dietary category). For secondary diets across all nervous tissues, there were again clear differentiations by size before the data were adjusted for size. These patterns follow the trend in that larger bodied primates (which have higher volumes of nervous tissues) consume leaves and some fruit as a secondary resource, with smaller bodied primates consuming animals, flowers, seeds, and gum (Kay, 1975). When the secondary dietary data was adjusted for size, there is again almost complete overlap between the ranges for all dietary categories. Overall, these results corroborate previous data in this dissertation in that the IAN size has a stronger relationship to mandible size (and by proxy, body size) than diet.

However, the analyses for phylogenetic multiple regressions did show some relationships between seed eating and the nerve CSA beneath M_1 and the nerve CSA at the mandibular foramen. While these relationships are significant, the R^2 values were relatively low (0.545 - 0.547) indicating that little more than half of the variation within the sample can be accounted for when using seed eating as a predicting variable. Within this sample, the species *Varecia variegata variegata* (0.4%), *Callicebus moloch* (34.2%), *Pithecia pithecia* (63.2%), *Chiropotes satanas* (66.2%), *Lagothrix lagotricha* (5.0%), *Pan paniscus* (9.0%), *Trachypithecus francoisi* (5.5%), *Semnopithecus entellus* (7.3%), *Colobus guereza* (0.23%), *Macaca mulatta* (0.8%), *Papio anubis* (8.5%) *Cercocebus agilis* (3.0%), *Cercopithecus neglectus* (4.0%), and *Erythrocebus patas* (8.7%) used seed eating to some extent as a dietary source (percentages

indicate the amount of seeds consumed in the overall species diet). When these species are compared by nervous tissue size at the mandibular foramen for primary resistant/non-resistant diet, there are no clear distinctions between these species and those that do not use seed eating as a dietary source. For example, although *M. mulatta* uses only 0.8% seeds, they have the same amount of nervous tissue (when size is adjusted for) at the mandibular foramen that *C. satanas* does, which use seed as their predominant dietary source. Very similar relationships are seen in the nerve CSA beneath M_1 in that there are no clear divisions within the data for seed eating and nervous tissue amount when size is accounted for.

However, all seed eating is not equal across primate species. For example, *Chiropotes* and *Pithecia*, two species that eat seeds as most of their diet, utilize puncture crushing with the anterior dentition to first break the seed up and then continue to masticate those pieces with the posterior dentition (Kinzey & Norconk, 1993; Kinzey, 1992; Mittermeier & van Roosmalen, 1981; Spencer, 2003). Other species, like *Pan paniscus*, eat seeds but do not masticate the seed and instead swallow it whole (Beaune et al., 2013). *Callicebus moloch* has been shown to first crack seeds/nuts in their mouths, pick the pieces out with their hands, and then consume the smaller pieces individually with their posterior teeth (Fragascy & Mason, 1983). Further, while seed eating can occur at both the anterior and posterior teeth, not all teeth are structured equally across groups. One adaptation to prevent teeth from fracturing during hard-object feeding is enamel thickness, with haplorrhines (apart from tarsiers) tending to show overall thicker enamel than strepsirrhines (Constantino et al., 2011; Lucas et al., 1994; Shellis et al., 1998). Although different primates have evolved to consume seeds in different ways, each of these primates would still need highly sensitive nerves in the posterior dentition to determine changes in stiffness of food objects to protect the dentition from damage.

All of this indicates that while some seed eating may be related to the posterior-most nervous tissues along the mandibular tooth row, the amount of nervous tissue does not change across dietary categories in primates when body size is adjusted for. Additionally, there were no

significant relationships between the nerve CSA at the mandibular foramen or beneath M_1 to any other stiff/tough dietary resource, indicating that this relationship to seed eating is not entirely influenced by the food material properties. However, seeds are the stiffest object assessed here across a wide range of diets and tend to be the stiffest objects that most primate species consume. This indicates that for the stiffest of all foods, the posterior dentition has potentially adapted in some way to assure better protection of the masticating teeth and better control of the chewing cycle during hard object feeding. Further investigation is warranted to establish if stiffness, rather than toughness, has a greater effect on posterior tooth morphology.

Many researchers (e.g., Davies et al., 1988; Ganzhorn et al., 2017; Kar-Gupta & Kumar, 1994; Prinz & Lucas, 2000) have argued various reasons as to why primates choose certain food sources such as fiber, protein, and tannin content. While higher fiber foods tend to show less intake across primates in the wild, there are no firm conclusions as to why primates choose certain tough/stiff foods over others. However, there is evidence that primates use sensory information from a "test" chew to establish if they are going to ingest it. For example, *Chiropotes satanas* and *Ateles paniscus* are sympatric species that both eat seeds and fruit pericarp, although *C. satanas* prefers to eat seeds/pericarp that is (on average) 15 times harder than those eaten by *A. paniscus* (Dominy et al., 2001; Kinzey & Norconk, 1993). Others (Kinzey & Norconk, 1993) argue that species like *Pithecia pithecia* prefer to ingest softer seeds with harder pericarps surrounding them which have been shown to have higher levels of nutrients but lower levels of tannins (Dominy et al., 2001). Additionally, humans (a species that does not necessarily specialize in hard-object feeding) have been shown to be able to detect incredibly small forces applied to the teeth – between 16g/mm^2 and 32g/mm^2, indicating that human teeth are highly touch sensitive (Linden, 1991; Yamada & Kumano, 1969). The data generated in this dissertation show that different species of primates tend to have, when body size is accounted for, very similar amounts of nervous tissues. In turn, this may indicate that many primate species may have the sensory ability to "test" food material properties but have not yet been

observed performing these behaviors. Additionally, this indicates that nerves are sensitive enough for material property testing even at a relatively conserved size, and/or that all primates are likely able to feel small changes in toughness/stiffness of food objects.

All cranial nerves across primates are highly conserved and derived from similar branchial arch tissues during embryonic development (Cochard, 2012; Trejo, 2019). The growth and development of the cranial nerves is an incredibly precise cascade event that involves specific genes, cell types, and stimulations to occur at certain times for proper development (Adameyko & Fried, 2016). This development process does not fall within the scope of this dissertation, but a discussion on the conservation of the trigeminal nerve across primates – and mammals – is necessary. All mammalian groups (Prototheria (Monotremata), Metatheria (marsupials), Eutheria (placentals)) progress through the same stages of peripheral and central trigeminal sensory system development in the same sequence largely based on body size, indicating the evolution of the development of the trigeminal system likely predates Mammalia (Ashwell, 2015; Benoit et al., 2016). Further, the trigeminal system is also found in most reptiles and birds, indicating not only a pre-mammalian evolutionary trajectory, but likely a pre-amniote evolutionary trait. Additionally, all groups of mammals show some sort of specialized sensory systems within the trigeminal that are all developed from the same epidermal peg and typically focus on somatosensory enhancements to the snout (Ashwell et al., 2012; Ashwell, 2015; Gemmell et al., 1988; Hughes et al. 1989). All these specializations, such as the star-nosed mole (Leitch et al., 2014) or the billed platypus (Ashwell & Hardman, 2012; Ashwell 2015), tend to have an increase in the surface area of the structures that trigeminal innervates, thus an increase in the number of nervous axons supplying somatosensory information from that area.

Leitch et al., (2014) were able to show that in shrews and moles, the total number of axons in the trigeminal nerve increased with both brain and body size – indicating that nervous tissue size is not entirely influenced by somatosensory capabilities. However, these researchers were also able to show that in the star-nosed mole (a mole that uses its snout much more than

all other species examined), the peripheral trigeminal nerve was significantly larger than all other species, although the brain size did not differ from species that were similar in body size. The star-nosed mole relies heavily on information gained from their snout and has thus undergone significant selection to increase the snout surface area and thus the number of nerve axons it contains. However, the star-nosed mole's elaborate snout would be much more related to the superior alveolar nerve rather than the IAN.

Although we see some instances of increased nervous tissue indicating more somatosensory capabilities in mammals, few studies have addressed if the size of nerves and foramina of the peripheral trigeminal can be used to estimate touch sensitivity in primates (Muchlinski, 2008, 2010). One of these studies, performed by Muchlinski (2010) assessed the superior alveolar nerve – a nerve directly related to the mid-facial or snout portion of the face – to establish if it had a relationship to primate diet. This study was able to show that in primates, the infraorbital foramen (IOF, the bony correlate of the superior alveolar nerve) cross-sectional area correlates with general descriptions of diets (i.e., frugivore, folivore, etc.). A larger IOF was directly associated with frugivory (a diet that often requires extensive manipulation of foodstuff outside of the oral cavity), with both folivores and insectivores having much smaller IOFs (indicating less food manipulation on the upper lip/mid-face) (Muchlinski, 2010). However, Muchlinski (2010) was unable to differentiate folivores and insectivores from each other based on IOF size. Further research (Muchlinski & Deane, 2016) argued that although the mental foramen is the mandibular correlate of the IOF, there were no clear distinctions by size across primate dietary groups. This led the authors to conclude that although the size of the IOF can be used to reconstruct diet in extinct primates, the mental foramen (and by proxy the mental nerve) cannot. The results found in this dissertation support these general conclusions in that although some primates specialize in certain feeding strategies, but when body size is accounted for there are no distinctions in the size of the IAN throughout the mandible based on feeding strategy.

The data collected here support the conclusion that the size of nervous tissues within the mandible are not under the same selective pressures as the teeth and do not have a relationship to either the shape of a tooth or the observed diets. These results also show that the size of the IAN has a strong relationship to mandible size and is heavily conserved across primates (and likely mammals by extension) in size, course, and shape. Additionally, this data shows that although there are clear implications for specializations and enlargements to the superior alveolar nerve, we continue to see no distinctions between primate groups in the IAN based on dietary patterns.

EVOLUTIONARY IMPLICATIONS

Although diet is perhaps one of the most studied aspects within biological anthropology in relation to primate tooth and mandibular form, there is substantial variation within feeding behaviors and dietary preferences of extant primates (Ross & Iriarte-Diaz, 2014). Even less is understood about the relationships between soft tissue and dietary variation across primates. However, it is necessary to understand the relationship between the soft- and hard-tissues of the masticatory apparatus because soft-tissues can have a dramatic effect on the forces that can be generated along the tooth row, thus affected the mechanical loads on the skeletal anatomy (Daegling & Grine, 2006; Lycett & Collard, 2005). Thus, phenotypic variation seen in parts of the primate cranium (such as the cranial buttressing system in extinct hominins) that are affected by mechanical loading during mastication must be assessed with caution when an attempt is made to establish diet using extant species. While the teeth, particularly the molars (Kay, 1975, Ungar et al., 2006), have been shown to be a very useful tool in establishing diet in extinct species via extant comparisons, any hard tissue that is affected by mechanical loading could show extensive variation due to functional bone adaptations (Ungar & Daegling, 2013). However, unlike the teeth, this dissertation has shown that the nervous tissues of the mandible

cannot be used to estimate diet in extant primates and thus should not be used (if soft tissues were ever found in the fossil record) to estimate the diet of extinct primate species.

This dissertation does contribute further evidence to the growing body of literature that post-canine teeth show allometric relationships between the root surface areas and enamel surface areas. This trend has been shown to be particularly prevalent in primates that utilize tough/stiff diets (Deines et al., 1993; Spencer, 2003) although the data collected here show that this is likely not influenced by stimulations relayed by the IAN. This indicates that sensation along the mandibular tooth row is not a driving force behind shape change in teeth because all primates have relatively the same amounts of nervous tissues supplying the mandibular tooth row. It is likely that nervous tissue size has been constrained throughout the evolutionary history of primates and thus could not be used as an effective tool to reconstruct diet if soft tissues were found in the archaeological or paleontological record.

Some researchers have argued that mandibular tooth form has changed throughout human evolution – particularly that of the premolars and molars – in that there has been an overall decrease in tooth size compared to other primates (Abbott, 1984; Riesenfeld, 1970). This overall decrease in facial size and tooth shape has influenced the mental foramen placement and number, with most humans having a single mental foramen that is regularly placed between P_3 and P_4. However, there is significant evidence that longer mandibles in non-human primates tend to have more posteriorly placed mental foramina and a higher likelihood of having accessory mental foramen (AMF) (Anderson et al., 1991; Coqueugniot, 2000; Coqueugniot & Minugh-Purvis, 2003; Liang et al., 2009b; Robinson & Yoakum, 2019; Rosas, 1997, 2001; Senyurek, 1946; Williams & Krovitz, 2004). This dissertation continues to support these arguments in that all five human individuals included had only one mental foramen on each side. Interestingly, this sample showed non-human primates with much smaller mandibles than humans in this sample (partiuclarly *Saimiri sciureus*) with many AMFs – sometimes up to five on a single side. This could potentially indicate that humans are much more constrained in

the number of mental foramen and placement – a trend we might not see across other primates. However this is likely not affected by the IAN size or use, as the data collected here showed there are no relationships between the IAN and diet nor did it show that the mental nerve comprises a majority of the mental foramen. While external soft-tisues (such as the chewing muscles) may play a role in MF placement, size, and number, the tissue that it contains, the mental nerve, does not appear to affect these physical attributes.

LIMITATIONS TO THE STUDY

The limitations to this study are numerous but do not detract from the work done. Limitations include but are not limited to the difficulty in assigning dietary categories to primates, the loss of knowledge in how many specimens were captured/killed/stored, the uncertainty in staining times and intensities when using diceCT, and the availability of specific specimens from collections. Each of these will be explained in full below to attempt to aid in future research in this area.

As discussed extensively in Chapter 2 (i.e., my background chapter), assigning dietary categories to primates is a difficult task. Many authors have chosen to use basic groupings (i.e., frugivore, folivore, etc.) based on the primary diet a species has been shown to consume. However, these diets are rarely defined the same in all studies (primary diet could mean a primate is choosing to eat a certain foodstuff 40-100% of the time) and no standard exists to precisely classify a primate's diet. While this study also used primary literature collected from observational studies, it should be noted that the same primate species may consume different proportions of food in different environments and during different seasons (Chapman & Fedigan, 1990; Hanya & Bernard, 2012; Janson & Boinski, 1992; Mittermeier & van Roosmalen, 1981; Ross & Iriarte-Diaz, 2014; Teaford, 1985). This work attempted to produce a more standardized way of assessing diet via tooth features (i.e., through the quantitative analysis utilizing the R software molaR) but even this is not a perfect way of establishing the diet of an individual. For

example, a captive and wild primate of the same species might have vastly different diets and dental surfaces, hindering our ability to accurately group species. Thus, future research should strive to assess a smaller number of species with known provenance in terms of actual diet consumed. This would aid in a better understanding of how the living surface of a tooth changes in a species based on diet and would give a much more controlled evaluation of the tooth's surface when using molaR.

The specimens collected for this experiment came from a variety of collections and researchers throughout the United States. In general, some history was available for the source of a specimen, but most specimens did not have a known origin. Specifically, many of the specimens for this project came from the Duke Miami Collections via Duke University and Doug Boyer and had no known histories. It is assumed they came from a captive collection that was fed a standard diet (likely monkey chow), but there is no evidence to support this. Additionally, many of the specimens collected from the University of Chicago via Callum Ross were either known or assumed to have come from the local Chicago Zoo after their natural death but again, no evidence supports this theory fully. However, many of the specimens, including all rats, rabbits, an otter, many of the strepsirrhines, and a few others either came from laboratories with known origins or were collected and preserved in the Terhune Lab. Along with the fact that the provenance has been lost for many specimens used here, the original fixatives were also unknown for many specimens. For example, the specimens obtained from the Duke Miami Collection were preserved in a mystery fluid (that was likely ethanol-based due to the smell) but could not be established based on the container. This limitation is most important when it came to deciding on which iodine solution to use during the diceCT process. However, in an ability to maintain consistency across the study, all specimens were fully immersed in a 10% NBF solution for a period of at least 30 days and were subjected to an aqueous-based iodine stain (I_2KI) until iodine uptake was complete. This meant that many of the specimens (that were likely

initially preserved in ethanol or ethanol-based products) had longer staining times regardless of size.

While iodine staining has been used for decades for medical research, the use of this technique in biological anthropology and anatomy studies is relatively novel (Hedrick et al., 2018; Li et al., 2016; Metscher, 2009; Vickerton et al., 2013; Witmer et al., 2018). Little was known (prior to this study) if staining fully fleshed adult heads was a possibility and even less was known if this was a potential avenue for staining nervous tissues. Because iodine bonds to lipids (i.e., fats) it was unknown if nervous tissues would have a substantial enough density of lipids to become radiopaque (Gignac et al., 2016). While the results of this study clearly show this is possible for a wide variety of primates, there were many unknowns as to staining times and results. For many of the heads, staining times were double what was anticipated and some tissues allowed the iodine to penetrate more efficiently than others (Gignac et al., 2016). Additionally, fresh iodine was necessary for most specimens every few weeks due to their large sizes and ready uptake of iodine. This meant that far more iodine solution was necessary than originally anticipated. Because the use of a microCT machine is costly and so many specimens were used in this study, it was difficult to adequately survey the amount of iodine uptake on a weekly basis (as proposed prior to the study beginning) and thus overstaining likely occurred.

Soft tissue studies are incredibly opportunistic and although I was able to survey a wide number of primate species, there is a definite gap in my ability to draw firm conclusions on the amount of variation seen in nervous structures. Essentially, this study had to use specimens that were available from researchers that were willing to donate them. This meant that while I set out to obtain a female and a male of multiple species in all the major groups of primates, the availability of specimens hindered my ability to do so. However, I am proud of the specimens that were able to be collected and recognize this effort was done to the best of my ability.

This dissertation has shown that nervous tissue size within the mandible cannot be used to establish the diet of an individual nor are there many significant relationships between

nervous tissue size and the hard-tissue components to which they are connected. However, it is imperative to recognize that the data collected here only represent half of the overall masticatory complex – the mandibular component. Further research is required to establish if the maxillary soft- and hard-tissues have significant relationships to one another and if the superior nervous tissues are affected by dietary differences in primates. This is particularly important because a body of literature already exists that shows when mammals have specialized snout sensory organs or extensively manipulate foods on the snout, there are larger amounts of nervous tissues innervating these regions (Ashwell & Hardman, 2012; Ashwell, 2015, Leitch et al., 2014; Muchlinski, 2010).

Finally, all these limitations were compounded by the fact that the data collection process for this sample occurred during the COVID-19 worldwide pandemic. Thus, access to scanning and lab facilities were severely limited, access to the materials themselves was not allowed for a period of two months (and thus the stain could not be refreshed), the shipping process for chemicals was substantially longer, and the ability to train/educate undergraduate researchers on data collection and anatomy was limited to virtual interactions.

Thus, future research should include specimens with known origin, that were ideally all preserved in a similar medium, that had known diets, and were preserved immediately after death to maintain the integrity of the nervous tissues. Additionally, future research should focus on the masticatory apparatus as a whole and include the nervous tissue of the maxillary tooth row to establish if the total amount of nervous tissue can be used more efficiently as a dietary predictor.

CONCLUSIONS

The results of this dissertation can be lumped into four major conclusions:

1. There were strong, significant relationships between the root surface area and enamel surface area of primate teeth, but there are few significant relationships between the IAN and the size and shape of teeth across primates.
2. The mandibular canal was most often not a true canal but was more of an open space within the body of the mandible in primates.
3. The IAN size was significantly related to the size of the mandibular canal but was not equal in size to the canal or its associated foramina.
4. There was no relationship between the size of the IAN and diet in primates.

In sum, this dissertation is the first work to discuss the variation seen in the IAN in primates. While this dissertation surveyed a wide variety of primates from many different family groups, future research will include a much smaller survey of a select number of species that are closely related but utilize different diets. This would allow researchers to gain a better understanding of the intraspecific variation of nervous tissues, if these are affected by phylogeny, and a better understanding of how these might be related to diet.

Further, this dissertation is the first to establish that there are few relationships between the nervous tissues of the mandible and the corresponding bony structures or diet in primates. While this dissertation used non-destructive methods on fixed specimens, future research will include a human sample of living individuals via MRI scans. Gaining access to human scans of in-vivo tissues would allow me to not only add 3D samples of human individuals into the collected data here but would also allow me to view the interactions between the soft- and hard-tissues in a living individual. It is known that preservatives (particularly alcohol based) and iodine staining can cause shrinkage during the fixation and staining processes. Because many of the specimens were preserved in unknown fluids here, it is difficult to assess how much shrinkage of soft tissues has occurred. Using in-vivo MRI scans would circumvent any problem of shrinkage for either preservation or staining and would allow me to establish if humans have separate evolutionary IAN trajectories in relation to other primates.

Finally, this work shows that the mandibular canal is most often not a true canal in primates and that it cannot be used as a proxy for the soft-tissue structures that are contained within this space. The mandibular canal is almost always described as that: a canal that begins at the mandibular foramen and proceeds anteriorly to the mental foramen. In medical textbooks, it is often shown as a bony tube with smooth sides that houses both the IAN and inferior alveolar artery (IAA). Future research will include more humans that are not elderly nor have extensive dental work to establish if having a canal is more common that what was seen here. Additionally, future research will examine the arterial system as it enters the mandibular canal to determine if an artery is always present, if it runs the entire length of the canal, and if a vein is present in any specimens. This work could be done on the scans produced here with further digital segmentation work.

This work shows that the IAN size is incredibly conserved across primate species, likely because most cranial nerves are highly conserved across all mammals in their path and structure (Trejo, 2019). Most medical textbooks (e.g., Cochard, 2012; Stern, 2003; Sudiwala & Knox, 2018) agree that all mammals (and most reptiles and birds) have 12 cranial nerves that come off the brain/brainstem in a specific order, follow the same pathways to the periphery, and transmit similar types of information back to the brain. This dissertation adds to this known literature by showing that nervous tissue amounts are likely determined by mandible size and thus, the amount of surface area the tissues must supply somatic sensation for, rather than varying in an adaptive manner in relation to diet or other factors.

LITERATURE CITED

Abbott, S. (1984). *A comparative study of tooth root morphology in the great apes, modern man and early hominids* (Unpublished doctoral dissertation). University of London, London.

Adameyko, I., & Fried, K. (2016). The nervous system orchestrates and integrates craniofacial development: a review. *Frontiers in Physiology, 19*, 1-49.

Adler, P. (1949). Sensibility of teeth to loads applied in different directions. *Journal of Dental Research, 26*, 279-289.

Agarwal, D. R., & Gupta, S. B. (2011). Morphometric analysis of mental foramen in human mandibles of South Gujarat. *People's Journal of Scientific Research, 4*(1), 15-18.

Agthong, S., Huanmanop, T., & Chentanez, V. (2005). Anatomical variations of the supraorbital, infraorbital, and mental foramina related to gender and side. *Journal of Oral Maxillofacial Surgery, 63*, 800-804.

Ahlgren, J. (1976). *Masticatory movements in man.* Paper presented at the Mastication: Proceedings of a Symposium on the Clinical and Physiological Aspects of Mastication, Bristol, United Kingdom.

Albrecht, P. (1967). The cranial arteries and cranial arterial foramina of the turtle genera Chrysemys, Sternotherus, and Trionyx: a comparative study with analysis of possible evolutionary implications. *Tulane Studies of Zoology, 14*, 81-99.

Aldridge, K., Kane, A. A., Marsh, J. L., Yan, P., Govier, D., & Richtsmeier, J. T. (2005). Relationship of brain and skull in pre- and postoperative sagittal synostosis. *Journal of Anatomy, 206*, 373-385.

Amorim, M., Prado, F., Borini, C., Bittar, T. O., Volpato, M. C., Groppo, F. C., & Caria, P. H. F. (2008). The mental foramen position in dentate and edentulous Brazilian's mandible. *International Journal of Morphology, 26*(4), 981-987.

Anderson, D., Hannam, A., & Matthews, B. (1970). Sensory mechanisms in mammalian teeth and their supporting structures. *Physiological Reviews, 50*(2), 171-195.

Anderson, D., & Hector, M. (1987). Periodontal mechanoreceptors and parotid secretion in animals and man. *Journal of Dental Research, 66*, 518-523.

Anderson, D., Hector, M., & Linden, R. (1985). The possible relation between mastication and parotid secretion in the rabbit. *Journal of Physiology, 364*, 19-29.

Anderson, L., Kosinski, T., & Mentag, P. (1991). A review of the intraosseous course of the nerves of the mandible. *Journal of Oral Implants, 17*, 394-403.

Angelopoulos, A. (1966). Anatomical variations in the distribution of the mandibular nerve and their significance to regional anesthesia. *Journal of the Oklahoma State Dental Association, 56*, 19-29.

Apinhasmit, W., Methathrathip, D., & Chompoopong, S. (2006). Mental Foramen in Thais: an anatomical variation related to gender and side. *Surgical and Radiological Anatomy, 28*, 529-533.

Appentag, K., Morimoto, T., & Taylor, A. (1980). Fusimotor activity in masseter nerve of the cat during reflex jaw movements. *Journal of Physiology, 305*, 415-431.

Ashkenazi, M., Taubman, L., & Gavish, A. (2011). Age-associated changes of the mandibular foramen position in antroposterior dimension of the mandibular angle in dry human mandibles. *The Anatomical Record, 294*(8), 1319-1325.

Ashwell, K. W., & Hardman, C.D. (2012). Distinct development of the trigeminal sensory nuclei in platypus and echidna. *Brain Behavioral Evolution, 79*, 261-274.

Ashwell, K. W. S. (2015). Timing of mammalian peripheral trigeminal system development relative to body size: A comparison of metatherians with rodents and monotremes. *Somatosensory and Motor Research, 32*(3), 187-199.

Avery, J. (1959). An investigation of the mechanism of neural impulse transmission in human teeth. *Oral Surgery, Oral Medicine, Oral Pathology, 12*, 190-198.

Avery, J. K., & Cox, C. F. (1977). *Role of nerves in teeth relative to pain and dentinogenesis.* Paper presented at the Pain in the trigeminal region, Department of Physiology, Bristol, United Kingdom.

Avizo [Computer software]. (2016). Waltham, MA: ThermoFisher Scientific.

Badrian, N., Badrian, A. l., & Susman, R. L. (1981). Preliminary observations on the feeding behavior of *Pan paniscus* in the Lomako Forest of Central Zaire. *Primates, 22*(2), 173-181.

Barclay, J. (1971). Enlarged mandibular canals. *Oral Surgery, Oral Medicine, and Oral Pathology, 32*, 665-666.

Baron, G., Stephan, H., & Frahm, H. D. (1990). Comparison of brain structure volumes in Insectivora and Primates. IX. Trigeminal complex. *Journal für Hirnforschung, 31*(2), 193-200.

Bearder, S. K., & Martin, R. D. (1980). *Acacia* gum and its use by bushbabies, *Galago senegalensis* (primates: lorisidae). *International Journal of Primatology, 1*, 103-128.

Beaudreau, D., & Jerge, C. (1968). Somatotopic representation in the Gasserian ganglion of tactile peripheral fields in the cat. *Archives of Oral Biology, 13*, 247-256.

Beaune, D., Bretagnolle, F., Bollache, L., Bourson, C., Hohmann, G., & Fruit, B. (2013). Ecological services performed by the bonobo (*Pan paniscus*): seed dispersal effectiveness in tropical forest. *Journal of Tropical Ecology*, *29*(5), 367-380.

Beecher, R., & Coruccini, R. (1981). Effects of dietary consistency on craniofacial and occlusal development in the rat. *Angle Orthodontist, 51*, 61-69.

Beertsen, W., McCulloch, C. A., & Sodek, J. (2000). The periodontal ligament: a unique, multifunctional connective tissue. *Periodontology, 13*, 20-40.

Beetson, W., Everts, V., & Van Den Hooff, A. (1974). Fine structure and possible function of cells containing leptomeric organelles in the periodontal ligament of the rat incisor. *Archives of Oral Biology, 19*, 1099-1100.

Benoit, J., Manger, P., & Rubidge, B. S. (2016). Paleonurological clues to the evolution of defining mammalian soft tissue traits. *Scientific Reports, 6*(1), 1-10.

Benoit, J., Angielczyk, K. D., Miyamae, J. A., Manger, P., Fernandez, V., & Rubidge, B. (2018). Evolution of facial innervation in anomodont therapsids (Synapsida): insights from x-ray computerized microtomography. *Journal of Morphology, 2018*(00), 1-29.

Bernick, S. (1952). Innervation of the primary teeth and surrounding tissues of monkeys. *The Anatomical Record, 113*, 215-237.

Bernick, S. (1966). Vascular and nerve supply to the molar teeth of guinea pigs. *Journal of Dental Research, 45*, 249-260.

Beyron, H. (1964). Occlusal relations and mastication in Australian Aborigines. *Acta Odontologica, 22*, 597.

Bicca-Marques, J. C., & Calegaro-Marques, C. (1994). Activity budget and diet of *Alouatta caraya*: an age-sex analysis. *Folia Primatologica, 63,* 216-220.

Blackmore, C., & Jennett, S. (2001). *The Oxford companion to the body*. Oxford University Press.

Boonratana, R. (2003). Feeding ecology of proboscis monkeys (*Nasalis larvatus*) in the lower Kinabatangan, Sabah, Malaysia. *Sabah Parks Nature Journal, 6*, 1-6.

Booth, K., Wyman, T., & Stoia, V. (2013). *Anatomy, physiology, and disease for the health professions*. McGraw Hill Education.

Bourque, M., & Kolta, A. (2001). Properties and Interconnections of trigeminal interneurons of the lateral pontine reticular formation in the rat. *Journal of Neurophysiology, 86*, 2583-2596.

Boyer, D. (2008). Relief index of second mandibular molars is a correlate of diet among prosimian primates and other mammals. *Journal of Human Evolution, 55,* 1118-1137.

Bradley, J. (1975). A radiological investigation into the age changes of the inferior dental artery. *British Journal of Oral Surgery, 13*, 82-90.

Brashear, A. (1936). The innervation of the teeth. An analysis of nave fiber components of the pulp and periodontal tissues and their probably significance. *Journal of Comparative Neurology, 64*, 169-185.

Britt, A., (2000). Diet and feeding behaviour of the Black-and-white ruffed lemur (*Varecia variegata variegata*) in the Betampona reserve, Eastern Madagascar. *Folia Primatologica, 71*(3), 133-141.

Budhiraja, V., Rastogi, R., Lalwani, R., Goel, P., & Bose, S. C. (2013). Study of Position, Shape, and Size of Mental Foramen Utilizing Various Parameters in Dry Adult Human Mandibles from North India. *ISRN Anatomy, 2013*, 1-5.

Bunn, J. M, Boyer, D. M., Lipman, Y., St Clair, E. M., Jernvall, J., & Daubechies, I. (2011). Comparing Dirichlet normal surface energy of tooth crowns, a new technique of molar shape quantification for dietary inference, with previous methods in isolation and in combination. *American Journal of Physical Anthropology, 145(2),* 247-261.

Burger, J. R., George Jr., M. A., Leadbetter, C., & Shaikh, F. (2019). The allometry of brain size in mammals. *Journal of Mammology, 100*(2), 276-283.

Burian, E., Sollmann, N., Ritschl, L. M., Palla, B., Maier, L., Zimmer, C., Probst, F., Fichter, A., Miloro, M., & Probst, M. (2020). High resolution MRI for quantitative assessment of inferior alveolar nerve impairment in course of mandible fractures: an imaging feasibility study. *Scientific Reports, 10*, 11566.

Burrows, A. M., & Smith, T. D. (2004). Three-dimensional analysis of mandiublar morphology in *Otolemur*. *American Journal of Physical Anthropology*, *127*(2), 219-230.

Byers, M. R. (1977). *Fine structure of trigeminal receptors in rat molars.* Paper presented at the Pain in the trigeminal region, Department in Physiology, Bristol, United Kingdom.

Byers, M. (1985). Sensory innervation of periodontal ligament of rat molars consists of unencapsulated Ruffini-like mechanoreceptors and free nerve endings. *Journal of Comparative Neurology, 231*, 500-518.

Byers, M. R., & Dong, W. K. (1983). Autoradiographic location of sensory nerve endings in dentin of monkey teeth. *The Anatomical Record, 205*, 441-454.

Byers, M. R., & Dong, W. K. (1989). Comparison of trigeminal receptor location and structure in the periodontal ligament of different types of teeth from the rat, cat, and monkey. *Journal of Comparative Neurology, 279*, 117-127.

Byers, M., O'Connor, T., Martin, R., & Doug, W. (1986). Mesencephalic trigeminal sensory neurons of a cat. Axon pathways and structure of mechanoreceptive endings in periodontal ligament. *Journal of Comparative Neurology, 250*, 181-191.

Capra, N. F., & Wax, T. (1989). Distribution and central projections of primary afferent neurons that innervate the masseter muscle and mandibular periodontal: a double label study. *Journal of Comparative Neurology, 279*, 341-352.

Capra, N. F., & Dessem, D. (1992). Central connections of trigeminal primary afferent neurons: topographical and functional considerations. *Critical Reviews in Oral Biology and Medicine, 4*(1), 1-52.

Carpenter, M. B. (1957). The dorsal trigeminal tract in the rhesus monkey. *Journal of Anatomy, 91*(1), 81-90.

Cartmill, M., Hylander, W. L., & Shafland, J. (1987). *Human Structure*. Harvard University Press.

Cash, R., & Linden, R. (1980). The effect of sympathetic stimulation on periodontal mechanoreceptor activity recorded in trigeminal ganglion of cat. *Journal of Dental Research, 59*(D), 1839.

Chapman, C., & Fedigan, L. (1990). Dietary differences between neighboring *Cebus capucinus* groups: local traditions, food availability or responses to food profitability? *Folia Primatologica (Basel), 54*, 177-186.

Charalampakis, A., Kourkoumelis, G., Psari, C., Antonio, V., Piagkou, M., Demesticha, T., Kotsiomitis, E., & Troupis, T. (2017). The position of the mental foramen in dentate and edentulous mandibles: clinical and surgical relevance. *Folia Morphology, 76*(4), 709-714.

Charles-Dominique, P., & Bearder, S. K. (1979). Field studies of lorisid behavior: methodological aspects. In G. A., Doyle, & R. D. Martin (Eds.), *The Study of Prosimian Behavior* (pp. 567- 629). American Press.

Chiego, D., Cox, C., & Avery, J. (1980). H3HRP analysis of the nerve supply to primate teeth. *Journal of Dental Research, 59*, 736-744.

Chávez-Lomeli, M., Mansilla Lory, J., Pompa, J. A., & Kjaer, I. (1996). The human mandibular canal arises from three separate canals innervating different tooth groups. *Journal of Dental Research, 75*, 1540-1544.

Clutton-Brock, T. H., & Harvey, P. H. (1980). Primates, brains, and ecology. *Journal of Zoology London*, *190*, 309-323.

Cochard, L. R. (2012) *Netter's atlas of human embryology*. Saunders Elsevier.

Cody, F., Harrison, L., Taylor, A., & Weghofer, J. (1974). Distribution of tooth receptor afferents in the mesencephalic nucleus of the fifth cranial nerve. *Journal of Physiology, 239*, 49P-50P.

Condemi, S. (1991). Some considerations concerning Neandertal features and the presence of Neandertals in the Near East. *Rivista di Antropologia (Roma), 69*, 27-38.

Constantino, P. J. (2009). The importance of fallback foods in primate ecology and evolution. *American Journal of Physical Anthropology, 140*(4), 599-602.

Constantino, P. J., Lee, J. J. W., Morris, D., Lucas, P. W., Harstone-Rose, A., Lee, W. K., Dominy, N. J., Cunningham, A., Wagner, M., & Lawn, B. R. (2011). Adaptation to hard-object feeding in sea otters and hominins. *Journal of Human Evolution*, *61*(1), 89-96.

Coqueugniot, H. (2000). La position du foramen mentonnier chez i'enfant: Révision ontogénétique et phylogénétique. *Bulletins et Mémoires de la Societe d'Anthropologie. (Paris), 12*, 227-246.

Coqueugniot, H., & Minugh-Purvis, N. (2003). Ontogenetic patterning and phylogenetic significance of mental foramen number and position in the evolution of upper Pleistocene *Homo sapiens*. In J. Thompson, G. Krovitz, & A. Nelson (Eds.), *Patterns of Growth and Development in the Genus Homo* (pp. 343-360). Cambridge University Press.

Corbin, K. (1940). Observations on the peripheral distribution of fibers arising in the mesencephalic nucleus of the fifth cranial nerve. *Journal of Comparative Neurology, 73*, 153-177.

Cords, M. (1986). Interspecific and Intraspecific variation in diet of two forest guenons, *Cercopithecus ascanius* and *C. mitis*. *Journal of Animal Ecology, 55,* 811-827.

Cowin, S. C. (2001). The false premis in Wolff's law. In: Cowin, S. C. (Ed.), *Bone biomechanics handbook, 2nd edition* (pp. P30-1-32-5). CRC press.

Crompton, A. W. (1989). The evolution of mammalian mastication. In D. B. Wake & G. Roth (Eds.), *Complex organismal functions: integration and evolution in vertebrates* (pp. 23-30). Wiley-Interscience.

Crompton, A. W. (1995). Masticatory function in non mammalian cynodonts and early mammals. In J. Thomason (Ed.), *Functional morphology in vertebrate paleontology* (pp. 55-75). Cambridge University Press.

Cryer, M. (1901). Cribiform tube. In S. White (Ed.), *Studies of the Internal Anatomy of the Face* (pp. 11-13). Dental Manufacturing Company.

Daegling, D. J., & Grine, F. E. (2006). Mandibular biomechanics and the paleontological evidence for the evolution of the human diet. In P. S. Ungar (Ed.), *Evolution of the human diet: the known, the unknown, and the unknowable* (pp. 107-154). Oxford University Press.

Daegling, D. J., McGraw W. S., Ungar P. S., Pampush J. D., Vick, A. E., & Bitty, E. A. (2011). Hard-object feeding in sooty mangabys (*Cercocebus atys*) and interpretation of early hominin feeding ecology. *PLOS One, 6*, e23095.

Davies, A. G., Bennett, E. L., & Waterman, P. G. (1988). Food selection by two south-east Asian colobine monkeys (*Presbytis rubicunda* and *Presbytis melalophos*) in relation to plant chemistry. *Biological Journal of the Linn Society, 34*, 33-56.

De Lange, A., Hannam, A., & Matthews, B. (1969). The diameters and conduction velocities of fibers in the terminal branches of the inferior dental nerve. *Archives of Oral Biology, 14*, 513-519.

Deacon, T. W. (1990). Rethinking mammalian brain evolution. *American Zoology*, *30*, 629-705.

DeGusta, D., Gilbert, W. H., & Turner, S. P. (1999). Hypoglossal canal size and hominid speech. *Proceedings for the National Academy of Sciences*, *96*, 1800-1804.

Delezene, L. K., Zolnierz, M. S., Teaford, M. F., Kimbel, W. H., Grine, F. E., & Ungar, P.S. (2013). Premoalr microwear and tooth use in *Australopithecus africanus. Journal of Human Evolution, 65*, 282-293.

Desjardins, R., Winkelmann, R., & Gonzalez, J. (1971). Comparison of nerve endings in normal gingiva with those in mucosa covering edentulous alveolar ridges. *Journal of Dental Research, 50*, 867-879.

Dew, J. L. (2005). Foraging, food choice, and food processing by sympatric ripe-fruit specialists: *Lagothrix lagotrich poppigii* and *Ateles belzebuth belzebuth*. *International Journal of Primatology, 26*(5), 1107-1135.

Dominy, N. (2004). Fruits, Fingers, and Fermentation: The sensory cues available to foraging primates. *Integrated Comparative Biology, 44*, 29-37.

Dominy, N. J., Lucas P. W., Osorio, D., & Yamashita, N. (2001). The sensory ecology of primate food perception. *Evolutionary Anthropology*, *10*, 171-186.

Donati, G., Bollen, A., Borgognin-Tarli, S. M., & Ganzhorn, J. U. (2007). Feeding over the 24-h cycle: dietary flexibility of cathemeral collared lemurs (*Eulemur collaris*). *Behavioral Ecology and Sociobiology, 61,* 1237-1251.

Dong, W., Chudler, E., & Marin, R. (1985). Physiological properties of interdental mechanoreceptors. *Brain Research, 334*, 389-395.

Dubner, R., Sessle, B. J., & Storey, A. T. (1978). *The neural basis of oral and facial function*. Plenum Press.

Dunham, N. T., & Lambert, A. L. (2016). The role of leaf toughness on foraging efficiency in Angola black and while colobus monkeys (*Colobus angolensis palliatus) American Journal of Physical Anthropology, 161*, 343-354.

Dupont, E. (1866). Etude sur les fouilles scientifiques executées pendant l'hiver de 1865 dans les cavernes des bordes de la Lesse. *Bulletins de l'Académie royale des sciences, des lettres et des beaux-arts de Belgique, 22*, 31-54.

Edin, B. B., & Trulsson, M. (1992). Neural network analysis of the information content in population responses from human periodontal receptors. *Science of Artificial Neural Networks, 1710*, 257-266.

Edwards, L. F., & Gaughran, G. R. L. (1971). *Concise anatomy*. McGraw-Hill.

El-Beheri, S. (1985). Antero-posterior journey of the mental foramen (birth to 7 years of age). *Egyptian Dental Journal, 31*(4), 313-320.

Elliott, J., & Dover, S. (1982). X-ray microtomography. *Journal of Microscopy, 126*, 211-213

Erisen, R., Yücel, T., & Kucukay, S. (1989). Endomethasone root canal filling material in the mandibular canal. *Oral Surgery, Oral Medicine, and Oral Pathology, 68*, 343-345.

Evans, A. R., Wilson, G. P., Fortelius, M., & Jernvall, J. (2007). High-level similarity of dentitions in carnivorans and rodents. *Nature, 445,* 78-81.

Falin, L. (1958). The morphology of receptors of the tooth. *Acta Anatomy, 35*, 257-276.

Falk, D., Hildebolt, C., Smith, K., Morwood, M., Sutikna, T., Brown, P., Jatmiko, Wayhu Saptomo, E., Brunsden, B., & Prior, F. (2005). The brain of LB1, *Homo floresiensis*. *Science, 308*(5719), 242-245.

Fearnhead, R. (1967). Innervation of dental tissues. In A. Miles (Ed.), *Structure and Chemical Organization of Teeth* (pp. 247-281). Academic Press.

Feuerstein, D., Costa-Mendes, L., Esclassan, R. Marty, M. Vaysse, F., & Noirrit, E. (2019). The mandibular plane: a stable reference to localize the mandibular foramen, even during growth. *Oral Radiology, 36*, 69-79.

Fleagle, J. G., & McGraw, W. S. (2002). Skeletal and dental morphology of African papionins: unmasking a cryptic clade. *Journal of Human Evolution, 42*, 267-292.

Fortelius, M. (1985). Ungulate cheek teeth: developmental, functional, and evolutionary interrelations. *Acta Zoologica Fennica, 180*, 1-76.

Fortelius, M., & Solounias, N. (2000). Functional characterization of ungulate molars using the abrasion-attrition wear gradient: A new method for reconstructing paleodiets. *American Museum Novitates, 3301*, 1-36.

Fox, C., Johnson, F., Whiting, J., & Roller, P. (1985). Formaldehyde fixation. *Journal of Histochemistry and Cytochemistry, 33*, 845-853.

Fragaszy, D. M., & Mason, W. (1983). Comparisons of feeding behavior in captive squirrel and titi monkeys (*Saimiri sciureus* and *Callicebus moloch*). *Journal of Comparative Psychology*, *97*(4), 310-326.

Fraipont, J., & Lohest, M. (1886). La race humaine de Néanderthal ou de Cannstadt en Belgique. Recherches ethnographiques sur les ossements humains découverts dans les dépôts quaternaries d'une grotte B Spy et détermination de leur âge géologique-Note Préliminaire. *Bulletins de l'Académie royale des sciences, des lettres et des beaux-arts de Belgique, 12*, 741-784.

Franciscus, R., & Trinkaus, E. (1995). Determinants of retro-molar space presence in leistocene *Homo* mandibles. *Journal of Human Evolution, 28*, 577-595.

Frank, R. (1968). Attachment sites between the odontoblast process and the interdental nerve fiber. *Archives of Oral Biology, 13*, 833-834.

Frank, V. (1966). Mandibular canal localization. *Oral Surgery, Oral Medicine, and Oral Pathology, 21*, 312-315.

Fujishita, A., Koga, Y., Utsumi, D., Nakamura, A., Yoshimi, T., & Yoshida, N. (2015). Effects of feeding a soft diet and subsequent rehabilitation on the development of the masticatory function. *Journal of Oral Rehabilitation, 42*, 266-274.

Gabriel, A. (1958). Some anatomical features of the mandible. *Journal of Anatomy, 92*, 580-586.

Galton, F. (1886). Regression towards mediocrity in hereditary stature. *Journal of the Anthropological Institue of Great Britain and Ireland, 15,* 246-263.

Ganzhorn, J. U., Arrigo-Nelson, S. J., Carrai, V., Chalise, M. K., Donati, G., Droescher, I., Eppley, T. M., Irwin, M. T., Koch, F., Koenig, A., Kowalewski, M. M., Mowry, C. B., Patel, E. R., Pichon, C., Ralison, J., Reisdorff, C., Simmen, B., Stalenber, E., Starrs, D., Terboven, J., Wrights, P. C., & Foley, W. J. (2017). The importance of protein in leaf selection of folivorous primates. *American Journal of Primatology, 79*, 1-13.

Garber, P. A. (1980). Locomotor behavior and feeding ecology of the Panamanian tamarin (*Saguinus oedipus geoffroyi*, Callitrichidae, Primates). *International Journal of Primatology, 1*(2), 185-201.

Garland Jr., T., Dickerman, A. W., Janis, C. M., & Jones, J. A. (1993) Phylogenetic analysis of covariance by computer simulation. *Systematic Biology, 42*, 265-292.

Gault, D., Renier, D., Marchac, D., & Jones, B. (1992). Intracranial pressure and intracranial volume in children with craniosynostosis. *Plastic Reconstructive Surgery, 90*, 377-381.

Gautier-Hion, A., Duplantier, J., Quris, R., Feel, F., Sourd, C., Decoux, J., Dubost, G., Emmons, L., Erard, C., Hecketsweiler, P., Moungazi, A., Roussilhon, C., & Thiollay, J. (1985). Fruit characters as a basis of fruit choice and seed dispersal in a tropical forest vertebrate community. *Oecologia (Berlin), 65*, 324-333.

Gemmell, R. T., Peters, B., & Nelson, J. (1988). Ultrastructural identification of Merkel cells around the mouth of the newborn marsupial. *Anatomical Embryology, 177*, 403-408.

Geomagic [Computer software]. (2013). Morrisville, NC: 3D Systems.

Gershenson, A., Nathan, H., & Luchansky, E. (1986). Mental foramen and mental nerve: changes with age. *Acta Anatomy, 126*, 21-28.

Gignac, P. M., Kley, N. J., Clarke, J. A., Colbert, M. W., Morhardt, A. C., Cerio, D., Cost, I. A., Cox, P. G., Daza, J. D., Early, C. M., Echols, M. S., Henkelman, R. M., Herdina, A. N., Holliday, C. M., Li, Z., Mahlow, K., Merchant, S., Muller, J., Orsborn, C. P., Paluh, D. J., Thies, M. L., Tsai, H. P., & Witmer, L. M. (2016). Diffusible iodine-based contrast-enhanced computed tomography (diceCT): an emerging tool for rapid, high-resolution, 3-D imaging of metazoan soft tissues. *Journal of Anatomy, 228*, 889-909.

Goldberg, L. (1971). Masseter muscle excitation induced by simulation of periodontal and gingival receptors in man. *Brain Research, 32*, 369-381.

Gordon, T. (1979). Alteration of patient chewing patterns after occlusal modification. *Quitessence International, 10*(4), 1.

Gould, L., & Gabriel, D. N. (2014). Wet and dry season diets of the endangered *Lemur catta* (ring-tailed lemur) in two mountainous rocky outcrop forest fragments in south-central Madagascar. *African Journal of Ecology, 53*(3), 320-330.

Gould, S., & Lewontin, R. (1979). The spandrels of San Marco and the Panglossian paradigm: a critique of the adaptationist programme. *Proceedings of the Royal Society of London (B), 205*, 581-598.

Gowgiel, J. (1992). The position and course of the mandibular canal. *Journal of Oral Implantology, 18*, 383-385.

Grafen, A. (1989). The phylogenetic regression. *Philosophical Transactions of the Royal Society B: Biological Sciences, 326,* 119-157.

Green, R., & Darvell, B. (1988). Tooth wear and the position of the mental foramen. *American Journal of Physical Anthropology, 77*, 69-75.

Greenfield, L. O. (1992). Relative canine size, behavior and diet in male ceboids. *Yearbook of Physical Anthropology, 35*, 153-185.

Greer, S. Y., George, I. D., & Aldridge, K. (2017). *Variation in the interface of brain and skull*. Paper presented at the American Association of Physical Anthropology, New Orleans, LA.

Griffin, C., & Harris, R. (1968). Unmyelinated nerve endings in the periodontal membrane of human teeth. *Archives of Oral Biology, 17*, 913-921.

Griffin, C., & Spain, H. (1972). The organization and vasculature of human periodontal ligament mechanoreceptors. *Archives of Oral Biology, 17*, 913-922.

Gupta, S., & Soni, J. S. (2012). Study of anatomical variations and incidence of mental foramen and accessory mental foramen in dry human mandibles. *National Journal of Medical Research, 2*(1), 28-30.

Göregen, M., Mīloglu, Ö., Ersoy, Ī., Bayrakdar, Ī. S., & Akgül, H. M. (2013). The assessment of accessory mental foramina using cone-beam computed tomography. *Turkish Journal of Medical Sciences, 43*, 479-483.

Hanihara, T., & Ishida, H. (2001). Frequency variations of discrete cranial traits in major human populations. IV. Vessel and nerve related variations. *Journal of Anatomy, 199*, 273-287.

Hannam, A. (1976). *Periodontal mechanoreceptors.* Paper presented at the Mastication: Proceedings of a Symposium on the Clinical and Physiological Aspects of Mastication, Bristol, United Kingdom.

Hannam, A. (1982). The innervation of the periodontal ligament. In B. K. B. Berkovitz (Ed.), *The periodontal ligament in health and disease* (pp. 173-196). Pergamon Press.

Hannam, A., & Farnsworth, T. (1977). Information transmission in trigeminal mechanosensitive afferents from teeth in the cat. *Archves of Oral Biology, 22*, 181-186.

Hannam, A., & Lund, J. (1981). The effect of intraoral stimulation on the human masticatory cycle. *Archives of Oral Biology, 26*(11), 865-870.

Hanya, G., & Bernard, H. (2012). Fallback foods of red leaf monkeys (*Presbytis rubicunda)* in Danum Valley, Borneo. *International Journal of Primatology, 33*, 322-337.

Harputluoglu, S. (1990). Effects of removing inferior alveolar neurovascular structures on mandibular growth and the eruption of permanent dentition in puppies. *Oral Surgery, Oral Medicine, and Oral Pathology, 70*, 147-149.

Harris, T. R., & Chapman, C. A. (2007). Variation in diet and ranging of black and white colobus monkeys in Kibale National Park, Uganda. *Primates, 48,* 208-221.

Harvey, P. H., Kavanagh, M., & Clutton-Brock, T. H. (1978). Sexual dimorphism in primate teeth. *Journal of Zoology (London)*, *186*, 474-485.

Hassanali, J. (1997). Quantitative and somatotropin mapping of neurons in the trigeminal mesencephalic nucleus and ganglion innervating teeth in monkey and baboon. *Archives of Oral Biology, 42*(10), 673-682.

Haywood, J., Richardson, E. R., & Malhortra, S. K. (1977). The mandibular foramen: Its anteroposterior position. *Oral Surgery, Oral Medicine, Oral Pathology, 44*(6), 837-843.

Heasman, P. (1984). The myelinated fibre content of human inferior alveolar nerves from dentate and edentulous subjects. *Journal of Dentistry, 12*, 283-286.

Hector, M. (1985). The masticatory-salivary reflex. In S. Lisney & B. Matthews (Eds.), *Current topics in oral biology* (pp. 311-320). University of Bristol Press.

Hedrick, B. P., Yohe, L., Vander Linden, A., Dávalos, L. M., Sears, K., Sadier, A., Rossiter, S. J., Davies, K. T. J., & Dumont, E. (2018). Assessing soft-tissue shrinkage estimates in museum specimens imaged with diffusable iodine-based contrast-enhanced computed tomography (diceCT). *Microscopy and Microanalysis, 24*(3), 284-291.

Herring, S. W. (1985). The ontogeny of mammalian mastication. *American Journal of Zoology, 25*, 339-349.

Hiiemäe, K. (1974). Mammalian mastication: a review of the activity of the jaw muscles and movements they produce in chewing. In P. Butler & K. Joysey (Eds.), *Studies on the development, structure and function of teeth* (pp. 360-398). Academic Press.

Hiiemäe, K., Heath, M., Heath, G., Kazazoglu, E., Murray, J., Sapper, D., & Hamlet, K. (1996). Natural bites, food consistency and feeding behavior in man. *Archives of Oral Biology, 41*(2), 175-189.

Hiiemäe, K. M., & Kay, R. F. (1973). Evolutionary trends in the dynamics of primate mastication. In M. R. Zingeser (Ed.), *Symp. Fourth Int. Congr. Primatology, Vol 3: Craniofacial Biology of Primates* (pp. 28-64). Karger.

Hill, D., & Lucas, P. (1996). Toughness and fiber content of major leaf food of Japanese macaques (*Macaca fuscata yakui*) in Yakushima. *American Journal of Primatology, 38*, 221-231.

Hock, L. B., & Sasekumar, A. (1979). A preliminary study on the feeding biology of mangrove forest primates. *The Malayan Nature Journal, 33,* 105-112.

Hofmann, R. R., Streich, W. J., Fickel, J., Hummel, J., & Clauss, M. (2008). Convergent evolution in feeding types: salivary gland mass differences in wild ruminant species. *Journal of Morphology, 269*, 240-257.

Hogg, R. T., Ravosa, M. J., Ryan, T. M., & Vinyard, C. J. (2011). The functional morphology of the anterior masticatory apparatus in tree-gouging marmosets (Cebidae, Primates). *Journal of Morphology, 272*, 833-849.

Holland, G. (1978). Fiber number and sizes in the inferior alveolar nerve of the cat. *Journal of Anatomy, 127*, 343-352.

Hu, G. (2011). Dietary breadth and resourse use of Francois' Langur in a seasonal and distrubed habitat. *American Journal of Primatology, 73*, 1176-1187.

Hublin, J. (1998). Climate change, paleogeography and the evolution of the Neandertals. In T. Akazawa, K. Aoki, & O. Bar-Yosef (Eds.), *Neandertals and modern humans in western Asia* (pp. 295-310). Plenum Publishing.

Hughes, R. L., Hall, L. S., Tyndale-Biscoe, C. H., & Hinds, L. A. (1989). Evolutionary implications of macropod organogenesis. In: G. Griggs, P. Jarman, I. Hume (Eds.), *Kangaroos, wallabies, and rat-kangaroos* (pp. 377-405). Surrey Beatty & Sons.

Hylander, W. L. (1975a). Incisor size and diet in anthropoids with special reference to cercopithecidae. *Science, 189*(4208), 1095-1098.

Hylander, W. L. (1975b). The human mandible: level or link? *American Journal of Physical Anthropology, 43*, 227-242.

Hylander, W. L. (1979). The functional significance of primate mandibular form. *Journal of Morphology, 160*, 223-240.

Hylander, W. L. (1985). Mandiublar function and biomechanical stress and scaling. *American Zoology, 25*, 315-330.

Hylander, W. L. (2006). Functional anatomy and biomechanics of the masticatory apparatus. In D. M. Laskin, C. Greene, & W. L. Hylander (Eds.), *Temporomandibular disorders: an evidenced approach to diagnosis and treatment* (pp. 3-34). Quintessence Publishing Co.

Imada, T. S. N., Paes da Silva, L. M., Fernandes, R., Centurion, B. S., de Oliveira-Santos, C., Honório, H. M., & Rubira-Bullen, I. R. F. (2012). Accessory mental foramina: prevalence, position and diameter assessed by cone-beam computed tomography and digital panoramic radiographs. *Clinical Oral Implants Research, 0*, 1-6.

Inagaki, N., Yamatodani, A., Shinoda, K., Shiotani, Y., Tohyama, M., Watanabe, T., & Wada, H. (1987). The histaminergic innervation of the mesencephalic nucleus of the trigeminal nerve in rat brain: a light and electron microscopical study. *Brain Research, 418*, 388-391.

Ingervall, B., & Helkimo, E. V. A. (1978). Masticatory muscle force and facial morhpology in man. *Archives of Oral Biology*, *23*, 203-206.

Inoue, T. (2015). Neural mechanisms of mastication. *Brain Nerve, 67(2),* 141-156.

Inoue, T., Kato, T., Masuda, Y., Nakamura, T., Kawamura, Y., & Morimoto, T. (1989). Modifications of masticatory behavior after trigeminal deafferentation in the rabbit. *Experimental Brain Research, 74*, 579-591.

Iranparvar, A., Nozariasbmarz, A., DeGrave, S., & Tayebi, L. (2020). Tissue engineering in periodontal regeneration. In: L. Tayebi (Ed.), *Applications of Biomedical Engineering in Dentistry* (pp. 301-327). Springer Nature.

Ito, G., Mitani, S., & Kim, J. (1988). Effect of soft diets on craniofacial growth in mice. *Anatomischer Anzeiger, 165*(2-3), 151-166.

Iwanaga, J., Anand, M. K., Jain, M. N., Nagata, M., Matsushita, Y., Ibaragi, S., Kusukawa, J., & Tubbs, R. S. (2019). Microsurgical anatomy of the superior wall of the mandibular canal and surrounding structures: Suggestion for new classifications for dental implantology. *Clinical Anatomy, 33*(2), 223-231.

Iwanaga, J., Saga, T., Tabira, Y., Nakamura, M., Kitashima, S., Watanabe, K., Kusukawa, J., & Yamaki, K. (2015). The clinical anatomy of accessory mental nerves and foramina. *Clinical Anatomy, 28*(7), 848-856.

Jacobs, R., Lambrichts, I., Liang, X., Martens, W., Mraiwa, N., Adriaensens, P., & Gelan, J. (2007). Neurovascularization of the anterior jaw bones revisited using high resolution magnetic resonance imaging. *Oral Surgery, Oral Medicine, Oral Pathology, Oral Radiology, and Endodontology, 103*(5), 683-693.

Jacobs, R., Mraiwa, N., Van Steenberghe, D., Giibels, F., & Quirynen, M. (2002). Appearance, location, course, and morphology of the mandibular incisive canal: an assessment on spiral CT scan. *Dentomaxillofacial Radiology, 5*, 322-327.

Jain, K. (2017). *Bite into this: preliminary analysis of jaw-adductor muscle architecture and bite force measured from diceCT images in Tupaia and strepsirrhine primates.* (Unpublished Honors Thesis), Duke University, Durham, North Carolina.

Jamniczky, H. A., & Russell, A. P. (2004). Cranial arterial foramen diameter in turtles: a quantitative assessment of size-dependent phylogenetic signal. *Animal Biology, 54*(4), 417-436.

Janis, C. M. (1990). The correlation between diet and dental wear in herbivorous mammals, and its relationship to the determination of diets in extinct species. In A. J. Boucot (Ed.), *Evolutionary paleobiology of behavior and coevolution* (pp. 241-259). Elsevier.

Janson, C. H., & Boinski, S. (1992). Morphological and behavioral adaptations for foraging in generalist primates: the case of the cebines. *American Journal of Physical Anthropology, 88*, 483-498.

Jerge, C. (1963). Organization and function of the trigeminal mesencephalic nucleus. *Journal of Neurophysiology, 26*, 372-392.

Jerge, C. (1965). Comments on the innervation of the teeth. *Dental Clinics of North America, 23*, 117-127.

Johnsen, S. E., & Trulsson, M. (2003). Receptive field properties of human periodontal afferents responding to loading of premolar and molar teeth. *Journal of Neurophysiology, 89*, 1478-1487.

Jones, C., & Anderson, S. (1978). *Callicebus moloch*. *Mammalian Species, 112,* 1-5.

Jonas, J. B., Schmidt, A. M., Müller-Bergh, J. A., Schlötzer-Schrehardt, U. M., & Naumann, G. O. H. (1992). Human optic nerve fiber count and optic disc size. *Investigative Ophthalmology and Visual Science, 33*(6), 2012-2018.

Julliot, C. (1996). Fruit choice by red howler monkeys (*Alouatta seniculus*) in a tropical rain forest. *American Journal of Primatology, 40*, 261-282.

Jungers, W. L., Falsetti, A. B., & Wall, C.E. (1995). Shape, relative size, and size-adjustments in morphometrics. *Yearbook of Physical Anthropology, 38,* 137-161.

Jungers, W. L, Pokempner, A. A., Kay, R. F., & Cartmill, M. (2003). Hypoglossal canal size in living hominoids and the evolution of human speech. *Human Biology, 75*(4), 473-484.

Kalender, A., Orhan, K., & Aksoy, U. (2012). Evaluation of the mental foramen and accessory mental foramen in Turkish patients using cone-beam computed tomography images teconstructed from a volumetric rendering program. *Clinical Anatomy, 25*, 584-592.

Kar-Gupta, K., & Kumar, A. (1994). Leaf chemistry and food selection by common langurs (*Presbytis entellus)* in Rajaji National Park, Uttar Pradesh, India. *International Journal of Primatology, 15*, 75-93.

Katakami, K., Mishima, A., Shiozaki, K., Shimoda, S., Hamada, Y., & Kobayashi, K. (2008). Characteristics of accessory mental foramina observed on limited cone-beam computed tomography Images. *Journal of Endodontists, 34*(12), 1441-1445.

Kay, R. F. (1975). The functional adaptations of primate molar teeth. *American Journal of Physical Anthropology, 42*, 327-352.

Kay, R. F. (1984). On the use of anatomical features to infer foraging behavior in extinct primates. In P. S. Rodman & J. G. H. Cant (Eds.), *Adaptations for foraging in nonhuman primates* (pp. 21-53). Columbia University Press.

Kay, R. F., Plavcan, J. M., Wright, P. C., & Glander K. E. (1988). Sexual selection and canine dimorphism in New World Monkeys. *American Journal of Phyiscal Athropology*, *77*, 385-397.

Kay, R. F., Cartmill, M., & Balow, M. (1998). They hypoglossal canal and the origin of human vocal behavior. *Proceedings for the National Academy of Sciences*, *95*, 5417-5419.

Kennett, C., & Linden, R. (1987). Do periodontal mechanoreceptors contribute to the control of normal bite forces in man? *Journal of Dental Research, 66*, 881.

Kieser, J., Kuzmanovic, D., Payne, A., Dennison, J., & Herbison, P. (2002). Patterns of emergence of the human mental nerve. *Archives of Oral Biology, 47*, 743-747.

Kiliaridis, S., Engström, C., & Thilander, B. (1985). The relationship between masticatory function and craniofacial morphology. *European Journal of Orthodontics, 7*(4), 273-283.

Kiliaridis, S. (1995). Masticatory muscle influence on craniofacial growth. *Acta Odontologica Scandinavica*, *53*, 196-202.

Kinzey, W. G. (1992). Dietary and dental adaptation in the Pitheciinae. *American Journal of Physical Anthropology, 88*, 499-514.

Kinzey, W. G., & Norconk, M. A. (1993). Physical and chemical properties of fruit and seeds eaten by *Pithecia* and *Chiropotes* in Surinam and Venezuela. *International Journal of Primatology*, *14*, 207-227.

Kjaer, I. (1989). Formation and early prenatal location of the human mental foramen. *Scandinavian Journal of Dental Research, 97*, 1-7.

Kleinman, P. K., Zito, J. L., Davidson, R. I., & Raptopoulos, V. (1983). The subarachnoid spaces in children: normal variations in size. *Radiology, 147*(2), 455-457.

Klinge, B., Petersson, A., & Maly, P. (1989). Location of the mandibular canal: comparison of macroscopic findings, conventional radiography, and computed tomography. *International Journal of Oral Maxillofacial Implants, 4*, 327-332.

Komuro, A., Morimoto, T., Iwata, K., Inoue, T., Masuda, Y., Kato, T., & Hidaka, O. (2001). Putative feed-forward control of jaw-closing muscle activity during rhythmic jaw movements in the anesthetized. *Journal of Neurophysiology, 86*, 2834-2844.

Kramer, A. (1989). *The evolutionary and taxonomic affinities of the Sangrian mandibles of Central Java, Indonesia*. University of Michigan Press.

Kress, B., Gottschalk, A., Anders, L., Stippich, C., Palm, F., Bahren, W., & Sartor, K. (2004). High-resolution dental magnetic resonance imaging of inferior alveolar nerve responses to the extraction of third molars. *European Radiology, 14*, 1416-1420.

Kubota, K., & Osanai, K. (1977). Periodontal sensory innervation of the dentition of the Japanese Shrew Mole. *Journal of Dental Research, 56*(5), 531-537.

Kuzentsova, L., & Smirnov, V. (1969). Individual variability of the form and position of the mandibular and mental foramina. *Stomatologia (Moskva), 48*, 54-57.

Lahann, P. (2006). Feeding ecology and seed dispersal of sympatric cheirogaleid lemurs (*Microbus murinus*, *Cheirogaleus medius*, *Cheirogaleus major*) in the littoral rainforest of south-east Madagascar. *Journal of Zoology, 271*(1), 88-98.

Lanyon, L., & Skerry, T. (2001). Postmenopausal osteoporosis as a failure of bone's adaption to functional loading: a hypothesis. *Journal of Bone Mineral Research, 16*, 1937-1947.

Lavigne, G., Kim, J., Valiquette, C., & Lund, J. (1987). Evidence that periodontal pressoreceptors provide positive feedback to jaw closing muscles during mastication. *Journal of Neurophysiology, 58*(2), 342-358.

Lee, J. J. W., Constantino, P. J., Lucas, P. W., & Lawn, B. R. (2011). Fracture in teeth - a diagnostic for inferring bit force and tooth function. *Biological Reviews, 86*, 959-974.

Leitch, D. B., Sarko, D. K., & Catania, K. C. (2014). Brain mass and cranial nerve size in shrews and moles. *Scientific Reports, 4*, 6241.

Leighton, M. (1993). Modeling dietary selectivity by Bornean orangutans: evidence for integration of multiple criteria in fruit selection. *International Journal of Primatology, 14*, 257-313.

Leutenegger, W., & Kelley, J. T. (1977). Relationship of sexual dimorphism in canine size and body size to social, behavior, and ecologicl correlates in anthropoid primates. *Primates, 18*, 117-136.

Lewinsky, W., & Steward, D. (1937). A comparative study of the innervation of teeth. *Proceedings for the Royal Society of Medicine, 30*, 1355-1369.

Li, Z., Ketcham, R. A., Yan, F., Maisano, J. A., & Clarke, J. A. (2016). Comparison and evaluation of the effectiveness of two approaches of diffusible iodine-based contrast-enhanced computed tomography (diceCT) for avian cephalic material. *Journal of Experimental Zoology (Mol. Dev. Evol.), 326B*, 352-362.

Liang, X., Jacobs, R., Corpas, L., Semal, P., & Lambrichts, I. (2009). Chronologic and geographic variability of neuromuscular structures in the human mandible. *Forensic Science International, 190*, 24-32.

Lima, E. M., & Ferrari, S. F. (2003). Diet of a free-ranging group of squirrel monkeys (*Saimiri sciureus*) in Eastern Brazilian Amazonia. *Folia Primatologica, 74*, 150-158.

Linden, R. W. A. (1991). Periodontal mechanoreceptors and their functions. In A. Taylor (Ed.), *Neurophysiology of the jaws and teeth* (pp. 52-88). Palgrave Macmillan.

Lindh, C., Petersson, A., & Klinge, B. (1995). Measurements of distances related to the mandibular canal in radiographs. *Clinical Oral Implants Research, 6*, 96-103.

Littner, M., Kaffe, I., Tamse, A., & Dicapue, P. (1986). Relationship between the apices of the lower molars and mandibular canal - a radiographic study. *Oral Surgery, Oral Medicine, and Oral Pathology, 62*, 595-602.

Loewenstein, W., & Rathkamp, R. (1955). A study on the pressoreceptive sensibility of the tooth. *Journal of Dental Research, 34*, 287-294.

Lucas, L. (2012). *Variation in dental morphology and bite force along the tooth row in anthropoids.* (Unpublished doctoral dissertation), Arizona State University, Arizona, United States.

Lucas, P. (1979). The dental-dietary adaptations of mammals. *Neus Jahrbuch Geology and Paleontology, 8*, 486-512.

Lucas, P. (1994). Categorization of food items relevant to oral processing. In D. Chivers & P. Langer (Eds.), *The digestive system in mammals: food, form, and function* (pp. 197-219). Cambridge University Press.

Lucas, P., Darvell, B., Lee, P., Yuen, T., & Choong, M. (1995). The toughness of plant cell walls. *Philosophical Transactions of the Royal Society of London B, 348*, 363-372.

Lucas, P., & Luke, D. (1980). Chewing it over: basic principles of food breakdown. In D. Chivers, B. Wood, & A. Bilsborough (Eds.), *Food Acquisition and Processing in Primates* (pp. 283-301). Plenum Press.

Lucas, P. W., Peters, C. R., & Arrandale, S. R. (1994). Seed-breaking forces exerted by orangutans with their teeth in captivity and a new technique for estimating forces produced in the wild. *American Journal of Physical Anthroplogy, 94*, 365-374.

Lucas, P., & Teaford, M. (1994). Functional morphology of colobine teeth. In A. Davies & J. Oates (Eds.), *Colobine monkeys: their ecology, behavior, and evolution* (pp. 173-204). Cambridge University Press.

Lucas, P. W. (2006). *Dental functional morphology*. Cambridge University Press.

Luke, D., & Lucas, P. (1983). The significance of cusps. *Journal of Oral Rehabilitation, 10*, 197-206.

Lumsden, A., & Osborn, J. (1977). The evolution of chewing: a dentist's view of paleontology. *Journal of Dentistry, 5*, 269.

Lund, J., McLachlan, R., & Dellow, P. (1971). A lateral jaw movement reflex. *Exploratory Neurology, 31*, 189-199.

Lund, J. P., & Kolta, A. (2006). Generation of the central masticatory pattern and its modification by sensory feedback. *Dysphagia, 2006*, 167-174.

Lund, J. P., Kolta, A., Westberg, K. G., & Scott, G. (1998). Brainstem mechanisms underlying feeding behaviors. *Current Opinion in Neurobiology, 8*, 718-724.

Lund, P. J. (1991). Mastication and its control by the brain stem. *Critical Reviews in Oral Biology and Medicine, 2*(1), 33-64.

Luo, P., & Dessem, D. (1996). Morphological evidence for recurrent jaw-muscle spindle afferent feedback within the mesencephalic trigeminal nucleus. *Brain Research, 710*, 260-264.

Luschei, E., & Goodwin, G. (1974). Patterns of mandibular movements and jaw activity during mastication in monkeys. *Journal of Neurophysiology, 37*, 954-966.

Luschei, E. S., & Goldberg, L. J. (2011). Neural mechanisms of mandibular control: mastication and voluntary biting. *Comprehensive Physiology*, *S2*, 1237-1274.

Lycett, S. J., & Collard, M. (2005). Do homologies impede phylogenetic analyses of the fossil hominids? An assessment based on extant papionin craniodental morphology. *Journal of Human Evolution, 5*, 618-642.

Mackinnon, S. E., & Dellon, A. L. (1995). Fascicular patterns of the hypoglossal nerve. *Journal of Reconstructive Microsurgery, 11*(3), 195-198.

Maeda, T. (1987). Sensory innervation of the periodontal ligament in the incisor and molar of the monkey *Mucaca fuscata.* An immunohistochemical study for neurofilament protein and glia-specific S-100 Protein. *Archives of Histology Japan, 501*, 437-454.

Mardinger, O., Chaushu, G., Arensburg, B., Taicher, S., & Kaffe, I. (2000). Anatomic and radiologic course of the mandibular incisive canal. *Surgical Radiological Anatomy, 22*, 157-161.

Martínez-Marcos, A., & Sañudo, J. R. (2019). Cranial Nerves: phylogeny and ontogeny. *The Anatomical Record, 302*, 378-380.

Marques, C., & Mathias, M.L. (2001). The diet of the European wild rabbit, *Oryctolagus cuniculus* (L.), on different coastal habitats of Central Portugal. *Mammalia, 65*(4), 437-449.

Matsuda, I., Clauss, M., Tuuga, A., Sugau, J., Hanya, G., Yumoto, T., Bernard, H., & Hummel, J. (2017). Factors affecting leaf selection by foregut-fermenting proboscis monkeys: new insight from in vitro digestibility and toughness of leaves. *Scientific Reports, 7*, 1-10.

Matsuda, Y. (1929). Future observations on the mental foramen in the human mandibles. *American Dental Surgery, 49*, 445-452.

Matthews, B. (1976). *Reflexes elicitable from the jaw muscles in man.* Paper presented at the Mastication: Proceedings of a Symposium on the Clinical and Physiological Aspects of Mastication, Bristol, United Kingdom.

Matthews, B. (1977). *Coupling between nerve terminals in teeth.* Paper presented at the Pain in the trigeminal region, Department of Physiology, Bristol, United Kingdom.

McDavid, S., Verdier, D., Lund, J. P., & Kolta, A. (2008). Electrical properties of interneurons found within the trigeminal motor nucleus. *European Journal of Neuroscience, 28*, 1136-1145.

McNamara, J. (1974). An electromyographic study of mastication in the rhesus monkey. *Archives of Oral Biology, 19*, 821-823.

Metscher, B. D. (2009). MicroCT for comparative morphology: simple staining methods allow high-contrast 3D imaging of diverse non-mineralized animal tissues. *BMC Physiology, 9*(11), 1-14.

Miles, A., & West, W. (1954). The relationship of the mandibular third molar to the mandibular canal. *Dental Practice, 4*, 370-375.

Mittermeier, R. A., & van Roosmalen, M. G. M. (1981). Preliminary observations on habitat utilization and diet in eight Surinam monkeys. *Folia Primatology (Basel), 36*, 1-39.

Montagu, A. (1954). The direction and position of the mental foramen in the great apes and man. *American Journal of Physical Anthropology, 12*, 503-518.

Moore, W., Lavelle, C., & Spence, T. (1968). Changes in the size and shape of the human mandible in Britain. *British Dental Journal, 4*, 163-169.

Morquette, P., Lavoie, R., Fhima, M.-D., Lamoureux, X., Verdier, D., & Kolta, A. (2012). Generation of the masticatory central pattern and its modulation by sensory feedback. *Progress in Neurobiology, 96*, 340-355.

Morris, H., Sir, & Jackson, C. M. (1933). *Morris' human anatomy: a complete systematic treatise*. P. Blakiston's son and co., inc.

Mosimann, J. E. (1970). Size allometry: size and shape variables with characterizations of the lognormal and generalized gamma distributions. *Journal of American Statistical Association, 65*(330), 930-945.

Moss, M. L., & Salentijn, L. (1969). The primary role of functional matrices in facial growth. *American Journal of Orthodontics*, *55*, 566-577.

Muchlinski, M. N. (2008). The relationship between the infraorbital foramen, infraorbital nerve, and maxillary mechanoreception: implications for interpreting the paleoecology of fossil mammals based on infraorbital foramen size. *The Anatomical Record, 291*, 1221-1226.

Muchlinski, M. N. (2010). Ecological Correlates of Infraorbital Foramen Area in Primates. *American Journal of Physical Anthropology,* 141, 131-141.

Muchlinski, M. N., & Deane, A. S. (2014). The interpretive power of infraorbital foramen area in making dietary inferences in extant apes. *The Anatomical Record, 297*, 1377-1384.

Muchlinski, M. N., & Deane, A. S. (2016). Dietary correlates associated with the mental foramen in primates: implications for interpreting the fossil record. *Journal of Morphology, 277*(7), 978-985.

Müller, K.H. (1996). Diet and feeding ecology of Masked Titis (*Callicebus personatus*). In M.A. Norconk, A. L. Rosenberger, & P. A. Garber (Eds.), *Adaptive radiation of neotropical primates* (pp. 383-401). Springer.

Murphy, T. (1968). Progressive reduction of tooth cusps as it occurs in the natural dentition. *Dental Practice and Dental Research, 19*(1), 8-14.

Murphy, T., & Grundy, E. (1969). The inferior alveolar neuromuscular bundle at the mandibular foramen. *Dental Practice and Dental Research, 20*, 41-48.

Mwaniki, D., & Hassanali, J. (1992). The position of mandibular and mental foramina in Kenyan African mandibles. *East African Medical Journal, 69*(4), 210-213.

Naitoh, M., Hiraiwa, Y., Aimiya, H., Gotoh, K., & Ariji, E. (2009a). Accessory mental foramen assessment using cone-beam computed tomography. *Oral Surgery, Oral Medicine, Oral Pathology, Oral Radiology, and Endodontics, 107*, 289-294.

Naitoh, M., Nakahara, K., Hiraiwa, Y., Aimiya, H., Gotoh, K., & Ariji, E. (2009b). Observation of buccal foramen in mandibular body using cone-beam computed tomography. *Okajimas Folia Anatomy Japan, 86*, 25-29.

Naitoh, M., Nakahara, K., Suenaga, Y., Gotoh, K., Kondo, S., & Ariji, E. (2010). Comparison between cone-beam and multislice computed tomography depicting mandibular neuromuscular canal structures. *Oral Surgery, Oral Medicine, Oral Pathology, Oral Radiology, and Endodontology, 109*(1), E25-E31.

Naitoh, M., Yoshida, K., Nakahara, K., Gotoh, K., & Ariji, E. (2011). Demonstration of the accessory mental foramen using rotational panoramic radiography compared with cone-beam computed tomography. *Clinical Oral Implants Research, 22*, 1415-1419.

Nakagawa, N. (2003). Difference in food selection between patas monkeys (*Erythrocebus patas*) and tantalus monkeys (*Cercopithecus aethiops tantalus*) in Kala Maloue National Park, Cameroon, in relation to nutrient content. *Primates, 44,* 3-11.

Nekaris, K., & Bearder, S. (2011). The lorisiform primates of Asia and mainland Africa. In C. Campbell, A. Fuentes, K. MacKinnon, S. Beader, R Stumpf (Eds.), *Primates in Perspective* (pp. 34-54). Oxford University Press.

Ness, A. (1954). The mechanoreceptors of the rabbit mandibular incisor. *Journal of Physiology (London),* 126, 475-493.

Nicholson, M. L. (1985). A study of the position of the mandibular foramen in the adult human mandible. *The Anatomical Record, 212*(1), 110-112.

Nickel, J. C., Iwasaki, L. R., & McLachlan, K. R. (1997). Effect of the physical environment on growth of the temporomandibular joint. In C. McNeill (Ed.), *Science and practice of occlusion* (pp. 115-124). Quntessence Publishing Co.

Norconk, M.A. & Conklin-Brittain, N.L. (2004). Variation on frugivory: the diet of Venezuelan white-faced Sakis. *International Journal of Primatology, 25*(1), 1-26.

Nortje, C., Farman, A., & Grotepass, F. (1977). Variations in the normal anatomy of the inferior dental (mandibular) canal: a retrospective study of panoramic radiographs from 3,612 routine dental patients. *British Journal of Oral Surgery, 15*, 55-63.

Nuwer, M.R., & Pouratian, N. (2017). Monitoring of neural function: electromyography, nerve conduction, and evoked potentials. In H. R. Winn (Ed.), *Youmans and Winn neurological surgery* (pp. 1996-2003). Elsevier.

O'Brien, H. D., & Bourke, J. (2015). Physical and computational fluid dynamics models for the hemodynamics of the artiodactyl carotid rate. *Journal of Theoretical Biology, 386*, 122-131.

O'Brien, H. D., & Williams, S. H. (2014). Using biplanar fluoroscopy to guide radiopaque vascular injections: a new method for vascular imaging. *PLOS One, 9*(5), e97940.

Okecha, A. A., & Newton-Fisher, N. E. (2006). The diet of olive baboons (*Papio anubis*) in the Budongo Forest Reserve, Uganda. In N.E. Newton-Fisher, H. Notman, J. D. Paterson, & V. Reynolds (Eds.), *Primates of Western Uganda* (pp. 61-73). Springer.

Oliveira-Santos, C., Souza, P. H. C., De Azambuja Berti-Couto, S., Stinkens, L., Moyaert, K., Van Assche, N., & Jacobs, R. (2011). Characterisation of additional mental foramina through cone beam computed tomography. *Journal of Oral Rehabilitation, 38*, 595-600.

Olivier, E. (1927). Le canal dentaire inférieur et son nerf chez l'adulte. *Annals of Anatomical Pathology (Paris), 4*, 975-987.

Olivier, E. (1928). The inferior dental canal and its nerve in the adult. *British Dental Journal, 49*, 356-358.

Orhan, A. I., Orhan, K., Aksoy, S., Özgül, Ö., Horasan, S., Arslan, A., & Kocyigit, D. (2013). Evaluation of perimandibular neurovascularization with accessory mental foramina using cone-beam computed tomography in children. *The Journal of Craniofacial Surgery, 24*(4), E365-E369.

Osburn, J. W., & Lumsden, A. G. S. (1978). An alternative to "thegosis" and re-examination of the ways in which mammalian molars work. *News Jahrbuch Geology and Paleontology, 156*, 371-386.

Overdorff, D. J., Strait, S. G., & Telo, A. (1997). Seasonal variation in activity and diet in small-bodied folivorous primate, *Hapalemur griseus*, in Southeastern Madagascar. *American Journal of Primatology, 43,* 211-223.

Pampush, J. D., Duque, A.C., Burrows, B.R., Daegling, D. J., Kenney, W., F., & McGraw, W. S. (2013). Homoplasy and thick enamel in primates. *Journal of Human Evolution*, *64*, 216-224.

Pampush, J. D., Winchester, J. M., Morse, P. E., Vining A. Q., Boyer, D. M., & Kay, R. F. (2016a). Introducing molaR: a new R package for quantitative topographic analysis of teeth (and other topgraphic surfaces). *Journal of Mammalian Evolution, 23*, 397-412.

Pampush, J.D., Spradley, J. P., Morse, P. E., Harrington, A. R., Allen, K. L., Boyer, D. M., & Kay, R. F. (2016b). Wear and its effect on dental topography measures in howling monkeys (*Alouatta palliata*). *American Journal of Physical Anthropology, 161*, 705-721.

Paraskevas, G., Mavrodi, A., & Natsis, K. (2015). Accessory mental foramen: an anatomical study on dry mandibles and review of the literature. *Oral Maxillofacial Surgery, 19*, 177-181.

Passamani, M., & Ryands, A. B. (2000). Feeding behavior of Geoffroy's marmoset (*Callitrhix geoffroyi*) in an atlantic forest fragment of South-eastern Brazil. *Primates, 41*(1), 27-38.

Pashley, D.H., Walton, R.E., & Slavkin, H.C. (2002). Histology and physiology of the dental pulp. In J. I. Ingle & L. K. Bakland (Eds.), *Endodontics* (pp. 25-55). PMPH-USA.

Passatore, M., Lucchi, M., Fillipi, G., Manni, E., & Bortalami, R. (1983). Localization of neurons innervating masticatory muscle spindle and periodontal receptors in the mesencephalic trigeminal nucleus and their reflex actions. *Archives of Italian Biology, 121*, 117-130.

Peyron, M., Lassauzay, C., & Woda, A. (2002). Effects of increased hardness on jaw movement and muscle activity during chewing of disco-elastic model foods. *Experimental Brain Research, 142*, 41-51.

Pickford, M. (1986). On the origins of body size dimorphism in primates. *Human Evolution, 1*(1), 77-90.

Plaffman, C. (1939). Afferent impulses from the teeth due to pressure and noxious stimulation. *Journal of Physiology (London), 97*, 207-219.

Placvan, J. M. (1993). Canine size and shape in male anthropoid primates. *American Journal of Physical Anthropology*, *92*(2), 201-216.

Plavcan, J. M., & van Schaik, C. P. (1992). Intrasexual competition and canine dimorphism in anthropoid primates. *American Journal of Physical Anthropology, 14*, 132.

Polland, K., Muro, S., Reford, G., Lockhart, A., Logan, G., & Brocklebank, L. (2001). The mandibular canal of the edentulous jaw. *Clinical Anatomy, 14*, 445-452.

Prabodha, L., & Nanayakkara, B. (2006). The position, dimensions and morphological variations of mental foramen in mandibles. *Galle Medical Journal, 11*(1), 13-15.

Prado, F. B., Groppo, F. C., Volpato, M. C., & Caria, P. H. F. (2010). Morphological changes in the position of the mandibular foramen in dentate and edentate Brazilian subjects. *Clinical Anatomy, 23*(4), 394-398.

Prinz, J., & Lucas, P. (2000). Saliva tannin interactions. *Journal of Oral Rehabilitation, 27*, 991-994.

Proffit, W. R., Fields, H. W., & Nixon, W. L. (1983). Occlusal forces in normal-and long-face adults. *Journal of Dental Research*, *62*, 566-570.

Quam, R., & Smith, F. (1998). A reassessment of the Tabun C2 mandible. In T. Akazawa, K. Aoki, & O. Bar-Yosef (Eds.), *Neandertals and modern humans in Western Asia* (pp. 405-421). Plenum Press.

Rees, L. A. (1954). The structure and function of the mandibular joint. *British Dental Journal, 96*, 125-133.

Riesenfeld, A. (1956). Multiple infraorbital, ethmoidal, and mental foramina in the races of man. *American Journal of Physical Anthropology, 14*, 85-100.

Riesenfeld, A. (1970). The effect of environmental factors on tooth development: an experimental investigation. *Acta Anatomica, 77*, 188-215.

Rilling, J. K. (2006). Human and nonhuman primate brains: are they allometrically scaled versions of the same design? *Evolutionary Anthropology, 14*, 65-77.

Roberts, N. M., Rabeni, C. F., Stanovick, J. S., & Hamilton, D. A. (2008). River Otter, *Lontra canadensis*, food habits in the Missouri Ozarks. *The Canadian Field-Naturalist, 122*(4), 303-311.

Robinson, C. & Yoakum, C. (2019). Variation in accessory mental foramen frequency and number in extant hominoids. *The Anatomical Record*, *303*(12): 3000-3013.

Rood, J. (1978). The diameter and intermodal lengths of the myelinated fibers in human alveolar nerve. *Journal of Dentistry, 6*, 311-315.

Rosas, A. (1997). A gradient of size and shape for the Atapuerca sample and middle Pleistocene hominid variability. *Journal of Human Evolution, 33*, 319-331.

Rosas, A. (2001). Occurrence of Neanderthal features in mandibles from the Atapuerca-SH site. *American Journal of Physical Anthropology, 33*, 319-331.

Rosenberger, A. L., & Kinzey, W. G. (1976). Functional patterns of molar occlusion in platyrrhine primates. *American Journal of Physical Anthropology, 45*, 281-298.

Rosenquist, B. (1996). Is there an anterior loop of the inferior alveolar nerve? *International Journal of Periodontics and Restorative Dentistry, 16*, 40-45.

Ross, C. F., Baden, A. L., Georgi, J., Here, A., Metzger, K. A., Reed, D. A., Schaerlaeken, V., & Wolff, M. S. (2010). Chewing variation in lepidosaurs and primates. *The Journal of Experimental Biology, 213*, 572-584.

Ross, C. F., & Iriarte-Diaz, J. (2014). What does feeding system morphology tell us about feeding? *Evolutionary Anthropology, 23*, 105-120.

Ruff, C., Holt, B., & Trinkaus, E. (2006). Who's afraid of the big bad Wolff?: "Wolff's Law" and bone functional adaptation. *American Journal of Physical Anthropology, 129*, 484-498.

Ruslin, F., Matsuda, I., & Md-Zain, B. M. (2019). The feeding ecology and dietary overlap in two sympatric primate species (*Macaca fascicularis*) and dusky langur (*Trachypithecus obscurus obscurus*), in Malaysia. *Primates, 60,* 41-50.

Sandring, S. (2015). *Gray's anatomy: the anatomical basis of clinical practice*. Elsevier Limited.

Sawyer, D. R., Kiely, M. L., & Pyle, M. A. (1998). The frequency of accessory mental foramina in four ethnic groups. *Archives of Oral Biology, 43*, 417-420.

Sayers, K., & Norconk, M. A. (2008). Himalayan *Semnopithecus entellus* at Langtang National Park, Nepal: diet, activity, patterns, and resources. *International Journal of Primatology, 29,* 509-530.

Scott, J. E., & Hogue, A. (2012). The adaptive signficance of mandiublar symphyseal fusion in mammals. *Journal of Evolutionary Biology*, *25*(4), 661-673.

Scott, J. E., Campbell, R. M., Baj, L. M., Burns, M. C., Price, M. S., Sykes, J. D., & Vinyard, C. J. (2018). Dietary signals in the premolar dentition of primates. *Journal of Human Evolution, 121*, 221-234.

Sella-Tunis, T., Pokhojaev, A., Sarig, R., O'Higgins, P., & May, H. (2018). Human mandibular shape is associated with masticatory muscle force. *Scientific Reports*, *8*, 6042.

Senyurek, M. (1946). Multiple mental foramina. *Nature, 157*, 792-793.

Sessle, B. J., Yao, D., Nishiura, H., Yoshino, K., Lee, J.-C., Martin, R. E., & Murray, G. M. (2005). Properties and plasticity of the primate somatosensory and motor cortex related to orofacial sensorimotor function. *Clinical and Experimental Pharmacology and Physiology, 32*, 109-114.

Seto, H. (1972). The sensory innervation of the oral cavity in the human fetus and juvenile mammals. In J. F. Bosma (Ed.), *Third symposium on oral sensation and perception* (Vol. Third, pp. 35-75). Washington, DC: U.S. Government Printing Office.

Shadad, O., Chaulagain, R., Luukko, K., & Kettunen, P. (2019). Establishment of tooth blood supply and innervation is developmentally regulated and takes place through differential patterning processes. *Journal of Anatomy, 234*(4), 465-479.

Shah, N. F. (2003). *Foraging strategies in two sympatric mangabey species (Cercocebus agilis and Lophocebus albigena)*. (Unpublished doctoral dissertation). State University of New York at Stony Brook, New York.

Shellis, R. P., Beynon, A., D., Reid, D. J., & Hiiemae, K. M. (1998). Variations in molar enamel thickness among primates. *Journal of Human Evolution*, *35*(4-5), 507-522.

Shigenaga, Y., Sera, M., Nishimori, T., Suemune, S., Nishimura, M., Yoshida, A., & Tsuru, K. (1988). The central projection of masticatory afferent fibers to the trigeminal sensory nuclear complex and upper cervical spinal cord. *The Journal of Comparative Neurology, 268*, 489-507.

Simmen, B., Hladik, A., & Ramasiarisoa, P. (2003). Food intake and dietary overlap in native *Lemur catta* and *Propitehcus verreauxi* and introduced *Eulemur fulvus* at Berenty, Southern Madagascar. *International Journal of Primatology, 24,* 949-968.

Simmen, B., Bayart, F., Marez, A., & Hladik, A. (2007). Diet, nutritional ecology, and birth season of *Eulemur macaco* in an anthropogenic forest in Madagascar. *International Journal of Primatology, 28*, 1253-1266.

Simonton, F. (1923). Mental foramen in the anthropoids and in man. *American Journal of Physical Anthropology, 6*, 413-421.

Singh, G. P. (2019). Anatomy of Trigeminal Nerve. In G. P. Rath (Ed.), *Handbook of Trigeminal Neuralgia* (pp. 11-22). Springer Nature Singapore Pte Ltd.

Singleton, M. (2004). Geometric morphometric analysis of functional divergence in mangabey facial form. *Journal of Anthropological Sciences, 82*, 27-44.

Smith, R. J. (1978). Mandibular biomechanics and temporomandibular joint function in primates. *American Journal of Physical Anthropology, 49*(3), 341-350.

Spencer, M. (2003). Tooth root form and function in platyrrhine seed-eaters. *American Journal of Physical Anthropology, 122*, 325-335.

Spriggs, A. N., Muchlinski, M. N., & Gordon, A. D. (2016). Does the primate pattern hold up? Testing the functional significance of infraorbital foramen size variation among Marsupials. *American Journal of Physical Anthropology, 160*, 30-40.

Starkie, C., & Stewart, D. (1931). The intra-mandibular course of the inferior dental nerve. *Journal of Anatomy, 65*, 319-323.

Stefan, V., & Trinkaus, E. (1998). Discrete trait and dental morphometric affinities of the Tabun 2 mandible. *Journal of Human Evolution, 34*, 443-468.

Stephans, H., Frahm, H., & Baron, G. (1981). New and revised data on volumes of brain structures in insectivores and primates. *Folia Primatologica*, *35*, 1-29.

Stephan, H., Baron G., & Frahm, H. (1988). Comparative size of brain and brain components. *Comparative Primate Biology*, *4*, 1-38.

Stern, J. T. (2003). *Essentials of gross anatomy*. F. A. Davis Company.

Stewart, D. (1927). Some aspects of the innervation of the teeth. *Proceedings for the Royal Society of Medicine, 20*, 1675-1686.

Stockdale, C. (1959). The relationship of the roots of mandibular third molars to the inferior dental canal. *Oral Surgery, Oral Medicine, and Oral Pathology, 12*, 1061-1072.

Strait, D. S., Weber, G. W., Neubauer, S., Chalk, J., Richmond, B. G., Lucas, P. W., Spencer, M. A., Schrein, C., Dechow, P. C., Ross, C. F., Grosse, I. R., Wright, B. W., Constantino, P., Wood, B. A., Lawn, B., Hylander, W. L., Wang, Q., Byron, C., Slice, D. E., & Smith, A. L. (2009). The feeding biomechanics and dietary ecology of *Australopithecus africanus*. *Proceedings of the National Academy of Sciences of the United States of America, 106*(7), 2124-2129.

Strait, S. (1993a). Molar microwear in extant small-bodied faunivorous mammals: An analysis of feature density and pit frequency. *American Journal of Physical Anthropology, 92*, 63-79.

Strait, S. (1993b). Molar morphology and food texture among small-bodied insectivorous mammals. *Journal of Mammology, 74*, 391-402.

Strait, S., & Overdorff, D. (1996). Physical properties of fruits eaten by Malagasy primates. *American Journal of Physical Anthropology (Supplemental), 22*, 224.

Strait, S. G. (1997). Tooth use and the physical properties of food. *Evolutionary Anthropology, 5*(6), 199-211.

Strait, S. G. (2001). Dietary reconstruction of small-bodied omomyoid primates. *Journal of Vertebrate Paleontology, 21*(2), 322-334.

Streicher, U. (2009). Diet and feeding behaviour of pygmy lorises (*Nycticebus pygmaeus*) in Vietnam. *Vietnamese Journal of Primatology, 3,* 37-44.

Stringer, C. (1987). A numerical cladistics for the genus *Homo*. *Journal of Human Evolution, 16*, 135-146.

Stringer, C., Hublin, J., & Vandermeersch, B. (1984). The origin of anatomically modern humans in Western Asia. In F. Smith & F. Spencer (Eds.), *The origins of modern humans: a world survey of the fossil evidence* (pp. 51-135). Alan R. Liss.

Sudiwala, S., & Knox, S. M. (2018). The emerging role of cranial nerves in shaping craniofacial development. *Genesis*, *57*, e23282.

Sutton, R. (1974). The practical significance of mandibular accessory foramina. *Australian Dental Journal, 19*, 167-173.

Taylor, A. B. (2002). Masticatory form and function in the African Apes. *American Journal of Physical Anthropology, 117*, 133-156.

Tang, C, Huang, L., Huang, Z., Krzton, A., Lu, C., & Zhou, Q. (2016). Forest seasonality shapes diet of limestone-living rhesus macaques at Nonggang, China. *Primates, 57,* 83-92.

Teaford, M. F. (1985). Molar micro wear and diet in the genus *Cebus. American Journal of Physical Anthropology, 66*, 363-370.

Teaford, M. F., (2007) What do we know and no know about diet and enamel structure? In P. S. Ungar (Ed.), *Evolution of the human diet; The known, the unknown, and the unknowable* (pp. 56-76). Oxford University Press.

Teaford, M. F., Lucas, P. W., Ungar, P. S., & Glander, K. E. (2006). Mechanical defenses in leaves eaten by Costa Rican howling monkeys (*Alouatta palliata)*. *American Journal of Physical Anthropology, 129*, 99-104.

Teaford, M. F., & Oyen, O. J. (1989). Differences in the rate of molar wear between monkeys raised on different diets. *Journal of Dental Research, 68*(11), 1513-1518.

Thangavelu, K., Kannan, R., Senthil Kumar, N., Rethish, E., Sabitha, S., & SayeeGanesh, N. (2012). Signficance fo localization of mandibular foramen in an inferior alveolar nerve block. *Journal of Natural Science, Biology, and Medicine, 3*(2), 156-160.

Thexton, A., & Hiiemae, K. (1997). The effect of food consistency upon jaw movement in the macaque: A cineradiographic study. *Journal of Dental Research, 76*(1), 552-560.

Thexton, A., Hiiemae, K. M., & Crompton, A. (1980). Food consistency and bite size as regulators of jaw movement during feeding in the cat. *Journal of Neurophysiology, 44*(3), 456-474.

Trejo, J. L. (2019). Cranial nerves: mind your head. *The Anatomical Record, 302*, 374-377.

Trinkaus, E. (1993). Variability in the position of the mandibular mental foramen and the identification of Neandertal apomorphies. *Riviste di Antropologia (Roma), 71*, 259-274.

Trulsson, M. (2006). Sensory-motor function of human periodontal mechanoreceptors. *Journal of Oral Rehabilitation, 33*, 262-273.

Trulsson, M., & Johansson, R. S. (1996). Encoding of tooth loads by human periodontal afferents and their role in jaw motor control. *Progress in Neurobiology, 49*, 267-284.

Trulsson, M., Johansson, R. S., & Olsson, K. A. (1992). Directional sensitivity of human periodontal mechanoreceptive afferents to forces applied to the teeth. *Journal of Physiology, 447*, 373-389.

Turman, J. E. (2007). the development of mastication in rodents: from neurons to behaviors. *Archives of Oral Biology, 52*, 313-316.

Udhaya, K., Saraladevi, K., & Sridhar, J. (2013). The morphometric analysis of the mental foramen in adult dry human mandibles: a study on the South Indian population. *Journal of Clinical Diagnosis Research, 7*(8), 1547-1551.

Ungar, P. (1998). Dental allometry, morphology, and wear as evidence for diet in fossil primates. *Evolutionary Anthropology*, *6*, 205-217.

Ungar, P. (2002). Reconstructing the diets of fossil primates. In M. Plavcan, R. Kay, W. Junger, & C. Van Schaik (Eds.), *Reconstructing behavior in the fossil record* (pp. 261-296). Kluwer Academic Plenum Publishers.

Ungar, P. (2015). Mammalian dental function and wear: A review. *Biosurface and Biotribology, 1*, 25-41.

Ungar, P. S., & Williamson, M. (2000). Exploring the effects of tooth wear on functional morphology: A preliminary study using dental topographic analysis. *Palaeontologia Electronica, 3*, 1-18.

Ungar, P., & M'Kierea, F. (2003). A solution to the worn tooth conundrum in primate functional anatomy. *Proceedings for the National Academy of Sciences, 100*(7)*,* 3874-3877.

van Roosmalen, M. G. M., Mittermeier, R. A., & Fleagle, J. G. (1988). Diet of the northern beaded saki (*Chiropotes satanas chiropotes*): A neotropical seed predator. *American Journal of Primatology, 14*(1), 11-35.

Van Steenberghe, D. (1979). The structure and function of periodontal innervation. A review of the literature. *Journal of Periodontal Research, 14*, 185-203.

Van Wowern, N., & Stoltze, K. (1978). Sex and age differences in bone morphology of mandibles. *Scan Journal of Dental Research, 86*, 478-485.

Vasey, N. (2000). Niche Separation in *Varecia variegata rubra* and *Eulemur fulvus albirons*: I. Interspecific patterns. *American Journal of Physical Anthropology, 112*, 411-431.

Vervust, B., Van Dongen, S., & Van Damme, R. (2009). The effect of preservation on lizard morphometrics - An experimental study. *Amphibians and Reptiles, 30*, 321-329.

Vickerton, P., Jarvis, J., & Jeffery, N. (2013). Concentration-dependent specimen shrinkage in iodine-enhanced microCT. *Journal of Anatomy, 223*, 185-193.

Vinyard, C. J. (2008). Putting shape to work: making functional interpretations of masticatory apparatus shapes in primates. In C. Vinyard (Ed.), *Primate craniofacial function and biology* (pp. 357-385). Springer Science+Business Media, LLC.

Vinyard, C. J., Taylor, A. B., Teaford, M. F., Glander, K. E., Ravosa, M. J., Rossie, J. B., Ryan, T. M., & Williams, S. H. (2011). Are we looking for loads in all the right places? New research directions for studying the masticatory apparatus of New World monkeys. *The Anatomical Record, 294*, 2140-2157.

Voljevica, A., Talović, E., & Hasanović, A. (2015). Morphological and morphometric analysis of the shape, position, number and size of mental foramen on human mandibles. *Acta Medica Academica, 44*(1), 31-38.

Wadu, S., Penhall, B., & Townsend, G. (1997). Morphological variatiability of the human inferior alveolar nerve. *Clinical Anatomy, 10*, 82-87.

Watanabe, S., & Dawes, C. (1988). A comparison of the effects of tasting and chewing foods on the flow rate of whole saliva in man. *Archives of Oral Biology, 33*, 761-764.

Watt, D., & Williams, C. (1951). The effects of the physical consistency of food on the growth and development of the mandible and maxilla of the rat. *American Journal of Orthodontics, 37*, 895-928.

Weijs, W., & De Jong, H. (1977). Strain in mandibular alveolar bone during mastication in the rabbit. *Archives of Oral Biology, 22*, 667-675.

Werner, J. A., Tillmann, B., & Schleicher, A. (1991). Functional anatomy of the temporomandibular joint. *Anatomy and Embryology, 183*, 89-95.

Westberg, K., Clavelou, P., Sandström, G., & Lund, J. (1998). Evidence that trigeminal brainstem interneurons form subpopulations to produce different forms of mastication in the rabbit. *The Journal of Neuroscience, 18*(16), 6466-6479.

Williams, F. L., & Krovitz, G. E. (2004). Ontogenetic migration of the mental foramen in Neandertals and modern humans. *Journal of Human Evolution, 4*, 199-219.

Witmer, L. M., Porter, R., Cerio, D., Nassif, J., Caggiano, E., Griffin, C., & Ridgely, R. (2018). *spiceCT-selectively perfusable iodine-based contrast-enhanced CT, a rapid alternative to diceCT for 3D visualization of vertebrate soft tissues*. Paper presented at the Society for Integrative and Comparative Biology meeting, San Francisco, CA.

Wolff, J. (1892). *Da gasetz der transformation der knoche*. A Hirshwald: Berlin.

Wright, P. C. (1989). The nocturnal primate niche in the New World. *Journal of Human Evolution, 18*(7), 635-658.

Wright, B. W. (2005). Craniodental biomechanics and dietary toughness in the genus *Cebus. Journal of Human Evolution, 48*, 473-492.

Xie, Q., Wolfe, A., Tilvis, R., & Ainamo, A. (1997). Resorption of the mandibular canal wall in the edentulous aged population. *Journal of Prosthetic Dentistry, 77*, 596-600.

Yamada, M., & Kumano, T. (1969). Mobility and assessment of the tactile sensation of teeth. *International Dental Journal, 19*(2), 295-296.

Yamashita, N. (1992). Mechanical variation in the diets of four Malagasy primates. *American Association of Physical Anthropologists (Supplemental), 14*, 176-177.

Yamashita, N. (1996). Functional dental correlates of food properties in five Malagasy lemur species. *American Journal of Physical Anthropology, 106*(2), 169-188.

Yeager, C. P. (1996). Feeding ecology of the long-tailed macaque (*Macaca fascicularis*) in Kalimantan Tengah, Indonesia. *International Journal of Primatology, 17,* 51-62.

Yesilyurt, H., Aydinlioglu, A., Kavakli, A., Ekinci, N., Eroglu, C., Hacialiogullari, M., & Diyarbakirli, S. (2008). Local differences in the position of the mental foramen. *Folia Morphologica, 67*(1), 32-35.

Young, R. F. (1977). *Fiber spectrum of the trigeminal sensory root of frog, cat, and man determined by electronmicroscopy.* Paper presented at the Pain in the trigeminal pain, Department of Physiology, Bristol, United Kingdom.

Zeigler, H. P., Jacquin, M. F., & Miller, M. G. (1984). Trigeminal sensorimotor mechanisms and ingestive behavior. *Neuroscience and Biobehavioral Reviews, 8*, 414-423.

Zhou, X., Wang, B., Pan, Q., Zhang, J., Kumar, S., Sun, X., Liu, Z., Pan, H., Lin, Y., Liu, G., Zhan, W., Li, M, Ren, B., Ma, X., Ruan, H., Cheng, C. Wang, D., Shi, F., Hui, Y., Tao, Y., Zhang, C., Zhu, P., Xiang, Z., Jiang, W., Chang, J., Wang, H., Cao, Z., Jiang, Z., Li, B., Yang, G., Roos, C., Garber, P. A., Bruford, M. W., Li, R., & Li, M. (2014). Whole-genome sequencing of the snub-nosed monkey provide insights into flavory and evolutionary history. *Nature Genetics, 46*(12), 1303-1312.

APPENDICES

APPENDIX A: SUMMARY STATISTICS OF RAW DATA

Table A.1. Summary statistics for the dentin exposure surface area variables by species/sex (mm^2)

Species/Sex	Number of Individuals	Molar Dentin Exposure		Premolar Dentin Exposure		Canine Dentin Exposure		Incisor Dentin Exposure	
		Mean	StdDev	Mean	StdDev	Mean	StdDev	Mean	StdDev
Allenopithecus nigroviridis	1	5.064413	NA	20.27728	NA	NA	NA	8.377586	NA
Male	1	5.064413	NA	20.27728	NA	NA	NA	8.377586	NA
Alouatta caraya	3	46.38942	NA	20.3995	19.88739	30.68278	11.49807	8.886637	6.238395
Female	1	46.38942	NA	41.40986	NA	43.80937	NA	13.29785	NA
Male	2	NA	NA	9.894315	11.3518	24.11949	2.43928	4.475426	NA
Alouatta palliata	2	17.17276	6.709419	22.81052	0.40089	63.74976	18.62973	7.878842	4.742727
Female	1	12.42849	NA	22.52705	NA	76.92298	NA	11.23246	NA
Male	1	21.91704	NA	23.09399	NA	50.57655	NA	4.525228	NA
Aotus trivirgatus	8	21.35858	16.61968	27.08366	22.08517	25.97257	15.76624	3.650712	1.483281
Female	5	20.39682	19.23173	18.91272	17.12814	19.10834	15.09574	2.85291	1.14543
Male	2	30.03163	11.90823	48.00282	32.10574	42.75728	5.374737	5.455317	0.559409
unknown	1	8.821256	NA	26.1	NA	26.72428	NA	4.030509	NA
Ateles geoffroyi	1	20.09723	NA	19.54446	NA	118.648	NA	6.231876	NA
Female	1	20.09723	NA	19.54446	NA	118.648	NA	6.231876	NA
Cacajao calvus	1	NA	NA	8.90506	NA	NA	NA	NA	NA
Male	1	NA	NA	8.90506	NA	NA	NA	NA	NA
Callicebus moloch	7	6.895352	6.179073	11.34501	10.65401	25.90149	16.44311	5.922162	4.50396
Female	1	1.464431	NA	1.572766	NA	7.96657	NA	2.311046	NA
Male	6	7.981536	6.235199	12.97372	10.67366	28.89064	15.7923	6.524014	4.615201
Callithrix argentata	2	14.32372	4.944923	25.47132	4.374043	42.89109	2.467255	4.390283	1.841436
Female	1	10.82713	NA	28.56424	NA	44.6357	NA	3.088191	NA
Male	1	17.82031	NA	22.37841	NA	41.14648	NA	5.692375	NA
Callithrix humeralifera	3	16.23215	2.885619	19.8479	3.408351	72.14193	21.64625	5.874665	1.733808
Female	2	17.47778	2.709981	20.92501	4.033958	76.29608	28.87176	6.746522	1.204729
Male	1	13.74088	NA	17.6937	NA	63.83364	NA	4.130951	NA
Callithrix jacchus	4	12.72637	13.35282	20.43666	25.74956	25.2917	10.10622	4.78626	3.379701
Female	3	14.87151	15.48667	25.78185	28.6903	26.58508	11.96523	5.62955	3.587024

unknown	1	6.290953	NA	4.401104	NA	21.41155	NA	2.256391	NA
Cebus apella	18	24.31715	21.96468	52.57102	62.07883	61.46213	61.00366	5.932315	6.741574
Female	10	14.11157	12.95345	24.46613	29.74141	23.31594	20.27166	3.375855	1.43864
Male	8	35.79844	25.0282	87.70213	75.38558	125.0391	51.6134	9.5844	9.572835
Cebus capucinus	10	57.40481	63.69362	59.30644	69.32287	56.13967	29.54027	5.470905	2.101841
Female	7	62.88805	73.68242	75.21769	78.57399	45.18577	26.33373	5.598646	2.192148
Male	3	44.61058	40.22291	22.18017	12.2567	81.69876	21.13216	5.172843	2.296278
Cercocebus agilis	5	5.047053	2.213972	12.04932	3.206618	23.62931	6.06049	8.235092	11.17193
Female	2	4.657059	3.008559	13.91158	2.728134	25.16832	8.20939	24.97525	NA
Male	3	5.307048	2.241458	10.8078	3.326165	22.09031	5.772379	2.655038	0.629206
Cercocebus torguatus	1	1.80107	NA	NA	NA	7.835958	NA	6.834032	NA
Female	1	1.80107	NA	NA	NA	7.835958	NA	6.834032	NA
Cercopithecus mitis	6	15.75575	8.301566	29.90931	11.20527	35.48776	13.59827	8.502631	3.577918
Female	6	15.75575	8.301566	29.90931	11.20527	35.48776	13.59827	8.502631	3.577918
Cercopithecus neglectus	1	2.55748	NA	4.275752	NA	115.3429	NA	4.167414	NA
Male	1	2.55748	NA	4.275752	NA	115.3429	NA	4.167414	NA
Cheirogaleus major	1	30.98658	NA	43.74214	NA	45.37778	NA	146.1791	NA
unknown	1	30.98658	NA	43.74214	NA	45.37778	NA	146.1791	NA
Chiropotes satanas	3	56.08974	16.86105	41.32122	11.38028	61.79709	73.11235	3.75177	1.44202
Female	1	39.7644	NA	31.60307	NA	113.4953	NA	4.771432	NA
Male	2	64.25241	12.99288	46.1803	10.83319	10.09885	NA	2.732107	NA
Colobus guereza	5	9.812657	6.141975	31.99291	33.57164	177.6926	155.7042	4.335033	1.423504
Female	1	11.57779	NA	NA	NA	55.66255	NA	NA	NA
Male	4	9.371373	7.000019	31.99291	33.57164	208.2001	161.6179	4.335033	1.423504
Colobus polykomos	4	10.03345	2.358494	22.36876	6.156329	101.1783	62.03823	8.440943	6.418374
Female	4	10.03345	2.358494	22.36876	6.156329	101.1783	62.03823	8.440943	6.418374
Erythrocebus patas	3	1.968037	0.503884	6.390038	4.106299	25.67813	11.12683	6.432924	1.989982
Female	2	1.968037	0.503884	8.687557	1.432417	25.67813	11.12683	5.025795	NA
Male	1	NA	NA	1.794999	NA	NA	NA	7.840054	NA
Eulemur fulvus collaris	1	2.933298	NA	3.617394	NA	12.80481	NA	7.247518	NA
unknown	1	2.933298	NA	3.617394	NA	12.80481	NA	7.247518	NA
Eulemur fulvus rufus	2	4.643106	3.293297	13.35984	9.391736	26.30726	37.20091	48.3725	10.07086
Female	1	6.971819	NA	20.0008	NA	52.61227	NA	41.25133	NA
Male	1	2.314393	NA	6.718879	NA	0.002246	NA	55.49367	NA

Eulemur macaco macaco	1	1.807343	NA	5.082679	NA	29.26083	NA	36.30785	NA
Male	1	1.807343	NA	5.082679	NA	29.26083	NA	36.30785	NA
Galago alleni	1	17.21027	NA	13.62876	NA	NA	NA	NA	NA
Female	1	17.21027	NA	13.62876	NA	NA	NA	NA	NA
Galago senegalensis	6	38.42101	15.74803	42.32259	32.9405	65.1809	16.75624	NA	NA
Female	3	38.19584	23.80168	40.03769	33.32315	44.20457	NA	NA	NA
Male	3	38.57113	14.58275	43.84586	40.07787	72.17301	11.30574	NA	NA
Gorilla gorilla gorilla	3	9.55742	NA	18.33131	8.157139	34.43497	46.14404	2.17388	0.925879
Female	2	NA	NA	24.09928	NA	7.827784	3.300176	2.353512	1.233246
Male	1	9.55742	NA	12.56334	NA	87.64933	NA	1.814614	NA
Hapalemur griseus	2	11.13963	9.907959	27.34668	14.02531	109.659	30.50903	NA	NA
Male	2	11.13963	9.907959	27.34668	14.02531	109.659	30.50903	NA	NA
Hapalemur griseus griseus	1	10.32395	NA	13.56133	NA	NA	NA	NA	NA
Female	1	10.32395	NA	13.56133	NA	NA	NA	NA	NA
Homo sapiens	3	NA	NA	3.197878	1.289539	5.237865	3.454317	3.57835	0.58161
Female	2	NA	NA	3.197878	1.289539	3.24357	0.036428	3.875174	0.384598
Male	1	NA	NA	NA	NA	9.226456	NA	2.984703	NA
Lagothrix logotricha	3	12.69812	7.171454	17.84056	6.670311	32.31754	2.067599	3.783794	2.213493
Female	1	4.417246	NA	11.78721	NA	31.54804	NA	2.274661	NA
Male	1	16.82721	NA	24.99164	NA	30.74503	NA	6.32482	NA
unknown	1	16.8499	NA	16.74282	NA	34.65955	NA	2.7519	NA
Lemur catta	1	5.925305	NA	15.23824	NA	93.93497	NA	26.41027	NA
Male	1	5.925305	NA	15.23824	NA	93.93497	NA	26.41027	NA
Lontra canadensis	1	241.8772	NA	257.6072	NA	105.5824	NA	8.273236	NA
Male	1	241.8772	NA	257.6072	NA	105.5824	NA	8.273236	NA
Lophocebus albigena	6	18.36229	5.097629	72.57837	52.56397	106.9989	123.5406	22.35165	11.77247
Female	2	17.55464	6.152692	116.9401	69.16195	14.64464	8.257176	NA	NA
Male	4	18.76612	5.480772	50.39749	32.28817	168.5683	127.5733	22.35165	11.77247
Macaca fascicularis	6	6.752537	3.798883	14.0843	4.049351	153.6367	266.0412	7.42292	5.696749
Female	3	5.126635	3.701779	13.65667	6.001824	24.41538	17.55973	9.334216	7.121666
Male	3	9.191389	3.239298	14.51193	2.103002	347.4686	396.5588	6.148722	5.784326
Macaca maura	1	27.21066	NA	66.94303	NA	90.70535	NA	NA	NA
Female	1	27.21066	NA	66.94303	NA	90.70535	NA	NA	NA
Macaca mulatta	10	4.545797	2.475711	8.807593	6.67363	28.76473	27.98975	4.260008	1.415146

Female	8	4.282436	2.728634	7.757638	6.01476	18.37648	18.57949	3.937904	1.448063
Male	2	5.599244	0.519429	12.48244	10.22296	70.31773	17.82754	5.387372	0.414286
Macaca nigra	1	NA	NA	NA	NA	149.0753	NA	NA	NA
Male	1	NA	NA	NA	NA	149.0753	NA	NA	NA
Macaca radiata	1	9.852914	NA	28.15476	NA	133.5306	NA	2.619811	NA
Male	1	9.852914	NA	28.15476	NA	133.5306	NA	2.619811	NA
Mandrillus leucophaeus	3	5.818345	6.13874	11.7643	2.887388	56.82114	NA	8.574497	5.88906
Male	3	5.818345	6.13874	11.7643	2.887388	56.82114	NA	8.574497	5.88906
Mandrillus sphinx	7	2.688344	1.26211	5.538444	4.123009	42.31513	50.37227	12.16618	9.236507
Female	4	1.889161	0.364293	3.120335	0.722453	3.453868	2.524279	7.134667	3.876521
Male	3	3.487527	1.390509	9.165607	4.806095	94.13014	23.55742	15.52053	10.99631
Microcebus murinus	1	79.13592	NA	227	NA	NA	NA	NA	NA
Female	1	79.13592	NA	227	NA	NA	NA	NA	NA
Miopithecus talapoin	2	7.800969	4.355131	19.77908	12.00182	81.98153	29.28368	14.92679	NA
Female	1	10.88051	NA	28.26564	NA	61.27484	NA	14.92679	NA
Male	1	4.721427	NA	11.29251	NA	102.6882	NA	NA	NA
Nasalis larvatus	8	10.98928	6.759989	21.45181	11.74976	68.09271	71.13571	8.475946	6.33547
Female	4	7.300853	NA	16.25069	8.316976	29.1076	10.09681	8.220554	2.862779
Male	4	12.21875	7.712103	28.38665	13.57097	107.0778	87.47854	8.731338	9.235058
Nycticebus coucang	2	16.9324	13.28921	57.37423	31.8691	38.19108	1.557282	43.75527	18.29358
Female	1	26.3293	NA	79.90909	NA	39.29225	NA	56.69078	NA
unknown	1	7.535509	NA	34.83938	NA	37.08992	NA	30.81975	NA
Otolemur crassicaudatus	1	3.090633	NA	3.53636	NA	15.5259	NA	22.66051	NA
unknown	1	3.090633	NA	3.53636	NA	15.5259	NA	22.66051	NA
Pan paniscus	1	4.799022	NA	11.61786	NA	22.69206	NA	2.775843	NA
Female	1	4.799022	NA	11.61786	NA	22.69206	NA	2.775843	NA
Pan troglodytes troglodytes	1	2.672476	NA	6.407498	NA	19.35025	NA	1.506041	NA
Male	1	2.672476	NA	6.407498	NA	19.35025	NA	1.506041	NA
Papio anubis	8	5.778731	3.23837	13.06188	6.196927	52.64341	54.70121	10.62252	10.0085
Female	3	6.372587	4.583454	10.48316	7.71649	12.64855	6.521917	3.589815	0.652369
Male	5	5.184874	2.037535	14.60911	5.426922	82.63956	56.18548	13.43561	10.74837
Papio ursinus	4	4.592264	NA	12.43439	2.328975	24.07959	19.9949	12.6193	10.77174
Female	2	4.592264	NA	10.78755	NA	12.79355	5.945088	8.563743	2.189474
Male	2	NA	NA	14.08122	NA	46.65167	NA	16.67487	16.65855

Perodicticus potto	1	26.01821	NA	24.40538	NA	99.12474	NA	NA	NA
Male	1	26.01821	NA	24.40538	NA	99.12474	NA	NA	NA
Piliocolobus badius	6	20.49679	13.94637	22.33633	9.860466	116.2334	94.39235	4.607986	1.202425
Female	2	30.43721	13.57605	35.29501	NA	79.82402	80.16591	5.871163	0.594708
Male	4	10.55637	1.986613	19.09666	7.724544	140.5063	111.3425	3.765868	0.235488
Pithecia pithecia	4	57.74837	49.1473	33.62487	27.39695	139.8294	68.91037	4.647122	1.581947
Female	3	76.43032	39.10364	43.68768	22.76683	144.6204	83.57771	4.647122	1.581947
Male	1	1.702537	NA	3.436439	NA	125.4562	NA	NA	NA
Pongo abelii	2	17.47499	5.336307	12.71159	0.61661	36.00988	NA	5.42158	2.181311
Female	1	13.70165	NA	12.27559	NA	36.00988	NA	3.87916	NA
Male	1	21.24832	NA	13.1476	NA	NA	NA	6.963999	NA
Presbytis comata	1	23.48217	NA	26.26705	NA	37.75265	NA	4.567398	NA
Female	1	23.48217	NA	26.26705	NA	37.75265	NA	4.567398	NA
Presbytis melalophos	2	5.839678	0.170983	15.65627	8.059554	39.21645	NA	6.96968	1.780541
Female	1	5.960581	NA	9.957301	NA	NA	NA	5.710647	NA
Male	1	5.718775	NA	21.35523	NA	39.21645	NA	8.228713	NA
Procolobus verus	2	26.60447	10.37801	64.84769	54.61171	127.9684	153.021	6.617561	0.919335
Female	1	33.94283	NA	103.464	NA	236.1706	NA	5.967492	NA
Male	1	19.26611	NA	26.23138	NA	19.76626	NA	7.267629	NA
Propithecus verreauxi	2	20.70501	22.68636	40.26298	50.01649	NA	NA	76.87868	78.25151
Male	2	20.70501	22.68636	40.26298	50.01649	NA	NA	76.87868	78.25151
Rattus norvegicus	5	2.794097	0.620278	NA	NA	NA	NA	NA	NA
Male	5	2.794097	0.620278	NA	NA	NA	NA	NA	NA
Saguinus oedipus	9	10.8044	3.765518	14.28952	5.392857	56.86481	39.97765	4.74773	4.195662
Female	3	13.31416	2.98878	17.27357	3.225911	45.89957	37.99061	7.909888	6.767163
Male	6	9.549525	3.66667	12.7975	5.861394	62.34743	43.26214	3.166651	0.9212
Saimiri oerstedii	2	22.62609	14.50749	20.10671	8.993108	71.2068	1.820304	5.121138	2.423316
Female	1	32.88444	NA	26.4658	NA	69.91966	NA	6.834681	NA
Male	1	12.36775	NA	13.74762	NA	72.49395	NA	3.407595	NA
Saimiri sciureus	32	37.32581	36.9969	68.90467	65.01513	47.49011	33.49981	6.893532	6.790206
Female	10	28.05861	29.51078	46.16676	46.26207	27.96347	25.72254	5.344272	7.209071
Male	22	41.11693	39.64539	78.20655	70.0785	59.5065	32.76911	7.631274	6.633396
Semnopithecus entellus	3	11.08402	NA	34.1295	19.96995	60.6599	54.06163	4.931946	1.612417
Female	1	NA	NA	48.25039	NA	114.3629	NA	3.42726	NA

Male	2	11.08402	NA	20.00861	NA	33.80841	38.97828	5.68429	1.343003
Symphalangus syndactylus	2	85.97833	NA	82.8665	56.28036	133.8173	NA	10.58849	NA
Female	2	85.97833	NA	82.8665	56.28036	133.8173	NA	10.58849	NA
Theropithecus gelada	4	2.771999	NA	22.54971	NA	42.05603	5.277279	6.516507	1.432338
Male	4	2.771999	NA	22.54971	NA	42.05603	5.277279	6.516507	1.432338
Trachypithecus cristatus	7	7.505319	3.145187	18.45697	7.28147	105.4397	200.5884	6.717608	4.166225
Female	6	8.24025	3.096574	19.08534	7.956973	114.6595	222.8387	5.334608	2.182274
unknown	1	4.565594	NA	15.31514	NA	59.34063	NA	15.01561	NA
Trachypithecus francoisi	1	3.048918	NA	5.310371	NA	4.449434	NA	2.389077	NA
Female	1	3.048918	NA	5.310371	NA	4.449434	NA	2.389077	NA
Trachypithecus obscurus	1	3.728162	NA	NA	NA	12.729	NA	2.827276	NA
Female	1	3.728162	NA	NA	NA	12.729	NA	2.827276	NA
Varecia rubra	1	3.702268	NA	3.416037	NA	NA	NA	NA	NA
Female	1	3.702268	NA	3.416037	NA	NA	NA	NA	NA
Varecia variegate variegata	3	2.111595	0.770948	2.541047	1.617031	90.11115	NA	55.71595	NA
Female	2	2.34272	0.931777	3.167339	1.695915	90.11115	NA	55.71595	NA
Male	1	1.649345	NA	1.288462	NA	NA	NA	NA	NA

Table A.2. Summary statistics for the root surface area variables by species/sex (mm^2)

Species/Sex	Number of Individuals	Molar Root SA		Premolar Root SA		Canine Root SA		Incisor Root SA	
		Mean	StdDev	Mean	StdDev	Mean	StdDev	Mean	StdDev
Allenopithecus nigroviridis	1	168.0821	NA	91.8084	NA	237.0443	NA	106.0409	NA
Male	1	168.0821	NA	91.8084	NA	237.0443	NA	106.0409	NA
Alouatta caraya	3	137.9172	NA	98.23295	20.4793	247.5712	127.1288	44.33565	9.781903
Female	1	137.9172	NA	83.7519	NA	101.034	NA	37.4188	NA
Male	2	NA	NA	112.714	NA	320.8398	10.66374	51.2525	NA
Alouatta palliata	2	141.719	26.99507	102.9022	18.95661	155.4904	51.25517	38.71073	17.54343
Female	1	160.8074	NA	116.3065	NA	191.7333	NA	51.1158	NA
Male	1	122.6306	NA	89.4978	NA	119.2475	NA	26.30565	NA
Aotus trivirgatus	8	31.14141	5.260383	20.72961	3.942418	29.05445	7.525307	21.01782	3.779761
Female	5	31.88451	4.409175	20.40492	3.56608	28.18662	6.744545	20.36222	4.418483
Male	2	25.84128	3.097517	18.2029	0.233275	24.75263	2.482546	20.46863	0.095919
unknown	1	38.02615	NA	27.4065	NA	41.99725	NA	25.3942	NA
Ateles geoffroyi	1	73.201	NA	62.25605	NA	156.0973	NA	63.5166	NA
Female	1	73.201	NA	62.25605	NA	156.0973	NA	63.5166	NA
Cacajao calvus	1	81.0167	NA	63.58585	NA	303.6526	NA	61.6422	NA
Male	1	81.0167	NA	63.58585	NA	303.6526	NA	61.6422	NA
Callicebus moloch	7	45.15425	6.645431	27.49085	3.152138	33.14	2.854849	19.33739	2.314718
Female	1	47.1947	NA	29.5292	NA	35.09415	NA	20.67305	NA
Male	6	44.81418	7.212671	27.15113	3.309637	32.81431	2.98147	19.11478	2.452191
Callithrix argentata	2	12.57958	1.072999	11.30265	1.31041	21.27225	2.075005	10.1383	0.713471
Female	1	11.82085	NA	10.37605	NA	19.805	NA	9.6338	NA
Male	1	13.3383	NA	12.22925	NA	22.7395	NA	10.6428	NA
Callithrix humeralifera	3	12.94563	0.535235	10.54132	0.830396	22.34813	1.32004	10.508	0.83809
Female	2	13.21815	0.356877	10.9815	0.465347	22.689	1.669691	10.05733	0.431441
Male	1	12.4006	NA	9.66095	NA	21.6664	NA	11.40935	NA
Callithrix jacchus	4	14.27451	3.472565	10.20759	2.721658	21.59526	7.887051	14.21768	6.230857
Female	3	13.98363	4.192898	9.974483	3.284069	20.67927	9.395429	13.72228	7.534115
unknown	1	15.14715	NA	10.9069	NA	24.34325	NA	15.70385	NA
Cebus apella	18	89.71756	14.18403	68.7305	9.237701	196.7943	51.56334	46.48538	7.428936
Female	10	83.39595	11.98123	65.76794	8.004328	159.476	25.96053	44.43618	7.394505
Male	8	96.82938	13.66069	72.43371	9.831407	243.4421	33.37871	49.04688	7.087451

Cebus capucinus	10	58.20131	5.28426	48.67809	4.524084	126.8039	33.14982	36.52251	6.826856
Female	7	57.28071	4.534277	48.26551	5.374363	118.2279	8.392162	33.51151	4.675595
Male	3	60.34937	7.354511	49.64078	1.861648	146.8146	62.25556	43.54818	6.194486
Cercocebus agilis	5	219.2163	64.40269	173.2939	54.03323	228.4808	111.7856	162.3559	73.60479
Female	2	210.8381	44.17367	159.2283	22.5485	156.9829	16.74616	151.1772	NA
Male	3	224.8018	84.86911	182.671	72.49294	276.146	127.7964	166.0821	89.68383
Cercocebus torguatus	1	201.1286	NA	170.8915	NA	129.4121	NA	180.3314	NA
Female	1	201.1286	NA	170.8915	NA	129.4121	NA	180.3314	NA
Cercopithecus mitis	6	92.96693	13.79564	54.34779	4.017515	85.16498	8.784573	66.45791	4.148563
Female	6	92.96693	13.79564	54.34779	4.017515	85.16498	8.784573	66.45791	4.148563
Cercopithecus neglectus	1	137.2218	NA	100.8063	NA	369.8647	NA	102.539	NA
Male	1	137.2218	NA	100.8063	NA	369.8647	NA	102.539	NA
Cheirogaleus major	1	4.5767	NA	2.9124	NA	2.5419	NA	2.0789	NA
unknown	1	4.5767	NA	2.9124	NA	2.5419	NA	2.0789	NA
Chiropotes satanas	3	65.95815	4.919371	56.7721	6.8944	224.3983	21.54184	62.8885	2.869188
Female	1	69.72795	NA	53.88805	NA	204.2126	NA	62.1365	NA
Male	2	64.07325	5.204164	58.21413	9.087842	234.4911	17.80187	63.2645	3.951737
Colobus guereza	5	188.2807	26.89669	147.0164	27.96543	320.9599	69.19884	107.1449	8.426657
Female	1	191.9334	NA	144.5747	NA	215.2594	NA	NA	NA
Male	4	187.3675	30.96799	147.6268	32.25322	347.385	41.58598	107.1449	8.426657
Colobus polykomos	4	186.2866	16.20291	134.8437	17.75793	165.3628	40.25204	88.0565	15.67774
Female	4	186.2866	16.20291	134.8437	17.75793	165.3628	40.25204	88.0565	15.67774
Erythrocebus patas	3	124.1136	19.21558	104.7271	22.90295	242.0264	151.4239	115.8457	26.35013
Female	2	116.2702	19.21884	94.70238	21.1216	155.1041	22.92472	116.8751	37.17932
Male	1	139.8004	NA	124.7765	NA	415.8709	NA	113.7871	NA
Eulemur fulvus collaris	1	57.5669	NA	56.97685	NA	38.49735	NA	23.8643	NA
unknown	1	57.5669	NA	56.97685	NA	38.49735	NA	23.8643	NA
Eulemur fulvus rufus	2	54.39193	13.1018	50.55995	12.50285	30.82845	7.10911	21.89443	4.192189
Female	1	45.12755	NA	41.7191	NA	25.80155	NA	18.9301	NA
Male	1	63.6563	NA	59.4008	NA	35.85535	NA	24.85875	NA
Eulemur macaco macaco	1	75.97905	NA	74.77245	NA	53.3029	NA	33.90765	NA
Male	1	75.97905	NA	74.77245	NA	53.3029	NA	33.90765	NA
Galago alleni	1	4.5487	NA	4.6953	NA	2.9826	NA	1.63075	NA
Female	1	4.5487	NA	4.6953	NA	2.9826	NA	1.63075	NA

Galago senegalensis	6	11.11545	2.219472	10.45604	2.248907	7.314883	1.244921	4.2131	0.293727
Female	3	10.6732	2.942011	10.36967	2.909001	7.39185	0.635529	4.3148	0.183802
Male	3	11.5577	1.752985	10.54242	2.039434	7.237917	1.858198	4.06055	0.447174
Gorilla gorilla gorilla	3	847.2043	129.0414	674.4642	57.94107	1166.757	444.9481	340.0556	65.96939
Female	2	817.7599	167.635	659.0003	72.66042	910.8466	54.91296	303.4241	25.54812
Male	1	906.0931	NA	705.3921	NA	1678.579	NA	413.3187	NA
Hapalemur griseus	2	63.4063	0.877661	53.96333	2.792895	17.86123	1.440836	12.12585	1.817264
Male	2	63.4063	0.877661	53.96333	2.792895	17.86123	1.440836	12.12585	1.817264
Hapalemur griseus griseus	1	67.10645	NA	56.38795	NA	18.32905	NA	13.13175	NA
Female	1	67.10645	NA	56.38795	NA	18.32905	NA	13.13175	NA
Homo sapiens	3	437.036	NA	221.2156	49.90466	250.9264	6.92342	145.9956	29.21719
Female	2	437.036	NA	221.2156	49.90466	248.0408	6.775391	145.9956	29.21719
Male	1	NA	NA	NA	NA	256.6977	NA	NA	NA
Lagothrix logotricha	3	104.1187	14.65618	75.77763	9.338132	168.3927	19.75447	51.739	9.125737
Female	1	112.7414	NA	78.4608	NA	146.3738	NA	56.804	NA
Male	1	87.19625	NA	65.39165	NA	184.5612	NA	41.2041	NA
unknown	1	112.4185	NA	83.48045	NA	174.2432	NA	57.2089	NA
Lemur catta	1	54.51675	NA	44.90675	NA	32.10435	NA	22.96715	NA
Male	1	54.51675	NA	44.90675	NA	32.10435	NA	22.96715	NA
Lontra canadensis	1	197.8406	NA	110.6302	NA	204.5623	NA	12.31685	NA
Male	1	197.8406	NA	110.6302	NA	204.5623	NA	12.31685	NA
Lophocebus albigena	6	182.2377	28.3886	108.2128	21.78304	204.1684	55.10794	191.5275	31.20626
Female	2	192.307	7.024929	106.1945	12.23889	152.2431	0.338457	NA	NA
Male	4	177.2031	35.00497	109.2219	27.14463	230.131	48.63338	191.5275	31.20626
Macaca fascicularis	6	128.1491	39.53537	104.7639	28.66338	197.9882	123.8623	156.7412	42.52615
Female	3	132.2488	56.47825	102.5379	34.78788	114.6682	12.99612	144.7035	50.11096
Male	3	124.0495	25.83409	106.99	28.7908	322.9682	94.6734	164.7663	46.04217
Macaca maura	1	152.6952	NA	98.7856	NA	269.8495	NA	NA	NA
Female	1	152.6952	NA	98.7856	NA	269.8495	NA	NA	NA
Macaca mulatta	10	176.6549	36.95035	124.7367	29.50477	185.0206	97.58145	134.6595	29.09683
Female	8	175.3406	40.07227	126.3419	31.06347	151.4252	64.92834	138.0109	30.74828
Male	2	181.9121	31.27862	118.3162	31.25935	319.4022	105.0876	121.2543	23.49843
Macaca nigra	1	177.3346	NA	118.9867	NA	320.3343	NA	176.0767	NA
Male	1	177.3346	NA	118.9867	NA	320.3343	NA	176.0767	NA

Macaca radiata	1	133.3089	NA	104.4011	NA	279.4029	NA	113.8442	NA
Male	1	133.3089	NA	104.4011	NA	279.4029	NA	113.8442	NA
Mandrillus leucophaeus	3	317.5063	13.78127	276.3545	22.13173	725.4795	74.64953	273.6705	12.84093
Male	3	317.5063	13.78127	276.3545	22.13173	725.4795	74.64953	273.6705	12.84093
Mandrillus sphinx	7	328.4451	65.77069	256.1831	65.50291	574.873	439.5535	268.1511	88.66285
Female	4	287.9024	42.64417	223.3436	52.96791	232.6734	41.11339	196.7142	33.97296
Male	3	382.502	50.78311	299.969	60.25633	1031.139	174.978	339.5879	56.47048
Microcebus murinus	1	5.9338	NA	5.2032	NA	4.6822	NA	3.222	NA
Female	1	5.9338	NA	5.2032	NA	4.6822	NA	3.222	NA
Miopithecus talapoin	2	50.24638	10.59257	33.36773	9.948179	49.7879	23.04553	32.63415	0.3771
Female	1	42.7563	NA	26.3333	NA	33.49225	NA	32.9008	NA
Male	1	57.73645	NA	40.40215	NA	66.08355	NA	32.3675	NA
Nasalis larvatus	8	159.705	25.71923	110.7735	13.77913	180.1813	81.96045	89.59751	15.69796
Female	4	149.7843	12.30912	107.6516	11.62639	106.5674	2.175206	86.98501	13.03424
Male	4	169.6256	33.6078	113.8953	16.78855	253.7953	34.91094	92.21001	19.66983
Nycticebus coucang	2	27.0877	3.37	21.5096	7.967043	24.72973	0.74971	9.611375	2.805694
Female	1	29.47065	NA	27.14315	NA	25.25985	NA	11.5953	NA
unknown	1	24.70475	NA	15.87605	NA	24.1996	NA	7.62745	NA
Otolemur crassicaudatus	1	33.73415	NA	34.4451	NA	26.71085	NA	14.6232	NA
unknown	1	33.73415	NA	34.4451	NA	26.71085	NA	14.6232	NA
Pan paniscus	1	554.8118	NA	432.599	NA	797.7258	NA	434.5623	NA
Female	1	554.8118	NA	432.599	NA	797.7258	NA	434.5623	NA
Pan troglodytes troglodytes	1	773.4435	NA	634.179	NA	820.7182	NA	476.3037	NA
Male	1	773.4435	NA	634.179	NA	820.7182	NA	476.3037	NA
Papio anubis	8	387.0389	64.17189	287.5961	60.41979	619.1485	304.0915	348.8598	61.90739
Female	3	385.9064	29.09143	270.4101	29.80905	313.8971	49.11355	316.7237	43.4671
Male	5	387.7184	82.35205	297.9078	74.76459	848.087	142.3833	368.1415	67.25288
Papio ursinus	4	329.3686	26.73282	262.6209	10.89086	650.9372	369.3402	359.0181	35.54704
Female	2	311.4413	23.14074	251.5208	NA	335.5378	6.854693	338.7195	39.29258
Male	2	347.2959	17.9691	268.171	7.238935	966.3365	106.2197	379.3167	24.46908
Perodicticus potto	1	28.39835	NA	25.5196	NA	31.41235	NA	14.0366	NA
Male	1	28.39835	NA	25.5196	NA	31.41235	NA	14.0366	NA
Piliocolobus badius	6	149.9975	31.83495	106.386	12.91816	206.5606	79.36804	85.2601	16.85712
Female	2	160.3188	54.1653	108.3086	13.19277	149.9549	54.46826	80.60805	19.12667

Male	4	144.8369	24.58901	105.4247	14.71117	234.8634	79.40833	87.58613	18.16643
Pithecia pithecia	4	58.68625	3.870751	48.0001	7.293067	144.917	47.66089	48.00732	8.444807
Female	3	59.50603	4.294391	48.01623	8.932059	136.1963	54.32343	48.00732	8.444807
Male	1	56.2269	NA	47.9517	NA	171.0792	NA	NA	NA
Pongo abelii	2	811.0382	14.78536	625.3747	100.5911	964.4865	437.8233	382.9773	84.41416
Female	1	821.4931	NA	554.2461	NA	654.8987	NA	323.2875	NA
Male	1	800.5834	NA	696.5034	NA	1274.074	NA	442.6672	NA
Presbytis comata	1	57.10705	NA	47.67405	NA	77.07735	NA	48.73675	NA
Female	1	57.10705	NA	47.67405	NA	77.07735	NA	48.73675	NA
Presbytis melalophos	2	125.1824	5.139676	99.0149	5.600639	125.8425	20.24228	68.12845	5.281098
Female	1	128.8167	NA	102.9752	NA	111.5291	NA	71.86275	NA
Male	1	121.5481	NA	95.05465	NA	140.156	NA	64.39415	NA
Procolobus verus	2	104.405	3.009871	87.55955	6.46437	172.5681	87.18584	68.6332	NA
Female	1	106.5333	NA	92.13055	NA	110.9184	NA	NA	NA
Male	1	102.2767	NA	82.98855	NA	234.2178	NA	68.6332	NA
Propithecus verreauxi	2	112.3617	1.017845	41.5834	0.150331	NA	NA	37.51578	5.693659
Male	2	112.3617	1.017845	41.5834	0.150331	NA	NA	37.51578	5.693659
Rattus norvegicus	5	20.92647	3.596539	NA	NA	NA	NA	NA	NA
Male	5	20.92647	3.596539	NA	NA	NA	NA	NA	NA
Saguinus oedipus	9	16.34853	2.107058	13.59448	2.374009	37.09666	4.403995	14.04774	1.35056
Female	3	17.26508	2.248048	14.18392	3.851904	39.8672	6.764187	14.38725	1.858027
Male	6	15.89026	2.079895	13.29977	1.664306	35.71138	2.412935	13.87798	1.197403
Saimiri oerstedii	2	21.24193	1.870616	18.9223	0.506571	44.11228	15.96849	13.31833	0.160266
Female	1	19.9192	NA	18.5641	NA	32.82085	NA	13.205	NA
Male	1	22.56465	NA	19.2805	NA	55.4037	NA	13.43165	NA
Saimiri sciureus	32	28.17196	3.789571	20.94666	2.684106	54.93088	12.51137	18.35191	2.988857
Female	10	27.4914	4.232625	19.72831	2.887029	47.61526	18.10228	17.08847	2.793357
Male	22	28.4813	3.633268	21.44507	2.494075	58.25616	7.318879	18.95354	2.951342
Semnopithecus entellus	3	146.88	48.85217	97.57252	30.23822	184.4045	89.43294	87.7462	2.491185
Female	1	166.7534	NA	107.956	NA	143.2778	NA	87.03265	NA
Male	2	136.9433	64.65788	92.3808	40.82863	204.9678	116.0146	88.10298	3.412957
Symphalangus syndactylus	2	165.8066	33.22765	113.5001	33.99122	165.1917	89.3037	75.95745	19.3707
Female	2	165.8066	33.22765	113.5001	33.99122	165.1917	89.3037	75.95745	19.3707
Theropithecus gelada	4	338.8539	17.83424	249.4808	11.90941	575.7856	20.84862	183.7903	5.175383

Male	4	338.8539	17.83424	249.4808	11.90941	575.7856	20.84862	183.7903	5.175383
Trachypithecus cristatus	7	109.2706	6.013588	85.54073	10.31504	107.3422	14.27095	47.94872	6.111779
Female	6	109.0176	6.546607	87.20896	10.21288	112.1164	7.27498	46.00953	3.638245
unknown	1	110.7889	NA	75.53135	NA	78.69655	NA	59.58385	NA
Trachypithecus francoisi	1	157.9812	NA	141.9819	NA	146.2392	NA	64.291	NA
Female	1	157.9812	NA	141.9819	NA	146.2392	NA	64.291	NA
Trachypithecus obscurus	1	130.2272	NA	103.969	NA	123.4309	NA	68.4131	NA
Female	1	130.2272	NA	103.969	NA	123.4309	NA	68.4131	NA
Varecia rubra	1	94.7055	NA	80.26335	NA	NA	NA	NA	NA
Female	1	94.7055	NA	80.26335	NA	NA	NA	NA	NA
Varecia variegate variegata	3	83.21322	7.34076	71.6551	9.430009	66.03148	21.44644	25.6196	NA
Female	2	81.62163	9.621567	71.2893	13.30591	50.86655	NA	25.6196	NA
Male	1	86.3964	NA	72.3867	NA	81.1964	NA	NA	NA

Table A.3. Summary statistics for the enamel surface area variables by species/sex (mm^2)

Species/Sex	Number of Individuals	Molar Enamel SA		Premolar Enamel SA		Canine Enamel SA		Incisor Enamel SA	
		Mean	StdDev	Mean	StdDev	Mean	StdDev	Mean	StdDev
Allenopithecus nigroviridis	1	68.76295	NA	55.9915	NA	NA	NA	47.76495	NA
Male	1	68.76295	NA	55.9915	NA	NA	NA	47.76495	NA
Alouatta caraya	3	102.9021	NA	73.25258	13.39894	145.8049	45.05873	25.5343	1.288914
Female	1	102.9021	NA	78.73475	NA	95.0588	NA	26.4457	NA
Male	2	NA	NA	70.5115	17.71953	171.1779	14.06524	24.6229	NA
Alouatta palliata	2	103.6986	1.126492	78.1297	0.85567	88.5801	10.57648	25.6607	1.110158
Female	1	102.9021	NA	78.73475	NA	96.0588	NA	26.4457	NA
Male	1	104.4952	NA	77.52465	NA	81.1014	NA	24.8757	NA
Aotus trivirgatus	8	23.4371	3.830877	16.63624	2.607037	16.66972	3.216175	14.55724	2.472695
Female	5	22.61776	4.445184	15.89207	2.631315	15.35351	3.185996	13.24368	1.563756
Male	2	24.88395	3.834074	17.67315	3.499896	18.05603	2.189592	16.91355	3.137645
unknown	1	24.6401	NA	18.28325	NA	20.47815	NA	16.41245	NA
Ateles geoffroyi	1	71.09195	NA	50.2303	NA	84.3339	NA	44.86135	NA
Female	1	71.09195	NA	50.2303	NA	84.3339	NA	44.86135	NA
Cacajao calvus	1	41.8362	NA	41.61885	NA	NA	NA	NA	NA
Male	1	41.8362	NA	41.61885	NA	NA	NA	NA	NA
Callicebus moloch	7	25.04722	1.734758	16.84824	2.279287	19.79926	1.343858	12.23769	1.22143
Female	1	22.645	NA	14.253	NA	20.1004	NA	10.13045	NA
Male	6	25.52766	1.424969	17.28078	2.159308	19.74907	1.464918	12.5889	0.868424
Callithrix argentata	2	11.0324	1.587738	8.6429	0.466337	14.49725	3.139696	5.975975	0.507031
Female	1	9.9097	NA	8.31315	NA	12.27715	NA	5.61745	NA
Male	1	12.1551	NA	8.97265	NA	16.71735	NA	6.3345	NA
Callithrix humeralifera	3	11.78143	0.80637	8.1935	0.922895	16.99763	1.930288	6.78615	0.813957
Female	2	12.20905	0.450922	8.72605	0.042568	17.99263	1.229623	7.1657	0.678752
Male	1	10.9262	NA	7.1284	NA	15.00765	NA	6.02705	NA
Callithrix jacchus	4	11.33564	3.58447	7.606263	2.18782	13.39506	4.89476	7.668213	3.543398
Female	3	11.30562	4.389445	7.672217	2.674646	12.64097	5.703161	6.91035	3.922674
unknown	1	11.4257	NA	7.4084	NA	15.65735	NA	9.9418	NA
Cebus apella	18	54.1334	6.194559	44.3715	5.419103	115.785	39.67819	26.83956	4.000854
Female	10	50.86807	4.581407	41.53681	4.353781	87.56906	9.8189	25.71877	4.460774
Male	8	57.80689	5.881309	47.91486	4.595595	162.8116	17.42007	28.4407	2.784347

Cebus capucinus	10	46.71347	5.266667	39.49126	3.499753	100.2539	29.65129	27.40114	5.121026
Female	7	47.41825	6.026454	39.59386	3.699955	83.81044	13.0254	27.31019	5.79616
Male	3	45.06897	3.173402	39.25183	3.731675	138.6221	17.11379	27.61335	4.13874
Cercocebus agilis	5	102.7533	16.77705	88.90679	17.07597	90.53338	41.22952	90.73366	38.44406
Female	2	104.1507	6.501705	87.94423	5.830414	77.1967	0.549776	115.096	NA
Male	3	101.8217	23.20664	89.5485	23.76207	103.8701	66.24084	82.61288	42.67594
Cercocebus torguatus	1	107.1015	NA	97.8214	NA	76.36475	NA	92.15745	NA
Female	1	107.1015	NA	97.8214	NA	76.36475	NA	92.15745	NA
Cercopithecus mitis	6	58.47492	12.06434	45.85029	5.590685	52.1015	5.844133	34.53973	10.65544
Female	6	58.47492	12.06434	45.85029	5.590685	52.1015	5.844133	34.53973	10.65544
Cercopithecus neglectus	1	70.48315	NA	60.4472	NA	162.7115	NA	41.89945	NA
Male	1	70.48315	NA	60.4472	NA	162.7115	NA	41.89945	NA
Cheirogaleus major	1	6.26265	NA	2.4543	NA	2.6994	NA	2.21595	NA
unknown	1	6.26265	NA	2.4543	NA	2.6994	NA	2.21595	NA
Chiropotes satanas	3	40.75062	1.60205	37.43905	0.946014	125.0884	0.558862	33.83908	7.384776
Female	1	39.42285	NA	38.5198	NA	125.4836	NA	28.61725	NA
Male	2	41.4145	1.577555	36.89868	0.19456	124.6932	NA	39.0609	NA
Colobus guereza	5	101.2634	7.613475	80.91642	5.122876	177.4038	35.8052	41.29385	5.058382
Female	1	NA	NA	NA	NA	150.8145	NA	NA	NA
Male	4	101.2634	7.613475	80.91642	5.122876	184.0511	37.61343	41.29385	5.058382
Colobus polykomos	4	94.97383	8.637812	81.07468	6.177852	98.94514	33.52357	49.4561	2.530801
Female	4	94.97383	8.637812	81.07468	6.177852	98.94514	33.52357	49.4561	2.530801
Erythrocebus patas	3	67.39842	12.49941	62.19302	9.00677	71.03513	10.33391	45.93855	6.593848
Female	2	72.59343	12.26954	61.99825	12.72856	71.03513	10.33391	46.90293	9.02095
Male	1	57.0084	NA	62.58255	NA	NA	NA	44.0098	NA
Eulemur fulvus collaris	1	53.19085	NA	48.07915	NA	29.30285	NA	16.3169	NA
unknown	1	53.19085	NA	48.07915	NA	29.30285	NA	16.3169	NA
Eulemur fulvus rufus	2	44.71365	7.965487	39.88453	4.41719	76.7574	67.79146	29.41408	13.64267
Female	1	50.3461	NA	43.00795	NA	28.8216	NA	19.76725	NA
Male	1	39.0812	NA	36.7611	NA	124.6932	NA	39.0609	NA
Eulemur macaco macaco	1	56.79765	NA	41.0645	NA	26.80515	NA	19.85125	NA
Male	1	56.79765	NA	41.0645	NA	26.80515	NA	19.85125	NA
Galago alleni	1	6.59925	NA	5.8236	NA	NA	NA	NA	NA
Female	1	6.59925	NA	5.8236	NA	NA	NA	NA	NA

Galago senegalensis	6	12.56056	1.936593	9.051383	1.129735	6.0501	1.229514	NA	NA
Female	3	12.56445	0.791111	8.743183	0.339199	6.1956	NA	NA	NA
Male	3	12.55797	2.681013	9.359583	1.670549	6.0016	1.501147	NA	NA
Gorilla gorilla gorilla	3	462.7466	97.03001	359.9433	62.44106	521.8496	260.0288	139.1833	61.88034
Female	2	394.136	NA	315.7908	NA	372.021	23.20286	123.3179	78.4098
Male	1	531.3572	NA	404.0958	NA	821.5067	NA	170.914	NA
Hapalemur griseus	2	32.24633	1.329325	33.21	0.158745	14.11753	0.595278	NA	NA
Male	2	32.24633	1.329325	33.21	0.158745	14.11753	0.595278	NA	NA
Hapalemur griseus griseus	1	31.13325	NA	29.29015	NA	NA	NA	NA	NA
Female	1	31.13325	NA	29.29015	NA	NA	NA	NA	NA
Homo sapiens	3	NA	NA	157.0499	14.97164	148.5666	15.7993	102.5836	3.843937
Female	2	NA	NA	157.0499	14.97164	140.7604	11.55918	101.1509	4.151601
Male	1	NA	NA	NA	NA	164.1791	NA	105.449	NA
Lagothrix logotricha	3	75.88702	7.33623	52.98013	3.299926	98.04142	32.46456	35.33708	5.595913
Female	1	69.6868	NA	49.4254	NA	71.34025	NA	28.9622	NA
Male	1	83.98595	NA	55.94595	NA	134.1787	NA	39.43825	NA
unknown	1	73.9883	NA	53.56905	NA	88.6053	NA	37.6108	NA
Lemur catta	1	43.94345	NA	34.91315	NA	28.5383	NA	22.7433	NA
Male	1	43.94345	NA	34.91315	NA	28.5383	NA	22.7433	NA
Lontra canadensis	1	227.8451	NA	94.8824	NA	131.0958	NA	8.1677	NA
Male	1	227.8451	NA	94.8824	NA	131.0958	NA	8.1677	NA
Lophocebus albigena	6	93.16046	2.407568	67.97572	3.367942	134.9252	45.91706	107.8239	6.783807
Female	2	95.17648	1.967772	67.28325	0.82682	76.13038	0.723406	NA	NA
Male	4	92.15245	2.074996	68.32195	4.265873	164.3226	7.547035	107.8239	6.783807
Macaca fascicularis	6	76.01556	16.09895	64.13214	12.97098	121.1275	80.92873	66.55519	14.0002
Female	3	70.84642	21.38446	55.84427	7.122488	62.93863	4.469503	55.39135	1.197485
Male	3	81.1847	10.51118	72.42002	12.79919	208.4107	27.62839	73.99775	13.54899
Macaca maura	1	119.5306	NA	105.5478	NA	258.8189	NA	NA	NA
Female	1	119.5306	NA	105.5478	NA	258.8189	NA	NA	NA
Macaca mulatta	10	89.3911	15.92277	71.21438	11.83019	101.9717	57.79046	57.74755	12.85737
Female	8	88.10218	17.78492	69.97804	12.99278	78.93559	34.84168	55.98811	14.10981
Male	2	94.54678	1.111254	76.15973	4.092982	194.1161	18.2634	63.9056	5.519251
Macaca nigra	1	99.0959	NA	NA	NA	259.3239	NA	NA	NA
Male	1	99.0959	NA	NA	NA	259.3239	NA	NA	NA

Macaca radiata	1	82.65825	NA	67.6482	NA	180.4107	NA	60.9584	NA
Male	1	82.65825	NA	67.6482	NA	180.4107	NA	60.9584	NA
Mandrillus leucophaeus	3	149.9616	31.94828	182.3217	18.1375	564.3605	NA	111.8617	5.186487
Male	3	149.9616	31.94828	182.3217	18.1375	564.3605	NA	111.8617	5.186487
Mandrillus sphinx	7	167.9536	28.67829	150.6028	21.52025	379.4043	358.9497	116.9007	58.28693
Female	4	142.4813	6.817236	133.7534	2.872758	92.07288	16.12592	64.8249	34.61358
Male	3	193.4259	7.945211	173.0687	7.218453	762.513	29.45274	151.6179	40.93742
Microcebus murinus	1	5.6444	NA	3.452	NA	NA	NA	NA	NA
Female	1	5.6444	NA	3.452	NA	NA	NA	NA	NA
Miopithecus talapoin	2	32.41695	3.985183	22.8328	3.677309	38.01215	18.98334	16.87585	2.05563
Female	1	29.599	NA	20.23255	NA	24.5889	NA	18.3294	NA
Male	1	35.2349	NA	25.43305	NA	51.4354	NA	15.4223	NA
Nasalis larvatus	8	96.59868	16.56465	71.79902	10.16417	113.8576	62.56206	46.39173	11.39897
Female	4	81.95045	0.057488	67.68651	5.799638	60.28833	2.06236	47.46595	4.240719
Male	4	106.3642	13.82592	77.28237	13.43693	167.427	38.41851	45.31751	16.79655
Nycticebus coucang	2	20.73448	6.887821	12.8177	3.444741	27.2007	20.52582	8.61725	2.230285
Female	1	25.6049	NA	15.2535	NA	41.71465	NA	10.1943	NA
unknown	1	15.86405	NA	10.3819	NA	12.68675	NA	7.0402	NA
Oryctolagus cuniculus	4	158.6799	22.56356	158.5565	24.71858	NA	NA	208.8623	36.96839
Female	2	168.8577	16.00038	171.2585	9.889843	NA	NA	230.8899	9.223607
Male	2	148.5021	29.27426	145.8544	33.0128	NA	NA	186.8347	45.54171
Otolemur crassicaudatus	1	25.7694	NA	18.5548	NA	15.14165	NA	16.36065	NA
unknown	1	25.7694	NA	18.5548	NA	15.14165	NA	16.36065	NA
Pan paniscus	1	269.4494	NA	188.4359	NA	378.0867	NA	261.0758	NA
Female	1	269.4494	NA	188.4359	NA	378.0867	NA	261.0758	NA
Pan troglodytes troglodytes	1	261.2444	NA	216.6391	NA	326.9401	NA	251.3475	NA
Male	1	261.2444	NA	216.6391	NA	326.9401	NA	251.3475	NA
Papio anubis	8	219.636	24.26985	183.5797	31.38463	354.3854	238.7649	173.2292	69.46505
Female	3	235.1388	18.41352	179.8268	37.26179	165.8305	31.75102	177.8144	68.66463
Male	5	210.3343	23.9345	185.8315	31.82169	542.9402	186.6944	171.3951	77.74744
Papio ursinus	4	208.2769	10.8388	170.4188	7.950108	348.7626	220.2426	151.1401	21.77376
Female	2	217.551	NA	176.0404	NA	158.3151	20.96292	134.8666	11.41196
Male	2	203.6399	10.293	164.7973	NA	539.21	0.224471	167.4136	15.25615
Perodicticus potto	1	20.27175	NA	12.57145	NA	18.09995	NA	NA	NA

Male	1	20.27175	NA	12.57145	NA	18.09995	NA	NA	NA
Piliocolobus badius	6	84.20149	16.1795	60.40582	8.227808	92.3645	24.22373	36.82952	9.22187
Female	2	95.73918	8.150219	60.5783	0.397677	73.9194	17.02741	34.2322	7.710717
Male	4	76.5097	16.38522	60.31958	10.61817	104.6612	21.48431	38.56107	11.36287
Pithecia pithecia	4	33.96839	1.864856	27.94593	4.109896	77.29703	25.44207	25.8335	4.79946
Female	3	34.46875	1.927267	28.81	4.566959	76.90092	31.14494	25.8335	4.79946
Male	1	32.4673	NA	25.3537	NA	78.48535	NA	NA	NA
Pongo abelii	2	391.6995	3.020053	378.2082	21.47582	500.3983	NA	328.1461	15.84492
Female	1	393.835	NA	393.3939	NA	500.3983	NA	339.3502	NA
Male	1	389.564	NA	363.0225	NA	NA	NA	316.9421	NA
Presbytis comata	1	41.239	NA	37.1677	NA	43.4727	NA	30.08595	NA
Female	1	41.239	NA	37.1677	NA	43.4727	NA	30.08595	NA
Presbytis melalophos	2	69.08858	3.031473	52.47143	1.331588	84.31335	NA	37.82073	6.224484
Female	1	66.945	NA	53.413	NA	NA	NA	42.2221	NA
Male	1	71.23215	NA	51.52985	NA	84.31335	NA	33.41935	NA
Procolobus verus	2	59.6651	0.824911	40.185	1.40587	84.76595	42.49945	36.8098	NA
Female	1	60.2484	NA	41.1791	NA	54.7143	NA	NA	NA
Male	1	59.0818	NA	39.1909	NA	114.8176	NA	36.8098	NA
Propithecus verreauxi	2	65.7081	10.60879	32.45235	7.99264	NA	NA	29.01325	6.492372
Male	2	65.7081	10.60879	32.45235	7.99264	NA	NA	29.01325	6.492372
Rattus norvegicus	5	14.08646	0.917381	NA	NA	NA	NA	85.72358	22.32021
Male	5	14.08646	0.917381	NA	NA	NA	NA	85.72358	22.32021
Saguinus oedipus	9	13.08198	0.773938	10.23502	1.292313	25.7192	2.724627	9.01635	0.913693
Female	3	13.35328	0.937498	10.20998	1.676348	24.9993	4.718678	9.019333	1.635298
Male	6	12.94633	0.735231	10.24754	1.243984	26.07915	1.582703	9.014858	0.5158
Saimiri oerstedii	2	17.5175	0.251942	15.01813	0.387883	29.31775	12.57837	7.9911	0.208526
Female	1	17.33935	NA	14.74385	NA	20.4235	NA	8.13855	NA
Male	1	17.69565	NA	15.2924	NA	38.212	NA	7.84365	NA
Saimiri sciureus	32	19.78739	2.963228	16.24328	2.382021	30.15171	9.388354	10.49014	1.858728
Female	10	18.94779	3.194629	15.57686	2.000258	22.56666	7.585715	9.774735	1.906702
Male	22	20.13087	2.868851	16.51591	2.512637	34.70273	7.26257	10.83081	1.780046
Semnopithecus entellus	3	86.1073	18.55604	71.73247	19.29525	102.965	45.27293	40.45878	15.48125
Female	1	NA	NA	89.8665	NA	102.219	NA	54.4978	NA
Male	2	86.1073	18.55604	62.66545	15.85397	103.338	64.01908	33.43928	13.5535

Symphalangus syndactylus	2	112.1466	15.02934	93.95223	21.32496	190.792	NA	45.61608	0.286696
Female	2	112.1466	15.02934	93.95223	21.32496	190.792	NA	45.61608	0.286696
Theropithecus gelada	4	185.5758	NA	141.1122	13.76786	345.5094	42.96981	71.95654	16.1123
Male	4	185.5758	NA	141.1122	13.76786	345.5094	42.96981	71.95654	16.1123
Trachypithecus cristatus	7	70.14902	11.75891	54.12019	6.673355	58.01325	7.174127	37.9923	12.1801
Female	6	73.1286	10.30803	56.12045	4.45326	59.67756	6.600051	37.48958	13.26284
unknown	1	55.2511	NA	42.1186	NA	49.6917	NA	41.00865	NA
Trachypithecus francoisi	1	72.0309	NA	58.9857	NA	57.5801	NA	30.5482	NA
Female	1	72.0309	NA	58.9857	NA	57.5801	NA	30.5482	NA
Trachypithecus obscurus	1	61.4712	NA	NA	NA	57.9192	NA	33.29975	NA
Female	1	61.4712	NA	NA	NA	57.9192	NA	33.29975	NA
Varecia rubra	1	80.0612	NA	64.1149	NA	NA	NA	NA	NA
Female	1	80.0612	NA	64.1149	NA	NA	NA	NA	NA
Varecia variegate variegata	3	69.2526	6.41517	44.29183	7.790624	49.37555	NA	23.66385	NA
Female	2	71.34523	7.485609	46.3179	9.836562	49.37555	NA	23.66385	NA
Male	1	65.06735	NA	40.2397	NA	NA	NA	NA	NA

Table A.4. Summary statistics for the molaR Dirichlet's Normal Energy variables by species/sex

Species/Sex	Number of Individuals	Molar DNE		Premolar DNE		Canine DNE		Incisor DNE	
		Mean	StdDev	Mean	StdDev	Mean	StdDev	Mean	StdDev
Allenopithecus nigroviridis	1	179.2338	NA	108.6603	NA	NA	NA	100.2972	NA
Male	1	179.2338	NA	108.6603	NA	NA	NA	100.2972	NA
Alouatta caraya	3	162.7137	NA	156.109	21.17369	147.7446	32.13859	104.2201	20.5468
Female	1	162.7137	NA	168.8078	NA	184.8009	NA	118.7489	NA
Male	2	NA	NA	149.7595	25.58825	129.2164	2.453699	89.69129	NA
Alouatta palliata	2	145.6368	16.91438	126.7005	12.00925	109.4572	2.230069	101.144	15.07576
Female	1	133.6765	NA	118.2087	NA	107.8803	NA	90.48384	NA
Male	1	157.5971	NA	135.1924	NA	111.0341	NA	111.8042	NA
Aotus trivirgatus	8	140.1961	17.5404	130.2393	27.7615	111.87	19.39068	112.7403	12.83691
Female	5	142.9977	21.82557	139.4166	32.36169	111.7052	22.84468	109.1603	14.86896
Male	2	132.2492	8.895492	111.4032	2.759231	103.117	7.423594	114.7761	2.357346
unknown	1	142.0821	NA	122.0253	NA	130.2002	NA	126.5689	NA
Ateles geoffroyi	1	121.2716	NA	100.9394	NA	104.7743	NA	93.50552	NA
Female	1	121.2716	NA	100.9394	NA	104.7743	NA	93.50552	NA
Cacajao calvus	1	171.082	NA	103.4485	NA	NA	NA	NA	NA
Male	1	171.082	NA	103.4485	NA	NA	NA	NA	NA
Callicebus moloch	7	163.1444	49.76407	125.8153	30.45946	99.2491	23.16748	111.6134	11.65334
Female	1	230.9876	NA	152.2836	NA	123.8824	NA	130.6499	NA
Male	6	149.5758	41.40977	121.4039	30.81992	95.14355	22.41633	108.4406	8.854535
Callithrix argentata	2	113.2317	14.65323	104.638	3.671994	85.40834	0.215334	90.55926	0.103417
Female	1	102.8703	NA	102.0415	NA	85.25607	NA	90.48613	NA
Male	1	123.5931	NA	107.2345	NA	85.5606	NA	90.63238	NA
Callithrix humeralifera	3	124.6355	1.821162	122.6588	1.644059	90.3629	10.80547	97.21347	4.588446
Female	2	124.1882	2.33084	122.4287	2.255671	91.44721	15.04865	95.4359	4.811341
Male	1	125.5301	NA	123.1191	NA	88.19427	NA	100.7686	NA
Callithrix jacchus	4	165.6831	28.95879	134.6325	17.22507	110.183	13.05213	107.0238	23.07118
Female	3	162.3792	34.53148	126.4266	6.405307	103.9228	4.516377	102.1208	25.57693
unknown	1	175.5947	NA	159.2504	NA	128.9636	NA	121.733	NA
Cebus apella	18	132.6391	43.29803	120.8617	26.26242	112.7293	16.13479	102.9872	15.1035

Female	10	149.3485	54.06976	123.7639	34.11405	107.9697	12.91451	103.9225	12.25095
Male	8	113.8412	13.45617	117.234	12.31567	120.6621	18.97258	101.6509	19.48432
Cebus capucinus	10	107.674	12.61658	110.4038	17.94143	112.5576	15.65613	88.36998	12.73372
Female	7	111.9264	11.84514	113.0207	20.79879	107.3088	15.79881	90.53297	14.76469
Male	3	97.75188	9.187825	104.2977	8.417992	124.805	5.725736	83.32301	4.592778
Cercocebus agilis	5	175.9463	16.89451	96.31781	28.98259	96.69901	10.42425	140.1549	14.20354
Female	2	173.8753	11.38265	87.96679	0.904889	90.64611	5.636053	138.9207	NA
Male	3	177.3269	22.33648	101.8851	39.53908	102.7519	12.15234	140.5663	17.3665
Cercocebus torguatus	1	161.6309	NA	102.9712	NA	108.3928	NA	115.2489	NA
Female	1	161.6309	NA	102.9712	NA	108.3928	NA	115.2489	NA
Cercopithecus mitis	6	131.141	16.32086	102.298	7.424185	82.76743	8.317128	94.94638	16.99284
Female	6	131.141	16.32086	102.298	7.424185	82.76743	8.317128	94.94638	16.99284
Cercopithecus neglectus	1	157.3913	NA	114.249	NA	135.8783	NA	87.48392	NA
Male	1	157.3913	NA	114.249	NA	135.8783	NA	87.48392	NA
Cheirogaleus major	1	177.3815	NA	152.9466	NA	131.8057	NA	186.5044	NA
unknown	1	177.3815	NA	152.9466	NA	131.8057	NA	186.5044	NA
Chiropotes satanas	3	128.5267	6.580995	118.4299	12.88463	110.0189	4.944483	131.2623	26.09325
Female	1	126.5714	NA	111.9967	NA	106.5226	NA	112.8116	NA
Male	2	129.5043	8.993578	121.6465	16.4301	113.5152	NA	149.7131	NA
Colobus guereza	5	184.5709	38.27103	128.1781	23.0354	121.6689	22.52123	95.82362	2.577713
Female	1	197.3965	NA	NA	NA	92.44641	NA	NA	NA
Male	4	181.3645	43.40917	128.1781	23.0354	128.9745	17.90141	95.82362	2.577713
Colobus polykomos	4	203.0138	29.69048	153.6022	27.74317	155.2828	50.38093	142.9663	18.35729
Female	4	203.0138	29.69048	153.6022	27.74317	155.2828	50.38093	142.9663	18.35729
Erythrocebus patas	3	220.9172	65.12041	141.517	23.95237	109.3517	30.81166	119.553	34.75419
Female	2	239.8611	79.5494	147.5684	30.45842	109.3517	30.81166	132.1783	38.20098
Male	1	183.0294	NA	129.4142	NA	NA	NA	94.30239	NA
Eulemur fulvus collaris	1	161.5012	NA	161.3047	NA	114.2552	NA	134.6342	NA
unknown	1	161.5012	NA	161.3047	NA	114.2552	NA	134.6342	NA
Eulemur fulvus rufus	2	177.9317	48.04223	158.7595	1.282926	157.2735	8.710634	183.1552	1.526611
Female	1	143.9607	NA	157.8523	NA	151.1142	NA	182.0757	NA
Male	1	211.9026	NA	159.6667	NA	163.4329	NA	184.2346	NA
Eulemur macaco macaco	1	198.7742	NA	135.862	NA	144.6249	NA	186.0209	NA
Male	1	198.7742	NA	135.862	NA	144.6249	NA	186.0209	NA

Galago alleni	1	166.324	NA	141.6107	NA	NA	NA	NA	NA
Female	1	166.324	NA	141.6107	NA	NA	NA	NA	NA
Galago senegalensis	6	195.0218	16.38462	171.3338	18.39452	165.5554	17.25435	NA	NA
Female	3	184.7603	8.142992	172.3266	28.17776	142.3322	NA	NA	NA
Male	3	205.2833	16.99817	170.341	6.996624	173.2965	9.328689	NA	NA
Gorilla gorilla gorilla	3	309.1229	192.4145	127.9717	3.375678	110.5763	21.45409	121.8221	39.40255
Female	2	383.912	201.2118	130.3587	NA	111.5187	30.25273	129.0014	52.87592
Male	1	159.5447	NA	125.5848	NA	108.6916	NA	107.4633	NA
Hapalemur griseus	2	202.8676	27.29127	207.9517	7.256969	189.5839	14.06675	NA	NA
Male	2	202.8676	27.29127	207.9517	7.256969	189.5839	14.06675	NA	NA
Hapalemur griseus griseus	1	173.8244	NA	152.0178	NA	NA	NA	NA	NA
Female	1	173.8244	NA	152.0178	NA	NA	NA	NA	NA
Homo sapiens	3	NA	NA	143.2646	29.63463	94.00172	13.67248	108.6497	16.75483
Female	2	NA	NA	143.2646	29.63463	95.16363	19.1252	112.3139	21.92923
Male	1	NA	NA	NA	NA	91.67792	NA	101.3214	NA
Lagothrix logotricha	3	142.3298	17.58914	113.1411	7.420245	116.267	6.222295	136.0976	48.08901
Female	1	162.2266	NA	105.7752	NA	123.3757	NA	105.9454	NA
Male	1	135.9118	NA	120.6145	NA	113.6166	NA	110.7918	NA
unknown	1	128.8509	NA	113.0336	NA	111.8087	NA	191.5554	NA
Lemur catta	1	154.7981	NA	129.196	NA	157.6407	NA	187.9078	NA
Male	1	154.7981	NA	129.196	NA	157.6407	NA	187.9078	NA
Lontra canadensis	1	266.1248	NA	162.1369	NA	74.5952	NA	148.1819	NA
Male	1	266.1248	NA	162.1369	NA	74.5952	NA	148.1819	NA
Lophocebus albigena	6	138.3765	15.00718	107.4935	9.58989	119.72	33.03126	118.4531	9.518855
Female	2	134.385	1.775424	102.2666	0.685638	91.49596	2.952802	NA	NA
Male	4	140.3723	18.93083	110.107	11.216	133.8321	31.92077	118.4531	9.518855
Macaca fascicularis	6	174.2157	15.52834	105.2681	12.2184	120.6335	24.88477	125.0999	28.57286
Female	3	174.4016	3.938914	100.9363	15.24511	102.6748	4.481234	108.5394	17.56142
Male	3	174.0298	24.2323	109.5999	9.193317	147.5715	4.240474	136.1401	31.96149
Macaca maura	1	141.3188	NA	138.3149	NA	145.5835	NA	NA	NA
Female	1	141.3188	NA	138.3149	NA	145.5835	NA	NA	NA
Macaca mulatta	10	171.6852	23.72343	114.5669	16.64213	96.14462	16.55995	85.3505	19.59691
Female	8	175.1065	25.34418	116.3318	17.42256	92.39952	16.50019	85.36984	17.33255
Male	2	158.0002	10.03605	107.5074	15.5959	111.125	1.123503	85.28281	35.63418

Macaca nigra	1	199.4406	NA	NA	NA	136.2443	NA	NA	NA
Male	1	199.4406	NA	NA	NA	136.2443	NA	NA	NA
Macaca radiata	1	156.0673	NA	113.515	NA	135.5475	NA	104.1101	NA
Male	1	156.0673	NA	113.515	NA	135.5475	NA	104.1101	NA
Mandrillus leucophaeus	3	167.547	22.12347	94.53626	6.198196	109.8371	NA	110.4464	3.885557
Male	3	167.547	22.12347	94.53626	6.198196	109.8371	NA	110.4464	3.885557
Mandrillus sphinx	7	183.2462	25.33183	115.8478	20.0136	119.8165	15.28856	116.8044	16.21482
Female	4	192.8493	19.0807	125.4767	18.55595	116.6089	16.48523	122.9624	15.15231
Male	3	173.6431	31.04066	103.0092	15.88937	124.0932	15.67045	112.699	18.65054
Microcebus murinus	1	233.1054	NA	157.1551	NA	NA	NA	NA	NA
Female	1	233.1054	NA	157.1551	NA	NA	NA	NA	NA
Miopithecus talapoin	2	146.4953	7.55215	123.3601	7.287316	107.1802	6.574141	117.9	32.56055
Female	1	151.8355	NA	128.513	NA	102.5315	NA	140.9238	NA
Male	1	141.1551	NA	118.2072	NA	111.8288	NA	94.87625	NA
Nasalis larvatus	8	187.2184	30.54228	133.4305	10.71642	115.3988	13.86811	113.3053	15.58585
Female	4	158.4818	16.42462	134.8116	10.81984	104.4072	4.497107	111.1547	5.595938
Male	4	206.3761	18.82704	131.589	12.64987	126.3904	10.31304	115.4559	22.87273
Nycticebus coucang	2	161.2868	24.6163	135.696	9.418146	111.3027	3.752451	160.9822	19.9667
Female	1	143.8805	NA	142.3556	NA	108.6494	NA	146.8636	NA
unknown	1	178.6932	NA	129.0364	NA	113.9561	NA	175.1008	NA
Otolemur crassicaudatus	1	176.899	NA	133.9438	NA	141.9156	NA	218.0417	NA
unknown	1	176.899	NA	133.9438	NA	141.9156	NA	218.0417	NA
Pan paniscus	1	156.9088	NA	131.4247	NA	135.3364	NA	162.1802	NA
Female	1	156.9088	NA	131.4247	NA	135.3364	NA	162.1802	NA
Pan troglodytes troglodytes	1	159.3486	NA	127.316	NA	111.6927	NA	127.007	NA
Male	1	159.3486	NA	127.316	NA	111.6927	NA	127.007	NA
Papio anubis	8	182.9274	31.93521	116.2428	12.84797	104.1351	18.22954	102.5266	20.81279
Female	3	181.1189	18.773	127.3019	7.40937	96.20424	24.19263	107.4829	49.59387
Male	5	184.0125	40.05762	109.6074	10.70791	112.0659	7.53741	100.544	4.204146
Papio ursinus	4	196.5498	29.75397	117.246	9.337469	143.102	68.03685	114.8707	4.537195
Female	2	162.7412	NA	110.6434	NA	96.48433	0.22479	118.6272	1.131023
Male	2	213.4542	7.48732	123.8486	NA	189.7197	72.07051	111.1141	2.008106
Perodicticus potto	1	163.2238	NA	146.585	NA	149.4736	NA	NA	NA
Male	1	163.2238	NA	146.585	NA	149.4736	NA	NA	NA

Piliocolobus badius	6	168.503	15.16645	111.1303	12.81142	110.0735	18.94441	107.0923	24.38459
Female	2	165.5487	0.949079	114.0008	16.72948	117.2343	12.51032	103.1406	13.46117
Male	4	170.4726	21.0961	109.695	13.11572	105.2996	23.53857	109.7268	32.7504
Pithecia pithecia	4	153.0157	58.35435	127.7543	18.48283	120.7043	22.46985	121.9265	4.704928
Female	3	125.4866	23.67977	124.6407	21.31328	110.8437	13.18894	121.9265	4.704928
Male	1	235.603	NA	137.095	NA	150.2862	NA	NA	NA
Pongo abelii	2	120.2114	32.63043	104.7869	2.824781	68.12702	NA	103.4704	4.113727
Female	1	97.13818	NA	102.7895	NA	68.12702	NA	100.5616	NA
Male	1	143.2846	NA	106.7843	NA	NA	NA	106.3792	NA
Presbytis comata	1	146.5585	NA	128.0899	NA	114.6577	NA	135.9487	NA
Female	1	146.5585	NA	128.0899	NA	114.6577	NA	135.9487	NA
Presbytis melalophos	2	204.1435	14.00718	157.1738	2.742476	112.7228	NA	134.8592	14.34238
Female	1	214.048	NA	155.2346	NA	NA	NA	145.0008	NA
Male	1	194.2389	NA	159.113	NA	112.7228	NA	124.7176	NA
Procolobus verus	2	191.3498	21.29499	129.2954	8.939055	100.9297	26.54171	116.8583	NA
Female	1	176.292	NA	135.6163	NA	82.16184	NA	NA	NA
Male	1	206.4076	NA	122.9746	NA	119.6975	NA	116.8583	NA
Propithecus verreauxi	2	171.7442	34.71561	137.7703	18.81566	NA	NA	161.5313	19.59583
Male	2	171.7442	34.71561	137.7703	18.81566	NA	NA	161.5313	19.59583
Rattus norvegicus	5	NA	NA	NA	NA	NA	NA	NA	NA
Male	5	NA	NA	NA	NA	NA	NA	NA	NA
Saguinus oedipus	9	157.8691	14.79996	140.5876	15.76426	118.5416	18.68131	114.4305	19.27988
Female	3	156.1138	12.77718	135.7592	11.62119	113.6039	21.56032	110.7585	29.2826
Male	6	158.7467	16.80436	143.0018	17.96152	121.0104	18.72177	116.2666	15.47959
Saimiri oerstedii	2	153.0088	12.87308	147.9874	13.8443	114.6787	12.13476	109.5229	24.79335
Female	1	162.1115	NA	157.7768	NA	106.0981	NA	127.0545	NA
Male	1	143.9062	NA	138.198	NA	123.2592	NA	91.9914	NA
Saimiri sciureus	32	173.503	21.85819	157.9115	16.93675	108.5777	17.98903	96.5865	19.00341
Female	10	177.6645	22.7048	155.1389	15.94656	93.29525	16.04663	105.4821	30.75848
Male	22	171.8006	21.81057	159.0458	17.55776	117.7472	12.01131	92.35048	7.586122
Semnopithecus entellus	3	174.9801	20.21432	145.7031	11.52233	121.816	13.86668	109.5486	13.78521
Female	1	NA	NA	151.7984	NA	135.4186	NA	112.4108	NA
Male	2	174.9801	20.21432	142.6554	14.48442	115.0146	10.34513	108.1175	19.17747
Symphalangus syndactylus	2	157.616	8.256614	125.8488	18.1423	126.3448	NA	86.37139	2.930537

Female	2	157.616	8.256614	125.8488	18.1423	126.3448	NA	86.37139	2.930537
Theropithecus gelada	4	190.5258	NA	144.7842	6.874445	160.1339	101.6798	111.7237	8.914753
Male	4	190.5258	NA	144.7842	6.874445	160.1339	101.6798	111.7237	8.914753
Trachypithecus cristatus	7	196.6548	39.47741	141.1714	29.28241	110.389	17.98066	122.1177	21.65537
Female	6	204.1501	39.07349	144.791	30.31336	115.8097	13.55536	122.4304	23.70495
unknown	1	159.1784	NA	119.4538	NA	83.28532	NA	120.2415	NA
Trachypithecus francoisi	1	189.3238	NA	136.4658	NA	120.5268	NA	91.53043	NA
Female	1	189.3238	NA	136.4658	NA	120.5268	NA	91.53043	NA
Trachypithecus obscurus	1	190.5361	NA	NA	NA	106.8666	NA	122.1221	NA
Female	1	190.5361	NA	NA	NA	106.8666	NA	122.1221	NA
Varecia rubra	1	152.9167	NA	170.5471	NA	NA	NA	NA	NA
Female	1	152.9167	NA	170.5471	NA	NA	NA	NA	NA
Varecia variegate variegata	3	167.9257	25.56495	171.7885	18.64946	137.41	60.53712	264.448	NA
Female	2	182.2916	8.29796	177.9121	21.69371	180.2162	NA	264.448	NA
Male	1	139.1938	NA	159.5414	NA	94.60378	NA	NA	NA

Table A.5. Summary statistics for the molaR Relief Index variables by species/sex

Species/Sex	Number of Individuals	Molar RFI		Premolar RFI		Canine RFI		Incisor RFI	
		Mean	StdDev	Mean	StdDev	Mean	StdDev	Mean	StdDev
Allenopithecus nigroviridis	1	0.52709	NA	0.68074	NA	NA	NA	0.886155	NA
Male	1	0.52709	NA	0.68074	NA	NA	NA	0.886155	NA
Alouatta caraya	3	0.565257	NA	0.580107	0.061106	0.73658	0.080123	0.775075	0.09094
Female	1	0.565257	NA	0.643423	NA	0.826193	NA	0.839379	NA
Male	2	NA	NA	0.548449	0.038138	0.691774	0.028177	0.71077	NA
Alouatta palliata	2	0.565206	0.022614	0.638277	0.033396	0.739142	0.00022	0.789048	0.024093
Female	1	0.549216	NA	0.614663	NA	0.739298	NA	0.772012	NA
Male	1	0.581197	NA	0.661891	NA	0.738987	NA	0.806084	NA
Aotus trivirgatus	8	0.547429	0.082187	0.59001	0.069716	0.715762	0.083714	0.755236	0.066193
Female	5	0.52372	0.096906	0.573107	0.086907	0.699055	0.092729	0.727448	0.068734
Male	2	0.605563	0.012039	0.617886	0.000676	0.785699	0.017606	0.807879	0.035169
unknown	1	0.549702	NA	0.618775	NA	0.659425	NA	0.788894	NA
Ateles geoffroyi	1	0.555604	NA	0.642398	NA	0.716251	NA	0.790167	NA
Female	1	0.555604	NA	0.642398	NA	0.716251	NA	0.790167	NA
Cacajao calvus	1	0.475562	NA	0.564523	NA	NA	NA	NA	NA
Male	1	0.475562	NA	0.564523	NA	NA	NA	NA	NA
Callicebus moloch	7	0.526875	0.038823	0.612165	0.02953	0.762504	0.042092	0.898761	0.066464
Female	1	0.474252	NA	0.568461	NA	0.733885	NA	0.819984	NA
Male	6	0.537399	0.032454	0.619449	0.024511	0.767274	0.043989	0.91189	0.062072
Callithrix argentata	2	0.600934	NA	0.628119	0.03107	0.822805	0.03969	0.82446	0.152881
Female	1	NA	NA	0.606149	NA	0.79474	NA	0.716357	NA
Male	1	0.600934	NA	0.650088	NA	0.85087	NA	0.932563	NA
Callithrix humeralifera	3	0.578938	0.010829	0.648914	0.004899	0.866397	0.030392	0.952671	0.039987
Female	2	0.580061	0.015065	0.646164	0.001618	0.850307	0.017146	0.960707	0.053013
Male	1	0.576693	NA	0.654415	NA	0.898577	NA	0.936599	NA
Callithrix jacchus	4	0.556261	0.04712	0.626623	0.031921	0.781344	0.072746	0.922169	0.027488
Female	3	0.557353	0.057647	0.61954	0.035034	0.767253	0.082138	0.925676	0.037913
unknown	1	0.552984	NA	0.647874	NA	0.823615	NA	0.915156	NA
Cebus apella	18	0.478238	0.034435	0.506075	0.040125	0.744826	0.071956	0.713325	0.030878
Female	10	0.461229	0.034707	0.482484	0.035733	0.697301	0.035974	0.704966	0.028464
Male	8	0.497372	0.023309	0.535563	0.021898	0.824034	0.034025	0.725266	0.032317

Cebus capucinus	10	0.500323	0.03085	0.543043	0.024131	0.776309	0.078056	0.76387	0.07231
Female	7	0.509127	0.032103	0.534928	0.022954	0.733923	0.04175	0.773113	0.08495
Male	3	0.479781	0.016927	0.561979	0.016472	0.87521	0.035047	0.742305	0.029718
Cercocebus agilis	5	0.539272	0.03227	0.60229	0.022137	0.775689	0.059718	0.774664	0.035726
Female	2	0.525089	0.022015	0.590906	0.0257	0.810255	0.027403	0.801263	NA
Male	3	0.548728	0.038795	0.60988	0.020829	0.741124	0.071893	0.765798	0.037985
Cercocebus torguatus	1	0.522045	NA	0.628284	NA	0.778132	NA	0.820686	NA
Female	1	0.522045	NA	0.628284	NA	0.778132	NA	0.820686	NA
Cercopithecus mitis	6	0.55834	0.031293	0.617763	0.021778	0.799962	0.039985	0.732108	0.089284
Female	6	0.55834	0.031293	0.617763	0.021778	0.799962	0.039985	0.732108	0.089284
Cercopithecus neglectus	1	0.515546	NA	0.567437	NA	0.839592	NA	0.581057	NA
Male	1	0.515546	NA	0.567437	NA	0.839592	NA	0.581057	NA
Cheirogaleus major	1	0.48302	NA	0.518281	NA	1.111743	NA	1.232477	NA
unknown	1	0.48302	NA	0.518281	NA	1.111743	NA	1.232477	NA
Chiropotes satanas	3	0.552072	0.022942	0.603158	0.00693	0.784091	0.003815	1.143958	NA
Female	1	0.577526	NA	0.607182	NA	0.781394	NA	1.143958	NA
Male	2	0.539346	0.008994	0.601146	0.008471	0.786788	NA	NA	NA
Colobus guereza	5	0.555567	0.04957	0.53379	0.037707	0.797321	0.053772	0.672707	0.040128
Female	1	0.59894	NA	NA	NA	0.733001	NA	NA	NA
Male	4	0.544723	0.049924	0.53379	0.037707	0.813401	0.046167	0.672707	0.040128
Colobus polykomos	4	0.595103	0.046243	0.630014	0.050533	0.750154	0.076522	0.757728	0.095057
Female	4	0.595103	0.046243	0.630014	0.050533	0.750154	0.076522	0.757728	0.095057
Erythrocebus patas	3	0.491724	0.066118	0.647606	0.058707	0.777564	0.017456	0.712879	0.065156
Female	2	0.52796	0.029408	0.675536	0.047033	0.777564	0.017456	0.750274	0.010006
Male	1	0.419253	NA	0.591744	NA	NA	NA	0.638088	NA
Eulemur fulvus collaris	1	0.454331	NA	0.514978	NA	1.047841	NA	NA	NA
unknown	1	0.454331	NA	0.514978	NA	1.047841	NA	NA	NA
Eulemur fulvus rufus	2	0.522475	0.002052	0.550131	0.018952	1.133761	0.005463	1.343826	0.022878
Female	1	0.521024	NA	0.563532	NA	1.137624	NA	1.360003	NA
Male	1	0.523926	NA	0.53673	NA	1.129898	NA	1.327648	NA
Eulemur macaco macaco	1	0.503576	NA	0.530489	NA	1.050207	NA	1.327053	NA
Male	1	0.503576	NA	0.530489	NA	1.050207	NA	1.327053	NA
Galago alleni	1	0.588954	NA	0.594471	NA	NA	NA	NA	NA
Female	1	0.588954	NA	0.594471	NA	NA	NA	NA	NA

Galago senegalensis	6	0.590883	0.051401	0.59919	0.040679	1.142622	0.034943	NA	NA
Female	3	0.577967	0.076687	0.586696	0.043644	1.152247	NA	NA	NA
Male	3	0.603798	0.014965	0.611685	0.041999	1.139414	0.042069	NA	NA
Gorilla gorilla gorilla	3	0.467945	0.052951	0.55554	0.024481	0.692535	0.015236	0.655915	0.110506
Female	2	0.459068	0.071657	0.572851	NA	0.6873	0.017317	0.64592	0.15435
Male	1	0.485699	NA	0.538229	NA	0.703005	NA	0.675903	NA
Hapalemur griseus	2	0.566803	0.02515	0.593183	NA	1.079804	NA	NA	NA
Male	2	0.566803	0.02515	0.593183	NA	1.079804	NA	NA	NA
Hapalemur griseus griseus	1	0.472797	NA	0.512862	NA	NA	NA	NA	NA
Female	1	0.472797	NA	0.512862	NA	NA	NA	NA	NA
Homo sapiens	3	NA	NA	0.605746	0.043379	0.729673	0.04015	0.799573	0.058308
Female	2	NA	NA	0.605746	0.043379	0.711425	0.035015	0.791147	0.079834
Male	1	NA	NA	NA	NA	0.766169	NA	0.816427	NA
Lagothrix logotricha	3	0.563149	0.024918	0.619281	0.003898	0.718644	0.063271	0.660123	0.063911
Female	1	0.535265	NA	0.619425	NA	0.647481	NA	0.586348	NA
Male	1	0.570943	NA	0.615313	NA	0.768548	NA	0.695424	NA
unknown	1	0.583238	NA	0.623105	NA	0.739903	NA	0.698596	NA
Lemur catta	1	0.526389	NA	0.526318	NA	1.085222	NA	1.266837	NA
Male	1	0.526389	NA	0.526318	NA	1.085222	NA	1.266837	NA
Lontra canadensis	1	0.528195	NA	0.583253	NA	0.65594	NA	0.889663	NA
Male	1	0.528195	NA	0.583253	NA	0.65594	NA	0.889663	NA
Lophocebus albigena	6	0.546061	0.015985	0.63306	0.007612	0.880723	0.062175	0.90942	0.060704
Female	2	0.549672	0.024088	0.630624	0.01187	0.813424	0.049094	NA	NA
Male	4	0.544255	0.014813	0.634278	0.006608	0.914372	0.033322	0.90942	0.060704
Macaca fascicularis	6	0.533169	0.026964	0.630153	0.025932	0.830399	0.069534	0.842969	0.040618
Female	3	0.520574	0.031842	0.616053	0.031612	0.793248	0.063317	0.815355	0.001428
Male	3	0.545764	0.018105	0.644253	0.009243	0.886126	0.031152	0.861377	0.045031
Macaca maura	1	0.608637	NA	0.670146	NA	0.860994	NA	NA	NA
Female	1	0.608637	NA	0.670146	NA	0.860994	NA	NA	NA
Macaca mulatta	10	0.501688	0.048952	0.570801	0.065673	0.730753	0.07333	0.662614	0.135632
Female	8	0.495998	0.053724	0.564099	0.069098	0.721747	0.072378	0.62448	0.119446
Male	2	0.52445	0.008242	0.597608	0.059988	0.766777	0.092097	0.796082	0.125526
Macaca nigra	1	0.545745	NA	NA	NA	0.814626	NA	NA	NA
Male	1	0.545745	NA	NA	NA	0.814626	NA	NA	NA

Macaca radiata	1	0.572315	NA	0.659782	NA	0.869728	NA	0.900671	NA
Male	1	0.572315	NA	0.659782	NA	0.869728	NA	0.900671	NA
Mandrillus leucophaeus	3	0.450805	0.064872	0.631142	0.054942	0.870738	NA	0.790314	NA
Male	3	0.450805	0.064872	0.631142	0.054942	0.870738	NA	0.790314	NA
Mandrillus sphinx	7	0.472575	0.022406	0.525341	0.037981	0.693358	0.133408	0.712526	0.115934
Female	4	0.459713	0.017462	0.508826	0.031781	0.602162	0.091926	0.643469	0.148351
Male	3	0.485437	0.021304	0.547361	0.039239	0.814953	0.043662	0.758564	0.089047
Microcebus murinus	1	0.512798	NA	0.59521	NA	NA	NA	NA	NA
Female	1	0.512798	NA	0.59521	NA	NA	NA	NA	NA
Miopithecus talapoin	2	0.574903	0.007118	0.643882	0.007457	0.828346	0.030062	0.717867	0.117887
Female	1	0.579936	NA	0.649155	NA	0.807088	NA	0.801226	NA
Male	1	0.56987	NA	0.638609	NA	0.849603	NA	0.634509	NA
Nasalis larvatus	8	0.587876	0.051057	0.629875	0.023935	0.767516	0.092213	0.750197	0.061476
Female	4	0.544085	0.062188	0.622109	0.028337	0.694307	0.035992	0.752159	0.080429
Male	4	0.61707	0.009158	0.640229	0.01526	0.840725	0.065218	0.748234	0.048365
Nycticebus coucang	2	0.540987	0.024985	0.63762	0.03478	0.871389	0.152481	1.266738	NA
Female	1	0.558655	NA	0.613027	NA	0.763568	NA	1.266738	NA
unknown	1	0.52332	NA	0.662213	NA	0.979209	NA	NA	NA
Otolemur crassicaudatus	1	0.502435	NA	0.539756	NA	0.899342	NA	1.061284	NA
unknown	1	0.502435	NA	0.539756	NA	0.899342	NA	1.061284	NA
Pan paniscus	1	0.486017	NA	0.585934	NA	0.668	NA	0.730166	NA
Female	1	0.486017	NA	0.585934	NA	0.668	NA	0.730166	NA
Pan troglodytes troglodytes	1	0.39836	NA	0.51357	NA	0.616009	NA	0.745829	NA
Male	1	0.39836	NA	0.51357	NA	0.616009	NA	0.745829	NA
Papio anubis	8	0.522684	0.035708	0.61274	0.041265	0.817244	0.087314	0.703611	0.152192
Female	3	0.51455	0.032734	0.59148	0.060092	0.743834	0.052917	0.654629	0.162477
Male	5	0.527565	0.040202	0.625495	0.025141	0.890653	0.009584	0.723204	0.162679
Papio ursinus	4	0.512334	0.015469	0.597374	0.027361	0.784485	0.078678	0.70975	0.061794
Female	2	0.529429	NA	0.578027	NA	0.717004	0.011679	0.688931	0.098356
Male	2	0.503787	0.006343	0.616722	NA	0.851966	0.014823	0.730569	0.006923
Perodicticus potto	1	0.572888	NA	0.616846	NA	1.060095	NA	NA	NA
Male	1	0.572888	NA	0.616846	NA	1.060095	NA	NA	NA
Piliocolobus badius	6	0.602314	0.042403	0.618635	0.038435	0.749614	0.04913	0.696722	0.040762
Female	2	0.618969	0.05761	0.624733	0.037109	0.710212	0.000246	0.707981	0.060957

Male	4	0.59121	0.038395	0.615586	0.044338	0.775882	0.047328	0.689215	0.03541
Pithecia pithecia	4	0.497757	0.014511	0.56161	0.029164	0.762227	0.034164	1.00519	0.020059
Female	3	0.499937	0.016951	0.557789	0.03447	0.768179	0.03922	1.00519	0.020059
Male	1	0.491216	NA	0.573075	NA	0.744372	NA	NA	NA
Pongo abelii	2	0.503199	0.06005	0.554907	0.0437	0.687178	NA	0.782519	0.016355
Female	1	0.545661	NA	0.585807	NA	0.687178	NA	0.794083	NA
Male	1	0.460737	NA	0.524006	NA	NA	NA	0.770954	NA
Presbytis comata	1	0.650752	NA	0.781113	NA	0.780319	NA	0.782726	NA
Female	1	0.650752	NA	0.781113	NA	0.780319	NA	0.782726	NA
Presbytis melalophos	2	0.551127	0.007764	0.59866	0.000821	0.79281	NA	0.697163	0.025748
Female	1	0.556617	NA	0.599241	NA	NA	NA	0.71537	NA
Male	1	0.545636	NA	0.59808	NA	0.79281	NA	0.678956	NA
Procolobus verus	2	0.627371	0.015161	0.633829	0.006801	0.722567	0.070995	0.64343	NA
Female	1	0.638091	NA	0.638639	NA	0.672366	NA	NA	NA
Male	1	0.61665	NA	0.62902	NA	0.772768	NA	0.64343	NA
Propithecus verreauxi	2	0.561248	0.036019	0.572364	0.01479	NA	NA	1.223726	0.008239
Male	2	0.561248	0.036019	0.572364	0.01479	NA	NA	1.223726	0.008239
Rattus norvegicus	5	NA	NA	NA	NA	NA	NA	NA	NA
Male	5	NA	NA	NA	NA	NA	NA	NA	NA
Saguinus oedipus	9	0.548105	0.03039	0.560122	0.036454	0.852237	0.039225	0.824671	0.03969
Female	3	0.548385	0.02313	0.566158	0.015064	0.847249	0.064481	0.834613	0.002191
Male	6	0.547965	0.035547	0.557104	0.044751	0.854731	0.027862	0.8197	0.049291
Saimiri oerstedii	2	0.581625	0.024338	0.618003	0.004651	0.831499	0.072367	0.796129	0.01207
Female	1	0.598835	NA	0.621292	NA	0.780328	NA	0.804664	NA
Male	1	0.564416	NA	0.614715	NA	0.88267	NA	0.787595	NA
Saimiri sciureus	32	0.555913	0.044259	0.599295	0.036967	0.783292	0.114524	0.791754	0.038301
Female	10	0.541249	0.070749	0.592589	0.059337	0.719312	0.069805	0.784659	0.061812
Male	22	0.561912	0.027598	0.602038	0.024161	0.821681	0.120633	0.794794	0.023801
Semnopithecus entellus	3	0.55381	0.033977	0.651996	0.031365	0.797702	0.039584	0.698333	0.060698
Female	1	NA	NA	0.683426	NA	0.765086	NA	0.748284	NA
Male	2	0.55381	0.033977	0.636282	0.022041	0.81401	0.039218	0.673357	0.060215
Symphalangus syndactylus	2	0.585465	0.001736	0.619385	0.001668	0.813306	NA	0.804228	0.087949
Female	2	0.585465	0.001736	0.619385	0.001668	0.813306	NA	0.804228	0.087949
Theropithecus gelada	4	0.522245	NA	0.585483	0.08896	0.841064	0.049244	0.622555	0.129523

Male	4	0.522245	NA	0.585483	0.08896	0.841064	0.049244	0.622555	0.129523
Trachypithecus cristatus	7	0.594101	0.04394	0.680849	0.037897	0.778375	0.049617	0.80795	0.05801
Female	6	0.604176	0.040648	0.694209	0.021364	0.763704	0.042983	0.815165	0.060008
unknown	1	0.543728	NA	0.614046	NA	0.83706	NA	0.76466	NA
Trachypithecus francoisi	1	0.529078	NA	0.663547	NA	0.730944	NA	0.717951	NA
Female	1	0.529078	NA	0.663547	NA	0.730944	NA	0.717951	NA
Trachypithecus obscurus	1	0.549071	NA	NA	NA	0.696624	NA	0.686849	NA
Female	1	0.549071	NA	NA	NA	0.696624	NA	0.686849	NA
Varecia rubra	1	0.438408	NA	0.506701	NA	NA	NA	NA	NA
Female	1	0.438408	NA	0.506701	NA	NA	NA	NA	NA
Varecia variegate variegata	3	0.435262	0.058365	0.410117	0.090649	1.183559	NA	NA	NA
Female	2	0.450481	0.073642	0.433626	0.114535	1.183559	NA	NA	NA
Male	1	0.404824	NA	0.363097	NA	NA	NA	NA	NA

Table A.6. Summary statistics for the molaR orientation patch count variables by species/sex

Species/Sex	Number of Individuals	Molar OPC		Premolar OPC		Canine OPC		Incisor OPC	
		Mean	StdDev	Mean	StdDev	Mean	StdDev	Mean	StdDev
Allenopithecus nigroviridis	1	94.75	NA	39.25	NA	NA	NA	19.125	NA
Male	1	94.75	NA	39.25	NA	NA	NA	19.125	NA
Alouatta caraya	3	66	NA	68.23167	9.182595	23.315	7.853533	14.745	0.176777
Female	1	66	NA	59.88	NA	32.38	NA	14.87	NA
Male	2	NA	NA	72.4075	8.000913	18.7825	0.307591	14.62	NA
Alouatta palliata	2	65.345	1.011163	43.4375	4.331029	15	1.583919	18.97	4.200214
Female	1	64.63	NA	40.375	NA	13.88	NA	16	NA
Male	1	66.06	NA	46.5	NA	16.12	NA	21.94	NA
Aotus trivirgatus	8	61.22688	16.15972	49.81188	16.63018	22.11	7.135388	28.24125	8.566553
Female	5	64.101	19.10655	54.261	20.21032	21.976	6.447927	30.612	8.885899
Male	2	50.4375	6.452349	39.875	0.176777	17.28	6.052834	20	3.535534
unknown	1	68.435	NA	47.44	NA	32.44	NA	32.87	NA
Ateles geoffroyi	1	53.37	NA	39.375	NA	17.38	NA	15.87	NA
Female	1	53.37	NA	39.375	NA	17.38	NA	15.87	NA
Cacajao calvus	1	83.935	NA	49.375	NA	NA	NA	NA	NA
Male	1	83.935	NA	49.375	NA	NA	NA	NA	NA
Callicebus moloch	7	81.2675	24.15548	57.00214	20.41422	20.30429	8.411767	26.66071	9.246898
Female	1	108.8	NA	86.19	NA	33.565	NA	41.75	NA
Male	6	75.761	22.40419	52.1375	17.35812	18.09417	6.624087	24.14583	7.034152
Callithrix argentata	2	59.685	15.2028	39.845	0.13435	12.25	0.353553	16.2175	0.137886
Female	1	70.435	NA	39.75	NA	12	NA	16.315	NA
Male	1	48.935	NA	39.94	NA	12.5	NA	16.12	NA
Callithrix humeralifera	3	53.22833	8.252018	48.665	1.225428	13.44	1.322876	17.43833	8.008824
Female	2	48.5275	1.898582	48.3125	1.502602	12.94	1.414214	12.815	0.176777
Male	1	62.63	NA	49.37	NA	14.44	NA	26.685	NA
Callithrix jacchus	4	73.24875	19.25239	52.34375	9.366399	18.68875	2.295308	17.78	3.069042
Female	3	67.93667	19.66399	49.00167	8.035984	17.62667	1.065145	16.87333	3.032533
unknown	1	89.185	NA	62.37	NA	21.875	NA	20.5	NA
Cebus apella	18	63.40088	17.38356	47.60417	11.57192	18.52438	4.4211	26.00735	7.534398
Female	10	70.70833	21.16343	51.294	14.17374	20.05	4.307798	29.1	7.531335
Male	8	55.18	5.74	42.99188	4.811765	15.98167	3.580789	21.58929	5.252071

Cebus capucinus	10	52.63	7.321079	42.075	6.278842	19.4375	3.773271	21.6495	7.082461
Female	7	55.12357	6.979998	40.16929	5.551444	20.42	4.103576	21.63286	7.392374
Male	3	46.81167	4.742216	46.52167	6.525443	17.145	1.513002	21.68833	7.860077
Cercocebus agilis	5	72.886	9.310841	48.786	7.513155	14.985	2.758164	25.3575	4.463938
Female	2	80.185	10.25305	52.22	0.92631	13.345	0.39598	20.44	NA
Male	3	68.02	5.65939	46.49667	9.6339	16.625	3.450681	26.99667	3.710648
Cercocebus torguatus	1	77.5	NA	43	NA	15.13	NA	22.94	NA
Female	1	77.5	NA	43	NA	15.13	NA	22.94	NA
Cercopithecus mitis	6	56.05083	10.33551	39.895	4.575064	12.4275	2.388641	19.23917	2.322758
Female	6	56.05083	10.33551	39.895	4.575064	12.4275	2.388641	19.23917	2.322758
Cercopithecus neglectus	1	101.13	NA	74.185	NA	15.38	NA	27.25	NA
Male	1	101.13	NA	74.185	NA	15.38	NA	27.25	NA
Cheirogaleus major	1	66.625	NA	36.5	NA	13.565	NA	18.88	NA
unknown	1	66.625	NA	36.5	NA	13.565	NA	18.88	NA
Chiropotes satanas	3	67.96	7.085358	56.33167	7.463003	12.095	0.219203	18.7475	4.331029
Female	1	63.5	NA	54.435	NA	11.94	NA	15.685	NA
Male	2	70.19	8.400429	57.28	10.29547	12.25	NA	21.81	NA
Colobus guereza	5	69.126	10.1141	52.10333	6.007665	14.7	3.391156	24.20667	4.100934
Female	1	75.75	NA	NA	NA	12.75	NA	NA	NA
Male	4	67.47	10.8679	52.10333	6.007665	15.1875	3.707948	24.20667	4.100934
Colobus polykomos	4	74.455	9.681273	55.6725	5.811274	22.235	6.547318	23.14333	2.07791
Female	4	74.455	9.681273	55.6725	5.811274	22.235	6.547318	23.14333	2.07791
Erythrocebus patas	3	87.74667	23.69236	59.31167	6.552206	16.9375	0.880348	25.12667	12.06133
Female	2	101.06	7.693322	63.0925	0.307591	16.9375	0.880348	29.125	13.96536
Male	1	61.12	NA	51.75	NA	NA	NA	17.13	NA
Eulemur fulvus collaris	1	89.565	NA	53.065	NA	14.815	NA	19.12	NA
unknown	1	89.565	NA	53.065	NA	14.815	NA	19.12	NA
Eulemur fulvus rufus	2	91.845	3.493107	62.4975	15.02955	12.91	1.371787	12.3125	0.265165
Female	1	89.375	NA	51.87	NA	11.94	NA	12.125	NA
Male	1	94.315	NA	73.125	NA	13.88	NA	12.5	NA
Eulemur macaco macaco	1	112.63	NA	44.065	NA	16.06	NA	13	NA
Male	1	112.63	NA	44.065	NA	16.06	NA	13	NA
Galago alleni	1	73.25	NA	44.25	NA	NA	NA	NA	NA
Female	1	73.25	NA	44.25	NA	NA	NA	NA	NA

Galago senegalensis	6	58.60417	7.666008	49.30333	5.764525	15.21875	1.933332	NA	NA
Female	3	62.02333	6.96108	51.64667	7.601737	13.185	NA	NA	NA
Male	3	55.185	7.961814	46.96	2.968893	15.89667	1.687967	NA	NA
Gorilla gorilla gorilla	3	123.9367	52.06751	59.25	1.06066	19.08333	7.217703	30.605	16.07048
Female	2	143.8125	55.24272	58.5	NA	20.815	9.284312	32.625	22.18194
Male	1	84.185	NA	60	NA	15.62	NA	26.565	NA
Hapalemur griseus	2	71.1875	13.16986	70.69	0.268701	14.7825	2.167282	NA	NA
Male	2	71.1875	13.16986	70.69	0.268701	14.7825	2.167282	NA	NA
Hapalemur griseus griseus	1	72	NA	70.56	NA	NA	NA	NA	NA
Female	1	72	NA	70.56	NA	NA	NA	NA	NA
Homo sapiens	3	NA	NA	49.25	1.767767	24.77	13.72217	28.73	10.09991
Female	2	NA	NA	49.25	1.767767	29.7175	15.15683	31.875	12.02789
Male	1	NA	NA	NA	NA	14.875	NA	22.44	NA
Lagothrix logotricha	3	69.08167	11.05074	53.22833	0.598589	19.73	5.718223	36.145	15.12701
Female	1	81.31	NA	53.13	NA	19.625	NA	34.565	NA
Male	1	59.81	NA	53.87	NA	14.065	NA	21.87	NA
unknown	1	66.125	NA	52.685	NA	25.5	NA	52	NA
Lemur catta	1	69.75	NA	45.935	NA	10.935	NA	14	NA
Male	1	69.75	NA	45.935	NA	10.935	NA	14	NA
Lontra canadensis	1	75.685	NA	42.44	NA	10.875	NA	23.06	NA
Male	1	75.685	NA	42.44	NA	10.875	NA	23.06	NA
Lophocebus albigena	6	60.69833	5.681546	46.39667	7.401436	15.20833	3.461771	19.46	1.95123
Female	2	56.785	2.340523	45.875	5.480078	15.47	0.311127	NA	NA
Male	4	62.655	6.05473	46.6575	9.001086	15.0775	4.457842	19.46	1.95123
Macaca fascicularis	6	80.59583	11.14325	53.45583	4.912412	15.187	2.317479	29.014	16.34563
Female	3	76.895	6.838675	56.37333	3.228221	15.125	2.517534	19.2525	1.240972
Male	3	84.29667	14.91892	50.53833	4.936867	15.28	2.962777	35.52167	19.35918
Macaca maura	1	53.69	NA	52.25	NA	19.31	NA	NA	NA
Female	1	53.69	NA	52.25	NA	19.31	NA	NA	NA
Macaca mulatta	10	77.692	10.64321	56.6815	8.554029	16.6375	3.998868	20.765	5.613109
Female	8	76.49	11.34655	57.18	9.562537	16.9925	4.448843	21.48357	6.168503
Male	2	82.5	7.778175	54.6875	2.916815	15.2175	0.576292	18.25	2.736503
Macaca nigra	1	81.12	NA	NA	NA	15.12	NA	NA	NA
Male	1	81.12	NA	NA	NA	15.12	NA	NA	NA

Macaca radiata	1	64.19	NA	44.565	NA	18	NA	21.69	NA
Male	1	64.19	NA	44.565	NA	18	NA	21.69	NA
Mandrillus leucophaeus	3	81.87667	12.67988	47.21	3.10382	12.12	NA	19.75	0.707107
Male	3	81.87667	12.67988	47.21	3.10382	12.12	NA	19.75	0.707107
Mandrillus sphinx	7	87.145	7.250665	64.06071	11.16102	25.86571	25.56787	19.487	2.254439
Female	4	85.52	3.446912	70.98125	5.231606	35.375	32.02806	19.155	2.694077
Male	3	88.77	10.56538	54.83333	10.44729	13.18667	0.67951	19.70833	2.520369
Microcebus murinus	1	63.875	NA	31.19	NA	NA	NA	NA	NA
Female	1	63.875	NA	31.19	NA	NA	NA	NA	NA
Miopithecus talapoin	2	64.655	0.219203	45.155	4.992174	21.0625	6.629126	20.8475	1.721805
Female	1	64.5	NA	48.685	NA	25.75	NA	22.065	NA
Male	1	64.81	NA	41.625	NA	16.375	NA	19.63	NA
Nasalis larvatus	8	58.976	8.919295	49.94786	3.531187	17.54813	3.596011	24.21938	4.568145
Female	4	55.44	7.863027	49.11125	3.952177	18.345	3.974705	23.90625	5.042555
Male	4	61.33333	10.36124	51.06333	3.272924	16.75125	3.561092	24.5325	4.796152
Nycticebus coucang	2	62.715	16.75136	35.8425	2.697612	13.1875	0.350018	12.9675	1.905653
Female	1	50.87	NA	37.75	NA	13.435	NA	11.62	NA
unknown	1	74.56	NA	33.935	NA	12.94	NA	14.315	NA
Otolemur crassicaudatus	1	108.5	NA	63.69	NA	19.125	NA	22.065	NA
unknown	1	108.5	NA	63.69	NA	19.125	NA	22.065	NA
Pan paniscus	1	103.44	NA	50.62	NA	21.065	NA	30.44	NA
Female	1	103.44	NA	50.62	NA	21.065	NA	30.44	NA
Pan troglodytes troglodytes	1	95.45	NA	65.435	NA	15.5	NA	26.125	NA
Male	1	95.45	NA	65.435	NA	15.5	NA	26.125	NA
Papio anubis	8	78.26625	5.083308	55.15	6.658717	15.5825	2.224657	22.10929	4.62141
Female	3	82.66667	0.721688	57.58333	11.02381	16.99833	1.637455	23.0975	7.378659
Male	5	75.626	4.660817	53.69	3.118469	14.16667	1.917742	21.714	4.212053
Papio ursinus	4	81.46	8.534184	48.78	0.834386	16.50125	3.940377	19.78125	2.190717
Female	2	73.75	NA	48.19	NA	15.4075	2.252135	21.28	1.994041
Male	2	85.315	7.516545	49.37	NA	17.595	6.059905	18.2825	1.198546
Perodicticus potto	1	61.69	NA	42.81	NA	12.315	NA	NA	NA
Male	1	61.69	NA	42.81	NA	12.315	NA	NA	NA
Piliocolobus badius	6	54.95	8.441176	43.72917	9.255818	17.188	3.995644	23.124	2.650015
Female	2	54.94	11.58241	37.6875	3.447146	18.785	6.498311	21.155	0.13435

Male	4	54.95667	8.685081	46.75	10.11538	16.12333	2.562349	24.43667	2.752187
Pithecia pithecia	4	81.07875	16.51269	65.11	12.02301	14.5475	2.063995	19.91667	4.783964
Female	3	73.77167	9.415023	60.41833	9.206444	13.56333	0.760663	19.91667	4.783964
Male	1	103	NA	79.185	NA	17.5	NA	NA	NA
Pongo abelii	2	68.4675	12.85874	53.375	6.625591	10.935	NA	20.655	0.749533
Female	1	59.375	NA	58.06	NA	10.935	NA	21.185	NA
Male	1	77.56	NA	48.69	NA	NA	NA	20.125	NA
Presbytis comata	1	41.19	NA	32.935	NA	17.125	NA	29.19	NA
Female	1	41.19	NA	32.935	NA	17.125	NA	29.19	NA
Presbytis melalophos	2	76.6875	6.805903	65.22	9.941921	14.06	NA	28.9375	4.946212
Female	1	81.5	NA	72.25	NA	NA	NA	32.435	NA
Male	1	71.875	NA	58.19	NA	14.06	NA	25.44	NA
Procolobus verus	2	62.94	8.570134	54.75	1.152584	16.31	0.975807	21.75	NA
Female	1	56.88	NA	55.565	NA	15.62	NA	NA	NA
Male	1	69	NA	53.935	NA	17	NA	21.75	NA
Propithecus verreauxi	2	69.565	1.506137	31.28	9.234815	NA	NA	12.095	1.98697
Male	2	69.565	1.506137	31.28	9.234815	NA	NA	12.095	1.98697
Rattus norvegicus	5	NA	NA	NA	NA	NA	NA	NA	NA
Male	5	NA	NA	NA	NA	NA	NA	NA	NA
Saguinus oedipus	9	71.09611	13.1544	55.50667	8.097717	18.75056	4.811299	28.61111	8.37059
Female	3	63.58333	9.194567	53.75	7.154544	17.355	6.093794	29.52167	11.56368
Male	6	74.8525	13.86534	56.385	9.036843	19.44833	4.520089	28.15583	7.607444
Saimiri oerstedii	2	54	1.59099	50.2525	0.088388	18.3775	0.003536	23.94	1.06066
Female	1	52.875	NA	50.19	NA	18.375	NA	23.19	NA
Male	1	55.125	NA	50.315	NA	18.38	NA	24.69	NA
Saimiri sciureus	32	63.88097	13.66257	55.81806	13.38224	17.39667	3.398486	21.93597	8.119074
Female	10	72.61722	19.63402	61.08944	20.1822	17.555	3.258672	25.7945	12.49443
Male	22	60.30705	8.586012	53.66159	9.158827	17.30167	3.588978	20.09857	4.200033
Semnopithecus entellus	3	78.405	12.15517	49.75	4.84876	19.5	1.984313	22.605	2.157099
Female	1	NA	NA	53.065	NA	21.75	NA	22	NA
Male	2	78.405	12.15517	48.0925	5.526039	18.375	0.53033	22.9075	2.959242
Symphalangus syndactylus	2	64.69	1.767767	47	9.984348	25.315	NA	27.405	15.6907
Female	2	64.69	1.767767	47	9.984348	25.315	NA	27.405	15.6907
Theropithecus gelada	4	92.12	NA	56.58333	16.14389	19.4825	10.9864	26.8425	2.236849

Male	4	92.12	NA	56.58333	16.14389	19.4825	10.9864	26.8425	2.236849
Trachypithecus cristatus	7	74.45917	14.64536	53.375	13.93693	20.49	7.378574	22.16929	5.059354
Female	6	72.139	15.09087	53.77083	15.22398	22.512	6.114783	22.92667	5.089009
unknown	1	86.06	NA	51	NA	10.38	NA	17.625	NA
Trachypithecus francoisi	1	87.75	NA	57.185	NA	14.75	NA	23.625	NA
Female	1	87.75	NA	57.185	NA	14.75	NA	23.625	NA
Trachypithecus obscurus	1	84.88	NA	NA	NA	18	NA	25.63	NA
Female	1	84.88	NA	NA	NA	18	NA	25.63	NA
Varecia rubra	1	78.81	NA	51.94	NA	NA	NA	NA	NA
Female	1	78.81	NA	51.94	NA	NA	NA	NA	NA
Varecia variegate variegata	3	78.91833	23.31387	46.95667	5.883174	11.125	NA	13.62	NA
Female	2	83.72	30.80157	49.03	6.590235	11.125	NA	13.62	NA
Male	1	69.315	NA	42.81	NA	NA	NA	NA	NA

Table A.7. Summary statistics for the molaR occlusal slope variables by species/sex

Species/Sex	Number of Individuals	Molar Slope		Premolar Slope		Canine Slope		Incisor Slope	
		Mean	StdDev	Mean	StdDev	Mean	StdDev	Mean	StdDev
Allenopithecus nigroviridis	1	71.39485	NA	78.91149	NA	NA	NA	81.98048	NA
Male	1	71.39485	NA	78.91149	NA	NA	NA	81.98048	NA
Alouatta caraya	3	75.03736	NA	76.39582	3.579385	78.12772	2.813697	81.57991	3.293842
Female	1	75.03736	NA	79.50108	NA	81.34816	NA	83.90901	NA
Male	2	NA	NA	74.84318	3.340658	76.51749	0.526173	79.25081	NA
Alouatta palliata	2	75.17403	1.747121	79.06946	2.295175	80.26127	1.072918	82.22036	1.328276
Female	1	73.93863	NA	77.44653	NA	79.5026	NA	81.28112	NA
Male	1	76.40943	NA	80.6924	NA	81.01993	NA	83.15959	NA
Aotus trivirgatus	8	75.59513	4.728283	79.32978	3.868858	80.14816	3.394743	81.40906	1.728909
Female	5	74.57425	5.825962	78.61483	4.797515	79.61772	3.985214	80.81314	1.777344
Male	2	78.34616	0.473139	81.48209	0.598723	82.524	0.195725	83.17145	0.056722
unknown	1	75.19754	NA	78.59988	NA	78.04867	NA	80.86388	NA
Ateles geoffroyi	1	76.55231	NA	80.82093	NA	79.19813	NA	81.59786	NA
Female	1	76.55231	NA	80.82093	NA	79.19813	NA	81.59786	NA
Cacajao calvus	1	71.06452	NA	74.32659	NA	NA	NA	NA	NA
Male	1	71.06452	NA	74.32659	NA	NA	NA	NA	NA
Callicebus moloch	7	74.46302	1.659427	77.77696	1.689903	80.47781	1.121576	82.57859	1.10215
Female	1	73.64394	NA	76.38459	NA	79.53291	NA	81.44161	NA
Male	6	74.62683	1.800237	78.00902	1.724693	80.63529	1.140698	82.76808	1.075197
Callithrix argentata	2	76.44956	2.779612	79.1901	1.370179	81.31505	1.857338	82.54406	2.394317
Female	1	74.48408	NA	78.22124	NA	80.00171	NA	80.85102	NA
Male	1	78.41505	NA	80.15897	NA	82.62839	NA	84.2371	NA
Callithrix humeralifera	3	77.37	0.569609	80.05134	0.107099	83.26171	0.452001	84.62073	0.865403
Female	2	77.0419	0.054993	80.02415	0.136025	83.00574	0.124424	84.85497	1.081043
Male	1	78.02619	NA	80.10573	NA	83.77366	NA	84.15227	NA
Callithrix jacchus	4	76.3291	1.243803	78.72041	1.218399	80.42149	2.275531	83.09285	1.817014
Female	3	76.25288	1.511858	78.332	1.149604	79.93867	2.523564	82.56397	1.80942
unknown	1	76.55776	NA	79.88563	NA	81.86995	NA	84.67951	NA
Cebus apella	18	71.14541	2.471279	73.65509	2.686624	78.70076	1.892444	80.53628	1.471138
Female	10	70.12654	2.483813	72.26922	2.448292	77.67102	1.35301	80.09887	1.675127
Male	8	72.29164	2.018034	75.38742	1.91027	80.41699	1.339268	81.16116	0.887591

Cebus capucinus	10	72.9577	0.982983	75.74195	1.176768	80.20516	1.495495	81.10329	2.350869
Female	7	73.11281	1.133092	75.37769	1.18924	79.79114	1.539056	81.32352	2.827837
Male	3	72.59578	0.464506	76.59189	0.663829	81.17119	0.978999	80.5894	0.56015
Cercocebus agilis	5	71.34102	2.036888	75.23209	2.024208	79.92257	1.139238	79.87227	1.13189
Female	2	70.68576	0.911721	74.21527	1.87075	80.71846	0.982086	80.76985	NA
Male	3	71.77786	2.677049	75.90997	2.172966	79.12668	0.62875	79.57308	1.17672
Cercocebus torguatus	1	72.33375	NA	79.59081	NA	80.40008	NA	82.26115	NA
Female	1	72.33375	NA	79.59081	NA	80.40008	NA	82.26115	NA
Cercopithecus mitis	6	74.3498	1.662448	77.4209	1.357814	79.9278	0.846744	78.32353	3.769783
Female	6	74.3498	1.662448	77.4209	1.357814	79.9278	0.846744	78.32353	3.769783
Cercopithecus neglectus	1	72.29267	NA	75.90004	NA	80.83654	NA	73.92783	NA
Male	1	72.29267	NA	75.90004	NA	80.83654	NA	73.92783	NA
Cheirogaleus major	1	78.18801	NA	77.30082	NA	86.40198	NA	87.02938	NA
unknown	1	78.18801	NA	77.30082	NA	86.40198	NA	87.02938	NA
Chiropotes satanas	3	73.99898	1.147844	76.08833	0.761069	79.813	0.429493	84.48416	0.453004
Female	1	75.31611	NA	76.83675	NA	79.5093	NA	84.80448	NA
Male	2	73.34042	0.181282	75.71411	0.564135	80.1167	NA	84.16384	NA
Colobus guereza	5	73.45347	3.502602	72.43586	3.428299	79.14432	1.527641	77.36937	1.969024
Female	1	75.3555	NA	NA	NA	76.89075	NA	NA	NA
Male	4	72.97796	3.853601	72.43586	3.428299	79.70771	0.997751	77.36937	1.969024
Colobus polykomos	4	74.59606	1.92934	77.81132	1.820945	79.99754	2.391031	80.40687	2.486051
Female	4	74.59606	1.92934	77.81132	1.820945	79.99754	2.391031	80.40687	2.486051
Erythrocebus patas	3	71.62643	2.971527	78.55942	0.852999	79.09333	1.316483	77.92382	1.65443
Female	2	73.31481	0.745804	79.02682	0.380083	79.09333	1.316483	78.84647	0.60546
Male	1	68.24968	NA	77.62463	NA	NA	NA	76.07852	NA
Eulemur fulvus collaris	1	73.76766	NA	77.451	NA	85.02955	NA	85.02983	NA
unknown	1	73.76766	NA	77.451	NA	85.02955	NA	85.02983	NA
Eulemur fulvus rufus	2	76.51215	0.338887	77.92865	1.458937	86.02982	0.002985	86.35333	0.157705
Female	1	76.27252	NA	78.96027	NA	86.03193	NA	86.24182	NA
Male	1	76.75178	NA	76.89702	NA	86.02771	NA	86.46485	NA
Eulemur macaco macaco	1	75.78258	NA	77.96879	NA	84.81513	NA	86.49566	NA
Male	1	75.78258	NA	77.96879	NA	84.81513	NA	86.49566	NA
Galago alleni	1	80.09893	NA	81.21476	NA	NA	NA	NA	NA
Female	1	80.09893	NA	81.21476	NA	NA	NA	NA	NA

Galago senegalensis	6	79.77405	2.768319	79.64938	2.349141	86.48319	0.245885	NA	NA
Female	3	79.38903	4.19983	79.18872	3.215761	86.68627	NA	NA	NA
Male	3	80.15907	1.037154	80.11004	1.678813	86.4155	0.251384	NA	NA
Gorilla gorilla gorilla	3	68.5135	1.224266	74.75121	1.049189	76.63262	0.656648	75.51594	5.166119
Female	2	68.54398	1.729764	75.4931	NA	76.9993	0.23583	75.23601	7.273748
Male	1	68.45255	NA	74.00932	NA	75.89924	NA	76.07579	NA
Hapalemur griseus	2	75.37039	0.968182	77.99365	0.239634	86.00645	0.241679	NA	NA
Male	2	75.37039	0.968182	77.99365	0.239634	86.00645	0.241679	NA	NA
Hapalemur griseus griseus	1	70.78904	NA	75.27619	NA	NA	NA	NA	NA
Female	1	70.78904	NA	75.27619	NA	NA	NA	NA	NA
Homo sapiens	3	NA	NA	76.9391	0.806466	78.12957	1.21949	80.46582	1.524629
Female	2	NA	NA	76.9391	0.806466	77.54452	0.959485	79.8794	1.607985
Male	1	NA	NA	NA	NA	79.29966	NA	81.63867	NA
Lagothrix logotricha	3	75.81599	0.720127	78.60009	0.726682	78.97043	1.142427	81.29903	1.479973
Female	1	75.15139	NA	78.75036	NA	77.7874	NA	79.64465	NA
Male	1	76.58108	NA	79.23989	NA	80.06738	NA	82.49714	NA
unknown	1	75.71551	NA	77.81002	NA	79.05652	NA	81.7553	NA
Lemur catta	1	76.05925	NA	75.81658	NA	85.75483	NA	87.00143	NA
Male	1	76.05925	NA	75.81658	NA	85.75483	NA	87.00143	NA
Lontra canadensis	1	72.30278	NA	76.15155	NA	78.90818	NA	86.11161	NA
Male	1	72.30278	NA	76.15155	NA	78.90818	NA	86.11161	NA
Lophocebus albigena	6	72.03634	1.624898	77.49266	0.905504	81.8699	1.421444	84.36461	1.698678
Female	2	72.27394	0.92853	77.55882	0.842498	80.49703	0.552372	NA	NA
Male	4	71.91755	2.014112	77.45957	1.060934	82.55633	1.17517	84.36461	1.698678
Macaca fascicularis	6	72.60172	1.976256	77.04392	1.887043	80.75664	1.477376	82.35023	1.994089
Female	3	71.60015	1.82625	76.19709	2.064335	80.23294	1.810241	81.21841	0.829812
Male	3	73.60329	1.849149	77.89075	1.577804	81.54218	0.345938	83.10478	2.339539
Macaca maura	1	75.95472	NA	80.11572	NA	81.50139	NA	NA	NA
Female	1	75.95472	NA	80.11572	NA	81.50139	NA	NA	NA
Macaca mulatta	10	69.56829	3.079207	73.56866	3.414619	78.26109	2.103841	75.81324	4.793741
Female	8	69.08528	3.25878	72.8878	3.443488	77.90887	1.7856	74.5985	4.501235
Male	2	71.50031	1.290105	76.29211	1.841334	79.66998	3.543214	80.06482	3.973903
Macaca nigra	1	72.72716	NA	NA	NA	80.27906	NA	NA	NA
Male	1	72.72716	NA	NA	NA	80.27906	NA	NA	NA

Macaca radiata	1	73.95065	NA	77.65888	NA	82.59338	NA	84.39379	NA
Male	1	73.95065	NA	77.65888	NA	82.59338	NA	84.39379	NA
Mandrillus leucophaeus	3	66.14003	5.084389	77.12062	2.886949	82.0826	NA	80.82156	0.119761
Male	3	66.14003	5.084389	77.12062	2.886949	82.0826	NA	80.82156	0.119761
Mandrillus sphinx	7	67.41475	1.267428	71.7904	1.96571	76.32143	4.599581	78.06216	3.42482
Female	4	67.18567	1.359372	71.11561	2.022712	73.54161	4.173912	75.74391	4.62729
Male	3	67.64382	1.417962	72.69012	1.82485	80.02786	1.129149	79.60766	1.948261
Microcebus murinus	1	75.91246	NA	79.37685	NA	NA	NA	NA	NA
Female	1	75.91246	NA	79.37685	NA	NA	NA	NA	NA
Miopithecus talapoin	2	77.26604	0.586274	80.03026	1.114295	82.52538	0.471957	79.8853	2.683111
Female	1	77.6806	NA	80.81818	NA	82.85911	NA	81.78254	NA
Male	1	76.85148	NA	79.24233	NA	82.19166	NA	77.98805	NA
Nasalis larvatus	8	73.67294	2.03107	77.9621	0.813741	80.69554	1.48141	80.84108	2.424787
Female	4	72.64651	3.360228	78.19814	1.017128	80.26965	1.26879	81.62094	3.123634
Male	4	74.35722	0.92142	77.64737	0.417951	81.12144	1.739872	80.06122	1.529751
Nycticebus coucang	2	78.02433	1.303351	79.75964	1.439204	81.98532	2.698992	87.1344	0.230111
Female	1	78.94594	NA	78.74197	NA	80.07685	NA	86.97169	NA
unknown	1	77.10272	NA	80.77731	NA	83.8938	NA	87.29711	NA
Oryctolagus cuniculus	4	NA	NA	NA	NA	NA	NA	NA	NA
Female	2	NA	NA	NA	NA	NA	NA	NA	NA
Male	2	NA	NA	NA	NA	NA	NA	NA	NA
Otolemur crassicaudatus	1	73.7087	NA	75.95067	NA	83.68398	NA	87.62781	NA
unknown	1	73.7087	NA	75.95067	NA	83.68398	NA	87.62781	NA
Pan paniscus	1	71.00171	NA	77.23548	NA	78.37358	NA	82.62498	NA
Female	1	71.00171	NA	77.23548	NA	78.37358	NA	82.62498	NA
Pan troglodytes troglodytes	1	61.45312	NA	70.29246	NA	74.44071	NA	80.41397	NA
Male	1	61.45312	NA	70.29246	NA	74.44071	NA	80.41397	NA
Papio anubis	8	70.80829	2.012751	75.9371	1.822672	80.28125	1.370303	77.66961	5.127505
Female	3	70.81223	1.738491	75.42881	2.80607	79.2845	1.202223	76.74294	5.532253
Male	5	70.80593	2.361852	76.24207	1.251679	81.27799	0.518152	78.04028	5.584299
Papio ursinus	4	69.75207	0.953991	75.17872	0.511911	79.43148	1.293227	78.2228	1.967753
Female	2	70.7934	NA	75.54069	NA	78.45795	0.627929	77.35967	2.664265
Male	2	69.2314	0.440032	74.81674	NA	80.40502	0.912097	79.08592	1.240124
Perodicticus potto	1	78.54584	NA	78.0415	NA	84.38569	NA	NA	NA

Male	1	78.54584	NA	78.0415	NA	84.38569	NA	NA	NA
Piliocolobus badius	6	76.32265	2.410626	76.89124	2.038584	79.86121	1.273473	79.66142	1.320379
Female	2	77.26374	3.577788	77.92143	2.678155	79.04227	1.715936	79.24164	1.143555
Male	4	75.69525	1.935424	76.37614	1.863931	80.40716	0.808391	79.94128	1.593502
Pithecia pithecia	4	71.62644	0.738514	74.26279	1.58305	78.48433	1.085146	82.75238	0.42162
Female	3	71.68528	0.892935	74.75147	1.525179	78.81173	1.0598	82.75238	0.42162
Male	1	71.44993	NA	72.79672	NA	77.50214	NA	NA	NA
Pongo abelii	2	70.64643	2.381114	74.34853	0.659704	76.4641	NA	81.28583	0.48137
Female	1	72.33013	NA	74.81501	NA	76.4641	NA	81.62621	NA
Male	1	68.96273	NA	73.88205	NA	NA	NA	80.94545	NA
Presbytis comata	1	80.2637	NA	84.02608	NA	83.68524	NA	83.14494	NA
Female	1	80.2637	NA	84.02608	NA	83.68524	NA	83.14494	NA
Presbytis melalophos	2	73.24835	0.764778	76.25804	0.635509	80.92406	NA	80.46537	0.181075
Female	1	72.70757	NA	75.80866	NA	NA	NA	80.59341	NA
Male	1	73.78913	NA	76.70741	NA	80.92406	NA	80.33733	NA
Procolobus verus	2	77.65114	0.554397	77.0977	NA	78.94378	1.517934	80.18534	NA
Female	1	78.04316	NA	NA	NA	77.87044	NA	NA	NA
Male	1	77.25912	NA	77.0977	NA	80.01712	NA	80.18534	NA
Propithecus verreauxi	2	74.29904	3.371727	79.12773	0.415445	NA	NA	86.41613	0.095166
Male	2	74.29904	3.371727	79.12773	0.415445	NA	NA	86.41613	0.095166
Rattus norvegicus	5	NA	NA	NA	NA	NA	NA	NA	NA
Male	5	NA	NA	NA	NA	NA	NA	NA	NA
Saguinus oedipus	9	77.19234	1.300821	78.28946	1.014047	81.21184	1.152313	81.68869	1.113612
Female	3	77.20769	1.170691	78.09652	0.775299	81.08495	1.64461	82.00728	1.087447
Male	6	77.18467	1.469353	78.38593	1.171037	81.27528	1.013969	81.52939	1.191572
Saimiri oerstedii	2	79.49301	1.676628	81.52072	1.397786	82.09965	0.067115	83.29213	0.962942
Female	1	80.67856	NA	82.50911	NA	82.05219	NA	83.97304	NA
Male	1	78.30745	NA	80.53234	NA	82.14711	NA	82.61123	NA
Saimiri sciureus	32	77.22577	1.765371	79.75582	1.436396	79.96781	3.302411	82.22663	1.578803
Female	10	76.49428	2.745821	79.63068	2.111116	79.25055	2.747219	81.86551	2.561961
Male	22	77.52501	1.121099	79.80702	1.113637	80.39817	3.615939	82.39859	0.830082
Semnopithecus entellus	3	73.65169	2.512425	79.41113	1.020322	80.7362	0.882128	78.90946	1.535724
Female	1	NA	NA	80.32418	NA	81.59932	NA	80.6123	NA
Male	2	73.65169	2.512425	78.9546	0.911928	80.30464	0.662446	78.05805	0.606158

Symphalangus syndactylus	2	75.37397	0.114103	78.78546	0.723368	80.45121	NA	81.71884	1.542085
Female	2	75.37397	0.114103	78.78546	0.723368	80.45121	NA	81.71884	1.542085
Theropithecus gelada	4	70.72734	NA	75.60045	2.564	80.09413	0.884978	75.64529	4.909503
Male	4	70.72734	NA	75.60045	2.564	80.09413	0.884978	75.64529	4.909503
Trachypithecus cristatus	7	76.06491	2.093708	80.1317	1.855958	80.59081	1.305637	81.92826	1.745296
Female	6	76.40166	2.151505	80.66569	1.318453	80.5378	1.45251	82.11815	1.830952
unknown	1	74.38111	NA	76.92779	NA	80.85585	NA	80.78893	NA
Trachypithecus francoisi	1	72.74338	NA	77.37389	NA	79.51626	NA	79.63958	NA
Female	1	72.74338	NA	77.37389	NA	79.51626	NA	79.63958	NA
Trachypithecus obscurus	1	72.68631	NA	NA	NA	78.14143	NA	78.65276	NA
Female	1	72.68631	NA	NA	NA	78.14143	NA	78.65276	NA
Tupaia sp.	1	81.23623	NA	80.28215	NA	83.62771	NA	87.28211	NA
Female	1	81.23623	NA	80.28215	NA	83.62771	NA	87.28211	NA
Varecia rubra	1	73.20228	NA	77.4262	NA	NA	NA	NA	NA
Female	1	73.20228	NA	77.4262	NA	NA	NA	NA	NA
Varecia variegate variegata	3	72.65094	4.357223	71.55194	5.900164	86.1547	NA	87.96376	NA
Female	2	73.98405	5.225669	72.54057	7.984956	86.1547	NA	87.96376	NA
Male	1	69.98471	NA	69.57468	NA	NA	NA	NA	NA

Table A.8. Summary statistics for the nervous tissue variables by species/sex

Species/Sex	Number of Individuals	Nerve Length (mm)		Nerve Volume (mm^3)		Molar Nerve CSA (mm^2)		Premolar Nerve CSA (mm^2)		Mandibular Foramen Nerve CSA (mm^2)		Mental Foramen Nerve CSA (mm^2)	
		Mean	StdDev	Mean	StdDev	Mean	StdDev	Mean	StdDev	Mean	StdDev	Mean	StdDev
Alouatta caraya	3	67.521	4.9589	39.186	9.85954	0.5770	0.05222	0.5086	0.0899	0.75665	0.457356	0.5842	0.16235
Female	1	NA	NA	NA	NA	NA	NA	NA	NA	NA	NA	NA	NA
Male	2	67.521	4.9589	39.186	9.85954	0.5770	0.05222	0.5086	0.0899	0.75665	0.457356	0.5842	0.16235
Aotus trivirgatus	8	20.457	NA	4.732	NA	0.1815	NA	0.1479	NA	0.3704	NA	0.21365	NA
Female	5	NA	NA	NA	NA	NA	NA	NA	NA	NA	NA	NA	NA
Male	2	NA	NA	NA	NA	NA	NA	NA	NA	NA	NA	NA	NA
unknown	1	20.457	NA	4.732	NA	0.1815	NA	0.1479	NA	0.3704	NA	0.21365	NA
Callicebus moloch	7	21.3582	1.4414	3.2962	0.80079	0.1228	0.00265	0.1176	0.0291	0.237725	0.019410	0.16645	0.03132
Female	1	20.339	NA	2.73	NA	0.121	NA	0.0970	NA	0.224	NA	0.1886	NA
Male	6	22.3775	NA	3.8625	NA	0.1247	NA	0.1382	NA	0.25145	NA	0.1443	NA
Callithrix jacchus	4	15.2533	4.3286	1.4336	0.79563	0.0793	0.02828	0.0676	0.0213	0.136533	0.057277	0.087583	0.02855
Female	3	14.4837	5.8240	1.3285	1.09530	0.0723	0.03613	0.0622	0.0271	0.141875	0.079938	0.09715	0.03288
unknown	1	16.7925	NA	1.644	NA	0.0933	NA	0.0784	NA	0.12585	NA	0.06845	NA
Cebus capucinus	10	28.3302	3.7190	8.272	0.54517	0.2796	0.08693	0.2733	0.0172	0.327275	0.056957	0.155625	0.03185
Female	7	NA	NA	NA	NA	NA	NA	NA	NA	NA	NA	NA	NA
Male	3	28.3302	3.7190	8.272	0.54517	0.2796	0.08693	0.2733	0.0172	0.327275	0.056957	0.155625	0.03185
Cercocebus agilis	5	38.416	NA	20.169	NA	0.3851	NA	0.1866	NA	0.86365	NA	0.1541	NA
Female	2	NA	NA	NA	NA	NA	NA	NA	NA	NA	NA	NA	NA
Male	3	38.416	NA	20.169	NA	0.3851	NA	0.1866	NA	0.86365	NA	0.1541	NA
Cercopithecus neglectus	1	47.009	NA	47.572	NA	1.0043	NA	0.8335	NA	0.9364	NA	0.6403	NA
Male	1	47.009	NA	47.572	NA	1.0043	NA	0.8335	NA	0.9364	NA	0.6403	NA
Cheirogaleus major	1	6.047	NA	0.2215	NA	0.0396	NA	NA	NA	0.04015	NA	0.01335	NA
unknown	1	6.047	NA	0.2215	NA	0.0396	NA	NA	NA	0.04015	NA	0.01335	NA
Chiropotes satanas	3	29.284	NA	13.006	NA	0.4578	NA	0.4277	NA	0.52425	NA	0.32725	NA
Female	1	NA	NA	NA	NA	NA	NA	NA	NA	NA	NA	NA	NA
Male	2	29.284	NA	13.006	NA	0.4578	NA	0.4277	NA	0.52425	NA	0.32725	NA
Colobus guereza	5	57.584	NA	36.794	NA	0.5526	NA	0.7685	NA	0.73005	NA	0.5965	NA
Female	1	NA	NA	NA	NA	NA	NA	NA	NA	NA	NA	NA	NA

Male	4	57.584	NA	36.794	NA	0.5526	NA	0.7685	NA	0.73005	NA	0.5965	NA
Erythrocebus patas	3	36.4375	NA	19.289	NA	0.2774	NA	NA	NA	1.0483	NA	0.2332	NA
Female	2	36.4375	NA	19.289	NA	0.2774	NA	NA	NA	1.0483	NA	0.2332	NA
Male	1	NA	NA	NA	NA	NA	NA	NA	NA	NA	NA	NA	NA
Eulemur fulvus collaris	1	39.819	NA	12.581	NA	0.3379	NA	0.23945	NA	0.575	NA	0.23785	NA
unknown	1	39.819	NA	12.581	NA	0.3379	NA	0.23945	NA	0.575	NA	0.23785	NA
Eulemur fulvus rufus	2	37.5245	NA	12.203	NA	0.2942	NA	0.2957	NA	0.7968	NA	0.32395	NA
Female	1	NA	NA	NA	NA	NA	NA	NA	NA	NA	NA	NA	NA
Male	1	37.5245	NA	12.203	NA	0.2942	NA	0.2957	NA	0.7968	NA	0.32395	NA
Eulemur macaco macaco	1	39.83	NA	21.429	NA	0.6006	NA	0.64775	NA	0.6296	NA	0.39195	NA
Male	1	39.83	NA	21.429	NA	0.6006	NA	0.64775	NA	0.6296	NA	0.39195	NA
Galago senegalensis	6	13.388	NA	1.0935	NA	0.0806	NA	0.0763	NA	0.10595	NA	0.0969	NA
Female	3	NA	NA	NA	NA	NA	NA	NA	NA	NA	NA	NA	NA
Male	3	13.388	NA	1.0935	NA	0.0806	NA	0.0763	NA	0.10595	NA	0.0969	NA
Hapalemur griseus griseus	1	22.7005	NA	4.966	NA	0.1318	NA	0.13505	NA	0.39305	NA	0.0898	NA
Female	1	22.7005	NA	4.966	NA	0.1318	NA	0.13505	NA	0.39305	NA	0.0898	NA
Lagothrix logotricha	3	42.3095	NA	40.415	NA	0.9619	NA	0.9123	NA	1.39825	NA	0.5913	NA
Female	1	NA	NA	NA	NA	NA	NA	NA	NA	NA	NA	NA	NA
Male	1	NA	NA	NA	NA	NA	NA	NA	NA	NA	NA	NA	NA
unknown	1	42.3095	NA	40.415	NA	0.9619	NA	0.9123	NA	1.39825	NA	0.5913	NA
Lemur catta	1	32.4635	NA	6.635	NA	0.1698	NA	0.13495	NA	0.3439	NA	0.1965	NA
Male	1	32.4635	NA	6.635	NA	0.1698	NA	0.13495	NA	0.3439	NA	0.1965	NA
Lontra canadensis	1	39.1845	NA	26.797	NA	0.6617	NA	0.2788	NA	0.959	NA	0.86575	NA
Male	1	39.1845	NA	26.797	NA	0.6617	NA	0.2788	NA	0.959	NA	0.86575	NA
Macaca fascicularis	6	40.205	NA	15.11	NA	0.2740	NA	0.33865	NA	0.48395	NA	0.3069	NA
Female	3	40.205	NA	15.11	NA	0.2740	NA	0.33865	NA	0.48395	NA	0.3069	NA
Male	3	NA	NA	NA	NA	NA	NA	NA	NA	NA	NA	NA	NA
Macaca mulatta	10	44.3545	6.3389	27.757	7.90907	0.5627	0.07054	0.50808	0.1236	0.92713	0.231905	0.57089	0.16762
Female	8	44.3545	6.3389	27.757	7.90907	0.5627	0.07054	0.50808	0.1236	0.92713	0.231905	0.57089	0.16762
Male	2	NA	NA	NA	NA	NA	NA	NA	NA	NA	NA	NA	NA

Nycticebus coucang	2	15.1825	NA	2.9605	NA	0.0921	NA	NA	NA	0.2223	NA	0.18235	NA
Female	1	NA	NA	NA	NA	NA	NA	NA	NA	NA	NA	NA	NA
unknown	1	15.1825	NA	2.9605	NA	0.0921	NA	NA	NA	0.2223	NA	0.18235	NA
Oryctolagus cuniculus	4	24.3031	1.8108	10.085	1.80988	0.2904	0.02896	NA	NA	0.5743	0.029034	0.220975	0.04209
Female	2	25.731	0.9913	11.394	1.11192	0.3096	0.01506	NA	NA	0.595325	0.024147	0.2354	0.02694
Male	2	22.8752	0.8361	8.7765	1.31734	0.2712	0.02856	NA	NA	0.553275	0.013328	0.20655	0.06130
Otolemur crassicaudatus	1	24.1955	NA	6.6815	NA	0.1762	NA	NA	NA	0.35775	NA	0.1624	NA
unknown	1	24.1955	NA	6.6815	NA	0.1762	NA	NA	NA	0.35775	NA	0.1624	NA
Pan paniscus	1	60.7035	NA	190.14	NA	3.0043	NA	3.0634	NA	2.56955	NA	3.95465	NA
Female	1	60.7035	NA	190.14	NA	3.0043	NA	3.0634	NA	2.56955	NA	3.95465	NA
Papio anubis	8	81.688	NA	123.10	NA	1.39	NA	1.446	NA	1.954	NA	1.5515	NA
Female	3	81.688	NA	123.10	NA	1.39	NA	1.446	NA	1.954	NA	1.5515	NA
Male	5	NA	NA	NA	NA	NA	NA	NA	NA	NA	NA	NA	NA
Pithecia pithecia	4	24.6157	6.2335	6.0255	2.54063	0.2425	0.05777	0.1893	0.0347	0.3717	0.008626	0.387366	0.15312
Female	3	20.208	NA	4.229	NA	0.2017	NA	0.1647	NA	0.3656	NA	0.2997	0.02800
Male	1	29.0235	NA	7.822	NA	0.2834	NA	0.2139	NA	0.3778	NA	0.5627	NA
Presbytis comata	1	NA	NA	NA	NA	NA	NA	NA	NA	NA	NA	NA	NA
Female	1	NA	NA	NA	NA	NA	NA	NA	NA	NA	NA	NA	NA
Rattus norvegicus	5	12.5563	1.4689	0.9631	0.27008	0.0532	0.00725	NA	NA	0.13793	0.026865	0.08599	0.01476
Male	5	12.5563	1.4689	0.9631	0.27008	0.0532	0.00725	NA	NA	0.13793	0.026865	0.08599	0.01476
Saguinus oedipus	9	16.391	1.3510	1.6927	0.43281	0.1152	0.03700	0.09115	0.0308	0.12309	0.025859	0.08999	0.02139
Female	3	16.6345	NA	2.324	NA	0.1729	NA	0.1421	NA	0.13595	NA	0.08965	NA
Male	6	16.3301	1.5521	1.5348	0.28932	0.1008	0.02097	0.07841	0.0136	0.119875	0.028682	0.090075	0.02470
Saimiri sciureus	32	16.464	1.6355	2.5525	0.71708	0.1476	0.03535	0.15984	0.0383	0.216316	0.055337	0.160661	0.06291
Female	10	15.577	1.7812	1.9797	0.94151	0.1311	0.04104	0.13453	0.0321	0.1582	0.026375	0.138275	0.11409
Male	22	16.7174	1.6433	2.7162	0.63028	0.1523	0.03562	0.16708	0.0389	0.232921	0.050195	0.167057	0.053785
Semnopithecus entellus	3	34.94	NA	21.172	NA	0.7189	NA	0.48615	NA	1.02585	NA	0.21185	NA
Female	1	NA	NA	NA	NA	NA	NA	NA	NA	NA	NA	NA	NA
Male	2	34.94	NA	21.172	NA	0.7189	NA	0.48615	NA	1.02585	NA	0.21185	NA
Trachypithecus cristatus	7	29.1985	NA	19.016	NA	0.6891	NA	NA	NA	0.74645	NA	0.30335	NA
Female	6	NA	NA	NA	NA	NA	NA	NA	NA	NA	NA	NA	NA
unknown	1	29.1985	NA	19.016	NA	0.6891	NA	NA	NA	0.74645	NA	0.30335	NA

Trachypithecus francoisi	1	45.048	NA	15.5505	NA	0.29795	NA	0.24345	NA	0.7021	NA	0.11795	NA
Female	1	45.048	NA	15.5505	NA	0.29795	NA	0.24345	NA	0.7021	NA	0.11795	NA
Varecia rubra	1	42.6545	NA	12.908	NA	0.2266	NA	0.2221	NA	0.30085	NA	0.3233	NA
Female	1	42.6545	NA	12.908	NA	0.2266	NA	0.2221	NA	0.30085	NA	0.3233	NA
Varecia variegata variegata	3	48.199	0.0608	17.361	2.24506	0.3777	0.10843	0.3104	0.0731	0.59255	0.0668215	0.20705	0.068447
Female	2	48.156	NA	15.774	NA	0.3011	NA	0.2587	NA	0.5453	NA	0.25545	NA
Male	1	48.242	NA	18.949	NA	0.4544	NA	0.3621	NA	0.6398	NA	0.15865	NA

Table A.9. Summary statistics for the mandibular canal variables by species/sex

Species/Sex	Number of Individuals	Mandible Length		Canal Length		Canal Volume		Molar Canal CSA		Premolar Canal CSA		Mandibular Foramen CSA		Mental Foramen CSA	
		Mean	StdDev	Mean	StdDev	Mean	StdDev	Mean	StdDev	Mean	StdDev	Mean	StdDev	Mean	StdDev
Allenopithecus nigroviridis	1	73.166	NA	44.25	NA	132.6	NA	2.349	NA	2.274	NA	4.5737	NA	1.648	NA
Male	1	73.166	NA	44.25	NA	132.6	NA	2.349	NA	2.274	NA	4.5737	NA	1.648	NA
Alouatta caraya	3	90.069	16.85	63.31	13.67	207.4	2.406	2.181	0.361	2.159	0.479	3.3484	0.695	3.075	1.229
Female	1	70.683	NA	47.52	NA	NA	NA	NA	NA	NA	NA	2.5478	NA	1.845	NA
Male	2	99.762	2.068	71.20	0.43	207.4	2.406	2.181	0.361	2.159	0.479	3.7488	0.068	3.691	0.867
Alouatta palliata	2	70.443	0.432	50.34	1.927	146.8	NA	2.041	NA	2.013	NA	6.4198	0.094	1.093	0.343
Female	1	70.138	NA	48.98	NA	NA	NA	NA	NA	NA	NA	6.3536	NA	1.336	NA
Male	1	70.749	NA	51.70	NA	146.8	NA	2.041	NA	2.013	NA	6.486	NA	0.850	NA
Aotus trivirgatus	8	37.954	1.947	21.24	1.353	NA	NA	NA	NA	NA	NA	1.19	0.238	0.738	0.178
Female	5	38.177	2.224	21.50	1.535	NA	NA	NA	NA	NA	NA	1.288	0.247	0.750	0.152
Male	2	36.796	1.547	20.51	1.395	NA	NA	NA	NA	NA	NA	0.964	0.048	0.622	0.27
unknown	1	39.151	NA	21.44	NA	NA	NA	NA	NA	NA	NA	1.1517	NA	0.907	NA
Ateles geoffroyi	1	67.769	NA	37.82	NA	NA	NA	NA	NA	NA	NA	4.0174	NA	1.632	NA
Female	1	67.769	NA	37.82	NA	NA	NA	NA	NA	NA	NA	4.0174	NA	1.632	NA
Cacajao calvus	1	65.032	NA	31.33	NA	NA	NA	NA	NA	NA	NA	2.1904	NA	0.551	NA
Male	1	65.032	NA	31.33	NA	NA	NA	NA	NA	NA	NA	2.1904	NA	0.551	NA
Callicebus moloch	7	39.157	0.857	21.64	0.971	18.87	3.374	0.789	0.202	0.761	0.161	1.0902	0.232	0.881	0.343
Female	1	40.345	NA	20.31	NA	21.81	NA	0.993	NA	0.833	NA	1.0881	NA	0.855	NA
Male	6	38.959	0.743	21.86	0.845	18.38	3.411	0.755	0.198	0.749	0.173	1.0905	0.254	0.885	0.376
Callithrix argentata	2	28.978	0.094	15.76	1.101	NA	NA	NA	NA	NA	NA	0.7102	0.135	0.558	0.066
Female	1	29.045	NA	16.54	NA	NA	NA	NA	NA	NA	NA	0.8058	NA	0.605	NA
Male	1	28.912	NA	14.99	NA	NA	NA	NA	NA	NA	NA	0.6146	NA	0.512	NA
Callithrix humeralifera	3	29.12	0.947	15.93	0.613	NA	NA	NA	NA	NA	NA	0.626	0.057	0.357	0.04
Female	2	29.051	1.329	15.69	0.644	NA	NA	NA	NA	NA	NA	0.6372	0.076	0.335	0.012
Male	1	29.26	NA	16.40	NA	NA	NA	NA	NA	NA	NA	0.6036	NA	0.402	NA
Callithrix jacchus	4	28.143	5.498	15.27	3.538	7.855	NA	0.546	NA	0.622	NA	0.5097	0.184	0.429	0.121
Female	3	27.777	6.674	15.00	4.284	7.855	NA	0.546	NA	0.622	NA	0.5184	0.224	0.461	0.125
unknown	1	29.238	NA	16.06	NA	NA	NA	NA	NA	NA	NA	0.4836	NA	0.332	NA

Cebus apella	18	59.034	3.93	33.10	4.147	NA	NA	NA	NA	NA	NA	2.591	0.607	1.193	0.456
Female	10	56.984	1.829	30.77	3.313	NA	NA	NA	NA	NA	NA	2.9159	0.559	1.076	0.244
Male	8	61.597	4.437	36.02	3.189	NA	NA	NA	NA	NA	NA	2.185	0.39	1.340	0.621
Cebus capucinus	10	53.622	2.728	29.78	2.289	NA	NA	NA	NA	NA	NA	1.7726	0.505	1.289	0.479
Female	7	54.403	2.814	30.27	2.323	NA	NA	NA	NA	NA	NA	1.8089	0.552	1.404	0.5
Male	3	51.801	1.622	28.63	2.134	NA	NA	NA	NA	NA	NA	1.6878	0.467	1.022	0.362
Cercocebus agilis	5	78.608	12.77	44.48	4.714	197.6	62.93	3.420	0.967	2.267	0.211	6.6601	2.262	1.800	0.681
Female	2	73.998	3.055	42.86	1.874	125.9	NA	2.303	NA	2.275	NA	7.6778	0.131	2.211	0.38
Male	3	81.681	16.92	45.57	6.187	233.4	14.67	3.978	0.018	2.263	0.298	5.9816	2.915	1.526	0.758
Cercocebus torguatus	1	79.052	NA	46.17	NA	NA	NA	NA	NA	NA	NA	4.3575	NA	1.514	NA
Female	1	79.052	NA	46.17	NA	NA	NA	NA	NA	NA	NA	4.3575	NA	1.514	NA
Cercopithecus mitis	6	61.797	5.347	34.37	2.483	NA	NA	NA	NA	NA	NA	2.7406	0.814	0.831	0.479
Female	6	61.797	5.347	34.37	2.483	NA	NA	NA	NA	NA	NA	2.7406	0.814	0.831	0.479
Cercopithecus neglectus	1	82.943	NA	48.87	NA	NA	NA	NA	NA	NA	NA	3.2218	NA	1.303	NA
Male	1	82.943	NA	48.87	NA	NA	NA	NA	NA	NA	NA	3.2218	NA	1.303	NA
Cheirogaleus major	1	17.364	NA	9.144	NA	NA	NA	NA	NA	NA	NA	0.1565	NA	0.059	NA
unknown	1	17.364	NA	9.144	NA	NA	NA	NA	NA	NA	NA	0.1565	NA	0.059	NA
Chiropotes satanas	3	55.751	2.757	22.09	5.234	NA	NA	NA	NA	NA	NA	3.1466	0.433	1.213	0.309
Female	1	52.797	NA	26.19	NA	NA	NA	NA	NA	NA	NA	3.0611	NA	1.539	NA
Male	2	57.228	1.453	20.03	5.436	NA	NA	NA	NA	NA	NA	3.1893	0.603	1.050	0.178
Colobus guereza	5	83.499	5.749	52.16	6.455	170.2	NA	1.846	NA	2.988	NA	3.2904	0.706	1.899	0.62
Female	1	74.804	NA	43.38	NA	NA	NA	NA	NA	NA	NA	2.0953	NA	1.737	NA
Male	4	85.673	3.545	54.36	4.842	170.2	NA	1.846	NA	2.988	NA	3.5891	0.264	1.939	0.709
Colobus polykomos	4	77.373	3.244	48.37	2.425	NA	NA	NA	NA	NA	NA	2.971	0.164	1.356	0.415
Female	4	77.373	3.244	48.37	2.425	NA	NA	NA	NA	NA	NA	2.971	0.164	1.356	0.415
Erythrocebus patas	3	85.668	16.01	43.36	6.322	191.9	75.11	3.618	0.22	NA	NA	4.5578	1.948	2.866	1.481
Female	2	76.649	4.983	39.82	2.194	138.8	NA	3.462	NA	NA	NA	3.7677	1.961	2.554	1.949
Male	1	103.71	NA	50.44	NA	245.0	NA	3.773	NA	NA	NA	6.1379	NA	3.490	NA
Eulemur fulvus collaris	1	65.909	NA	42.99	NA	NA	NA	NA	NA	NA	NA	3.4503	NA	4.632	NA
unknown	1	65.909	NA	42.99	NA	NA	NA	NA	NA	NA	NA	3.4503	NA	4.632	NA
Eulemur fulvus rufus	2	57.157	3.93	33.7	5.724	117.4	NA	2.561	NA	2.814	NA	3.1633	1.191	1.558	1.46
Female	1	54.378	NA	29.65	NA	NA	NA	NA	NA	NA	NA	2.3211	NA	0.526	NA

Male	1	59.936	NA	37.74	NA	117.4	NA	2.561	NA	2.814	NA	4.0055	NA	2.590	NA
Eulemur macaco macaco	1	64.606	NA	42.53	NA	NA	NA	NA	NA	NA	NA	2.8154	NA	2.051	NA
Male	1	64.606	NA	42.53	NA	NA	NA	NA	NA	NA	NA	2.8154	NA	2.051	NA
Galago alleni	1	17.631	NA	10.32	NA	NA	NA	NA	NA	NA	NA	0.1442	NA	0.12	NA
Female	1	17.631	NA	10.327	NA	NA	NA	NA	NA	NA	NA	0.1442	NA	0.12	NA
Galago senegalensis	6	23.942	2.162	13.60	1.019	4.504	2.272	0.332	0.2	0.379	0.222	0.3014	0.099	0.321	0.098
Female	3	24.18	1.57	13.96	1.214	3.679	0.621	0.248	0.043	0.273	0.092	0.3006	0.091	0.341	0.051
Male	3	23.703	3.009	13.24	0.853	5.329	3.518	0.416	0.3	0.485	0.308	0.3021	0.128	0.300	0.142
Gorilla gorilla gorilla	3	164.3	23.6	97.76	17.78	NA	NA	NA	NA	NA	NA	20.80	12.17	13.59	4.062
Female	2	150.7	0.725	87.50	0.173	NA	NA	NA	NA	NA	NA	14.021	4.449	13.72	5.735
Male	1	191.56	NA	118.2	NA	NA	NA	NA	NA	NA	NA	34.384	NA	13.31	NA
Hapalemur griseus	2	40.947	1.073	21.34	1.084	16.76	0.24	0.716	0.037	0.685	0.048	1.37	0.214	0.247	0.088
Male	2	40.947	1.073	21.34	1.084	16.76	0.24	0.716	0.037	0.685	0.048	1.37	0.214	0.247	0.088
Hapalemur griseus griseus	1	40.848	NA	28.20	NA	31.78	NA	1.110	NA	0.754	NA	1.4999	NA	1.641	NA
Female	1	40.848	NA	28.20	NA	31.78	NA	1.110	NA	0.754	NA	1.4999	NA	1.641	NA
Homo sapiens	5	108.97	6.919	59.79	5.164	389.5	NA	NA	NA	NA	NA	15.878	5.014	12.57	4.293
Female	3	104.61	4.347	56.33	2.419	389.5	NA	NA	NA	NA	NA	16.421	6.966	14.91	3.604
Male	2	115.5	3.404	64.97	2.344	NA	NA	NA	NA	NA	NA	15.063	1.129	9.077	2.619
Lagothrix logotricha	3	69.003	2.496	41.37	2.172	137.2	19.05	2.617	0.342	2.679	0.291	5.8609	0.579	2.405	0.262
Female	1	71.001	NA	42.67	NA	150.3	NA	3.003	NA	3.002	NA	5.2058	NA	2.685	NA
Male	1	66.205	NA	38.86	NA	115.4	NA	2.354	NA	2.436	NA	6.0746	NA	2.166	NA
unknown	1	69.805	NA	42.57	NA	146.0	NA	2.494	NA	2.599	NA	6.3023	NA	2.365	NA
Lemur catta	1	55.492	NA	32.91	NA	NA	NA	NA	NA	NA	NA	1.9426	NA	0.706	NA
Male	1	55.492	NA	32.91	NA	NA	NA	NA	NA	NA	NA	1.9426	NA	0.706	NA
Lontra canadensis	1	67.606	NA	39.16	NA	154.4	NA	5.720	NA	2.084	NA	4.1088	NA	3.827	NA
Male	1	67.606	NA	39.16	NA	154.4	NA	5.720	NA	2.084	NA	4.1088	NA	3.827	NA
Lophocebus albigena	6	78.73	6.167	47.29	4.521	129.2	42.91	1.995	0.651	3.865	2.447	6.1184	2.378	1.387	0.586
Female	2	74.441	4.802	46.02	0.999	NA	NA	NA	NA	NA	NA	4.549	0.444	1.687	1.004
Male	4	80.875	6.107	47.92	5.668	129.2	42.91	1.995	0.651	3.865	2.447	6.9032	2.626	1.238	0.384
Macaca fascicularis	6	76.512	11.78	44.33	6.584	NA	NA	NA	NA	NA	NA	4.1223	0.879	1.837	0.625
Female	3	67.28	3.997	38.96	2.274	NA	NA	NA	NA	NA	NA	4.4216	0.854	1.454	0.611
Male	3	85.745	8.673	49.71	4.063	NA	NA	NA	NA	NA	NA	3.823	0.967	2.220	0.401

Macaca maura	1	94.088	NA	55.71	NA	NA	NA	NA	NA	NA	NA	4.8548	NA	4.424	NA
Female	1	94.088	NA	55.71	NA	NA	NA	NA	NA	NA	NA	4.8548	NA	4.424	NA
Macaca mulatta	10	80.884	9.087	46.56	6.035	142.8	0.381	2.548	0.375	2.577	0.077	4.8574	1.326	2.872	1.507
Female	8	79.75	9.267	45.92	6.29	142.8	0.381	2.548	0.375	2.577	0.077	4.643	1.377	2.846	1.527
Male	2	85.423	9.513	49.15	5.838	NA	NA	NA	NA	NA	NA	5.7149	0.842	2.978	2.021
Macaca nigra	1	93.352	NA	48.51	NA	NA	NA	NA	NA	NA	NA	4.5414	NA	0.267	NA
Male	1	93.352	NA	48.51	NA	NA	NA	NA	NA	NA	NA	4.5414	NA	0.267	NA
Macaca radiata	1	81.754	NA	39.77	NA	79.30	NA	1.276	NA	NA	NA	3.4081	NA	1.398	NA
Male	1	81.754	NA	39.77	NA	79.30	NA	1.276	NA	NA	NA	3.4081	NA	1.398	NA
Mandrillus leucophaeus	3	145.76	6.756	92.46	3.146	599.4	56.8	5.019	1.223	5.712	0.786	10.175	0.79	9.400	4.137
Male	3	145.76	6.756	92.46	3.146	599.4	56.8	5.019	1.223	5.712	0.786	10.175	0.79	9.40	4.137
Mandrillus sphinx	7	121.65	24.13	72.98	14.9	511.2	220.2	5.851	1.949	5.431	2.154	13.544	5.106	5.045	1.976
Female	4	103.37	5.216	61.31	3.979	372.1	98.72	5.083	1.754	4.017	1.06	11.525	4.151	3.787	1.528
Male	3	146.03	12.1	88.53	2.738	696.6	201.5	6.874	2.007	7.316	1.705	16.236	5.775	6.723	0.906
Microcebus murinus	1	17.729	NA	8.911	NA	1.544	NA	0.22	NA	NA	NA	0.213	NA	0.094	NA
Female	1	17.729	NA	8.911	NA	1.544	NA	0.22	NA	NA	NA	0.213	NA	0.094	NA
Miopithecus talapoin	2	42.625	5.06	22.41	3.894	NA	NA	NA	NA	NA	NA	1.4097	0.375	0.775	0.047
Female	1	39.048	NA	19.66	NA	NA	NA	NA	NA	NA	NA	1.1444	NA	0.808	NA
Male	1	46.203	NA	25.16	NA	NA	NA	NA	NA	NA	NA	1.675	NA	0.742	NA
Nasalis larvatus	8	76.106	9.37	42.02	5.14	NA	NA	3.859	2.329	NA	NA	3.6384	0.808	2.596	1.885
Female	4	70.158	4.285	38.54	3.493	NA	NA	NA	NA	NA	NA	3.34	0.986	1.748	1.019
Male	4	82.055	9.6	45.49	4.155	NA	NA	3.859	2.329	2.578	NA	3.9369	0.559	3.445	2.31
Nycticebus coucang	2	33.533	0.048	15.20	1.477	11.37	0.692	0.864	0.035	NA	NA	0.9497	0.081	1.140	0.011
Female	1	33.499	NA	14.15	NA	10.88	NA	0.889	NA	NA	NA	1.0069	NA	1.133	NA
unknown	1	33.568	NA	16.24	NA	11.85	NA	0.839	NA	NA	NA	0.8925	NA	1.148	NA
Oryctolagus cuniculus	4	65.835	7.107	2796.	5544	NA	NA	NA	NA	NA	NA	2.6018	0.427	3.775	0.792
Female	2	69.576	2.376	25.03	1.246	NA	NA	NA	NA	NA	NA	2.6991	0.07	4.226	0.525
Male	2	62.094	9.483	5568.	7841	NA	NA	NA	NA	NA	NA	2.5045	0.71	3.324	0.89
Otolemur crassicaudatus	1	43.819	NA	23.61	NA	32.03	NA	1.301	NA	NA	NA	1.5615	NA	1.254	NA
unknown	1	43.819	NA	23.61	NA	32.03	NA	1.301	NA	NA	NA	1.5615	NA	1.254	NA
Pan paniscus	1	82.345	NA	61.51	NA	NA	NA	NA	NA	NA	NA	7.5809	NA	5.878	NA
Female	1	82.345	NA	61.51	NA	NA	NA	NA	NA	NA	NA	7.5809	NA	5.878	NA

Pan troglodytes troglodytes	1	148.85	NA	64.48	NA	NA	NA	NA	NA	NA	NA	11.219	NA	9.772	NA
Male	1	148.85	NA	64.48	NA	NA	NA	NA	NA	NA	NA	11.219	NA	9.772	NA
Papio anubis	8	141.22	18.11	92.12	11.79	810.7	307.7	5.469	2.606	5.886	3.018	13.837	4.286	4.852	1.863
Female	3	123.99	8.182	81.56	6.159	NA	NA	NA	NA	NA	NA	12.13	1.026	5.407	0.042
Male	5	151.56	13.58	96.35	11	810.7	307.7	5.469	2.606	5.886	3.018	14.861	5.304	4.630	2.234
Papio ursinus	4	135.06	18.02	81.75	4.769	517.3	87.92	4.621	0.228	4.934	0.615	10.918	1.168	8.006	1.475
Female	2	119.74	1.053	77.81	2.377	453.8	29.74	4.474	0.128	4.498	0.033	10.17	0.711	7.681	0.481
Male	2	150.38	5.845	85.69	0.598	580.7	78.81	4.769	0.229	5.369	0.614	11.666	1.162	8.331	2.424
Perodicticus potto	1	37.104	NA	17.48	NA	16.05	NA	1.029	NA	NA	NA	1.2794	NA	0.543	NA
Male	1	37.104	NA	17.48	NA	16.05	NA	1.029	NA	NA	NA	1.2794	NA	0.543	NA
Piliocolobus badius	6	73.043	5.187	44.78	4.663	81.66	NA	1.650	NA	1.584	NA	3.2861	0.736	1.446	0.774
Female	2	75.477	9.024	47.64	6.98	NA	NA	NA	NA	NA	NA	4.0207	0.634	2.174	1.026
Male	4	71.826	3.431	43.35	3.437	81.66	NA	1.650	NA	1.584	NA	2.9188	0.48	1.083	0.344
Pithecia pithecia	4	52.184	3.357	26.36	3.028	NA	NA	NA	NA	NA	NA	2.034	0.509	1.258	0.18
Female	3	50.783	2.265	25.59	3.193	NA	NA	NA	NA	NA	NA	1.8164	0.322	1.253	0.22
Male	1	56.387	NA	28.67	NA	NA	NA	NA	NA	NA	NA	2.6869	NA	1.271	NA
Pongo abelii	2	168.94	35.07	93.23	27.25	1049.4	468.3	10.557	2.405	7.891	0.338	13.402	0.992	14.30	5.312
Female	1	144.14	NA	73.97	NA	718.21	NA	8.856	NA	7.652	NA	14.104	NA	10.55	NA
Male	1	193.73	NA	112.5	NA	1380.5	NA	12.25	NA	8.130	NA	12.7	NA	18.06	NA
Presbytis comata	1	51.236	NA	28.07	NA	NA	NA	NA	NA	NA	NA	2.6014	NA	0.428	NA
Female	1	51.236	NA	28.07	NA	NA	NA	NA	NA	NA	NA	2.6014	NA	0.428	NA
Presbytis melalophos	2	61.144	0.67	36.04	0.983	NA	NA	NA	NA	NA	NA	2.1858	0.05	0.679	0.696
Female	1	61.618	NA	35.34	NA	NA	NA	NA	NA	NA	NA	2.221	NA	1.171	NA
Male	1	60.671	NA	36.74	NA	NA	NA	NA	NA	NA	NA	2.1507	NA	0.187	NA
Procolobus verus	2	67.522	9.574	39.21	8.334	NA	NA	NA	NA	NA	NA	3.4657	0.722	1.655	1.393
Female	1	74.292	NA	45.10	NA	NA	NA	NA	NA	NA	NA	3.976	NA	0.670	NA
Male	1	60.753	NA	33.32	NA	NA	NA	NA	NA	NA	NA	2.9554	NA	2.640	NA
Propithecus verreauxi	2	52.854	0.607	29.51	1.421	NA	NA	NA	NA	NA	NA	1.3683	0.413	1.149	0.098
Male	2	52.854	0.607	29.51	1.421	NA	NA	NA	NA	NA	NA	1.3683	0.413	1.149	0.098
Rattus norvegicus	5	23.132	2.358	12.45	1.559	3.1144	0.934	0.109	0.032	NA	NA	0.5285	0.111	0.182	0.046
Male	5	23.132	2.358	12.45	1.559	3.1144	0.934	0.109	0.032	NA	NA	0.5285	0.111	0.182	0.046
Saguinus oedipus	9	30.712	1.355	16.02	1.474	5.9955	NA	0.411	NA	0.474	NA	0.4579	0.066	0.411	0.078

Female	3	31.193	1.734	15.96	1.611	NA	NA	NA	NA	NA	NA	0.4512	0.02	0.423	0.108
Male	6	30.471	1.235	16.05	1.561	5.9955	NA	0.411	NA	0.474	NA	0.4612	0.082	0.405	0.071
Saimiri oerstedii	2	33.404	2.326	16.70	1.622	NA	NA	NA	NA	NA	NA	0.6494	0.176	0.561	0.008
Female	1	31.759	NA	15.55	NA	NA	NA	NA	NA	NA	NA	0.774	NA	0.556	NA
Male	1	35.049	NA	17.84	NA	NA	NA	NA	NA	NA	NA	0.5249	NA	0.567	NA
Saimiri sciureus	32	34.547	2.073	17.43	1.168	56.463	81.66	0.829	0.145	0.851	0.113	1.0103	0.218	1.194	0.319
Female	10	33.703	2.907	17.30	1.549	71.033	93.43	0.880	0.127	0.903	0.058	1.1509	0.228	1.261	0.387
Male	22	34.931	1.492	17.49	0.988	12.754	NA	0.677	NA	0.697	NA	0.9464	0.186	1.163	0.288
Semnopithecus entellus	3	75.263	12.69	45.67	9.584	171.05	NA	3.638	NA	2.637	NA	3.3057	0.636	1.398	0.612
Female	1	82.408	NA	53.29	NA	171.05	NA	3.638	NA	2.637	NA	2.5822	NA	2.060	NA
Male	2	71.69	15.67	41.85	9.821	NA	NA	NA	NA	NA	NA	3.6674	0.152	1.067	0.302
Symphalangus syndactylus	2	67.525	10.2	36.38	4.505	NA	NA	NA	NA	NA	NA	3.4509	0.309	1.767	0.06
Female	2	67.525	10.2	36.38	4.505	NA	NA	NA	NA	NA	NA	3.4509	0.309	1.767	0.06
Theropithecus gelada	4	124.16	3.27	75.19	2.703	447.45	56.28	5.55	1.302	4.129	1.144	13.748	1.345	4.840	1.888
Male	4	124.16	3.27	75.19	2.703	447.45	56.28	5.55	1.302	4.129	1.144	13.748	1.345	4.840	1.888
Trachypithecus cristatus	7	61.602	3.532	37.74	3.56	NA	NA	NA	NA	NA	NA	2.1837	0.107	0.849	0.461
Female	6	62.854	1.346	38.94	1.761	NA	NA	NA	NA	NA	NA	2.1987	0.109	0.758	0.431
unknown	1	54.092	NA	30.54	NA	NA	NA	NA	NA	NA	NA	2.0937	NA	1.392	NA
Trachypithecus francoisi	1	65.85	NA	47.49	NA	NA	NA	NA	NA	NA	NA	2.0022	NA	0.614	NA
Female	1	65.85	NA	47.49	NA	NA	NA	NA	NA	NA	NA	2.0022	NA	0.614	NA
Trachypithecus obscurus	1	67.925	NA	35.14	NA	NA	NA	NA	NA	NA	NA	3.9841	NA	3.190	NA
Female	1	67.925	NA	35.14	NA	NA	NA	NA	NA	NA	NA	3.9841	NA	3.190	NA
Varecia rubra	1	73.787	NA	49.50	NA	NA	NA	NA	NA	NA	NA	1.9185	NA	2.899	NA
Female	1	73.787	NA	49.50	NA	NA	NA	NA	NA	NA	NA	1.9185	NA	2.899	NA
Varecia variegata variegata	3	70.703	3.162	46.71	1.674	107.52	NA	2.553	NA	1.155	NA	2.0583	0.539	2.301	1.182
Female	2	70.172	4.279	46.30	2.14	107.52	NA	2.553	NA	1.155	NA	1.7478	0.041	1.629	0.288
Male	1	71.765	NA	47.54	NA	NA	NA	NA	NA	NA	NA	2.6793	NA	3.645	NA

APPENDIX B: BIOSAFETY PROTOCOL APPROVAL

UNIVERSITY OF ARKANSAS

Office of Research Compliance

June 21, 2018

MEMORANDUM

TO:	Dr. Claire Terhune
FROM:	Ines Pinto, Biosafety Committee Chair
RE:	New Protocol
PROTOCOL #:	18045
PROTOCOL TITLE: and their relation	An assessment of the neurovascular structures of the trigeminal nerve
APPROVED PROJECT PERIOD:	**Start Date** June 14, 2018 **Expiration Date** June 13, 2021

The Institutional Biosafety Committee (IBC) has approved Protocol 18045, "An assessment of the neurovascular structures of the trigeminal nerve and their relation". You may begin your study.

If modifications are made to the protocol during the study, please submit a written request to the IBC for review and approval before initiating any changes.

The IBC appreciates your assistance and cooperation in complying with University and Federal guidelines for research involving hazardous biological materials.

1424 W. Martin Luther King, Jr. • Fayetteville, AR 72701
Voice (479) 575-4572 • Fax (479) 575-6527